

PALEOHYDROLOGY AND SIMULATION OF THREE KARST BASINS

PALEOHYDROLOGY AND STREAMFLOW SIMULATION OF THREE KARST BASINS

IN

SOUTHEASTERN WEST VIRGINIA, U.S.A.

By

JULIAN MICHAEL HENRY COWARD, B.Sc., M.Sc.

A Thesis

Submitted to the School of Graduate Studies

in Partial Fulfilment of the Requirements

for the Degree

Doctor of Philosophy

McMaster University

March, 1975

DOCTOR OF PHILOSOPHY
(Geology)

McMASTER UNIVERSITY
Hamilton, Ontario

TITLE: Paleohydrology and Streamflow Simulation of three Karst Basins in Southeastern West Virginia, U.S.A.

AUTHOR: Julian Michael Henry Coward, B.Sc. (University College,
London)
M.Sc. (University College,
London)

SUPERVISOR: Dr. D.C. Ford

NUMBER OF PAGES: xvi, 394

SCOPE AND CONTENTS: Streams in limestone areas initially flow on the surface, but as the area matures the flow becomes almost entirely underground, through caves and other conduits. For this study three small karst drainage basins in West Virginia were chosen, the present hydrological conditions and the caves studied in detail, and the past hydrological conditions inferred. The controls on the drainage development were determined.

A computer simulation of the hydrology was carried out to determine the quantitative hydrology of the basins, and to infer some of the characteristics of the inaccessible flow paths. The model was used to simulate the streamflows in the basins, using known climatic data. The type of inaccessible flow paths was inferred from the type of computer model used.

ABSTRACT

This study was undertaken to gain a better understanding of karst hydrology. To do this, the present day hydrology and the paleohydrology were determined in three karst basins. The basins chosen were the Swago, Locust and Spring Creek basins in Pocahontas and Greenbrier Counties, West Virginia. A number of conventional field techniques were used successfully in this study, including the following: current meter and dye dilution gauging; dye and lycopodium stream tracing; geological and cave mapping; the setting up of stage recorders; geochemistry; and limestone erosion measurements. The climate of the region was investigated to obtain realistic precipitation, temperature and potential evaporation data over the study basins.

It was found that the mean precipitation over two of the basins was 30% higher than recorded data in the valleys. The karst development of the basins was found to take place in four major stages. These were: A) initial surficial flow, B) strike controlled drainage, C) major piracy from one sub-basin to another, and D) shortening of the flow routes. The major controls on the karst development were found to be: A) the Taggard shale, B) the strike direction, which controlled early basin development, and C) the hydraulic gradient from the sink to rising, which controlled later basin development.

To better assess the quantitative hydrology, and to assist in determining the type of unexplorable flow paths, a watershed model was

developed. This modelled the streamflow from known climatic inputs using a number of measured or optimized parameters. The simulation model handled snowmelt, interception, infiltration, interflow, baseflow, overland flow, channel routing, and evaporation from the interception, soil water, ground water, snowpack and channel water. The modelled basin could be split up into 20 segments, each with different hydrological characteristics, but a maximum of 3 segments was used in this study.

A total of 29 parameters was used in the model although only 10 (other than those directly measurable) were found to be sensitive in the three basins. The simulated streamflow did not match the real flows very well due to errors in the data input and due to simplifications in the model. It was found, however, that as the proportion of the limestone in a segment increased the overland flow decreased, the interflow increased, the baseflow and interflow recessions were faster, the soil storages were smaller and the infiltration rate was higher, than in segments with a larger proportion of exposed clastics. The flow characteristics of the inaccessible conduits were inferred from the channel routing parameters and it was postulated that the majority of the underground flow in the karst basins was taking place under vadose conditions.

ACKNOWLEDGEMENTS

I would like to thank my supervisor Dr. Derek Ford for his constant encouragement, advice and suggestions throughout the preparation of this thesis. Also my thanks to Dr. W. James, Dr. N. Wilson and Dr. J. Kramer, as members of my committee who gave much valuable help.

I am also indebted to Bill Stickers for help during field work; Bob Bignell for printing the photographs; John Drake for dyeing great quantities of lycopodium spores; Dallas McKeever and several other land-owners in West Virginia who allowed access to their caves; staff at the West Virginia Geological Survey, particularly Dr. Price (now retired) and Dr. Erwin, for advice and information; U.S. Geological Survey at Charleston (District Chief, Dr. Griffin) for the loan of four stage recorders and other assistance; and the Ministry of the Environment of Ontario for support and indulgence during the final preparation of this report.

My sincere thanks go to my wife, Mary, for her constant encouragement, support and friendship during the preparation of this work, and for the monumental task of deciphering my writing, correcting my spelling and typing all the drafts of this thesis.

And last, my gratitude to all fellow cavers for companionship in the caves, in the pubs and around the campfires.

TABLE OF CONTENTS

	<u>Page</u>
ABSTRACT	iii
TABLE OF CONTENTS	vi
LIST OF FIGURES	xi
LIST OF TABLES	xv
CHAPTER I INTRODUCTION	1
1.1 Paleohydrology	2
1.2 Objectives of the Study	3
1.3 Choice of Study Area	4
1.4 Description of the Study Area	6
1.4.1 Description of the Swago Creek Basin	10
1.4.2 Description of the Locust Creek Basin	10
1.4.3 Description of the Spring Creek Basin	13
1.5 Bedrock Geology	15
1.5.1 Superficial Deposits, Soils and Vegetation	19
1.6 Previous Work	20
CHAPTER II FIELD RESEARCH TECHNIQUES	23
2.1 Stream Gauging	23
2.1.1 Current Meter Gauging	23
2.1.2 Dye Dilution Gauging	24
2.1.2.1 Fluorometer Calibration	25
2.1.2.2 Constant Rate Dye Injection	29
2.1.2.3 Slug Injection	32
2.2 Hydrograph Measurements	34
2.2.1 Recorder Sites	37
2.2.2 Hydrograph Record Lengths	39
2.3 Cave Mapping	42
2.4 Flood and Dye Test	42
2.5 Stream Tracing	43
2.5.1 Lycopodium Tracing	46
2.5.2 Dye Tracing	50
2.6 Geochemical Methods	53
2.7 Erosion Measurements	54
2.7.1 Micro-erosion Instrument	56
2.7.2 Erosion Site	58
2.7.3 Calibration	58

	<u>Page</u>
CHAPTER III CLIMATE AND FIELD RESULTS	61
3.1 Climate	61
3.1.1 Precipitation	63
3.1.2 Areal Variation in Precipitation	65
3.1.3 Variation of Precipitation with Altitude	67
3.1.4 Mean Basin Precipitation	70
3.1.5 Evaporation and Temperature	77
3.2 Streamflow	77
3.3 Erosion Results	80
3.3.1 Past Climatic Conditions and Past Erosion Rates	82
 CHAPTER IV SIMULATION	 85
4.1 Description of the Real System being Modelled	86
4.1.1 Description of Model Used	87
4.2 Details of the Algorithms Used in the Model	90
4.2.1 Interception	90
4.2.2 Snow	93
4.2.3 Infiltration	94
4.2.4 Evapotranspiration	97
4.2.5 Channel Routing	99
4.2.6 Overland Flow	99
4.3 Objective Function	100
4.3.1 Purpose and Choice of Objective Function	100
4.3.2 Description of Objective Functions Used	102
4.4 Organization of the Computer Program	105
4.4.1 Climatic Data Input	107
4.4.2 Description of Program REEDAT	107
4.4.3 Description of Program PRECON	108
4.4.4 Description of the Streamflow Data and the Program RATNG	109
4.4.5 Description of the Program KARST	110
4.4.5.1 Descriptions of the Subroutines Used in KARST	112
4.5 Optimization of the Simulation Program	117
4.5.1 Automatic Methods of Optimization	117
4.5.2 Manual Methods of Optimization	120
4.6 Sensitivity Analysis	121
 CHAPTER V THE GENESIS OF THE SWAGO CREEK BASIN	 127
5.1 Hydrological Description of the Present Basin	127
5.1.1 Sinks along Dry Creek	131

	<u>Page</u>
5.2 Description of the Caves in the Swago Creek Basin	135
5.2.1 Cave Creek Cave	136
5.2.2 Barnes Pit Cave	136
5.2.3 Tub Cave	138
5.2.4 Swago-Carpenters Cave	139
5.2.4.1 The Flood and Dye Test at Swago Creek	141
5.2.5 Hause Waterfall Cave	144
5.2.6 Overholts Blowing Cave	146
5.3 Description of the Four Stages of Karst Development in the Swago Basin	150
5.3.1 Stage 1: Surficial Flow	151
5.3.2 Stage 2: Initial Karst Development	151
5.3.3 Stage 3: Present Conditions	155
5.3.4 Stage 4: Future Conditions	157
5.4 Simulation of the Swago Creek Basin	158
5.4.1 Description of the Real and Simulated Streamflows	161
5.4.2 Geomorphic Significance of the Model Parameters	164
 CHAPTER VI THE GENESIS OF THE LOCUST CREEK BASIN	 166
6.1 Hydrological Description of the Surficial Basin	168
6.2 Description of the Caves and Major Flow Routes in the Locust Creek Basin	174
6.2.1 Hills-Bruffey Cave	174
6.2.2 Cutlip Cave	177
6.2.3 Clyde Cochran Cave	181
6.2.4 Snedegars and Friars Hole Caves	181
6.2.5 Hughes Creek Caves	194
6.2.6 Marthas Caves	196
6.2.7 Beards Blue Hole	198
6.2.8 Poor Farm Cave	198
6.2.9 Locust Creek Cave	201
6.2.10 Description of the Bruffey to Upper Hughes Creek Cave and to Locust Creek Flow Routes	201
6.3 Description of the Five Stages of Development	206
6.3.1 Stage 1: Surficial Flow	208
6.3.2 Stage 2: Initial Karst Development	210
6.3.3 Stage 3: Major Piracies	215
6.3.4 Stage 4: Shortening of the Flow Routes	218
6.3.5 Stage 5: Future Shortening of the Flow Routes	220
6.4 The Simulation of Locust Creek	222
6.4.1 Comparison Between the Real and Simulated Streamflows	224
6.4.2 Geomorphic Significance of the Model Parameters	226

	<u>Page</u>
CHAPTER VII THE GENESIS OF THE SPRING CREEK BASIN	229
7.1 Description of the Spring Creek Basin	229
7.1.1 The Culverson Creek Sub-basin	231
7.1.2 The Upper Spring Creek Sub-basin	233
7.1.3 The Great Savanna Sub-basin	234
7.1.4 The Lower Spring Creek Sub-basin	236
7.2 The Development of the Spring Creek Basin	237
7.2.1 Stage 1: Surficial Flow	238
7.2.2 Stage 2: Underdraining of the Valleys	240
7.2.3 Stage 3: Major Piracies of the Streams	246
7.2.4 Stage 4: Shortening of the Flow Routes	250
7.3 The Simulation of Spring Creek	251
7.3.1 Comparison Between the Real and Simulated Flows	254
7.3.2 Geomorphic Significance of the Model Parameters	254
CHAPTER VIII DISCUSSION AND CONCLUSIONS	257
8.1 Summary of the Basin Genesis	257
8.1.1 Development of the Swago Creek Basin	258
8.1.2 Development of the Locust Creek Basin	260
8.1.3 Development of the Spring Creek Basin	260
8.2 Generalized Development of the Karst Basins	261
8.2.1 Stage A: Surficial Flow	262
8.2.2 Stage B: Strike Oriented Drainage and Underdraining of the Valleys	262
8.2.3 Stage C: Major Piracies and Diversions	265
8.2.4 Stage D: Opening Up and Development of the Flow Routes	266
8.3 Major Controlling Factors in the Development of the Basins	267
8.3.1 The Taggard Shale	267
8.3.2 Strike Direction	271
8.3.3 Hydraulic Gradients	271
8.4 Simulation Results	275
8.4.1 The Objective Functions for the Basins	278
8.4.1.1 Peak Objective Function	278
8.4.1.2 Mean Objective Function	282
8.4.1.3 Temporal Objective Function	283
8.4.1.4 Total Objective Function	284
8.4.2 The Water Balances for the Basins	284
8.4.3 Errors in the Model Responses	288
8.4.4 Geomorphic Significance of the Parameter Values found in the Segments in the Four Basins	289
8.5 Conclusions	292
8.5.1 Basin Genesis	292
8.5.2 Simulation	294

	<u>Page</u>
BIBLIOGRAPHY	295
APPENDIX I	304
APPENDIX II	355
APPENDIX III	390

LIST OF FIGURES

	<u>Page</u>
1.1 Map of Eastern West Virginia showing the basins studied.	5
1.2 Map of the study area.	7
1.3 View of the karst near Snedegars Cave at the northern end of the Spring Creek basin.	9
1.4 Stream profiles for Swago, Locust and Spring Creeks.	11
1.5 The Locust Creek valley in winter.	14
1.6 General columnar section of the geology of the field area in West Virginia.	16
2.1 Fluorometer calibration curve for Rhodamine dye.	27
2.2 Concentration time graph for the slug dye dilution gauging at Fullers Cave.	33
2.3 Location of gauging sites and resurgences and sinks for the lycopodium test.	35
2.4 The stage recorder at Swago Creek.	36
2.5 Installation of the first Spring Creek recorder.	38
2.6 Final site for the stage recorder at Spring Creek during average flow conditions.	40
2.7 The stage recorder at Spring Creek during high water conditions.	41
2.8 Construction of the Swago Dam for the flood and dye test.	44
2.9 The micro-erosion meter.	55
2.10 The micro-erosion site in Lower Hughes Cave.	57
2.11 View of the limestone surface at the micro-erosion site.	59
3.1 Location of climatic stations.	62
3.2 Monthly precipitation at Marlinton and Buckeye, 1969-1971.	64

	<u>Page</u>
3.3 Plot of daily precipitation for June, 1969 at Marlinton, Buckeye and Renick.	66
3.4 Hypsometric curves for Swago, Locust and Spring Creeks, and the mean annual precipitation at different elevations.	71
3.5 Rating Curve for Swago Creek.	75
3.6 Rating Curve for Locust Creek.	76
3.7 Rating Curve for Spring Creek.	78
3.8 Monthly mean runoff at Swago, Locust and Spring Creeks.	81
3.9 Erosion at Hughes Creek Cave.	83
4.1 Idealized hydrological cycle in a karst basin.	87
4.2 Flow diagram for the hydrologic model.	89
4.3 Modelled infiltration rate with varying rainfall.	96
4.4 Flow chart for the data input and program divisions.	106
4.5 Flow chart for the simulation program KARST.	113
5.1 Swago Creek basin—topography and drainage.	128
5.2 Swago Creek basin—caves, underground drainage and present flow routes.	130
5.3 Swago Creek basin—surficial flow during Stage 1.	132
5.4 Swago Creek basin—karst development during Stage 2.	134
5.5 Barnes Pit Cave.	137
5.6 Swago-Carpenters Caves.	140
5.7 Results of the flood and dye test.	143
5.8 Hause Waterfall Cave.	145
5.9 Overholts Blowing Cave.	147
5.10 The stream passage near the entrance to Overholts Cave.	148
5.11 The Bypass Passage near the entrance to Overholts Cave.	148
5.12 The stream passage in Overholts Cave.	149

	<u>Page</u>
5.13 The real and modelled hydrographs for Swago Creek.	160
6.1 Locust Creek basin—topography, surficial drainage and location of caves.	169
6.2 Locust Creek basin—high water sink points.	171
6.3 Locust Creek basin—low water sink points and caves.	173
6.4 Hills-Bruffey Cave.	175
6.5 Cutlip Cave.	178
6.6 Clyde Cochrane Cave.	180
6.7 Snedegars Cave.	182
6.8 Friars Hole.	186
6.9 Friars Hole Cave: the main trunk passage near the downstream end of the cave.	188
6.10 Friars Hole Cave: near the upstream end of the main trunk passage.	190
6.11 Friars Hole Cave entrance series.	193
6.12 Hughes Creek Caves.	195
6.13 Marthas Caves.	197
6.14 Beards Blue Hole.	199
6.15 Poor Farm Cave.	200
6.16 Locust Creek Cave.	202
6.17 Chemical characteristics during the flood pulse test at Locust Creek Cave.	205
6.18 Locust Creek basin—surficial flow during Stage 1.	207
6.19 Long profile of Hills Creek, the Cherry River and the Friars Hole valley.	209
6.20 Locust Creek basin—initial underdraining of the valleys during Stage 2.	211
6.21 Locust Creek basin—piracy of the Hills drainage to Locust Creek during Stage 3.	216

	<u>Page</u>
6.22 Locust Creek basin—capture of the Clyde Cochrane and Rush Run drainage during Stage 4.	219
6.23 Locust Creek basin—the three segments used in the model.	223
6.24 The real and modelled hydrographs for Locust Creek.	225
7.1 The Spring Creek basin—topography and drainage.	230
7.2 The Spring Creek basin—major sub-basins, towns and cave locations.	232
7.3 Cross section across the "Great Savanna" region.	235
7.4 Spring Creek basin—surficial flow during Stage 1.	239
7.5 Spring Creek basin—initial underdraining of the valleys during Stage 2.	241
7.6 Stream profiles and competence of Hills, Spring and Culverson Creeks near the sink points.	243
7.7 Boulders moved during the Camille Flood in August 1969.	244
7.8 Spring Creek basin—major diversions.	247
7.9 The real and modelled hydrographs for Spring Creek.	252
7.10 The real and modelled hydrographs for Wildcat Cave.	255
8.1 The caves developed above and below the Taggard shale.	269
8.2 Relationship between the peak objective function and the ratio of the flows.	281
8.3 Relationship between the percentage overland flow, interflow and baseflow to the limestone area in each segment.	287

LIST OF TABLES

	<u>Page</u>
1.1 Comparison of the Swago, Locust and Spring Creek Basins	12
2.1 Fluorometer Readings for Mixtures of Fluorescein and Rhodamine Dyes	28
2.2 Average Number of Spores per Slide from Background	49
2.3 Average Number of Spores per Slide After 27 Days	49
3.1 Comparison of Rainfall from Existing Climatological Stations in the Valleys and from a Temporary Station in the Hills	68
3.2 Average Precipitation Calculated for Locust Creek	73
3.3 Weights Used to Obtain Basin Precipitation from the Climatic Station Figures	74
3.4 Monthly Streamflow	79
4.1 List of Parameters Used in the Model	91
4.2 Comparison of Recorded and Simulated Flows Using OPSET on the Elkhorn Creek, Kentucky	119
4.3 Results of Sensitivity Analysis	123
5.1 Comparison of the Real and Modelled Pool Areas and Spillway Widths in Swago Cave.	144
5.2 Sensitive Parameter Values Used at Swago Creek	162
6.1 Geological Section of the Upper Part of the Greenbrier Limestone at Julia, and Comparison with the Passages in the Snedegars and Friars Hole Systems	184
6.2 Sensitive Parameter Values Used at Locust Creek	227
7.1 Hydraulic Straight Line Gradients from Various Caves to Spring Creek, Fort Spring and Mill Creek	249
7.2 Sensitive Parameter Values Used at Spring and Wildcat Creeks	253

	<u>Page</u>
8.1 Characteristics of the Basin Development	259
8.2 Orientation of Drainage Routes During Stages B to D	264
8.3 Hydraulic Straight Line Gradients of the Routes in the Swago, Locust and Spring Creek Basins, from Various Sinks to Nearby Resurgences.	273
8.4 Parameter Values Used in the Model which were Constant for all Segments in all the Basins	276
8.5 Comparison of the Sensitive Parameter Values at the Four Basins	277
8.6 Comparison of the Objective Functions for Selected Periods in the Four Basins	279
8.7 Summary of the Objective Functions and Water Balances for the Four Basins	285

CHAPTER I

INTRODUCTION

Carbonate rocks outcrop over approximately ten percent of the earth's surface (Sanders and Friedman, 1967). Karst areas, where the landforms are developed predominantly by solution, occur principally upon limestones, which are the most common carbonate rocks. Although not all limestones develop into karst, several percent of the earth's surface is karstified.

In karst regions, the majority of streams flow underground for at least part of their courses, thus creating a large recharge to the ground water reservoir. Due to the development of solutional conduits and channels, limestones can have extremely high permeabilities. For example a permeability of 250,000 Meinzers (gallons/day/square foot) has been quoted for a limestone aquifer (Meinzer, 1949), which is larger than any other permeability measured by the U.S.G.S. The permeability of other rocks varies widely but, by comparison, an aquifer with a permeability of over 20 Meinzers is considered to have a good yield (Todd, 1959).

The high ground water recharge and high permeabilities in limestone areas leads to the formation of large springs. Over half of the First Order springs, which are defined as having an annual average discharge of at least 100 cfs. (cubic feet per second), occur in limestone regions (Meinzer, 1927).

Due to the large permeabilities, high recharge to the ground water,

and widespread outcrop, limestone aquifers are important sources of water. However limestone hydrogeology is still in its infancy, as White and Schmidt (1966) state:

"The study of ground water in karsted terrain is beset with problems. In general, efforts to understand karst hydrology have been much less successful than efforts to understand ground water in other types of aquifers."

This study was undertaken to contribute to the knowledge of karst hydrogeology.

1.1 Paleohydrology

All basins develop in the course of geological time. Karst basins can develop in very complex ways, and evidence for the former modes of development are often preserved in the form of caves. From a study of the hydrological conditions existing in the past, inferences about the probable mode of development in the future can be made.

The future hydrology of a karst region can be adversely modified by the intervention of man. The construction of dams in karst regions has often been beset with difficulties (e.g. Barwell and Moneymaker, 1950; Hantush, 1955) and several dams and reservoirs in karst regions have had to be abandoned due to leakage. The leakage often does not develop for several years due to the karst conduits from the reservoir being opened up slowly by the water flowing through them. For example the Lake Cumberland Dam in Kentucky is being re-grouted now at an estimated cost of \$64 million. It is the second re-grouting in its twenty year history.

The dam is an earth filled structure on limestone which has developed (evidently) significant and dangerous cavernous flow within the past ten years or so.

In areas without extreme man-made modifications the karst hydrology is still in a state of flux, with diversions and piracies continuing as the basin develops. Although the development is slow, significant natural changes can occur in a lifetime. Catastrophic changes can take place overnight. Springs can form or dry up, streamflows can increase or decrease, lakes can appear or disappear, and well levels can change, as the basin develops naturally. The effects on the water users and local residents can be extreme. Studies of the development of karst basins are therefore important, and were carried out as part of this study.

1.2 Objectives of the Study

The present study was undertaken to gain a better understanding of karst hydrology. In particular the following objectives were set:-

- a) To choose and study in detail a number of small karst basins. In these basins the present day hydrology and cave and conduit flow characteristics were to be determined in as much detail as possible.
- b) To quantify the hydrology in the basins by using a model to simulate the streamflow using climatic input data.
- c) From the model parameters some predictions of the type of inaccessible flow paths were to be made. This objective was not fully met as the model parameters could not be defined with sufficient accuracy

to allow detailed predictions to be made of all the flow paths.

d) To determine the paleohydrology, and to use this information to predict the future hydrology of the basins. The paleohydrology had to be considered when the present day flow paths were being determined.

e) To determine the mode of formation of all the accessible caves in the basins. This information was needed to predict the paleohydrology of the basins.

1.3 Choice of Study Area

As one of the objectives of the project was to study a real basin, it was necessary to choose a field area where this could be done. A number of criteria limited the choice of field areas, and these were the following:-

a) As part of the study was to determine the quantitative hydrology of the chosen area, it was necessary to instrument that area, particularly to collect streamflow data. Visits to the field would therefore have to be made regularly for two or three years. The field area therefore had to be readily accessible from Hamilton.

b) The proposed study required extensive knowledge of the cave systems and of the karst hydrology. To gain this knowledge, much field work must be undertaken. By choosing an area which had been previously studied and well documented, a considerable amount of extra field work would be saved.

c) The karst should be well developed. This usually occurs when the limestone is fairly pure and thick. Unless the karst is well developed,

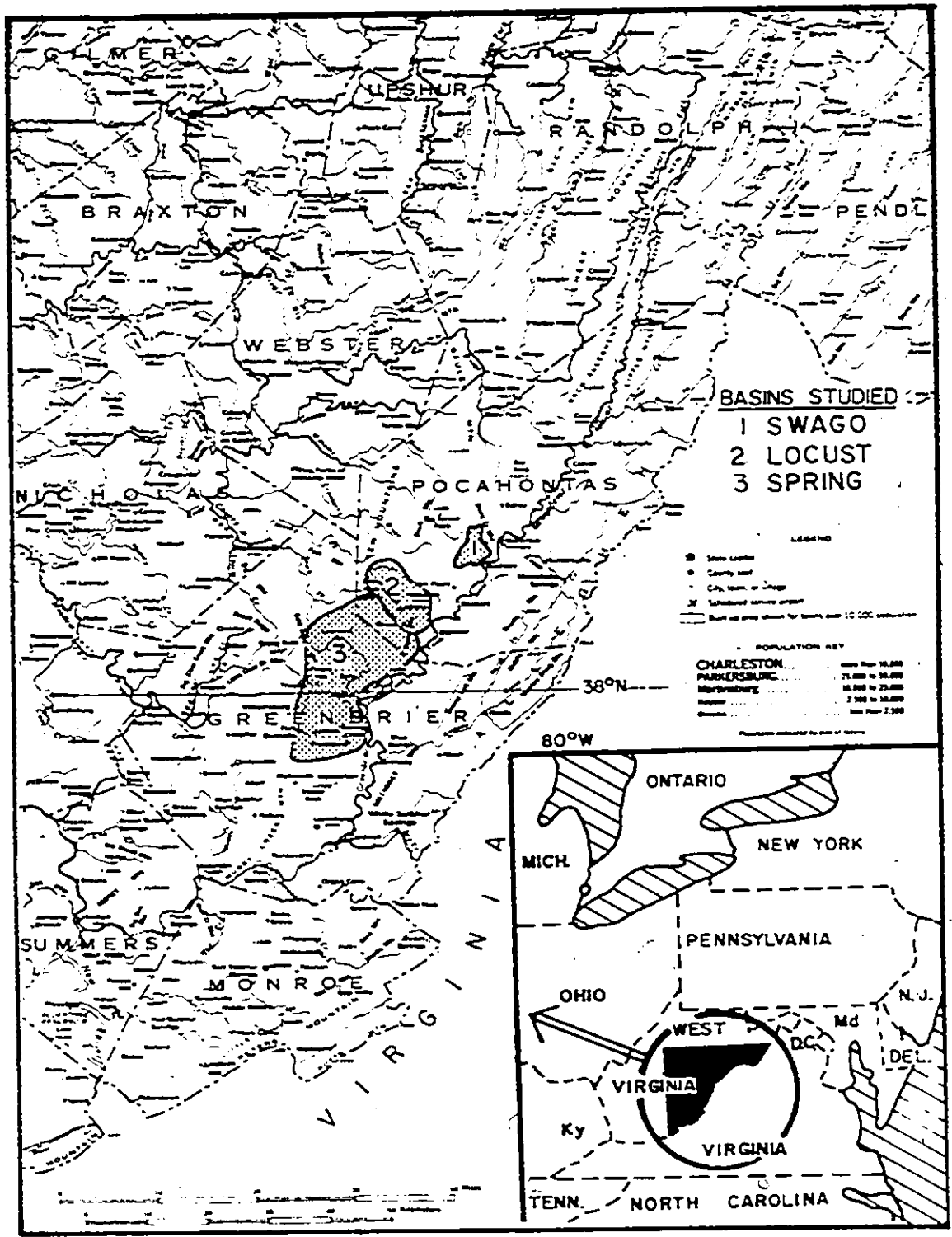


Figure 1.1 Map of Eastern West Virginia showing the basins studied.

caves are not common and a study of the former flow patterns is trivial.

d) As the study involved cave genesis and paleohydrology, an area that had varied types of karst development would allow comparisons to be made of the effects of karstification on the hydrology. One aspect of the study was to predict the type of inaccessible cave passages from a study of the hydrology. A variety of cave passage types was needed to achieve this prediction, so a field area containing a variety of karst development was needed.

Exposed karst areas occur widely in North America, with the exception of the Prairies and the Canadian Shield. Karst areas in Canada are not well developed (in the east) or are too inaccessible (in the Rockies), and prior to 1969 even these areas had not been extensively studied. In the United States the only areas that were suitable, on the basis of the above criteria, were the Mammoth Cave area in Kentucky and the West Virginian karst.

The area in West Virginia (Figure 1.1) was chosen as it was slightly more accessible than the Mammoth Cave area, and had a more varied relief and thus a more varied karst development. In West Virginia, the karst is developed down a belt parallel to the Allegheny Front (Figure 1.2). The area in Pocahontas and Greenbrier Counties has been extensively studied, and for this reason was adopted as the field area.

1.4 Description of the Study Area

The study area lies in the valley of the Greenbrier River in Pocahontas and Greenbrier Counties, West Virginia (Figure 1.2). This

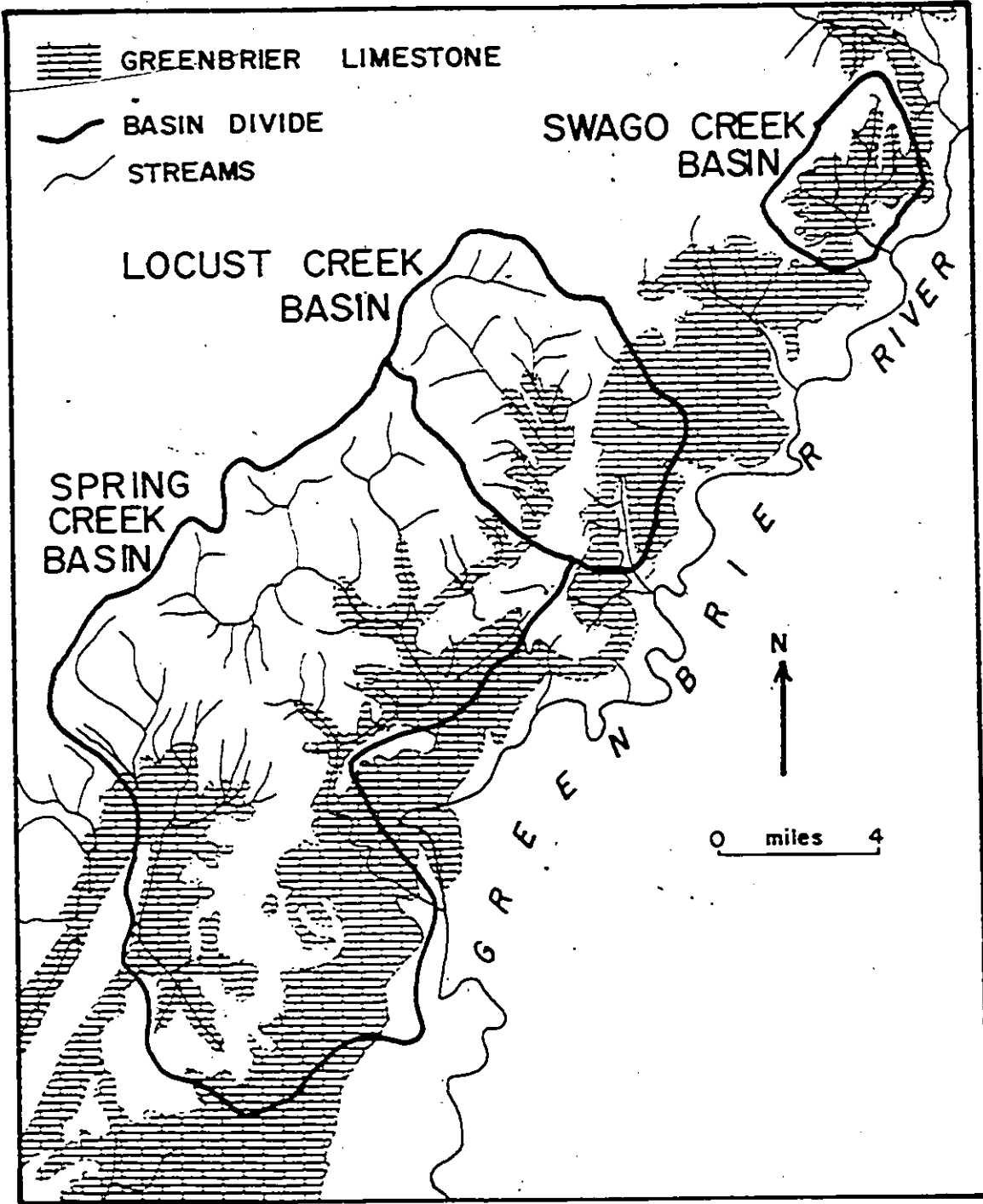


Figure 1.2 Map of the study area.

area is covered by the 15 minute topographic quadrangle maps of Marlinton, Lobelia, and White Sulphur Springs, and by small parts of the Mingo, Clintonville, and Rockwood maps. The 7½ minute quadrangle maps of this area have not yet been published.

In this region, limestone outcrops in a belt 2 to 10 miles wide, parallel to and just west of the Greenbrier River. High ground above the limestone outcrop is developed on clastic rocks. Many streams flow from the clastic hills, sink through the Greenbrier limestone, and resurge at the contact with an underlying shale formation. The limestone, particularly in the south of the area, has well developed, classic karst features upon it (Figure 1.3), including sinkholes, uvalas, blind valleys, sinking streams and caves. There are very few permanent surface streams running on the limestone, although a number of small streams are perched upon alluvium and flow intermittently.

This area has a humid temperate climate, with mean precipitation in the valleys of about 46 inches a year (Thorntwaite, 1955). The mean annual temperature at the lower elevations is about 55°F, dropping to 45°F on the hills. The climate is discussed in more detail in Section 3.1.

Three contrasting basins were picked for detailed study on the basis of relief. Swago Creek is a high relief basin, Spring Creek a low relief basin, and Locust Creek of moderate relief. Stream profiles for the main stream channels for the three basins are shown in Figure 1.4, from which their contrasting relief can be seen. A comparison of some of the topographic, morphologic and geologic characteristics of the three basins is shown on Table 1.1. The basins are described in the following sub-sections.



Figure 1.3 View of the karst near Snedegars Cave at the northern end of the Spring Creek basin.

1.4.1 Description of the Swago Creek Basin

This is the most northerly and smallest basin (Figure 5.1). It has the highest relief of the three examples and a geographic area of 12.0 square miles above the gauge, of which 42% is outcropping limestone, 9% underlying McCrady shale, with the rest being overlying clastic rocks. Several streams run off the hills, sink through the limestone and resurge at the two major springs—Cave Creek and Overholts Spring. In high water the streams off the hills can inundate the sinks and flow over the surface down the normally dry streambeds of Dry Creek, Swago Creek, Overholts Run and McClintocks Run (Figure 5.1). In the Swago basin the ground water shed follows the topographic divide fairly closely, except in the headwaters of Dry Creek, where the uppermost sink, draining 1.1 square miles, flows beneath a ridge to Price Run resurgence, which is outside of the basin.

The gauge at Swago is set on the McCrady shale and is at an altitude of 2150 feet. The peaks enclosing the basin rise to 4700 feet within two miles of the gauge. Because of the high relief, steep slopes and consequent rapid erosion, karst features other than caves are not well developed in the Swago basin.

1.4.2 Description of the Locust Creek Basin

The Locust Creek basin is the intermediate basin in size, relief, and position. The topographic divide of Locust Creek is considerably

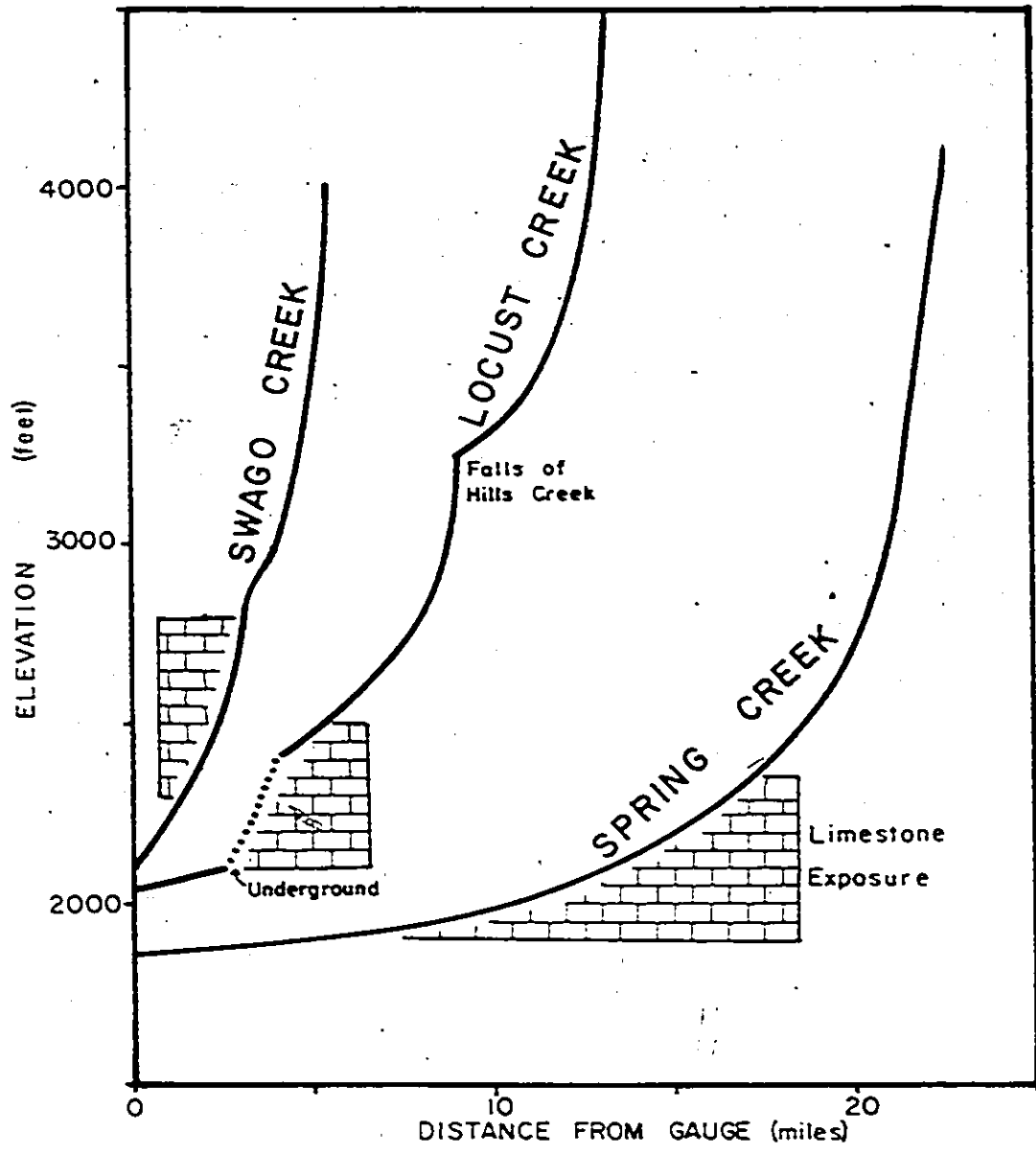


Figure 1.4 Stream profiles for Swago, Locust and Spring Creeks.

Table 1.1Comparison of the Swago, Locust and Spring Creek Basins

	<u>Swago</u>	<u>Locust</u>	<u>Spring</u>
Groundwater Basin Area (sq. mi.)	10.1*	37.4	129
Topographic Area (sq. mi.)	12.0	5.5	130
Lowest Point in Basin (feet)	2150	2070	1855
Highest Point in Basin (feet)	4700	4525	4518
Relief (feet)	2550	2455	2663
Major Stream Length (miles)	5.5	16**	35
Average Channel Slope (%)	8.8	2.9	1.44
Stream Order (Strahler, 1962)	3	4**	5
Exposed Mauch Chunk and Overlying Rocks in the Basin (%)	49	72	62
Exposed Greenbrier Limestone in Basin (%)	42	27	37
Exposed McCrady Shale and Underlying Rocks in Basin (%)	9	1	1

*This area increases during floods to 12 square miles.

**With an assumed straight line connection between Hills and Locust Creeks.

different in size from the ground water shed, as the topographic area above the gauge (Figure 6.1) is only 5.5 square miles while the drainage area is about 37 square miles. Locust Creek has captured the drainage of the Hills and Bruffey Creeks as well as the Little Levels drainage (Figure 6.1), none of which drain to Locust Creek on the basis of the topography. Locust Creek, therefore, flows from an under-sized spring and down an underfit river valley (Figure 1.5).

Basin elevation ranges from 2070 feet at the stream gauge to 4525 feet on Kennison Mountain. The major portion of the basin (72%) has the Mauch Chunk and younger rocks exposed, while only 27% of the basin has outcropping limestone, and about 1% exposed McCrady shale. The dry valley below Hills Creek and the limestone plateau south of Hillsborough have well developed karst features on them, such as uvalas and many sinkholes.

1.4.3 Description of the Spring Creek Basin

Spring Creek is the largest, most southerly and lowest relief basin of the three (Figure 7.1). The basin has developed into a more mature karst area than the northerly basins, with a classic sinkhole plain (Watson, 1966; Miotke and Palmer, 1972) formed in its southern part. This sinkhole plain contains numerous uvalas, sinkholes and dolinas. The drainage divide is not well defined on the sinkhole plain although a number of stream tracings allow an estimation of its position to be made. The drainage divide for the basin is of similar size (130 square miles) to the topographic divide, but of different shape. Culverson Creek, which



Figure 1.5 The Locust Creek valley in winter. The Locust spring is at the head of this valley below the photographer.

formerly flowed down the Great Banana valley (Wolfe, 1974), has been captured by Spring Creek, while the Hills-Bruffey drainage has been captured away from the Spring Creek drainage.

The basin relief is 2663 feet (Table 1.1), comparable to the relief of the other basins, but due to the larger size of the basin the average channel slope is considerably less than at Swago or Locust. In the Spring Creek basin about 37% of the area has outcropping limestone.

1.5. Bedrock Geology

The geology of the region is fairly simple, with the regional dip of the beds being about 5° to the west-north-west. The Greenbrier River flows southeastwards along the strike, and marks the approximate division between Devonian strata to the east of the river and the Mississippian strata to the west.

The succession in this part of West Virginia is shown in Figure 1.6. The uppermost beds exposed in the basins are the Pottsville Series (Pennsylvanian). They consist of interbedded sandstones and shales containing some coal formations which are stripmined in parts of the Spring Creek basin. The Pottsville only outcrops on the hilltops of the basins.

Below the Pottsville is the Bluestone, Princeton and Mauch Chunk Series (Mississippian), which consist of about 2300 feet of sandstones and shales, containing some thin beds of coal and limestones. The limestones are impure, non-cavernous, and disrupt the surface streams very little.

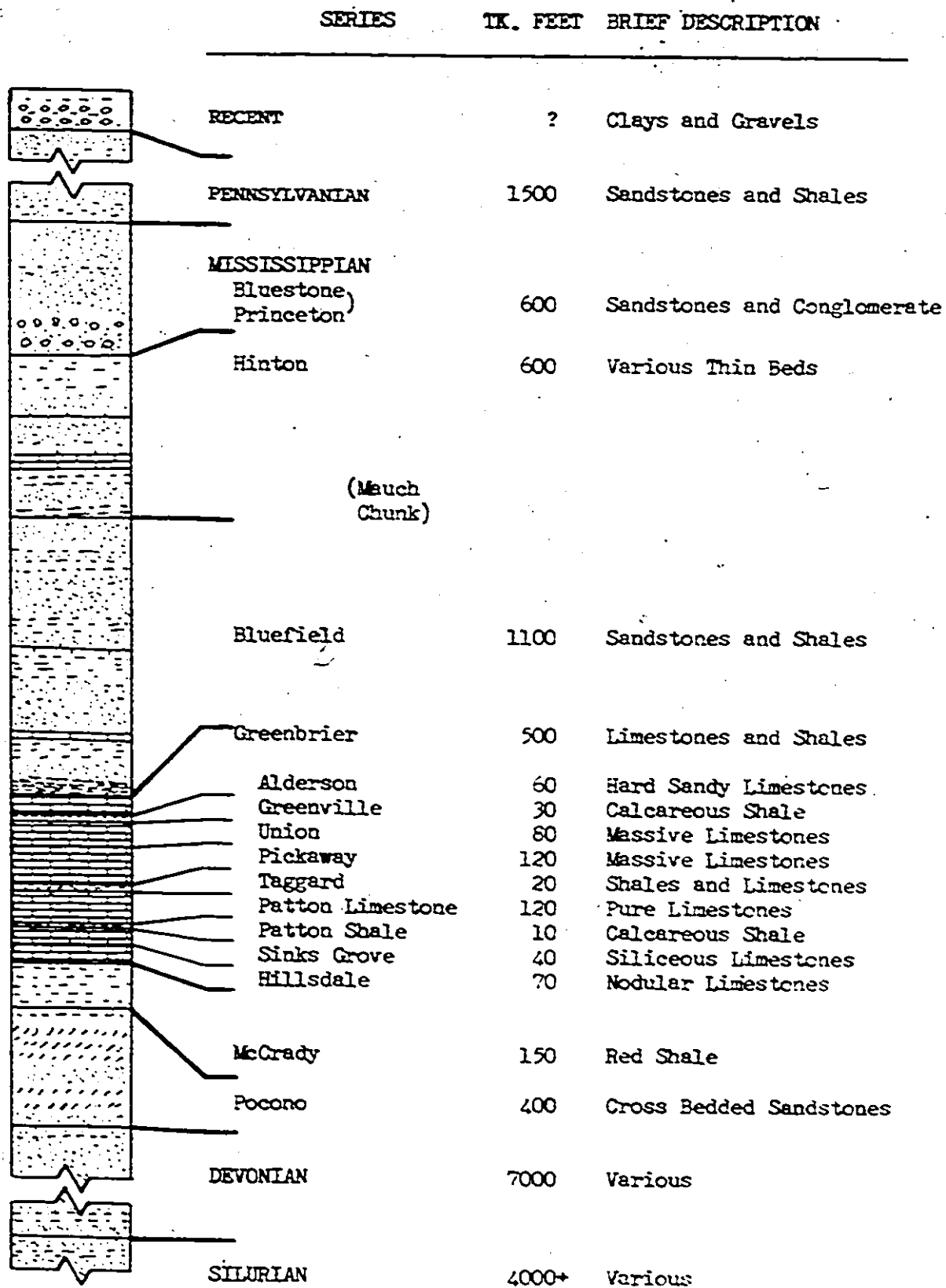


Figure 1.6 General columnar section of the geology of the field area in West Virginia.

Most of the streams in the basins have their headwaters in the Mauch Chunk Series, flow as surface streams onto the Greenbrier limestone where they sink, to resurge at the base of the limestone. The lowest bed of the Mauch Chunk Series is the Lillydale shale, which is a greenish-grey impervious shale fifty feet thick. Boulders and pebbles of the Lillydale and of the other upper members of the Mauch Chunk are common in the Greenbrier limestone caves, and in the dry streambeds on the limestone.

The Greenbrier limestone forms the important aquifer for this study and has developed, particularly to the south, heavily karsted topography. The limestone has been sub-zoned into nine units which include three shale bands. The limestone as a whole is about 450 feet thick at Swago and thickens to 650 feet at the southern end of the Spring Creek basin, while the interbedded shales thicken to the north. The shales therefore influence the hydrology far more at Swago than further south.

The uppermost unit, the Alderson limestone, is a 40 to 50 foot thick, bluish limestone containing some minor interbedded shales. At Swago no caves are known in the Alderson, although some of the streams sink through it to resurge on the underlying shale. In the Spring and Locust Creek basins however, several caves are known in this limestone and a few streams sink into it and breach the underlying Greenville shale.

The Greenville shale is a brown, calcareous shale, commonly 20 feet thick but locally absent in the south, and thickening to about 30 feet at Swago. It functions as an efficient aquiclude at Swago, but is more easily breached to the south.

The Union limestone is the most massive and pure member of the

Greenbrier Series. It is from 100 to 150 feet thick, gray to dark gray in colour, but weathering white and containing many marine fossils.

The underlying Pickaway limestone, from 100 to 130 feet thick, is similar to the Union but is less pure, less soluble and contains fewer fossils. In much of the area the lower part of the Pickaway contains many shale bands which have influenced cave development, particularly in Carpenters and Snedegars Caves (Sections 5.2.4 and 6.2.4). Together the Union and Pickaway constitute the most important cave forming section in the region. The Union is particularly soluble, and most of the shafts and avens within the caves occur in it.

The Taggard formation consists of grey oolitic limestones interbedded with red shales, which are thicker and more persistent in the north. At Swago the formation is relatively impervious, so that several streams resurge at the top of it, to sink again into the top of the underlying Patton limestone. Some caves at Swago do break through the shales, but its presence is generally indicated by perched horizontal galleries, often with pitches immediately below the shales. Farther south the Taggard is more calcareous and less disruptive to the hydrology and cave formation.

The Patton shale is found only at Swago. It is calcareous and only 5 feet thick, and does not perch the water at all. The Patton, Sinks Grove and Hillsdale limestones are all similar, consisting of blue, massive, fossiliferous limestones containing a few chert nodules. They are together about 200 feet thick in the Spring Creek area, and about 220 feet thick at Swago.

The red McCrady shales and sandstones underlie the limestones and act as an aquiclude throughout the region, with all of the resurg-

ences coming out on top of this shale. The McCrady is about 50 feet thick, and lies unconformably on the Pocono Series which are the lowest beds of the Mississippian. In a number of caves in the region, particularly to the south, streams have cut deep vadose trenches into the McCrady shale by mechanical erosion.

In all three of the basins under study, the stream gauges were set up on the McCrady shale. At Swago the gauge was on McCrady bedrock, while at Locust and Spring the sites were on alluvium, which from nearby exposures was estimated to be less than five feet thick. The flow of ground water through the alluvium on the shale was considered to be negligible.

1.5.1. Superficial Deposits, Soils and Vegetation

In this part of West Virginia the superficial deposits are generally thin or absent. Along the valleys of Spring, Hills and Locust Creeks and the Greenbrier River, there are thin deposits of alluvium. A major deposit of alluvium, which is at least 165 feet thick (Wolfe, 1973), is present in the lower part of the Roaring Creek valley (Figure 7.1).

The soils belong to the Grey-Brown Podzolic soil group (Vessel, 1939), which is the major soil group in the northeastern United States (Strahler, 1963). There is a contrast between the soils developed over the limestone and those developed from other parent material. On the limestone, the Frederick or Hagerstown soils (Vessel, 1939) are developed which, although often thin, are relatively productive and are often

cultivated if the relief is not too steep. The Westmorland soils, developed on the Mauch Chunk Series, are poorer and are unsuitable for agriculture. In addition, the relief is usually steep, thus limiting cultivation.

The natural vegetation in the valleys of the area is eastern deciduous forest, which includes maples, oaks, basswood, black walnut and cherry (Price and Heck, 1939). In the hills above 4200 feet, spruce becomes more common than the deciduous trees (Darlington, 1943), and a transitional forest of hard and softwoods grows between the elevations of 3000 and 4200 feet. Much of the forest on the limestone area has been cleared for agriculture, and in most places the present edge of the forest matches the top of the Union limestone very closely. Lumbering has been carried on in most of the forests, and nearly all the black walnuts and other fine hardwoods have been taken out. Extensive areas were clear cut near the turn of the century and are now in second growth.

1.6 Previous Work

Previous work of the geology of this part of West Virginia includes the publications by the West Virginia Geological Survey. Price and Heck mapped the geology of Pocahontas and Greenbrier Counties (Price, 1929; Price and Heck, 1939). McCue and Lucke (1939) described the limestones in more detail. Little work on the karst of West Virginia was published until the late 1950's when cavers started to explore the caves in the region. Most of the caving was done by members of the Pittsburgh, Nittany and Baltimore Grottos, all member clubs of the National Speleological

Society, and the results of their work are to be found in their publications—The Netherworld News, the Nittany Grotto Newsletter, and the Baltimore Grotto News—as well as in the N.S.S. News and Bulletin.

Davies (1958 and 1965) collected together the information on the caves and associated karst features in West Virginia, and described many of the caves studied in this work.

Wolfe (1962 and 1964) discussed the development of the caves in Pocahontas County, West Virginia. He found that many of the major horizontal passages in the caves were developed at certain elevations, and considered four factors which could control the passage development. The factors were the following: structural control, erosion level control, water table control, and lithologic control. He concluded that a major erosion level, called the Harrisburg Peneplain, appeared to be the key factor in the development of the major horizontal cave passages.

White and Schmidt (1966) have studied the caves and karst in this area, particularly in the Swago and Locust Creek basins. They have delineated much of the drainage in the basins and have stressed that the underground or true drainage divides are totally different from the topographic drainage divides in this region. These authors also described the influence that the Taggard shale has had on the local hydrology, causing what are termed "lost waterfalls" when the streams resurge above the Taggard, flow over the shale, and sink as soon as they reach the underlying limestone.

Jones (1973) has studied the limestone hydrology in Greenbrier County, which includes the southern part of the Spring Creek basin. He determined the drainage divides in the region on the basis of dye tracing

work and cave maps. He described and studied the "contact" caves along the eastern edge of the limestone outcrop as well as the other major caves in Greenbrier County. Jones, however, did not discuss in any detail paleohydrology or the evolution of the caves.

CHAPTER II

FIELD RESEARCH TECHNIQUES

A number of conventional field techniques were used to aid in this study. These included the following: the establishment of gauging stations on the major streams; mapping accessible cave conduits; tracing the paths of inaccessible sinking streams to define drainage divides; measurements of flood pulses and variations of water chemistry in order to categorize the inaccessible flows; and the establishment of erosion sites to estimate the age of the caves.

2.1 Stream Gauging

The streams in the region were gauged using conventional current meter and dye dilution techniques. All stage recorder sites were rated using a current meter. Dye dilution was also used to check the discharge of Swago Creek, and to measure the discharge in some smaller streams.

2.1.1 Current Meter Gauging

In shallow streams during low flows, a Price-type current meter was mounted on a rod and the gauging done by wading. At Spring Creek, and at times of higher flows in the other streams, the meter was supported on a wire from a bridge. The wire was weighted with a 40 pound block of

iron. The bridge used at Swago Creek was 200 yards downstream of the stage recorder, at Locust Creek was 50 yards upstream, and at Spring Creek the nearest bridge was almost one mile downstream from the recorder. Care was taken not to measure the discharge when the stage was changing rapidly, in order to prevent hysteresis type errors.

Between fifteen and twenty measurements of current velocity were made across each stream at 0.6 of the depth below the water surface. About twenty revolutions of the impellor were timed, after letting the meter settle down for half a minute or so. Calculations of the discharge were by the standard midsection formula method (Church and Kellerhals, 1970) assuming that velocity varies linearly between verticals. No tests of errors were made but it is probable that 95% of the measurements of discharge are accurate to $\pm 8\%$ (Carter and Anderson, 1963). The current meter stream gaugings were used to develop the rating curves shown in Figures 3.5 to 3.7.

2.1.2 Dye Dilution Gauging

Dye dilution gauging was applied at the Swago, Fullers and Wildcat streams. Both slug and constant injection techniques were used, using Rhodamine WT dye.

The principle of dilution gauging is to insert a known amount of tracer into the stream and to allow it to mix thoroughly with the water. The observed dilution of the tracer then gives the discharge of the stream directly. The concentration of the dye in surface streams is usually kept below the visibility limit (10 ppb, Turner (1968)) to prevent upsetting local residents and to prevent dangers to health from

ingestion of the dye. At these low concentrations the dye is detected and measured using a calibrated fluorometer, which is described in Section 2.1.2.1.

During dye dilution gauging it is important that the dye becomes thoroughly mixed with the stream water. This is best achieved at a waterfall or some other hydraulic discontinuity. If no discontinuities are present, as at Swago Creek, the tracer can be mixed by turbulent flow in the stream. The simple empirical formula for mixing length, from Hull (1962) was used here:

$$L = 50 Q^{\frac{1}{3}} \quad (2.1)$$

where L is the mixing length in feet, and

Q is the discharge of the stream in cusecs.

This formula applies if the dye is injected in midstream and a mixing length 4 times larger used if the dye is injected at the side of the stream. The discharge and mixing time were estimated for use in the formula by timing twigs along the reach. The mixing time is the time taken for the water to flow along the stream for the mixing length. For constant rate dye injection gauging, the dye should be injected for a time greater than the mixing time to assure that steady state conditions have been achieved.

2.1.2.1 Fluorometer Calibration

Dye from a single 50 pound drum of 20% (weight, volume) Rhodamine WT solution was used for all dilution gauging, as it was considered

likely that different drums could have different concentrations of dye. The fluorometer used for the dye tests was calibrated with a sample of dye from this drum.

One (1) ml of the concentrated dye was diluted with distilled water to 100 ml, and a sample of this solution similarly diluted twice more to give a final dilution of 10^6 . From this dilute solution a number of standards were made up, ranging from 1 ppb (part per billion of original dye solution) to 1000 ppb. These standards were run on a Turner Mark III fluorometer using 546-590 filters (Wilson, 1968) at all possible scales. Samples were also run on the x30 scale with a 1% neutral density filter in front of the secondary filters. Graphs were drawn up for the fluorometer scale reading against dye concentrations for the dilution gaugings, and are shown in Figure 2.1.

In addition, the fluorometer was calibrated for the dye Fluorescein, and for mixtures of Fluorescein and Rhodamine. The results of this calibration were used during simultaneous dye tracing tests. The Fluorescein standards were made up by weighing the powdered dye, and mixing it with distilled water to give final standard solutions of 10^{-6} to 10^{-9} gms/ml. These standards, the Rhodamine standards, and mixtures of the dyes were run on the Turner fluorometer using 2A-47B and 2A-12 filters, which are the recommended filters to detect Fluorescein (Wilson, 1968) and also the Rhodamine filters 546 and 590.

The fluorometer readings are shown in Table 2.1. Similar results were obtained with 900 ppb dye concentrations, with the fluorometer readings being approximately 100 times larger.

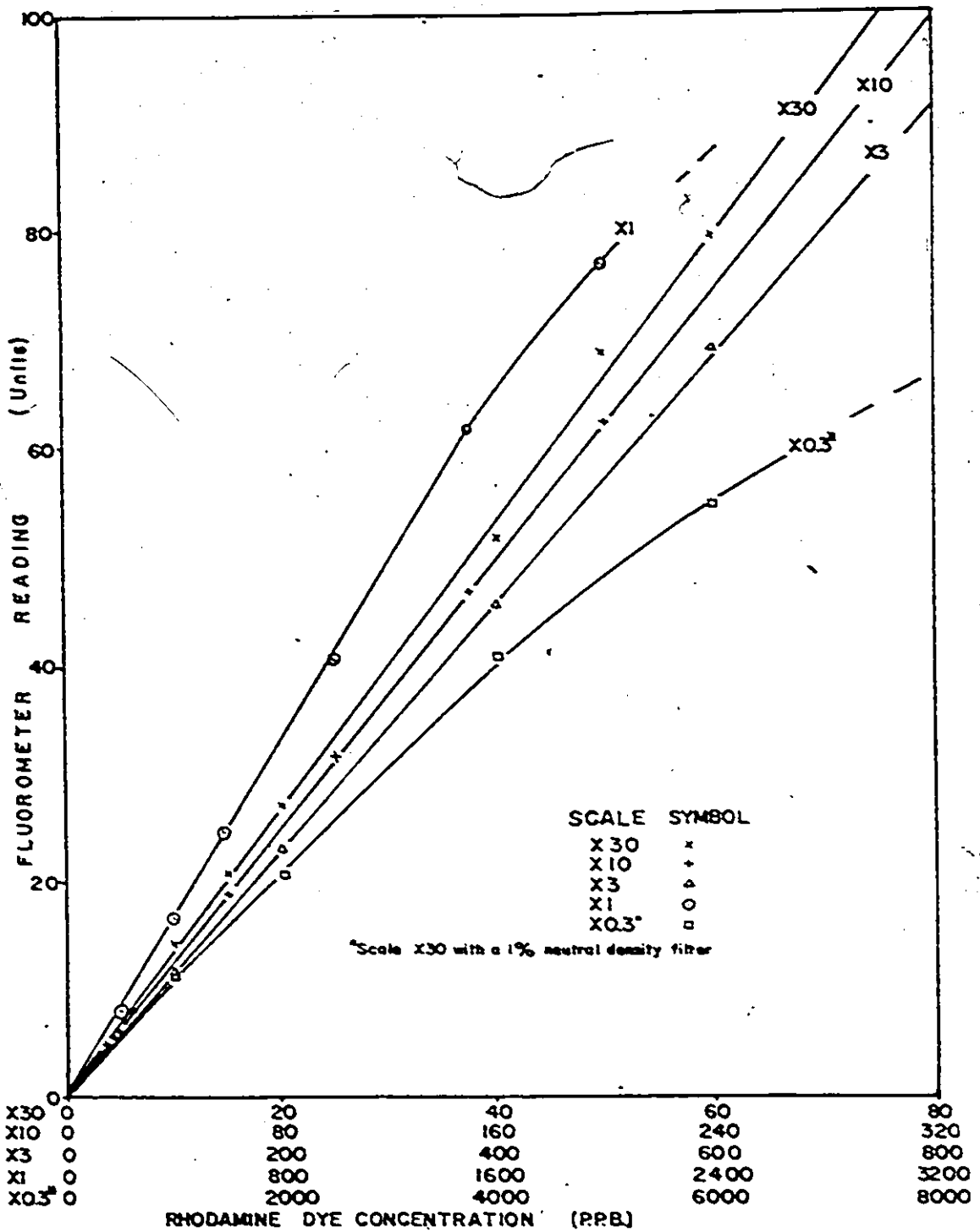


Figure 2.1 Fluorometer calibration curve for Rhodamine dye.

Table 2.1Fluorometer Readings for Mixtures
of Fluorescein and Rhodamine Dyes

<u>DYE</u>	<u>2A-47B and 2A-12 (Filters usually used for Fluorescein)</u>	<u>546 and 590 (Filters usually used for Rhodamine)</u>
Distilled Water	0	0
9 ppb Fluorescein	11	0
50% Mixture	6.7	6.9
9 ppb Rhodamine	2.9	12.0

Turner Model III Fluorometer, scale x30.

It can be seen from the readings that either of the dyes, or a mixture of the dyes, can be distinguished by considering the fluorometer readings using both sets of filters. Aley (1971), however, stated that he was unable to separate the two dyes even using a fluorometer. The reason for his failure to distinguish the dyes is unknown.

It follows from Table 2.1 that if a mixture of dye is tested, which contains \underline{r} ppb of Rhodamine and \underline{f} ppb of Fluorescein, the fluorometer readings will be:

$$MR = 1.3 \underline{r} \quad \text{with the Rhodamine filters, and} \quad (2.2)$$

$$MF = 1.2 \underline{f} + 0.3 \underline{r} \quad \text{with the Fluorescein filters,} \quad (2.3)$$

where MR and MF are the fluorometer readings using the Rhodamine and Fluorescein filters respectively.

From these equations the dye concentrations can be found as:

$$\bar{x} = 0.75 MR \quad (2.4)$$

$$\bar{f} = 0.85MR - 0.19 MR \quad (2.5)$$

These calibration figures were used to interpret the simultaneous dye tracing results.

2.1.2.2 Constant Rate Dye Injection

For the constant rate dye injection method a Mariotte flask (Church and Kellerhals, 1970) was used to continuously inject a solution of Rhodamine WT into the middle of the stream. The flow rate and concentration from the Mariotte flask were adjusted to give a final concentration which was just below visibility in the stream. A sample of the dye being injected was collected for a timed period before and after the injection period. Because the streams were small the dye was injected for considerably longer than the mixing time. While the dye was being injected, stream samples were collected in the stream below the calculated mixing length. Usually several samples were collected across the stream in order to check that good mixing had taken place.

In the laboratory the sample of the dye taken before injection was diluted to 100 ml with distilled water. One (1) ml of this solution was diluted with distilled water to 100 ml, and further diluted 100 to 1 using undyed stream water. This final solution had the same concentration as if the original dye sample had been diluted with 10^6 ml (35.2 cu. ft.)

of stream water. This solution and the stream samples were run on the calibrated fluorometer (Section 2.1.2.1) to find the mean concentration in the stream (C_s) and in the diluted injected dye (C_D). The flow rate in the stream (Q) can then be given by:

$$Q = \frac{C_D}{C_s} \times \frac{35.2}{t} \text{ cfs} \tag{2.6}$$

where t is the time in seconds for which the injected dye sample was collected.

It is also possible to dye gauge two or more stream tributaries simultaneously. The dye is inserted upstream of the junction, and stream samples are taken above and below the junction.

A simultaneous gauging of two streams was carried out at the Overholts and Cave Creek streams on July 23, 1969. These two streams join just north of the village of Buckeye, to form Swago Creek.

The flow rate was estimated by timing twigs and measuring the cross section areas of the streams, and was found to be about 2 cfs. in the Overholts stream and 5 cfs. in the Swago stream. The mixing length was calculated using equation 2.1 at 60 feet for the Overholts stream as the dye was injected in the middle of the stream, and about 350 feet for Swago Creek where the dyed water from Overholts Creek entered at the edge of the stream.

As the streams were small, the concentrated Rhodamine dye was diluted about 100 to 1 before injection, so that a reasonable injection rate could be maintained without appreciably colouring the stream below the gauging site.

The dye was continuously injected into the middle of the Overholts stream about 200 feet above its junction with Cave Creek. A sample of the injected dye was collected for 30 seconds before and after the test. Stream samples were taken in the Overholts stream just above the junction and about 300 feet below the junction in Swago Creek. Several samples were taken across the stream to check for adequate mixing, as the second site was sampled just before the theoretical mixing length.

The concentration of the injected dye sample taken before the test and diluted with 10^6 ml of water was 65 ppb. The sample taken after the test was 68 ppb. The difference between the above two readings was due to slight variations in the injection rate, and the average figure was used in the discharge calculations that follow.

The concentration of samples taken from the stream was 45 ppb in Overholts and 13, 14 and 14 ppb taken from three samples across Swago Creek. Thus using equation 2.6 the discharge at Overholts was:

$$Q_o = \frac{66.5}{45} \times \frac{35.2}{30} = 1.76 \text{ cfs.}, \quad (2.7)$$

and in Swago Creek was:

$$Q_s = \frac{66.5}{13.66} \times \frac{35.2}{30} = 5.71 \text{ cfs.} \quad (2.8)$$

The discharge from the Cave Creek stream must be the difference between the figures:

$$Q_{cc} = 5.71 - 1.76 = 3.95 \text{ cfs.} \quad (2.9)$$

2.1.2.3 Slug Injection

For the slug injection method small bottles were filled in the laboratory with from about one to twenty grams of undiluted Rhodamine WT solution, the dye in each being carefully weighed. At the gauging site one bottle was emptied into the stream, rinsed out, and then several samples of the stream water were collected downstream beyond the calculated mixing length. It was found that most of the dye passed the sampling point in from one-third of, to three times the mixing time. About ten stream samples were collected before the mixing time and ten more after. The samples were run on a calibrated fluorometer and a graph of dye concentration versus time drawn. The area under the graph was measured by counting squares, and the stream discharge can be given by:

$$Q = \frac{w}{\rho \int_0^{\infty} c(t) dt} \quad (2.10)$$

where w is the weight of dye added,

ρ is the dye density,

$c(t)$ is the concentration of dye at time t , and

$\int_0^{\infty} c(t) dt$ is the area under the graph.

The stream entering Fullers Cave was gauged by slug injection. A quantity of 0.8 gms of dye was put into the stream and samples taken every 15 seconds up to $3\frac{1}{2}$ minutes, then every 30 seconds to $4\frac{1}{2}$ minutes, and at $5\frac{1}{2}$ and 7 minutes. The concentrations of the dye against time are shown in Figure 2.2. The area under the graph is 12.5 ppm-minutes, and

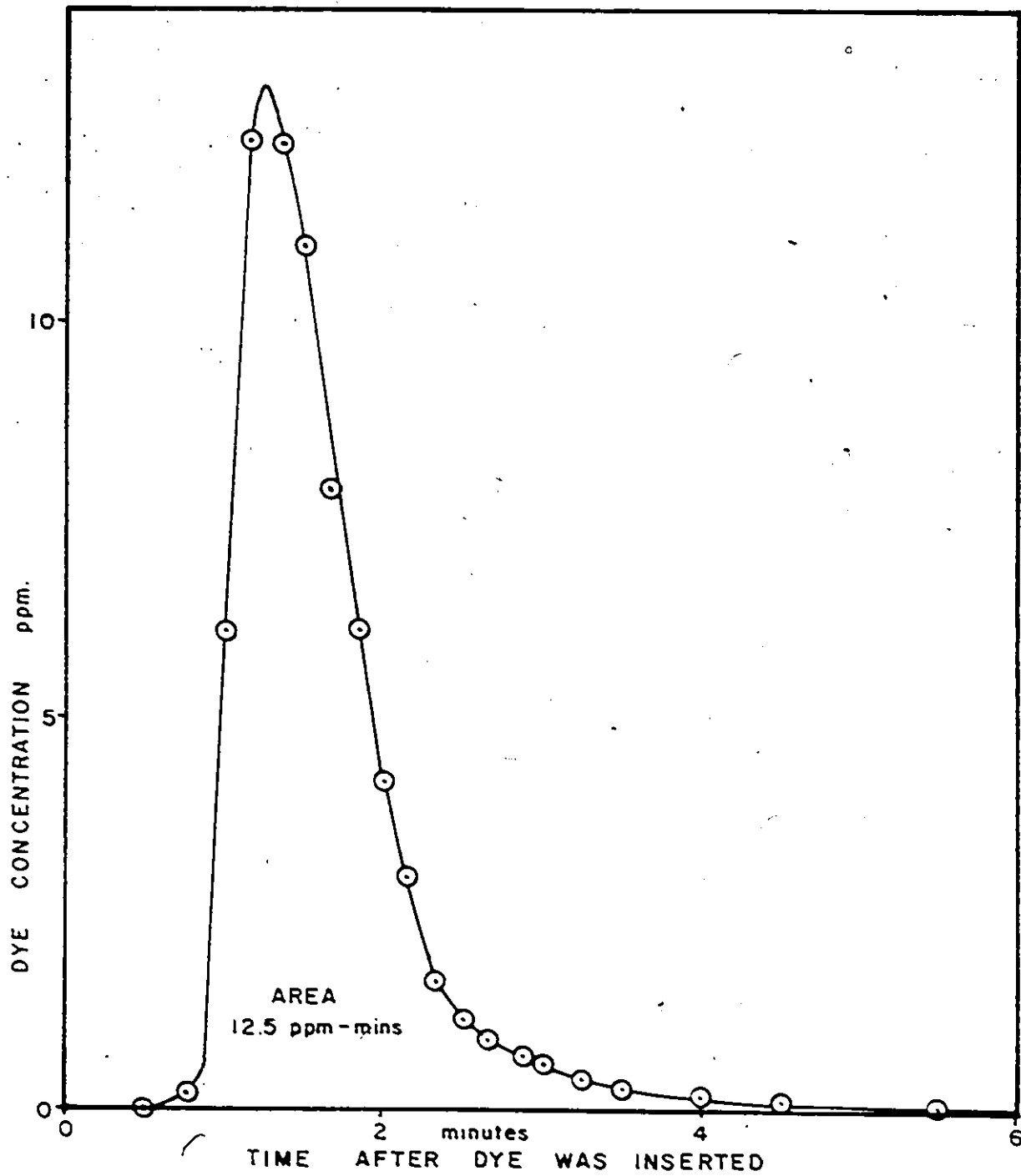


Figure 2.2 Concentration time graph for the slug dye dilution gauging at Fullers Cave.

thus the flow is given by:

$$(2.10) \quad Q = \frac{w}{\rho \int_0^{\infty} c(t) dt}$$

$$= 3.35 \times 10^{-2} \text{ cfs.}$$

as the dye density was 1.12 gms/cm.

The flow was sufficiently small that a bucket was used to test the dye gauging. A flow of 0.0305 cfs. was obtained by timing the filling of the bucket. The lower figure was obtained as not all of the stream flow could be diverted into the bucket.

2.2 Hydrograph Measurements

Gauging sites were set up for the three basins, on Swago, Locust and Spring Creeks, and at Wildcat Cave (Figure 2.3), with staff gauges and stage recorders installed at each site. The staff gauges formed an absolute datum and were used to set up and correct the recorders during the gauging period. The stage recorders were Fisher and Porter series 1540 recorders, on loan from the United States Geological Survey. The output was a two inch wide paper tape, punched with a special decimalized binary code, that can be read by eye or with a reader. With the float pulley that was used the instrument can record up to 100 feet change in stage at 0.01 foot intervals. The recorders were battery driven and a reading was taken every 15 minutes. The recorders were installed in galvanised steel cases, (Figure 2.6), mounted on top of a 3 inch diameter aluminum pipe. The pipes were set in concrete beside the stream with an

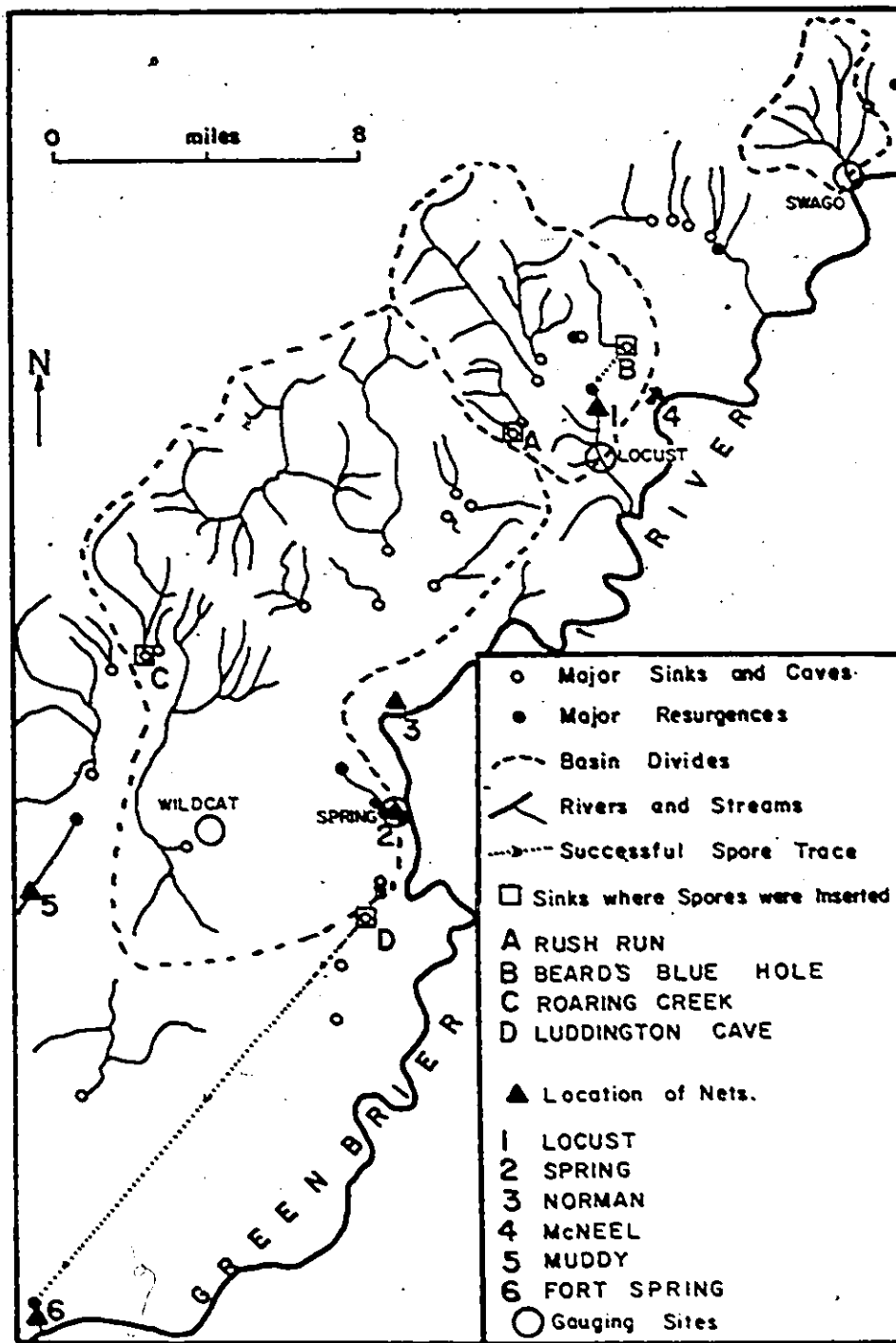


Figure 2.3 Location of gauging sites and resurgences and sinks for the lycopodium test.

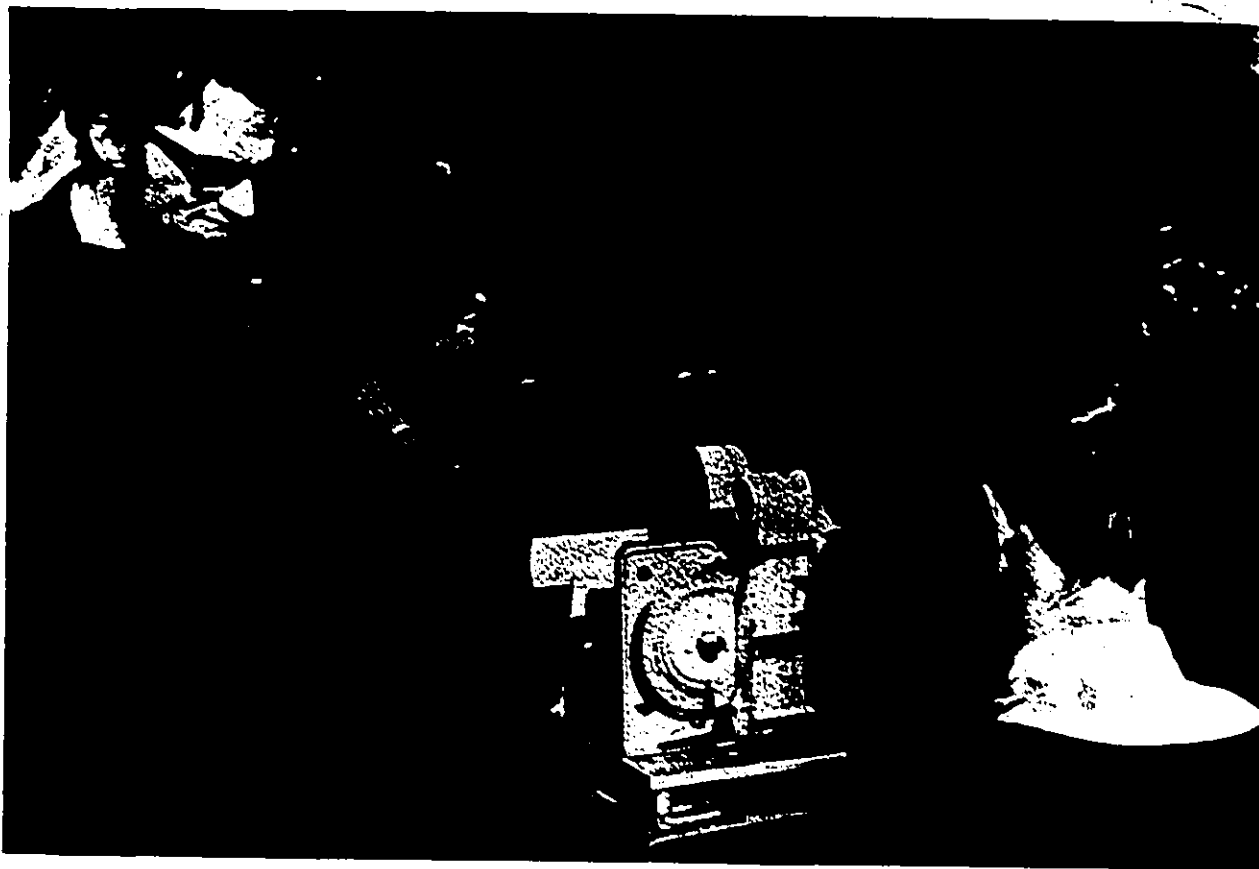


Figure 2.4 The stage recorder at Swago Creek. The paper tape output from the recorder can be seen.

inlet pipe connecting the recorder to the water in the stream. The float for the recorder was $2\frac{1}{2}$ inches in diameter, and floated inside the down pipe.

In winter a layer of about six inches of kerosene was poured into the down pipe to delay freezing of the float. The kerosene raised the level of the float slightly, therefore the recorder had to be corrected relative to the staff gauge, after addition of the kerosene.

2.2.1 Recorder Sites

The Swago gauge was set up behind a garage at Buckeye (Figure 2.3), in a pool just above a small waterfall. The streambed was McCredy shale with a few boulders and cobbles in it, and the lip of the waterfall formed a good control for the site. The garage owner told me that the water level had not risen more than five feet above normal in the last ten years and so the recorder was set up atop a six foot pipe. The recorder is shown in Figure 2.4.

The Locust recorder was set up beside an old mill about three miles below the Locust resurgence. No information was available on flood levels. The recorder was set on a twelve foot pipe concreted beside the stream. The control was a constriction over large cobbles and, as far as could be seen by inspection and by looking at the rating, the control did not shift during the period of gauging.

At Spring Creek the recorder was first set up on a bridge pier half a mile above the junction of Spring Creek and the Greenbrier River.

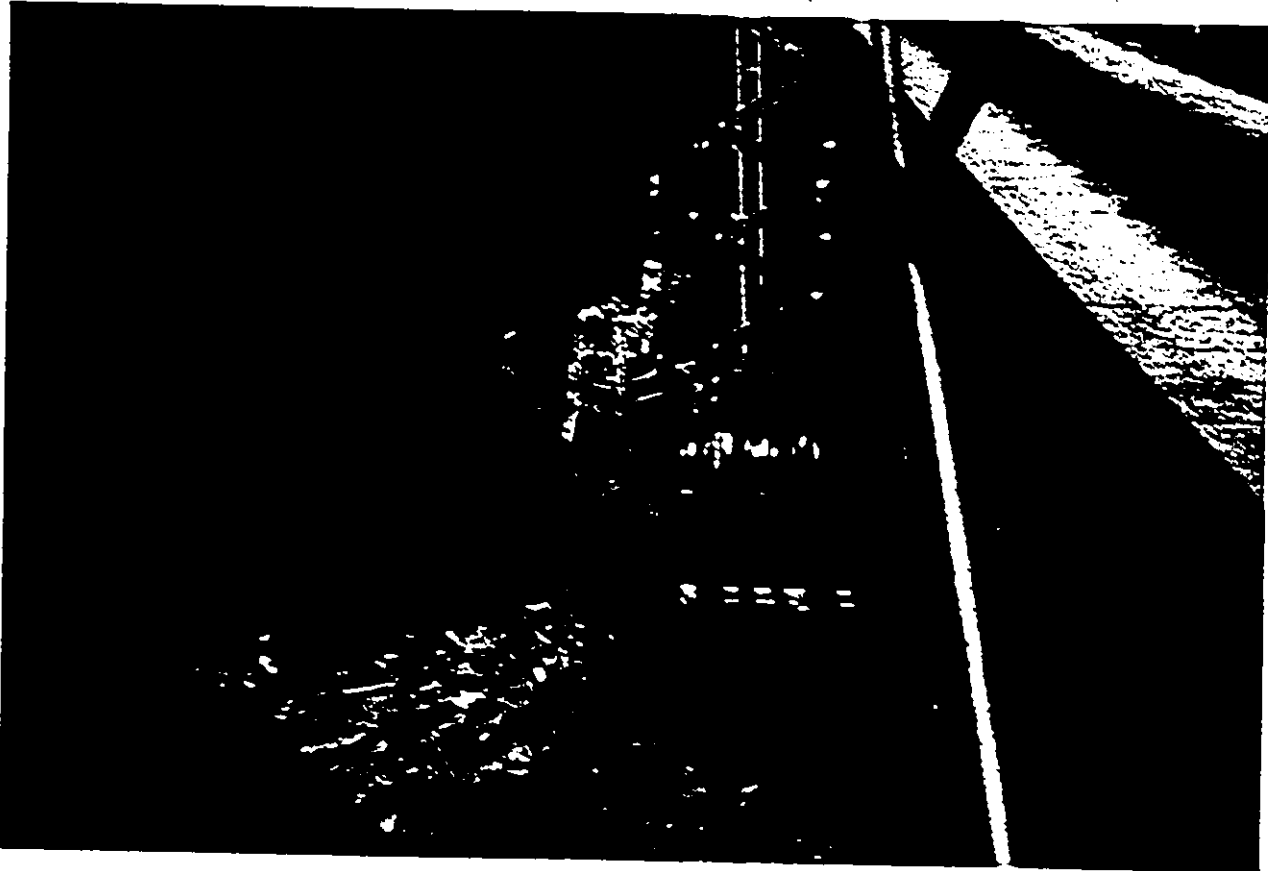


Figure 2.5 Installation of the first Spring Creek recorder. The recorder was set up on the bridge pier but was affected by backwater and was subsequently moved upstream.

Figure 2.5 shows work in progress on installing this recorder. It was found that the recorder was affected by backwater effects from the river, so it was later moved a further mile upstream (Figure 7.1), and set on top of a 15 foot pipe held by a half ton of concrete. A support and platform were built from the recorder to a large tree immediately upstream (Figure 2.6). This also protected the recorder at high water from logs and other debris (Figure 2.7). The control was a constriction over large cobbles and did not appear to shift.

A recorder was set up inside Wildcat Cave on the underground stream of Culverson Creek, a tributary of Spring Creek. The recorder was set up on a 15 foot pipe bolted to the cave walls. The control was a bedrock waterfall.

2.2.2 Hydrograph Record Lengths

Stage records were obtained at each creek for the following periods:

- a) Swago Creek from September 20, 1969 to October 11, 1971,
- b) Locust Creek from November 21, 1969 to October 11, 1971,
- c) Spring Creek from July 14, 1970 to October 10, 1971, and
- d) Wildcat Cave Creek from June 3 to October 9, 1971.

Records from all stations were lost from June 12 to July 13 1970, and there were problems during the winter due to the freezing in of the floats or ice in the streams. At Swago during low flows in the summer of 1970 and 1971 some readings were lost when the float rested on the bottom of the pipe.



Figure 2.6 Final site for the stage recorder at Spring Creek during average flow conditions. The discharge is about 30 cfs.



Figure 2.7 The stage recorder at Spring Creek during high water conditions. This photograph should be compared to Figure 2.6. The discharge is about 1200 cfs.

2.3 Cave Mapping

Most of the caves carrying streams in the area were explored, and the passage sizes and shapes and the flows of water in the caves noted. Some of the caves in the area had been mapped already by others. The remainder of the hydrologically important caves were mapped using conventional techniques with Brunton or Suunto compasses and survey tapes. The caves mapped included the following: Barnes Pit, Overholts, Cutlip, Hills-Bruffey, Clyde Cochrane, Canadian Hole and Beards Blue Hole.

Surveys for a number of other caves were obtained. These surveys were checked in the field and hydrological observations added to the maps. Maps of the various caves are shown in Chapters 5, 6 and 7.

Entrance elevations were obtained using altimeter traverses. The traverses were run from a bench mark on a circular tour to include where possible several other bench marks. The elevations of the points obtained were corrected for temperature effects and for a linear barometric change with time (American Paulin System, undated).

The positions of the cave entrances were obtained from aerial photos or from topographic maps. The map positions were checked and corrected in the field.

2.4 Flood and Dye Test

A simultaneous flood and dye test was carried out at Swago Cave to determine the relative speeds of the flood pulse and water pulse through a known portion of a cave. The cave, which has been surveyed,

consists of 600 feet of steep-gradient stream passage, four waterfalls up to 55 feet high, two pools, and a canal section 50 feet long.

A dam four feet high was constructed across the streambed on the surface above the cave (Figure 2.8). About 2000 cubic feet of water was held back by the dam. It was allowed to overflow for three hours before release, so that water conditions in the cave were steady. The undisturbed flow in the stream was measured at 0.84 cfs. Then 4 oz. of 20% Rhodamine WT were quickly stirred into the dam pool and the dam broken, releasing the dyed water.

Measurements of the stage of water were taken 800 feet inside the cave every minute for 15 minutes during the passage of the flood, and less frequently after that, for a total of two hours. The passage of the dye was also noted. Results of this test are discussed in Section 5.2.4.1.

2.5 Stream Tracing

Stream tracing was carried out to determine the path and resurgence points of sinking streams. A quantity of a tracer is inserted into a sinking stream and detectors placed at all possible resurgences. The detectors from each resurgence are later tested to see if any of the tracer has been picked up. If so, this proves the connection through to the resurgence. Various methods of stream tracing have been reviewed by Hass (1959) and by Drew and Smith (1969).

Possible tracers are dyes (Fluorescein, Rhodamine, etc.), mechanical tracers (Lycopodium spores, various plastic floats), bacterial

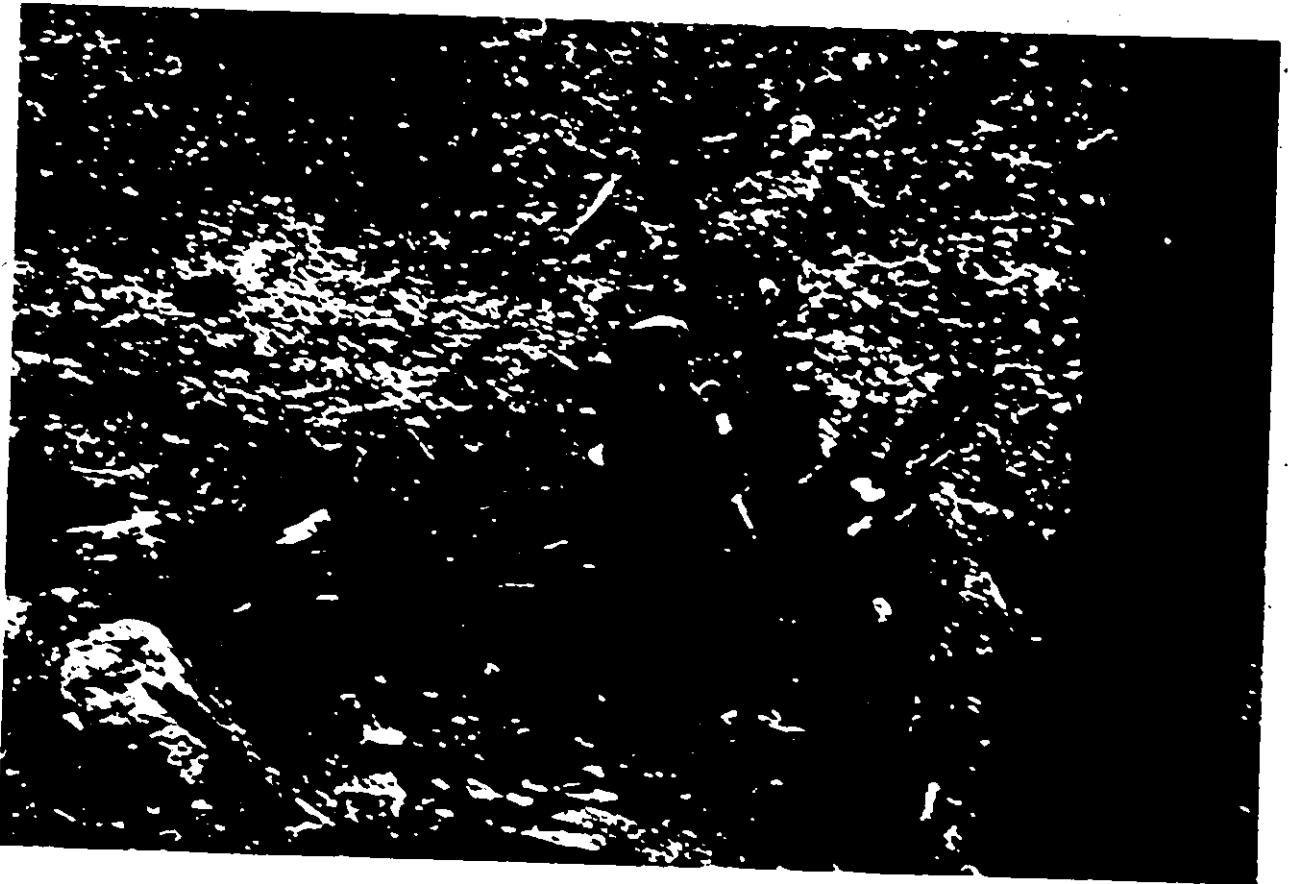


Figure 2.8 Construction of the Srago Dam for the flood and dye test.

cultures, radioactive tracers and various soluble salts. The salts are not generally very sensitive, therefore considerable quantities of salt need to be inserted into the stream for long tests. For example, three tons of common salt were used for a $1\frac{1}{2}$ mile test in Yorkshire (Howath, 1900). Radioactive tracers can be very sensitive but require considerable care in handling, expensive equipment, and there are difficulties in obtaining permission to run the tests. Bacterial cultures require time to grow a tagged culture, and knowledge of bacteriological techniques to grow and detect the bacteria (Ferrano, 1970, person communication). Lycopodium spores and dyes are both relatively sensitive, easy and cheap techniques to employ, and have been used with good results in a number of karst drainage studies (Palmer 1969, Boon et al. 1966, Aley 1972, Zotter 1963). These techniques were used for this study.

Once a tracer has been introduced into a stream it is difficult to carry out another test using that tracer in the area, until all detectable tracer has been swept out of the system. This usually means waiting for several months before another test can be carried out. For this study it was necessary to trace a number of adjacent streams. To test these in the limited field seasons available, simultaneous tracing using distinguishable tracers was carried out. Dyed Lycopodium spores and two different dyes, Rhodamine and Fluorescein, were used simultaneously.

2.5.1 Lycopodium Tracing

Stream tracing using Lycopodium spores was pioneered by Zotl (1965) in the Dachstein, Austria, where he found well integrated diffuse flow from a number of sinks. Atkinson and Drew (1967) have used the technique successfully in Mendips, and Brown (Boon et al., 1966) used Lycopodium spores very successfully in Jamaica for distances of up to 13 miles. Recently Aley (1972) and Moitke and Palmer (1972) have tried tracing with spores in karst at Missouri and Kentucky respectively.

Lycopodia are spores of a Moroccan moss. They have a diameter of about 30 μ . For tracing, the spores may be dyed with a number of colours and each different coloured batch introduced into a separate sink in a region. Fine mesh nets are placed in each possible resurgence to collect the spores. They are then identified by inspecting the contents of the nets under a microscope.

The nets are made of 25 micron nylon plankton netting, sewn into a canvas funnel to form a conical net (Drew and Smith, 1969) 20 inches long. This net was held inside a steel stove pipe section 12 inches in diameter and 2 feet long. A $\frac{1}{2}$ inch steel netting over each end keeps out twigs, leaves and crayfish, etc. The complete net assembly is placed in a fast flowing portion of the resurgence stream and wired securely to trees and boulders.

On May 4, 1970 nets were placed in the following streams: Locust Creek, Spring Creek, Fort Spring, Normans, McNeels Mill Run, and Muddy Creek (see Figure 2.3). Two nets were placed in the first three streams and one net in each of the other streams. The Lycopodium spores were

dyed, using the method of Drew and Smith (1969), with Methyl Violet, Bismark Brown, Malachite Green and Magenta. Spores were put into the streams as follows:

- a) May 15, 1970, 10 lbs. (dry) of Violet spores put into Rush Run,
 - b) May 15, 1970, 5 lbs. of Magenta spores put into Beards Blue Hole,
 - c) May 16, 1970, 10 lbs. of Brown spores put into Roaring Creek,
 - d) May 16, 1970, 5 lbs. of Green spores put into Luddingtons sink,
- (see Figure 2.3). The nets were sampled on May 12 (for background), May 20th, June 12th and July 8-9th, although not all sites were recovered every time.

The plankton nets may become clogged with mud. The amount of mud removed from the nets in West Virginia varied according to the site, from about 20 cc to 2 liters of sediment. In the laboratory a simple separation was performed to extract the spores from the mud. The samples from the nets were shaken up and 10 ml of the sample was left to settle in a test tube for a minute to remove sand and other large particles. The suspension was then decanted and centrifuged for 30 seconds at approximately 200 rpm when it was found that the spores came down as a sediment, leaving clays and finer particles in suspension. The sediment from the tube was spread out on a microscope slide, and the spores counted under a binocular microscope at x25 magnification.

It was found to be very difficult to distinguish the spores from detritus on the slides and it was necessary to use statistical tests to determine the successful traces. Slides were prepared from six background samples taken from the nets before the spores were inserted into the sinks, and from each of the nets recovered 4, 27 and 53-54

days after the spores were inserted.

Each slide was placed over a grid, and the number of spores of each of the four colours was counted on each slide. The background slides were counted twice by two observers, to reduce subjective errors. The samples obtained from the nets 27 days after the spores were inserted were counted six, seven, or eight times (depending on the resurgence) by four observers. The McNeel Run net was not sampled after 27 days however, and the sample obtained after 53 days was used for this analysis.

It was found difficult to distinguish on the slides the Magenta and Violet coloured spores from naturally occurring spores and detritus. The brown and green spores were easy to differentiate.

The average background count is shown in Table 2.2. The average number of spores on each slide, from the nets recovered after 27 days, is shown in Table 2.3.

A Student "t" test (Gregory, 1963) was performed on the number of spores of each colour found from each resurgence. The null hypothesis was that the number of spores found on the slide from the actual sample was the same as the number from the background. As the number of spores in the sample should be larger than the background the test is one tailed. A 1% significance level was chosen for the test. The null hypothesis was found to be true for colours of spores from all resurgences except for Green spores from Fort Spring and Violet spores from Spring Creek.

Slides were counted from the nets 4 days after the spores were inserted, but were found not to differ significantly from background. After 53 days the number of Green spores from Fort Spring was signifi-

Table 2.2Average Number of Spores per Slide from Background

<u>Colour of Spores</u>	<u>Locust</u>	<u>Spring</u>	<u>Norman</u>	<u>McNeel</u>	<u>Muddy</u>	<u>Fort Spring</u>
Red	2.5	1.5	3.0	4.0	1.0	11.5
Violet	<u>0.5</u>	1.	35.	3.5	1.9	52.5
Magenta	36.	44.	46.	32.5	30.	57.5
Green	1.	2.	1.5	2.5	3.5	<u>2.5</u>

Table 2.3Average Number of Spores per Slide After 27 Days

	<u>Locust</u>	<u>Spring</u>	<u>Norman</u>	<u>McNeel*</u>	<u>Muddy</u>	<u>Fort Spring</u>
No. of Slides Counted	7	7	6	6	8	6
<u>Colour of Spores</u>						
Red	1.71	0.71	1.5	3.17	1.50	10.77
Violet	<u>3.29</u>	2.0	13.33	3.50	3.13	13.83
Magenta	28.71	29.86	125.33	43.17	24.12	81.83
Green	0.86	2.57	0.83	1.33	1.63	<u>8.67</u>

*After 53 days.

Note: underlined values are significantly different. All other pairs of figures are not significantly different.

cantly above background, but the numbers of all the other spores were not significantly different from background.

The test indicates that Luddingtons Cave (where the Green spores were put in) drains to Fort Spring, which is 13 miles distant, in more than four days; and that Beards Blue Hole (where the Violet spores were inserted) drains to Locust Creek, taking between 4 and 27 days to travel the $1\frac{1}{2}$ miles between sink and rising.

2.5.2 Dye Tracing

Dye tracing using both Fluorescein and Rhodamine dyes was carried out to determine the resurgence points of sinking streams.

The quantity of dye to be inserted is difficult to determine (Zotter, 1963). There should be sufficient to give a positive test, but not enough to colour any of the resurgences. Zotter (1963) recommends using 2 oz. per mile during "low" flow and $\frac{1}{2}$ oz. per mile during "high" flows (note that Zotter uses less dye as the flow increases), and does not recommend tracing during droughts. Drew and Smith (1969) give an estimate of 1 oz. of dye per mile of straight line travel per cfs. of discharge at the most likely resurgence. Theoretically this amount of dye should not be visible (e.g. less than 10 ppb) unless the water travels faster than 100 feet per hour and all the dye is recovered. Conversely it should be detectable (more than 0.1 ppb) in the stream unless the water travels slower than 1 foot per hour and/or a considerable amount of the dye is adsorbed on muds and clays. However the adsorption of

the dye on the detectors is a cumulative process and the detectability limit on charcoal is considerably more sensitive than the detectability limit in the stream. This process increases the range between the visibility and detectability concentration in the water and allows a greater latitude of injected dye for dye tracing.

Aley (1971), from his experience in Missouri, has suggested using the non-linear empirical formula shown below to predict the quantity of dye to be used for tracing:

$$W = 0.021 \left(\frac{DQ}{V} \right)^{0.498} \quad (2.8)$$

where W is the weight of Fluorescein injected, in pounds,

D is the straight line distance to resurgence in miles,

Q is the flow rate at the resurgence in cfs., and

V is the estimated velocity of flow in ft./sec.

The reason for the exponent of 0.498 (and not, say, 0.5) is unknown.

For short tests with the usual West Virginia flow conditions, Aley calculates the dye amount to be similar to the amount used by Drew and Smith (1969). With larger tests however, Aley would use less dye. Hass (1959) recommends using 1/5 of the amount of dye that Drew and Smith used, and this amount would be comparable to the amount used by Aley (1971) in larger tests.

In this study the quantity recommended by Drew and Smith (1969) of 1 oz. of dye per mile per cfs. was used as the first approximation. In the larger tests a trial was often made using about 1/10 of the calculated amount of dye in order to insure against brightly coloured streams, which seemed to upset the local residents.

It was found in West Virginia that Rhodamine was a considerably more successful tracer than Fluorescein, which appear to be absorbed on clays. Zotter (1963) however, has had good success using Fluorescein on shorter tests in the same area.

The dye is collected on activated charcoal placed in any possible resurgence. For these tests, the charcoal was held in small bags (about 2 inches square) of aluminum window screen netting, stapled down the edges. About 5 ml of charcoal was placed in each bag. These detectors were tied to stones placed in a fast flowing part of the resurgence and were changed several times during a test. For each test, 2 ml of the charcoal was removed from the detector, and eluted with a solution of KOH in methanol (2 pellets in 10 cc). This was then tested on the Turner fluorometer using the general purpose lamp and 546-590 filters for Rhodamine and a 2A-47B and a 2A-12 filters for the Fluorescein (Wilson, 1968). For most tests a background detector was obtained at each spring before the dye had been inserted, and a dye test was considered positive if the elutriant had a fluorometer reading of more than 5 times the background reading. Background readings for the Rhodamine were generally less than 2 ppb (elutriant strength) but were commonly over 50 ppb for Fluorescein, due to green algae growth in the stream.

One combined Rhodamine and Fluorescein dye test was tried at two neighbouring streams--Snedegars Creek and a small unnamed creek just to the north. Five pounds of 20% Rhodamine WT was inserted in the Snedegars streamway, and 2 pounds of powdered Fluorescein in the smaller stream, and detectors placed in all nearby resurgences. After eluting the detectors the elutriant was run on both Fluorescein and Rhodamine

filters. It was found that the Snedagers stream flowed to Spring Creek. However the Fluorescein dye in the other stream was not recovered, probably due to absorption on mud. A later test using Rhodamine showed that this stream flowed north to Locust Creek.

Results of the dye tests will be described in Chapters 5, 6 and 7 on the descriptions of the present day basins.

2.6 Geochemistry Methods

Waters were analysed for calcium, magnesium, alkalinity (bicarbonate ions), pH, temperature and, in some cases, conductivity. A few early samples were analysed for sulphate and chloride, but as all were found to be less than 1 ppm, these ions were neglected thereafter. All analyses were carried out in the field, and the methods checked in a laboratory against known waters. Calcium and magnesium were measured with EDTA by standard methods (Rainwater and Thatcher, 1960), but using a syringe instead of a burette, and a volumetric flask in place of a pipette; these were stronger and easier to carry. Results to ± 2 ppm were found on laboratory duplicates. Alkalinity was measured with standardized acid and a methyl orange type indicator (B.D.H. 4460), again using syringes and flasks. A Lovibond colorimetric pH comparator was used with Cresol Red and Bromo-Thymol Blue indicators, and was found in the laboratory to give the pH to within 0.3 units compared to a calibrated Metrohm meter. Most samples were in the overlap range of the two indicators and both colours were used. On a few samples the Blue and Red

indicators gave pH's which were considerably different, for some unknown reason. These samples were rejected. The geochemistry results were used in the pulse test described in Section 6.2.12.

2.7. Erosion Measurements

There are a number of methods of estimating the ages of caves, none of which gives the absolute age. Isotopic dating of cave speleothems (Thompson, 1973) or isotopic dating of ancient wood in the cave (Ford, 1973) or the study of sediments (Wolfe, 1973; Reams, 1968; etc.) only give the minimum age of cave formation, as these deposits are laid down after the cave has formed. More direct methods include calculations on the amount of limestone picked up in cave streams (Hanna, 1966) or the direct measurement of the erosion of the limestone surface (High and Hanna, 1970). The latter method was used in this study to estimate the length of time that caves have been eroding.

Micro-erosion measurements are carried out by inserting stainless steel screws into the limestone rock. A jig is then placed on these screws and readings taken with a dial gauge down to the limestone surface. The jig is then removed. Several months or years later the jig can be replaced on the screws in exactly the same position and more readings taken. The difference between the first and second set of readings is the amount of erosion.

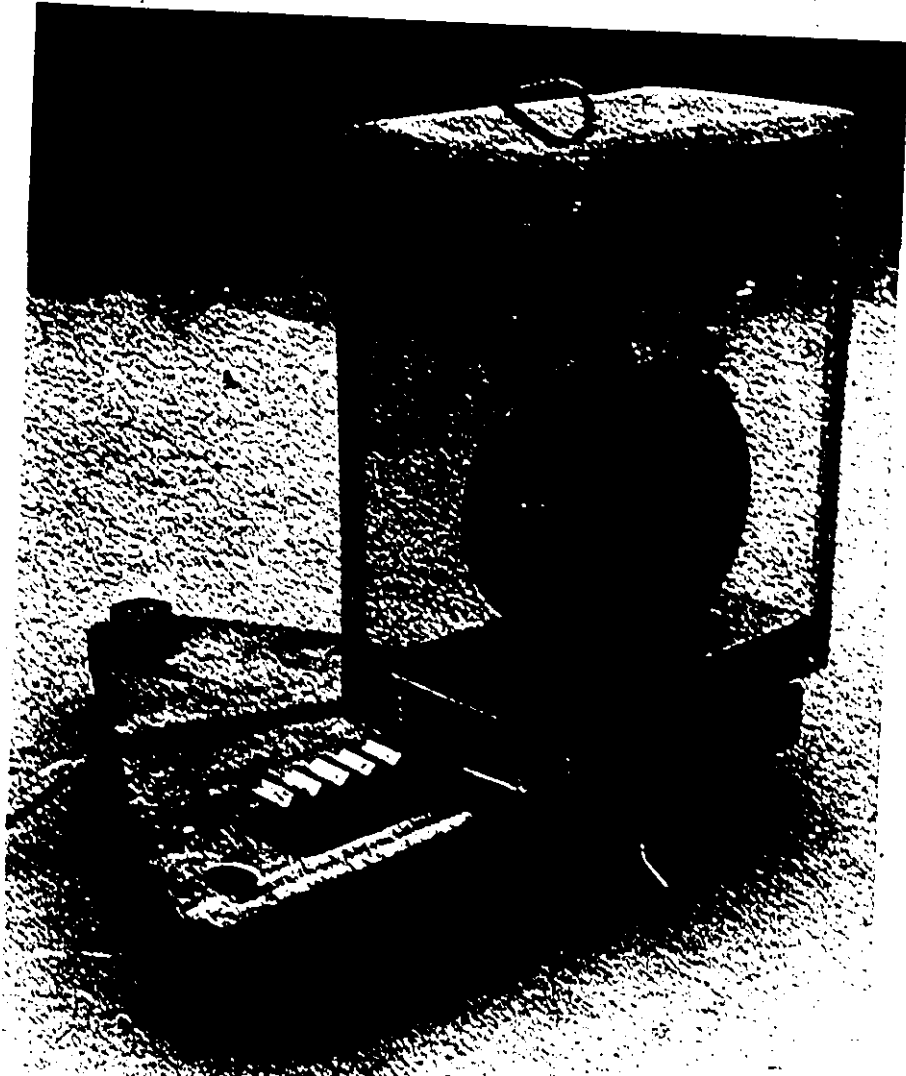


Figure 2.9 The micro-erosion meter.

2.7.1 Micro-erosion Instrument

The screws used for the micro-erosion device were No. 6 x 3/4" stainless steel sheet metal screws, which are similar to wood screws. A small cone was drilled into the head of each screw and a stainless steel ball bearing was silver soldered onto the head of each screw.

The screws were set into lead anchors, which were placed in three holes drilled in the rock exactly five inches apart in an equilateral triangular configuration (Figure 2.11). The balls on the screws were arranged to be about 1/8" below the rock surface, so that stones and debris carried along by the stream would not knock the ball-headed screws. Between measurements the screws were protected by a thick layer of heavy grease to prevent corrosion.

The erosion meter comprised a base plate and a carriage (Figure 2.9). The base plate was a 1/4" thick aluminum plate with three bolts placed in a 5 inch equilateral triangular configuration. The end of one bolt was turned down to an internal conical shape, another had a groove, and the third had a flat end. When placed on the ball-headed screws, the baseplate could be relocated on the screws in exactly the same position each time.

The carriage was similarly restrained by three pins which could slide in crossed "V" grooves. The carriage held the dial gauge and could traverse over a total of 52 positions over the baseplate. If the baseplate were rotated, 156 different measurements could be taken on three ball-headed screws.

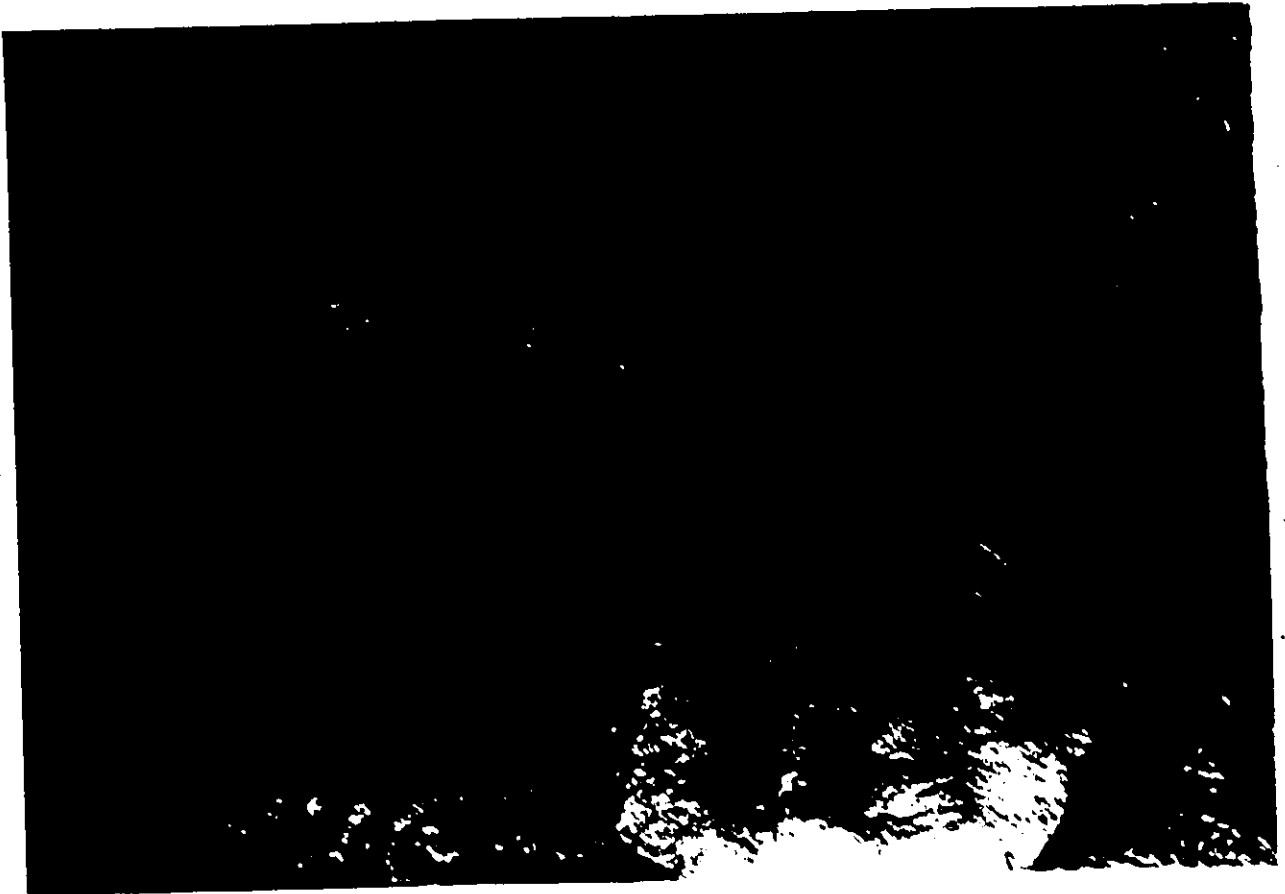


Figure 2.10 The micro-erosion site in Lower Hughes Cave. The pipe was used to temporarily deflect the water while measurements were taken. The micro-erosion sites are across the stream behind the pipe.

2.7.2 Erosion Site

The Locust Creek basin has undergone several stages of development (Chapter 6). A recent stage is the development of Lower Hughes Cave, which now takes the waters issuing from Upper Hughes Cave. An erosion site was set up in Lower Hughes Cave to measure the erosion in the active streambed, in order to estimate the age of the cave. The cave was convenient for erosion measurements as it is a short cave with easy access, and carries a small perennial stream.

The site chosen was in the stream, at a place where the passage is about 8 feet high and about 2 feet wide (Figure 2.10). The stream flowing in the cave discharges about 0.1 cfs. during dry summer conditions, rising to many tens of cfs. in the spring. The cave is flooded to the roof during high water, several times a year.

A series of screws was put into the rock in the passage, starting from the centre of the stream and continuing to a point on the wall about one foot above the normal stream level. A total of 91 measurements was taken in August 1969 across half the stream. These were remeasured in July and October of 1971. The results are discussed in Section 3.3.

2.7.3 Calibration

The erosion meter was calibrated before and after each measurement, in order to detect any strains that may have occurred in the meter during the field trip to the erosion site. The erosion device was placed on three 3/16" ball bearings on a small sheet of plate glass and

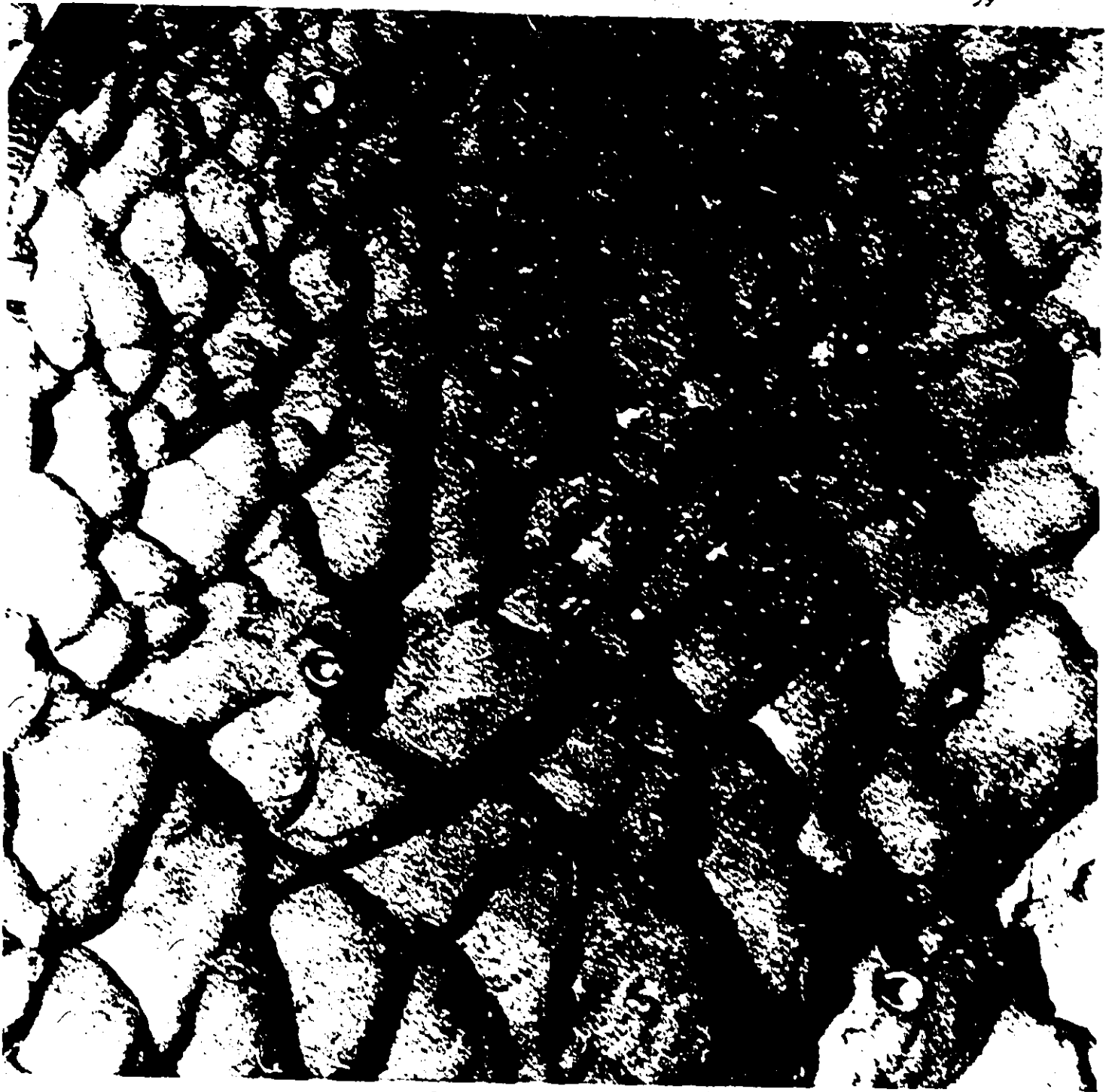


Figure 2.11 View of the limestone surface at the micro-erosion site.
The stainless steel ball-headed screws are 3 inches apart.
The stream flows from right to left, as indicated by
the scallop direction.

readings taken as the carriage was traversed over the baseplate. The ball bearings were held 5 inches apart by a plastic calibration plate. The calibration reading did not vary appreciably before or after any real measurements, but was used to detect any instrument error and to correct for repositioning of the dial gauge in the carriage.

CHAPTER III

CLIMATE AND FIELD RESULTS

In this chapter the field results are presented for use in later analysis. The first and second sections concern the climate and stream-flow in the the area; these data were used in the simulation runs. The last section describes the erosion results which were used to measure the age of one cave and to estimate the time span for the development of the karst in the basins.

3.1 Climate

The climatic conditions over the area were investigated for use in the simulation runs. It was necessary to obtain the precipitation, potential evaporation and temperature figures for the basins being simulated. Time did not allow the establishment of a climatic network, so the climatic information was obtained from the existing climatic stations, which in this region were all located in the valleys (Figure 3.1). It was found that there were large variations in the precipitation throughout the area, and that precipitation increased considerably with altitude. The precipitation on the hilltops was found to be 70% higher than in the valleys. The mean precipitations over the three study basins were obtained from the climatic stations, using the estimated rate of increase in precipitation with altitude to adjust the figures. Daily potential

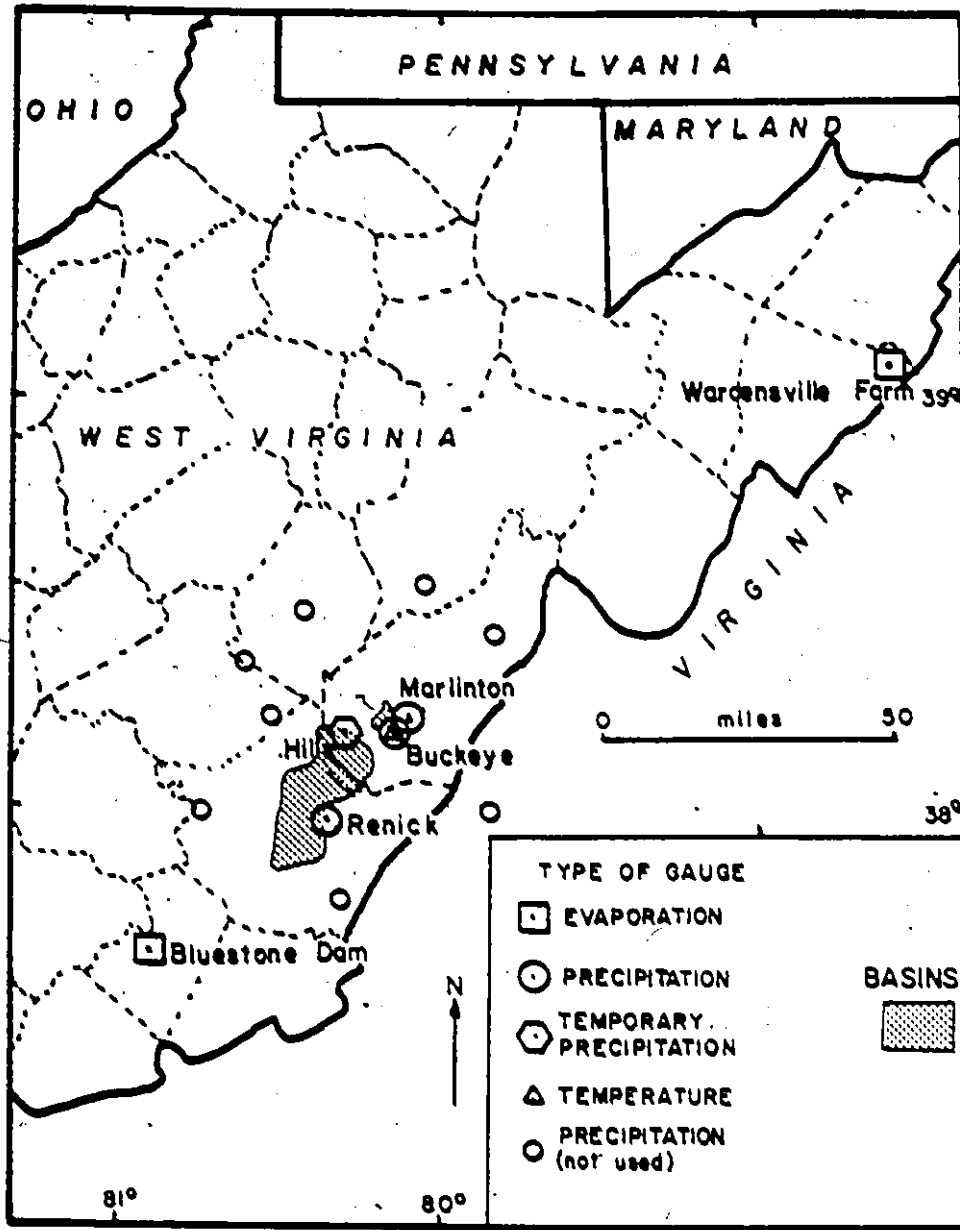


Figure 3.1 Location of climatic stations.

evaporation and mean temperature figures were also obtained from the existing climatic stations.

Southeast West Virginia has a humid temperate climate with a mean (1899-1930) annual precipitation of 46 inches (Thorntwaite, 1955) at Marlinton. At an altitude of 2000 feet, the summer temperatures are lower than those of the surrounding lowlands; daytime temperatures over 90°F are rare. In winter, in the valleys, there are usually 10 nights a year with minimum temperatures below zero. Winter also brings about 30 days each year with more than one inch of snow on the ground. About once a year storms deposit more than a foot of snow in the valleys.

3.1.1 Precipitation

Three major types of precipitation fall in this part of West Virginia:-

- a) Throughout the year, particularly in winter and spring, showers are common, usually of low intensity and spread over a large area.
- b) In summer the moist air blowing from the south, off the Gulf of Mexico or South Atlantic, causes thunderstorms. In most areas there are about ten thunderstorms a year, usually localized but often producing large amounts of rain.
- c) The third type of precipitation is the remnants of coastal hurricanes, blowing in from the southeast. Although not common, these hurricanes can cause considerable damage over wide areas. In 1969 Hurricane Camille deposited almost four inches of rain at Renick

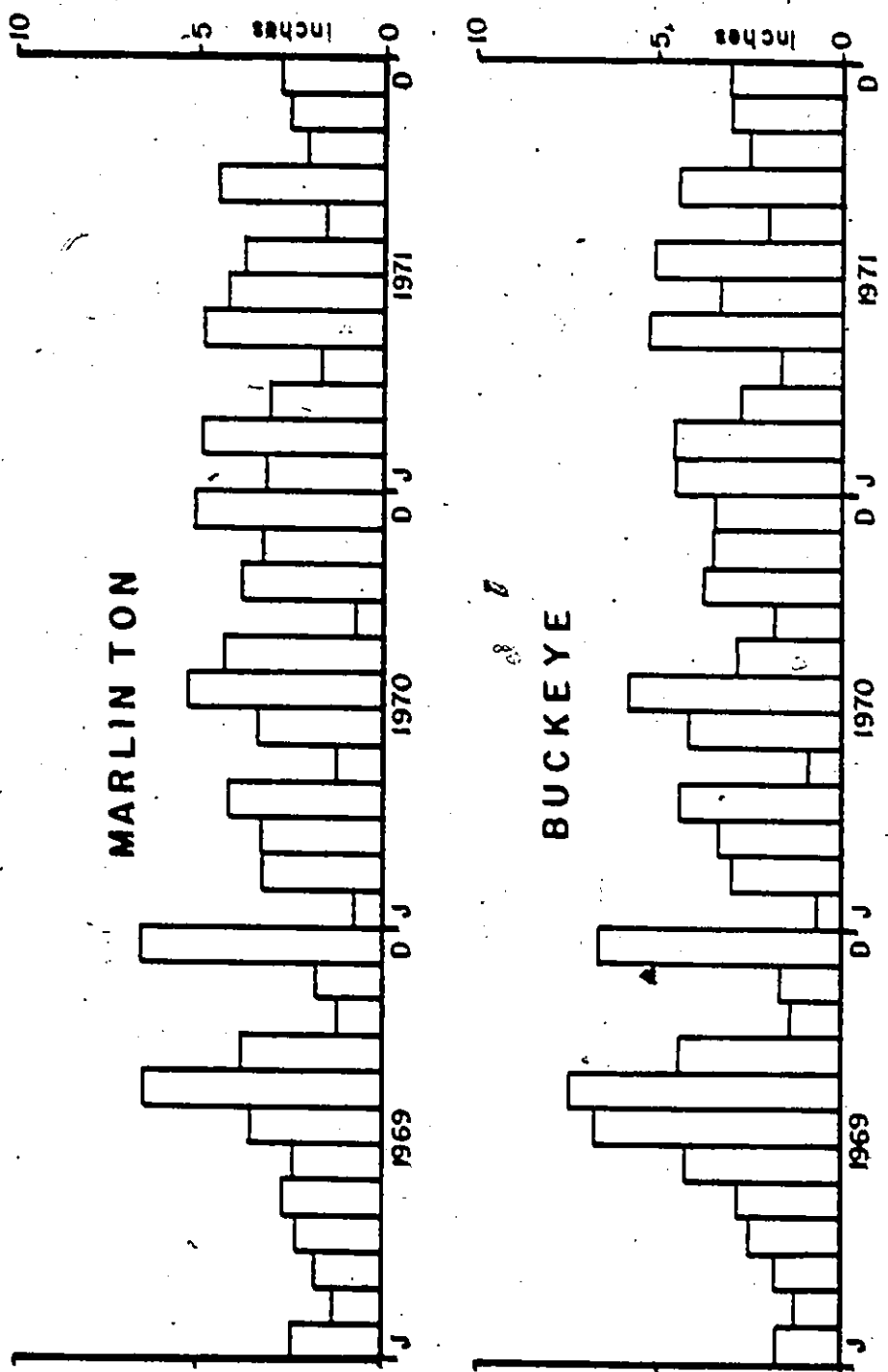


Figure 3.2 Monthly precipitation at Marlinton and Buckeye, 1969-1971.

(and 27 inches near Richmond, Virginia) and caused considerable flooding damage along Spring Creek (Williams and Guy, 1973).

Due to the prevailing winds the southwestern sides of the hills tend to receive more rain than the northeastern sides. Fortunately the three basins face southeast, so an increase in precipitation on the southwestern sloping sides of the basin tends to be counteracted by a decrease on the northeastern sloping sides.

3.1.2 Areal Variations in Precipitation

It was found that there were considerable areal variations in the precipitation in this region. Figure 3.2 shows the monthly precipitation figures for Buckeye and Marlinton in the years 1968 to 1971. It will be observed from Figure 3.2 that there is considerable variation between the monthly figures for the two stations.

The variation in precipitation between the two stations is more extreme if daily figures are considered. Figure 3.3 shows a plot of daily precipitation figures for June 1969 at Marlinton, Buckeye and Renick. It is seen that there are large variations among the three stations, although Marlinton and Buckeye are only four miles apart and Buckeye and Renick are twenty miles apart. The three stations are at similar elevations and all are within the Greenbrier River valley. These large variations among the daily precipitations at the three stations are most marked in the summer, due to the localized effects of thunderstorms. Frontal rains in the winter cause less spatial variation.

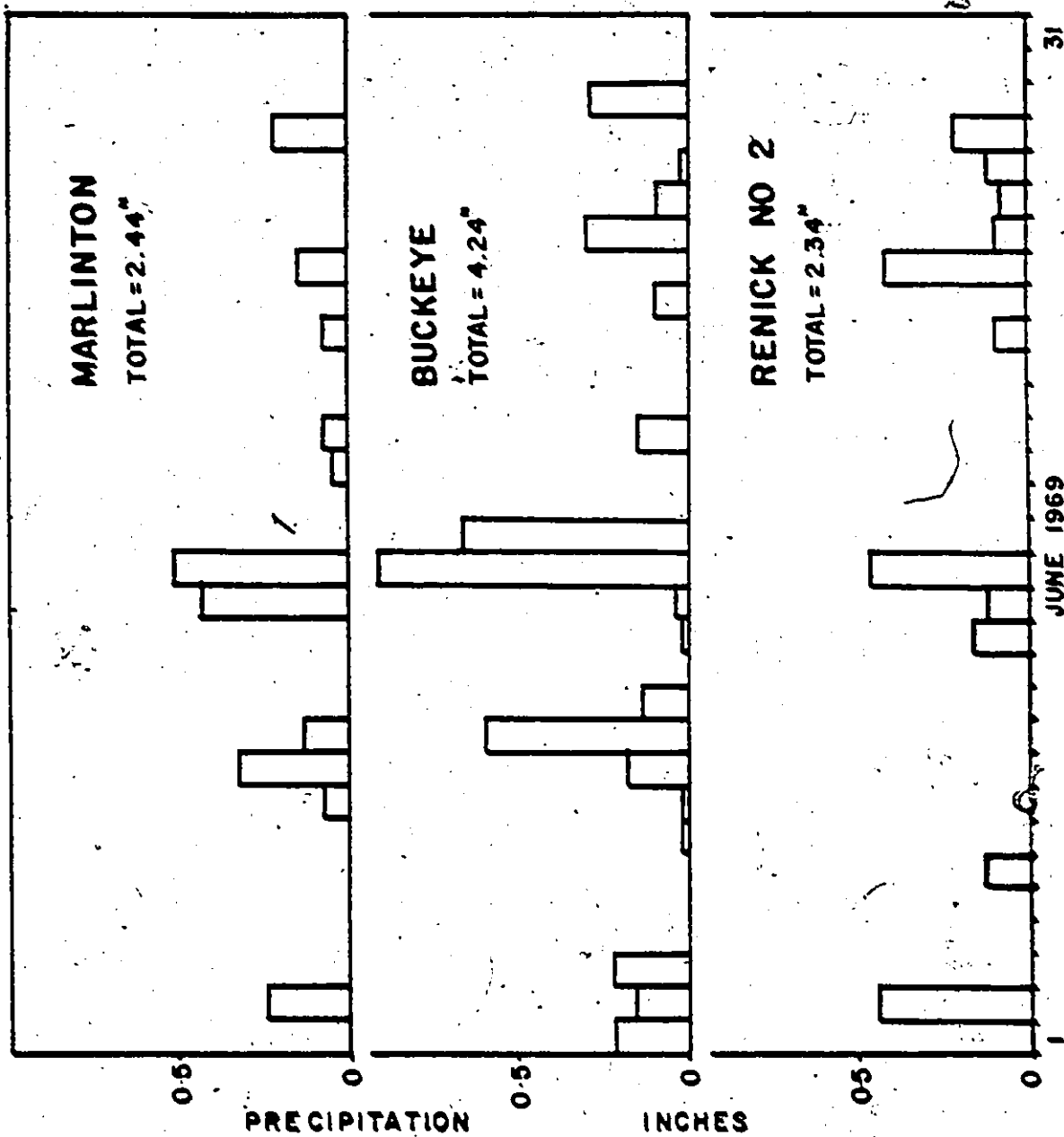


Figure 3.3

Plot of daily precipitation for June, 1969 at Marlinton, Buckeye and Renick. Marlinton is 4 miles from Buckeye and 24 miles from Renick. The wide differences between the three stations can be seen.

With the limited number of gauges available it is difficult to assess the mean precipitation over the basins. In the summer, mean precipitation figures obtained from existing stations could be considerably in error. However, time did not allow the establishment of a more extensive precipitation network; precipitation figures were used from the existing stations, but there were understood to be probable errors.

3.1.3 Variation in Precipitation with Altitude

Precipitation generally increases with altitude (Speen, 1947). In order to derive the mean precipitation over a basin from a number of climatic stations, the change in precipitation with altitude and the elevations of the climatic stations, as well as the elevations throughout the basin, must be known.

In order to estimate the change in precipitation with altitude in this part of West Virginia, a rain gauge was set up near the headwaters of Hills Creek in the Locust Creek basin (see Figure 3.1) at an elevation of 3450 feet. The gauge was a simple three inch brass funnel gauge set up in a clearing in a woodland on September 3, 1969, and read on September 12 and October 5, 1969. The rainfall collected is shown in Table 3.2, with precipitation readings from nearby stations shown as comparisons. In Table 3.1 the official October figures for Renick are missing, but have been estimated by the U.S. Department of Commerce. The average precipitation figures were obtained by a weighted mean, weighted according to the distances from the Hills Creek station. It is seen that

Table 3.1

Comparison of Rainfall from Existing Climatological Stations
in the Valleys and from a Temporary Station in the Hills

<u>Station</u>	<u>Station Elevation (feet)</u>	<u>Rainfall in the Period (in inches)</u>		
		<u>Sept. 3-12</u>	<u>Sept. 13-Oct. 2</u>	<u>Sept. 3-Oct. 2</u>
Buckeye	2100	2.43	2.61	5.04
Renick	2150	2.50	1.17 (est)	3.67 (est)
Camden on Gauley	2030	1.71	1.89	3.60
Weighted Mean	(2100)	2.31	1.81	4.12
Temporary Hills Gauge	3450	3.2	2.7	5.9
Increase in Precipitation of Hills Creek Gauge (%)		39	49	43

the precipitation at the Hills Creek station is over 40% higher than the mean precipitation in the valleys.

Donley and Mitchell (1939) determined the relation of precipitation to elevation in the southern Appalachian region. They assumed that the increase in precipitation due to elevation was linear and could be expressed as:

$$R_2 = R_1 \left(1 + \frac{K}{100} (A_2 - A_1) \right) \quad (3.1)$$

where R_1 and R_2 are the mean precipitations,

A_1 and A_2 are the elevations of two stations, and

K is a factor relating precipitation to elevation.

In order to obtain good correlation between the precipitation and elevation figures, Donley and Mitchell had to divide their area into five zones, based on geographical provinces. They then obtained values of K in each zone, ranging from 0.013 to 0.037 per 100 feet.

Projecting the increase in precipitation found at Hills Creek throughout the year, a value was obtained for K of 0.032 per 100 feet (from the data in Table 3.1), which compares well with Donley's and Mitchell's values in Zones 1 and 2 ($K = 0.025$ and 0.031 per 100 feet) where the elevation difference and exposure are similar to those at Hills Creek. Duchstein, et al. (1972), in a study of the number and magnitude of rainfall-events in the summer in Arizona, also correlated rainfall to altitude. From his data K can be calculated as 0.024 per 100 feet.

The variation in precipitation is dependent on a number of factors other than elevation. Spreen (1947), in a study of the effects

of topography on precipitation in Colorado, found that only 30% of the variation in precipitation is attributable to elevation, while 85% of the variation can be explained if four other factors—rise, orientation, exposure, and zone of environment—are included. However, using typical figures for these four factors from Spreen's data, we can calculate the value of K to be 0.026 per 100 feet in Colorado.

The variations in precipitation can also vary from season to season. Thus Harmon (1971) found in Idaho that the winter precipitation increases with altitude ($K = 0.1$ per 100 feet) far more than does summer precipitation ($K = 0.04$ per 100 feet).

Clearly the effect of topography on precipitation is not a simple matter. However most studies have shown that at moderate elevations precipitation does increase with altitude. As a large proportion of the area of the West Virginia basins was considerably higher than the climatic stations, the average basin precipitation will be larger than that shown by the low level climatic stations, and was calculated assuming that the precipitation increases with altitude at the rate found at the Hills Creek gauge.

3.1.4 Mean Basin Precipitation

Assuming that the precipitation increases linearly with altitude, we can calculate the mean precipitation over the basins, if we know the precipitation in the valleys and the height to area distribution in the basins. The hypsometric curves (area-height curves for basins) are shown

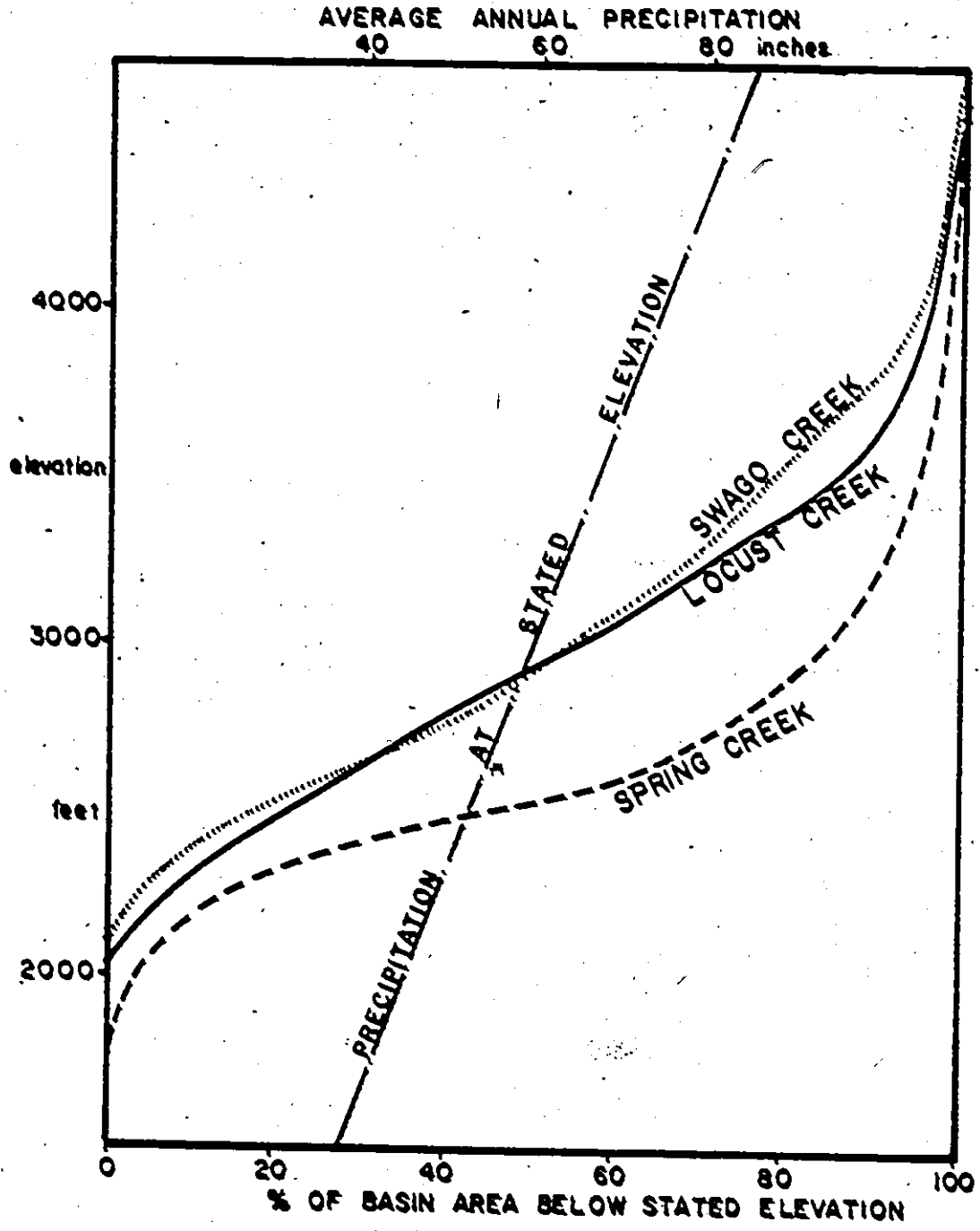


Figure 3.4 Hypsometric curves for Swago, Locust and Spring Creeks, and the mean annual precipitation at different elevations.

in Figure 3.4. The hypsometric curves for Locust and Swago Creek are seen to be similar, while the curve for Spring Creek is considerably lower than the other two curves.

The total precipitation over the basin can be obtained by summing the product of the proportion of land between two elevations and the precipitation at the mean elevation. Thus the basin precipitation can be approximated as:

$$\bar{R} = \sum_{E=E_{min}}^{E_{max}} R_E (\phi_{E-1} - \phi_{E+1}) \quad (3.2)$$

where \bar{R} is the mean precipitation,

R_E is the precipitation at elevation E ,

ϕ_E is the proportion of land lying below elevation E (thus a hypsometric curve is a plot of ϕ_E to E), and

E_{min} and E_{max} are the minimum and maximum basin elevations.

The basin precipitations were obtained from the climatic stations of Buckeye, Renick and Marlinton which are at elevations of 2100, 2150 and 2150 feet respectively. Equation 3.2 was used to calculate the basin precipitation relative to a precipitation station elevation of 2130 feet, which is approximately the mean elevation. The calculation for Locust Creek is shown in Table 3.2.

From Table 3.2 the precipitation over the Locust Creek basin is almost 30% larger than the precipitation in the valleys. Although the increase in precipitation with height at the other two basins is not known, we can assume that it would increase at about the same rate as at Locust Creek. As the hypsometric curve for Swago Creek is similar to that for Locust Creek, we can take the Swago basin precipitation to

Table 3.2

Average Precipitation Calculated for Locust Creek

<u>Elevation Range (feet)</u>	<u>% of Area Between Elevations</u>	<u>Mean Elevation (feet)</u>	<u>Precip. Increase Calculated from Eqn. 3.2, Rel. to 2130 ft.</u>	<u>Contribution to Total Precip. (B x D)</u>
A	B	C	D	E
2050	4	2150	1.0064	0.040
2250	35	2500	1.106	0.387
2750	28	3000	1.29	0.362
3250	19	3500	1.45	0.276
3750	13	4000	1.61	0.209
4250	1	4384	1.73	0.017
4518				
Total	100			1.291 x R₁

be 30% higher than the valley precipitation.

At Spring Creek, however, the basin is considerably lower. The basin precipitation was found to be only 15% larger than the valley precipitation.

The precipitation figures for the basins were obtained from the three existing U.S. climatological stations of Marlinton, Buckeye, and Renick. An approximated Thiessen (1911) mean averaging method was used, and the weights assigned to each station were arranged to give an increased basin precipitation according to the calculations above. The weights adopted are shown in Table 3.3.

Table 3.3

Weights Used to Obtain Basin Precipitation
from the Climatic Station Figures

<u>Climatic Station</u>	<u>Station Height</u> (feet)	<u>Weights</u>		
		<u>Summer</u>	<u>Lowest</u>	<u>Spring</u>
Marlinton	2150	0.5	0.1	0.1
Buckeye	2100	0.8	0.8	0.1
Renick No. 2	2150	0.0	0.4	.95

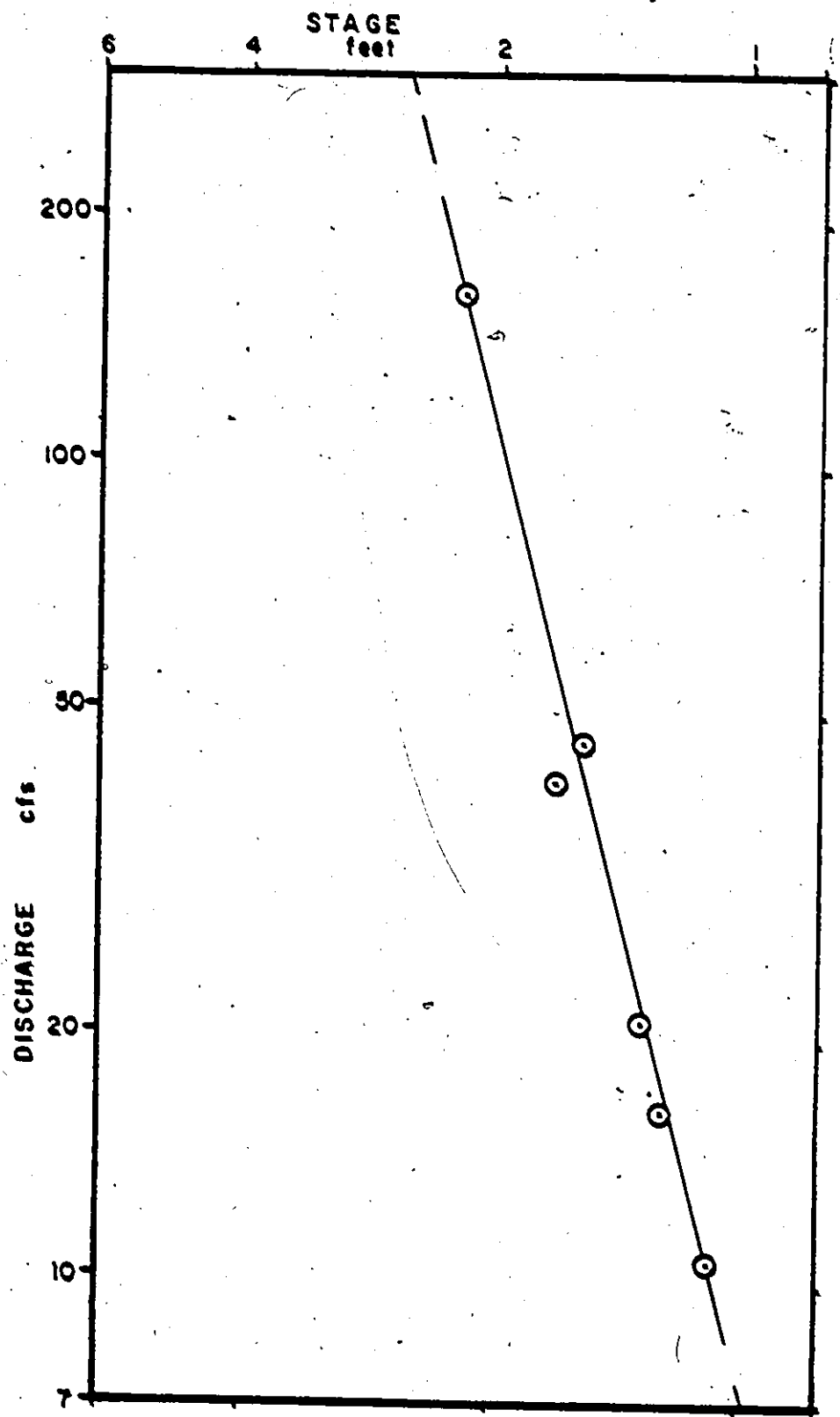


Figure 3.5 Rating curve for Swago Creek.

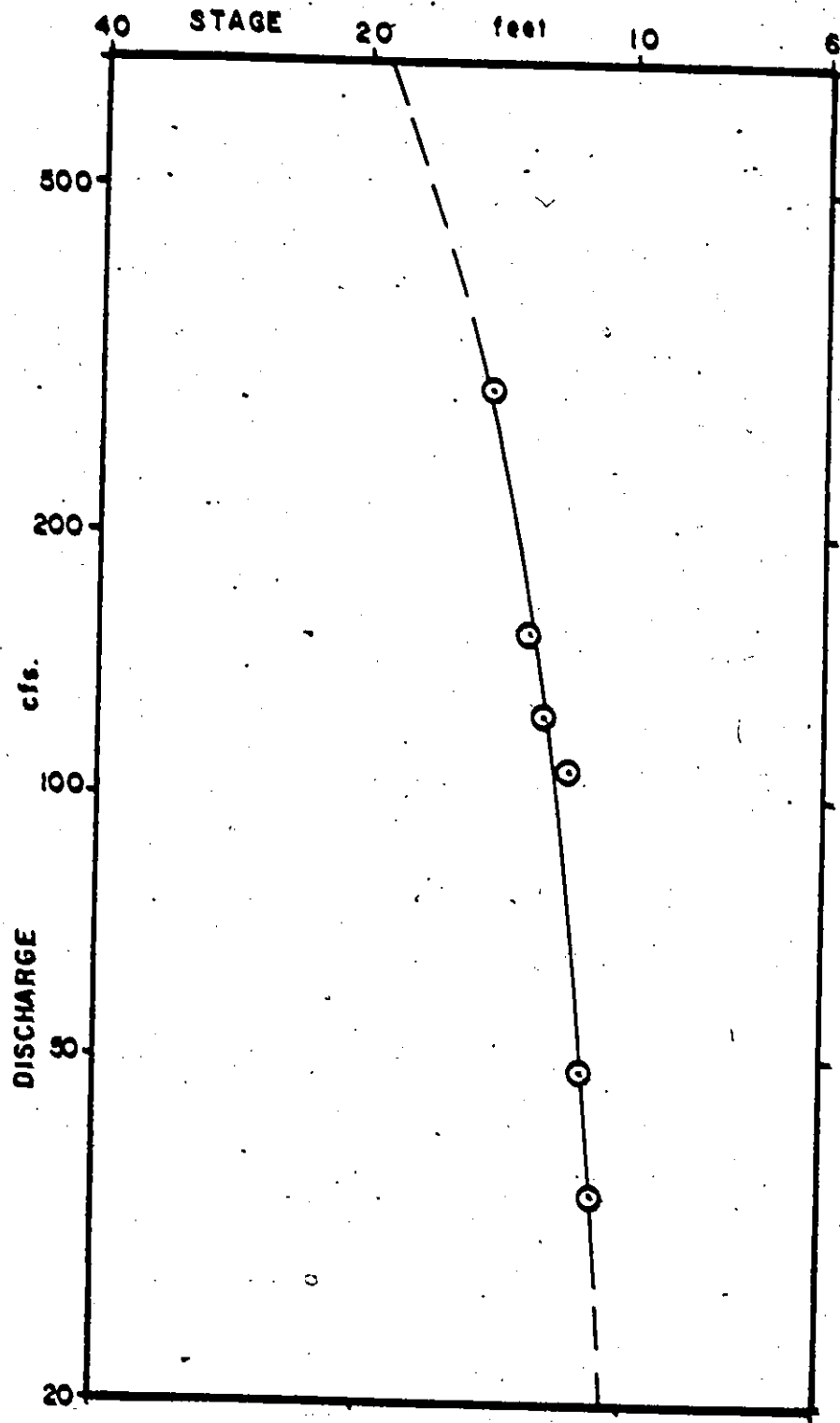


Figure 3.6 Rating curve for Locust Creek.

3.1.5 Evaporation and Temperature

The two nearest potential evaporation stations were at Bluestone Dam (30 to 60 miles southwest of the basins) and at Wardensville farm (80 to 110 miles northeast of the basins), Figure 3.1. In spite of the large distances involved, the potential evaporation figures were obtained from the average of these two stations. It was realized that the figures could be considerably in error.

Temperature data were obtained from the Buckeye minimum and maximum temperatures, corrected for a lapse rate of $3\frac{1}{2}^{\circ}\text{F}/1000$ feet (Linsley et al., 1949).

3.2 Streamflow

The streamflow was measured using Curley meters and dye dilution techniques, as described in Sections 2.2 and 2.3. The rating curves obtained at Swago, Locust, and Spring Creeks are shown in Figures 3.5 to 3.7. The curves had to be extrapolated for high and low flows. The stage-discharge relationship was assumed to take the form:

$$Q = c(H - B)^n \quad (\text{Rantz, 1968}) \quad (3.3)$$

where c and n are constants,

H is the measure stage,

B is the elevation above gauge datum at zero flow, and

Q is the discharge.

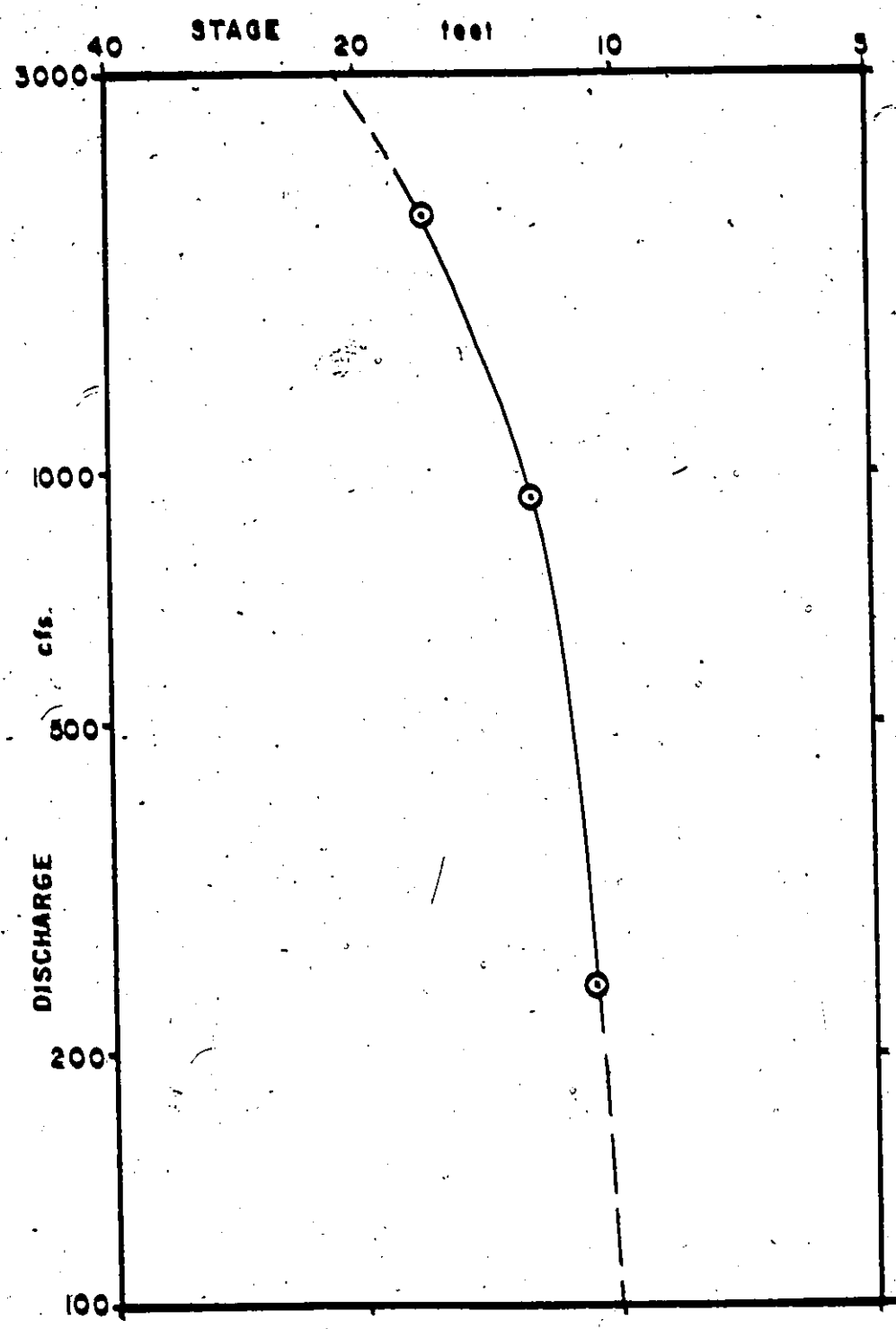


Figure 3.7 Rating curve for Spring Creek.

Table 1.4

79

Monthly Streamflow

MONTH	PRECIP. at		STREAMFLOW				
	Marlinton (inches)	Swago (cfs) (inches)	Locust (cfs) (inches)	Locust (cfs) (inches)	Spring (cfs) (inches)	Spring (cfs) (inches)	
Sept./69	3.86	12.9*	1.15*				
Oct. /69	1.17	6.8	0.61				
Nov. /69	1.83	11.9	1.07	40.5	0.96		
Dec. /69	6.59	59.5	5.30	14.4	0.34		
Jan. /70	0.79	22.1	1.97	58.6	1.38		
Feb. /70	3.27	34.5	3.07	134.4	3.17		
Mar. /70	3.30	43.2	3.82	159.0	3.76		
Apr. /70	4.07	35.2	3.16	148.1	3.50		
May /70	1.21	7.9	0.71	28.5	0.67		
June /70	3.36	5.3*	0.48*	36.2*	0.85*		
July /70	5.27	6.4*	0.57*	8.7*	0.21*	25.4*	0.22*
Aug. /70	4.27	7.47	0.67	20.7	0.49	50.2	0.43
Sept./70	0.81	4.55	0.41	8.3	0.20	20.2	0.18
Oct. /70	3.87	9.41	0.84	22.9	0.54	18.9	0.17
Nov. /70	3.33	27.35	2.46	114.7	2.71	223.1	1.97
Dec. /70	5.01	44.65	4.16	134.3	3.17	161.5	1.42
Jan. /71	3.14	36.2	3.22	113.7	2.69	350.1	3.09
Feb. /71	4.98	61.6	5.50	188.0	4.44	540.6	4.75
Mar. /71	3.01	40.8	3.63	140.3	3.31	347.6	3.06
Apr. /71	1.68	17.2	1.53	61.4	1.45	246.8	2.17
May /71	4.87	30.7	2.23	90.1	2.13	269.9*	2.39*
June /71	4.21	11.9	1.06	36.2	0.86	136.0*	1.20*
July /71	3.74	3.8	0.34	21.5	0.51	66.7	0.59
Aug. /71	1.51	4.5	0.40	24.3	0.57	89.7	0.79
Sept./71	4.45	4.5	0.40	59.3	1.40	169.9	1.49
Oct. /71	2.05	6.3*	0.56*	15.6*	0.37*	81.6*	0.72*

* Indicates an incomplete month's record.

Taking logs we get:

$$\text{Log } (Q) = \text{Log } (c) + n\text{Log } (H - B) \quad (3.4)$$

Thus a plot of $(H - B)$ against Q on log-log graph paper should plot on a straight line. Values of B were chosen by trial and error for the Locust, Spring and Swago Creeks rating curve until a reasonably straight line was obtained on a log-log graph of $(H - B)$ to Q . The curve was then extended to high and low discharges, in order to obtain a rating table for all stage values obtained. At Wildcat Cave only one measurement of stage and discharge was obtained, and the rating curve was assumed to take the form of equation 3.4 above. Leopold, et al. (1964), tabulated the mean values for the exponent n in equation 3.1 for various types of channels. From these a value of 2.4 was used for n . B was set at 2:0 feet by inspection of the gauging site.

A simple program was written to convert the two hourly stage figures into discharges at all four stations using the derived rating curves. The mean monthly streamflows for the sites are given in Table 3.4, both in cfs. and in inches of runoff from the basins, and the streamflow shown in Figure 3.8.

3.3 Erosion Results

The erosion meter was described in Section 2.8. From the erosion figures the approximate age of Hughes Creek Cave was estimated. The erosion figures across the stream for the period September 1969 to July 1971, and to October 1971, are shown in Figure 3.9. The maximum erosion

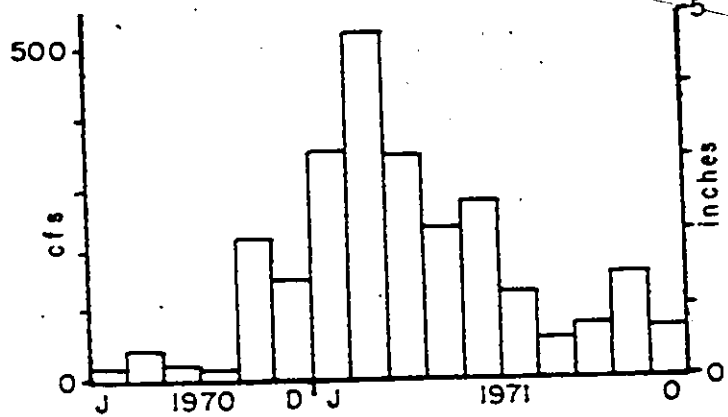
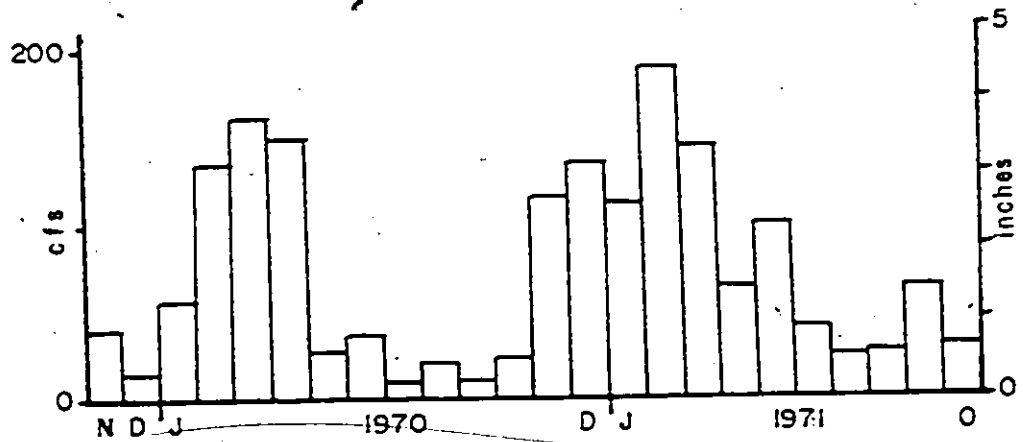
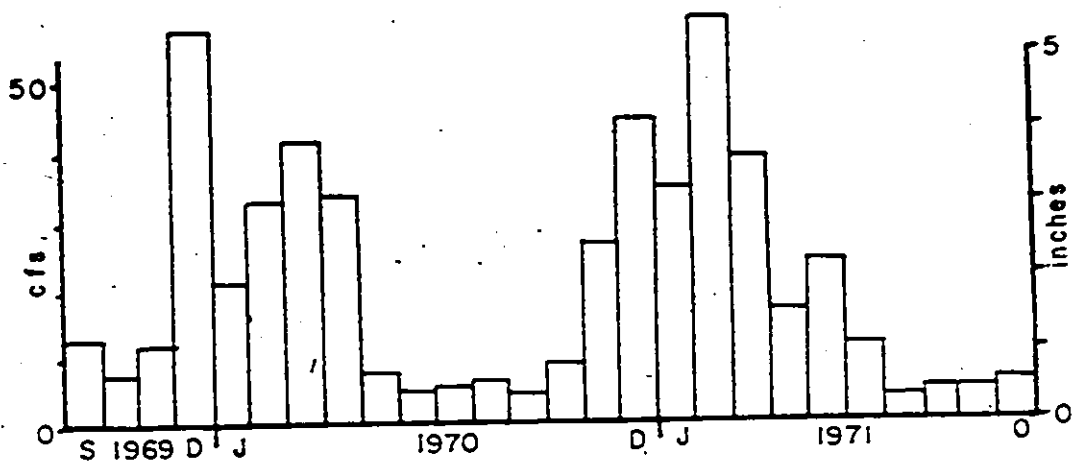


Figure 3.8 Monthly mean runoff at Swago, Locust and Spring Creeks..

at one position is 53-thousandths of an inch a year, and the minimum an apparent deposition of 8-thousandths per year. The reason for the apparent deposition is not known. The position of this erosion site was on a thin shale band above the normal stream level, and the reading could be due to expansion of the shale, true deposition, or to a measuring error.

The average erosion during the period September 1969 to July 1971 is 30.5 thou/year, from July 1971 to October 1971 is 25.2 thou/year, and for the total period is 29.8 thou/year. The lowered erosion during the summer of 1971 is due to drier conditions.

Taking the mean erosion throughout the total period, the stream is eroding at a rate of 1 inch per 34 years, or 1 foot in 400 years.

The erosion of the streambed depends on a number of variables such as the flow rate, chemical characteristics of the water, and temperature. In order to relate the erosion figures to the age of the caves, some idea of past climatic conditions must be known.

3.3.1 Past Climatic Conditions and Past Erosion Rates

Climatic conditions in the eastern part of the U.S.A. in the past have been inferred from a number of diverse studies. Thompson (1973) studied the past climatic conditions in West Virginia in order to confirm his paleotemperature estimates which were based on the isotopic composition of speleothems. Thompson concluded that the climatic conditions have warmed up in the last 10,000 or so years, based on evidence of

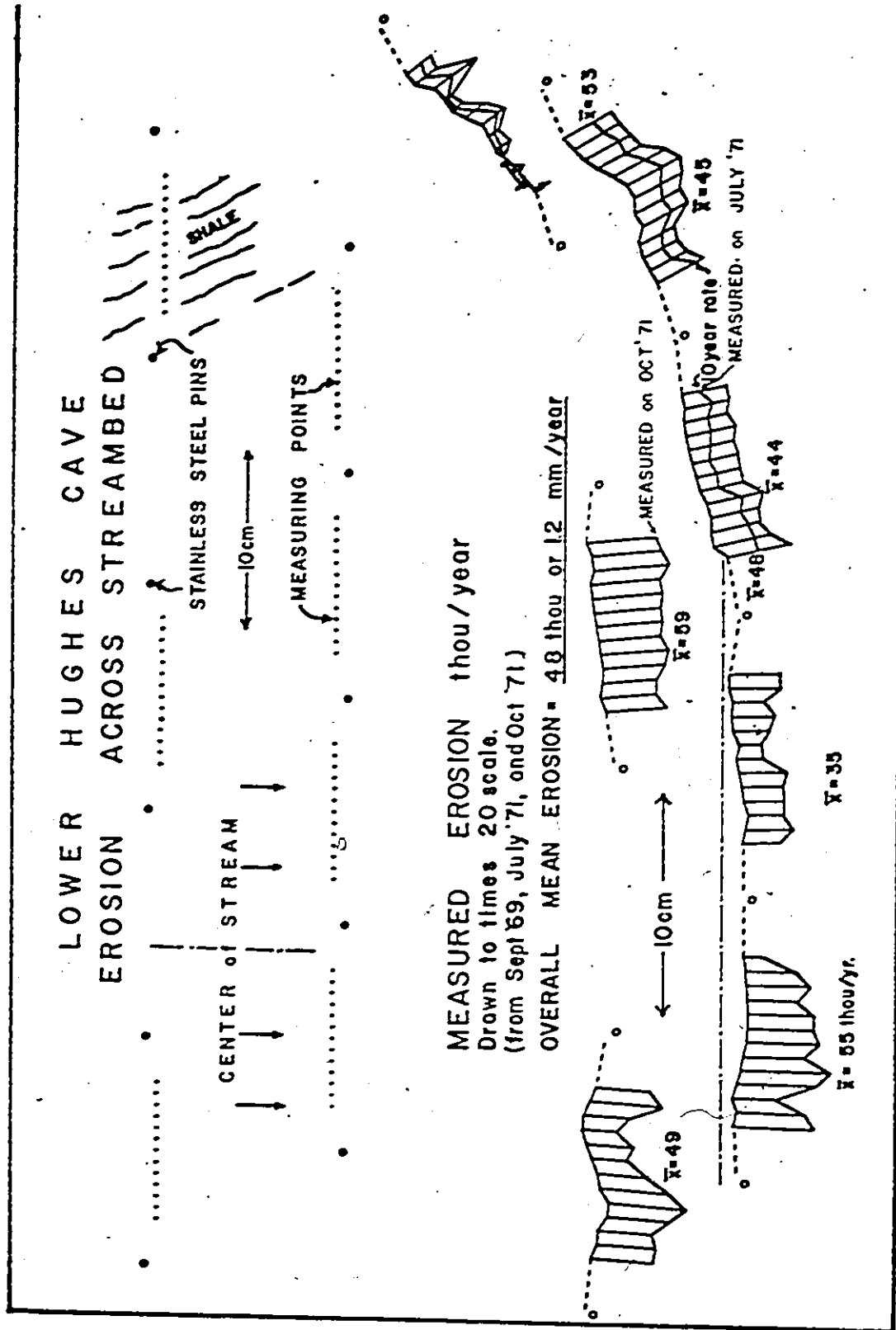


Figure 3.9 Erosion at Hughes Creek Cave. The diagrams show the erosion that would take place in 20 years.

patterned ground (Clark, 1968), pollen studies (Craig, 1969) and his own work.

In the past when the temperature was lower, the relative erosion rate would be smaller than today due to the lowered aggressiveness of the water caused by the lowering of CO_2 in the soil, other factors being equal. Evidence is given in Section 6.3 that the proportionate flow through Upper Hughes Cave is decreasing as the Hills Creek stream is finding a more direct route to Locust Spring. During Stage 4 (Section 6.3.4) the whole of Hills Creek flowed through Hills-Bruffey Cave to Upper Hughes Cave. At present, however, most of the Hills water is diverted to Clyde Cochrane Cave, and does not pass through Lower Hughes Cave. It is likely therefore that during the last few thousand years the flow in Hughes Cave has decreased.

The lowering of temperatures in the past few thousand years will tend to decrease the rate of erosion. The increased flow rate, however, will tend to increase the erosional rate. Overall the erosional rate will probably not be markedly different than that at present.

The cave was initiated under phreatic conditions and now floods to the roof occasionally; in each case the erosion would take place on the roof as well as on the floor. The roof erosion, however, has not been large, as there are still anastomoses and half tubes in the ceilings of nearby passages, and was neglected in this age calculation. As the cave is now eroding at the rate of 1 foot per 400 years, and as the passage is 8 feet high, the Hughes Creek Cave is about 3200 years old, if the erosion rate has been constant during that period.

CHAPTER IV

SIMULATION

Water movement in a river basin is a dynamic process. Water enters a basin by precipitation and leaves by streamflow, by evapotranspiration, and possibly by ground water flow. The response of streamflow to precipitation is not instantaneous, but depends on the holdup of water as snow, by vegetation, by the soil, by the stream channel, or as ground water. The routing of the water through the basin can be represented by a set of mathematical algorithms. The set of algorithms is one type of deterministic simulation model. This type of model generates streamflows from known climatic conditions, using a defined set of algorithms.

For this study the three basins (Swago, Locust and Spring Creeks) were modelled using a deterministic model. The algorithms and parameters in the model were altered until a good fit was obtained between the simulated and real streamflows. Certain characteristics of the basin were then inferred from the parameter values that were used to model each basin.

It was found that the objectives of the simulation study were not fully met. The climatic data available were poor, and it was not possible to achieve a good match between the simulated and real streamflows. For this reason the output was found to be fairly insensitive to the model algorithms used and the basin characteristics could not be well defined from the type of model used. However some general characteristics of the basins were determined from the simulation study.

4.1 Description of the Real System Being Modelled

The system being modelled is shown in Figure 4.1. Precipitation falls as rain or snow, and may deplete or increase any snowpack. Some of the rain or snow may be intercepted by vegetation, while the remaining water falls onto the ground. Depending on the dryness of the soil, a portion of this water infiltrates the soil, and the rest runs off as overland flow. Three underground storages are modelled—an upper zone in the soil, a lower zone in the soil, and a ground water storage. The water percolates from the upper zone through the lower zone in the soil to the ground water storage. Water flows from the lower zone and ground water storages into the stream to give a fast and a slow ground water component.

The two outflows from the ground water and the overland flows are combined to give the simulated streamflow. Evapotranspiration takes place from the upper zone storage, from the snowpack, from the interception storage, and possibly from the ground water storage and channel surfaces.

4.1.1 Description of Model Used

For modelling, the basins were divided up into a number of segments, or sub-basins, on the basis of lithology and vegetation cover. Throughout each segment the hydrological characteristics such as soil type, vegetation cover, and infiltration capacity, were assumed to be the same. The program modelled each segment in turn to obtain a segmental streamflow. The streamflows were then summed and routed to give the

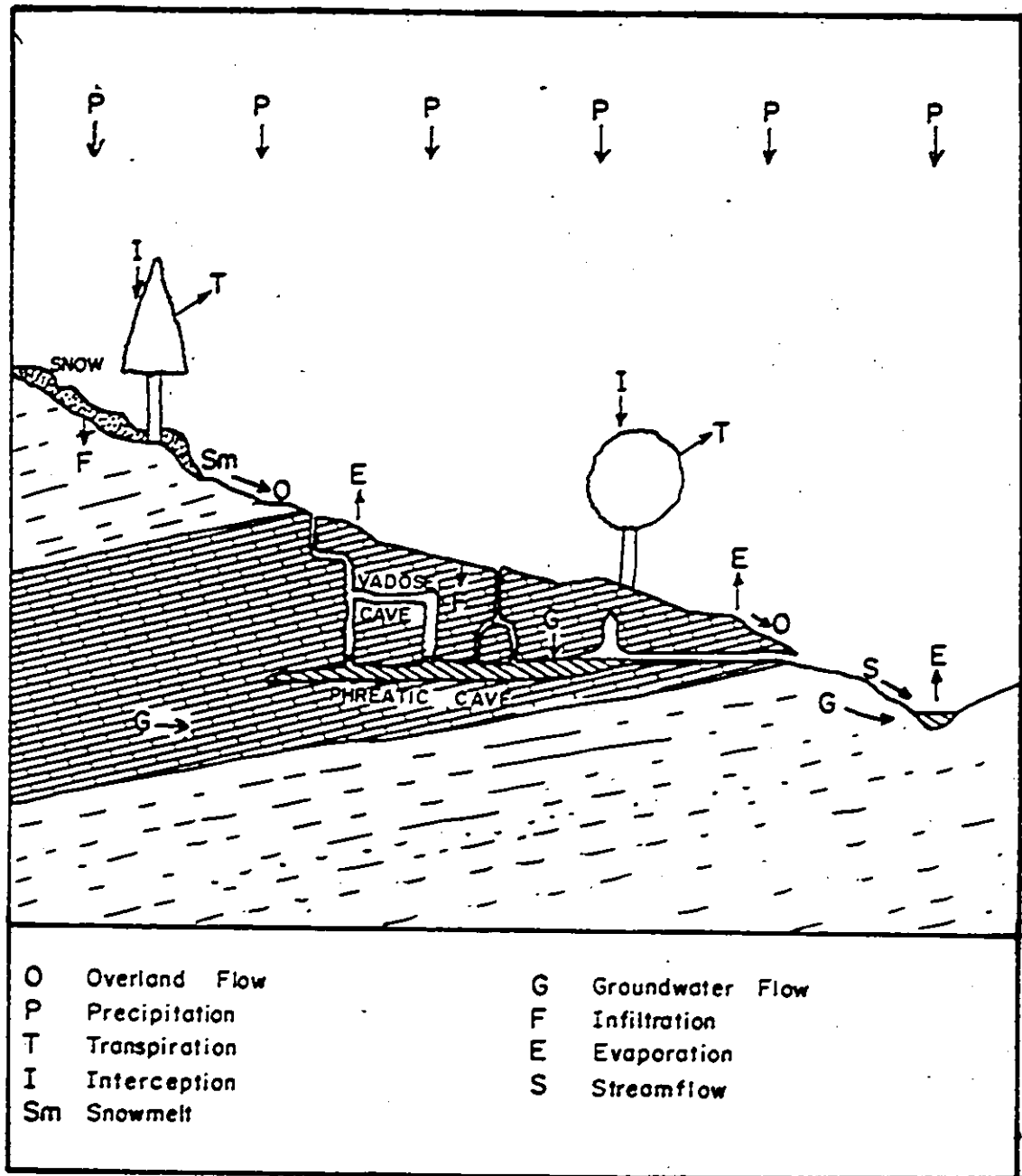


Figure 4.1 Idealized hydrological cycle in a karst basin.

final basin streamflow. During initial simulation runs only one segment was modelled. As the simulation was developed, more segments were used.

The hydrological system being modelled is shown in Figure 4.1, and the flow diagram of the computer program to simulate the hydrology is shown in Figure 4.2. The model consists of a number of storage locations with water flowing between the different storages according to defined mathematical relationships. The mathematical relationships were arranged to be continuous over normal values, and checks were made for negative or excessive storages or water flows, and counter action taken.

The mathematical relationships were based on the known properties of the hydrologic cycle, and are described in detail in Section 4.2. The relationships include a number of parameters which are selected by the user. The parameters include such quantities as the basin area, infiltration rates, and maximum water storage in various locations (Table 4.1). When modelling, the parameters are initially chosen from experience or from hydrological information, and the parameters are changed to obtain a good simulation match.

This type of simulation model was largely developed at Stanford University between 1959 and 1965 (Crawford and Linsley, 1966). The program was originally written in ALGOL but has been translated to FORTRAN by James (1966) and by Claborn and Moore (1970). The translation by James, known as the Kentucky Watershed Model, has been widely used (for example by Drooker (1968), James et al. (1969), Miller (1968), Ross (1970), and Villines (1968)).

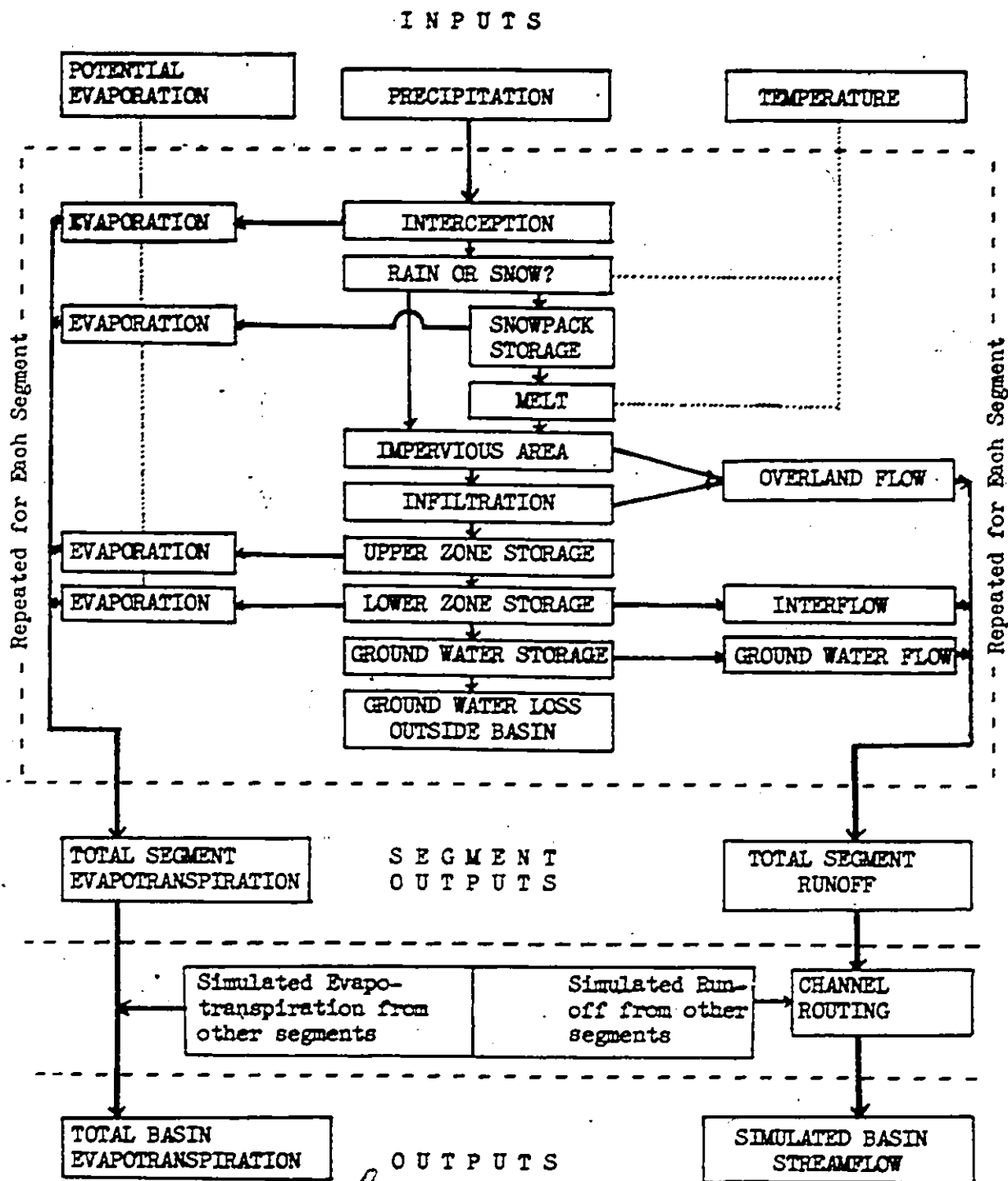


Figure 4.2 Flow diagram for the hydrologic model.

The Stanford and Kentucky models are large comprehensive programs which use a great deal of computer storage and time, and are therefore expensive to run. Although good results have been achieved by these models, simpler versions can often be run satisfactorily (for example Porter and McMahon (1971), England and Coates (1971)). For this study a shorter version of the Kentucky model was implemented, as it was relatively fast and used a small amount of computer storage.

4.2 Details of the Algorithms Used in the Model

4.2.1 Interception

A portion of the precipitation falling on trees, vegetation and surface litter is stored and subsequently evaporated off. For this model the interception process was assumed to consist of a fixed sized reservoir which was allowed to fill up before any rain would reach the surface. The water in the interception storage was evaporated off at the potential rate at each time interval. The maximum interception storage was set initially at 0.2 inches for forests and at 0.1 inches for grassland or other low vegetation.

Little is known of snow interception (Miller, 1965) and its magnitude is hard to determine. For simplicity, snow interception was assumed to occur at the same rate as that of rain.

Table 4.1

List of Parameters Used in the Model

<u>Name</u>	<u>Description</u>	<u>Units</u>
PARAMETERS EASILY MEASURABLE FROM MAPS AND AIR PHOTOS		
AREA	segment area	square miles
HTSTA	mean elevation of the climatic stations	feet
HTSEG	mean elevation of the segment	feet
SIA	proportion of impervious area in segment	--
SAWT	proportion of lakes, channels and open water in the segment	--
ART	proportion of segment where interception does not occur	--
EASILY ESTIMATED PARAMETERS		
LPSRT	lapse rate	°F/1000 ft.
GWRRT	ground water recession rate	days
BZK	interflow recession rate	1/days
TIMET	time delay histogram	1/analysis time
IADD	time delay between segments	days
ASM	interception storage	inches
EVAPC	evaporation constant	--
GWEA	ground water evaporation coefficient	--
SNOW PARAMETERS		
GM	ground melt	inches/day
TCOFF	temperature index for snowmelt	inches/day/°F

(cont'd...)

Table 4.1 (cont'd)List of Parameters Used in the Model

<u>Name</u>	<u>Description</u>	<u>Units</u>
INITIAL CONDITIONS		
AST INT	interception storage	inches
UZS INT	upper zone storage	inches
LZS INT	lower zone storage	inches
GWS INT	ground water storage	inches
WE INT	snow pack storage	inches of water equivalent
PARAMETERS FOUND BY OPTIMIZATION		
INFMAX	infiltration rate, maximum	inches/day
INFMIN	infiltration rate, minimum	inches/day
INFRT	infiltration coefficient	--
SOILE	soil evaporation coefficient	--
UBCOF	upper to lower zone percolation coefficient	--
BGCOF	lower zone to ground water percolation coefficient	--
LZSN	nominal lower zone storage	inches
UZSN	nominal upper zone storage	inches

4.2.2 Snow

The precipitation was divided into rain or snow on the basis of temperature. If the mean temperature was above 33°F the precipitation was assumed to be rain, which, if any snowpack was present, contributed to the snowmelt. Falling snow increased the snowpack.

On days without precipitation the snow melts due to a number of factors such as absorbed radiation, condensation, conduction of heat from the ground and convection from the air. The U.S. Corps of Engineers (1960) have evolved relationships to describe the melt, which have been programmed by Anderson and Crawford (1964). The relationships are fairly complicated however, and require detailed input data of radiation, wind, etc. The relationships have been found to give poor representation in some situations (Pysklywec, 1966). The simpler degree-day or temperature index method was used here (Woo, personal communication, 1972), where the melt is made proportional to the temperature above freezing. Thus:

$$M = DDF(T - 32) \quad (4.1)$$

where M is the melt in inches of water equivalent a day,

DDF is the index for temperature melt, and

T is the mean daily temperature in degrees F.

The index DDF controls the rate of melting. Published values range from 0.05 to 0.15 inches/day/°F (Davar, 1970). Horton (1945) found DDF values of 0.06 inches/day/°F on heavily forested basins, and 0.09 inches/day/°F on basins with thin cover in western Pennsylvania.

These values were used for the basins in West Virginia.

Other forms of melt are modelled by allowing a constant amount of the snow to melt each day. This approximates the melt due to radiation, condensation and ground melt. Davar (1970) suggests using 0.02 inches/day for this constant melt, a figure which was used in this study.

4.2.3 Infiltration

Rain falling on the surface can infiltrate up to the infiltration capacity of the soil, then the excess fills up detention storage and starts overland flow. The infiltration capacity is related to the amount of water in the soil: as the soil gets wet the infiltration capacity decreases towards some low constant amount.

For this model the infiltration capacity was determined by the water level in the upper zone (soil) storage, using the relationship found by Philip (1963), which is:

$$F = b \exp\left[\frac{-c \text{ UZS}}{\text{UZSN}}\right] + a \quad (4.2)$$

where F is the infiltration capacity,

UZS is the water in the upper zone storage,

UZSN is the maximum amount of water that the upper zone can hold,

a is the minimum infiltration capacity when the soil is wet,

b is a constant such that a + b is the maximum infiltration capacity when the soil is dry, and

c is a constant relating the infiltration capacity to the soil moisture.

In any real basin, the soil conditions will not be the same throughout the basin, as some areas will be wetter than other areas, and so the infiltration rate will also vary throughout the basin. In order to model this condition the infiltration rate was assumed to vary linearly from zero up to the maximum rate determined by equation 4.2, as shown in Figure 4.3 (Crawford and Linsley, 1966). With a certain rainfall excess (rainfall plus snowmelt minus interception) the infiltration will be given by the shaded area in Figure 4.3. This area can be given by:

$$I = P - \frac{P^2}{2F}, \text{ if } F > P \quad (4.3)$$

$$I = \frac{F}{2}, \text{ if } F < P \quad (4.4)$$

where I is the actual infiltration rate, and

P is the rainfall excess.

Water is lost from the soil storage by evapotranspiration and by percolation downwards to the ground water storage. The percolation is considered to take place in two stages from the soil storage to the lower zone storage, and from the lower zone storage to the ground water storage.

Both percolations were modelled by making the flow dependant on the moisture conditions in the top storage location as:

$$UBF = UBCO \times \frac{UZS^2}{UZSN} \quad (4.5)$$

where UBF is the upper to lower zone percolation, and

$UBCO$ is upper to lower zone percolation coefficient.

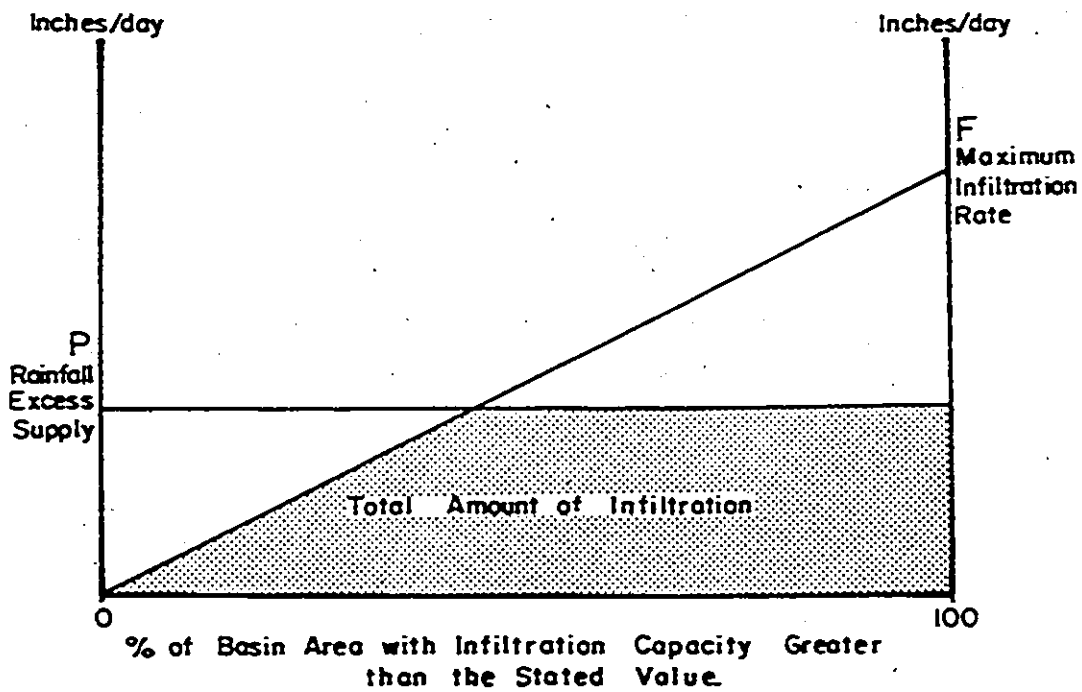


Figure 4.3 Modelled infiltration rate with varying rainfall excess. The rainfall excess is the rainfall plus the snowmelt minus the interception.

Also:

$$BGF = BGCO \times \frac{LZS^2}{LZSN} \quad (4.6)$$

where BGF is the lower zone to ground water percolation,
 BGCO is the lower zone to ground water percolation coefficient,
 LZS is the lower zone storage level, and
 LZSN is the nominal lower zone storage.

The lower zone and ground water storages were modelled as contributing to the fast and slow baseflow component of the streamflow. The flow took the form of the well-known exponential decay function as:

$$GWF = GWK \times GWS \quad (4.7)$$

where GWF is the ground water flow and
 GWK is the ground water recession-constant,
 and:

$$UZF = UZK \times LZS \quad (4.8)$$

where UZF is the interflow and
 UZK is the interflow recession constant.

4.2.4 Evapotranspiration

The amount of water that is evaporated off the various storage locations depends on the potential evaporation rate. The evaporation occurs first from the interception storage, then from the snow pack, and then from the upper and lower zone storages, until all the potential

evaporation has been satisfied.

The evapotranspiration from the soil will not be equal throughout a basin, as some areas of soil will be dry while other areas will be wet. Therefore the evapotranspiration opportunity of the soil is assumed to vary linearly from zero up to some maximum value R , in the same way as the infiltration shown in Figure 4.3.

The maximum evapotranspiration was related to the soil moisture as:

$$R = B \frac{UZS}{UZSN} \quad (4.9)$$

where B is a constant.

By analogy with Figure 4.3 it can be seen that the actual evapotranspiration ET can be given by:

$$ET = PE - \frac{PE^2}{2R}, \text{ if } PE \leq R, \text{ or} \quad (4.10)$$

$$ET = \frac{R}{2}, \text{ if } PE > R \quad (4.11)$$

where PE is the remaining potential evaporation, after evaporation from the snowpack and from interception.

In winter the evapotranspiration will be considerably reduced due to snow cover. Some transpiration will still take place from trees, although soil evaporation and transpiration from low vegetation will be negligible. The reduction in evapotranspiration was not taken into account in this model. In winter the potential evaporation is small and the evaporation from interception and from the snowpack often exceeds

the potential evaporation, in which case no evapotranspiration is assumed to occur from the soil.

4.2.5 Channel Routing

A time area method was used for channel routing (Crawford and Linsley, 1966). This method is simple but suffers from several sources of errors. The time of travel at one particular flow will not equal the time of travel at other flow rates. As the routing of floods tends to be more important than the routing of small peaks, a time area histogram for high flows was used in all cases. The time area histogram is estimated by using Manning's equation to calculate the flow times along the major reaches of the basin.

The addition of the segmental streamflow was also performed using a time delay summation method. If a basin was being simulated using several segments, the upstream segment streamflows are added to the lower segment streamflows with a specified time delay. This represents tributaries joining the main channel with the specified channel hydraulic delay to the gauging site.

4.2.6 Overland Flow

Overland flow is an important function for flood flows. In a small basin, however, the flow is usually fast and takes less than a day to arrive at the channel. As the modelling period was usually one day, no overland flow modelling was performed in this study.

4.3 Objective Function

During simulation optimization and testing, the model is adjusted and parameters are changed until a good "fit" is obtained between the real and the simulated responses. An objective function can be a measure of the degree of fit between the responses. Usually the objective function is minimized when the fit is good.

In some simulation programs a discrete objective function is not calculated, and the model is optimized by visually comparing the real and simulated responses. A discrete objective function is essential for automatic optimization techniques, and can be very useful during manual optimization. Some objective functions can also be used to compare the results of simulating different basins.

4.3.1 Purpose and Choice of Objective Function

The objective function is a measure of the goodness of fit of a model and must be chosen to stress important objectives of the simulation. For streamflow generators the objective function could be chosen to optimize the following conditions:

- a) peak flows for flood control,
- b) temporal relationships in the flood peaks,
- c) base flows for droughts or pollution control,
- d) average flows for resource planning.

For many studies, several or all of the above four criteria need to be met. The objective of the present study was to use the model to

predict characteristics of the real system. As the real system can affect peak flows, base flows, mean flows and the temporal relationships during flood pulses, an attempt was made to optimize the model using all of the above criteria. It was realized that optimizing using all four objectives may impair the optimization on any one of the conditions.

No single objective function can be used to optimize well all four criteria. Thus it was decided to generate three objective functions—one which optimized peak and base flows, one the mean flows, and one for the temporal relationships. A composite objective function was generated by summing the three individual objective functions.

The objective functions chosen should possess certain attributes. It is important that the objective function should be:

- a) powerful and sensitive,
- b) physically based, so that the rationale and magnitude of the parameter can be understood,
- c) relevant, that is it should stress important objectives in the simulation,
- d) non-dimensional with analysis time or flow volumes, so that different models and basins can be compared,
- e) easy to calculate, to economize on computer time.

All objective functions used in this study possessed the above attributes, as far as possible.

4.3.2 Description of Objective Functions Used

A number of different objective functions have been used in published simulation studies. A least squares criterion is commonly used, for example by Hudlow (1969), Nash and Sutcliffe (1970), O'Connell et al. (1970), and Manderville (1970). A least squares criteria, however, only optimizes peak values. In streamflow generation in small basins, where the flood values may be an order of magnitude larger than the average flows, the largest flood has an exceedingly large weight in the objective function, and low, average and even moderately high flows hardly affect the objective function. Optimization using a least squares objective function will only match the peak flows, and can leave the base flows considerably in error.

Absolute values (Sittner et al. (1969), Crawford and Linsley (1966)), and correlation coefficients (Betson (1965), Crawford and Linsley (1966)), have also been used, but these also emphasize flood values.

Liety and Dawdy (1969) have used an objective function of the form:

$$Z = \sum_{i=1}^N (\log Q_i - \log F_i)^2 \quad (4.12)$$

where Z is the objective function,

Q_i is the real flow at step i,

F_i is the simulated flow at step i.

This objective function gives equal weights to high and low values, and effectively considers the ratio of the real and simulated flows. The

objective function (equation 4.12) is dimensioned with regards to time, and because of the squared term also emphasizes values which are greatly in error. Equation 4.12 was modified here to:

$$U_1 = \frac{1}{N} \sum_{i=1}^N \text{ABS} (\log Q_i - \log F_i) \quad (4.13)$$

where U_1 is the "peak" objective function,

ABS is the positive value of the expression,

N is the number of analysis points.

This objective function is sensitive to both flood and drought conditions, is non-dimensional, and gives a proportioned amount of weight to values greatly or slightly in error.

The mean flows were optimized using a simple objective function, as follows:

$$U_2 = \frac{\bar{Q} - \bar{F}}{\bar{Q}} \quad (4.14)$$

where U_2 is the "mean objective function,

\bar{Q} is the mean real flow, and

\bar{F} is the mean simulated flow.

The temporal relationships have not been well investigated except by workers on discrete parts of the hydrological cycle, for example by Hudlow (1969) and Henderson and Wooding (1964) who were studying lag times.

For this study a temporal objective function was calculated as:

$$U_3 = \frac{1}{N} \sum_{i=2}^N \text{ABS} (\log Q_i - \log F_{i-1}) - \frac{1}{N} \sum_{i=2}^N \text{ABS} (\log Q_{i-1} - \log F_i) \quad (4.15)$$

where U_3 is the "temporal" objective function.

U_3 is positive if the real hydrograph (Q) lags the simulated hydrograph (F), and negative if the real hydrograph leads the simulated.

All three optimization functions tend to zero as optimization is improved. U_1 can only be positive, but U_2 and U_3 can be either positive or negative. A final single objective function was obtained by summing the three functions U_1 , U_2 , and U_3 . As it was decided to give equal weight to each function, and as the magnitudes of the functions were similar, the final objective function U_4 was given as:

$$U_4 = U_1 + \text{ABS}(U_2) + \text{ABS}(U_3) \quad (4.16)$$

where U_4 is the "total" objective function.

The four objective functions were calculated for different selected periods throughout the analysis (e.g. in summer and winter, or by months) and also summed for the total period. A sensitivity analysis was carried out (Section 4.6) to determine the effects of each model parameter on each objective function. Optimization of the model was carried out using the sensitive objective function values while optimizing each parameter in turn. The total objective function was used to compare the simulation in different basins, and also to determine the effects of different algorithms in the model.

4.4 Organization of the Computer Program

During testing and optimization of the model the simulation program was run many times with different parameters but with the same climatic and streamflow data. As the handling, converting, and checking of the climatic and streamflow data took an appreciable amount of computer time, three subsidiary programs were used to generate the basic input data in a form that could be quickly used by the simulation program, which was called KARST. The purpose of the three subsidiary programs--REEDAT, PRECON, and RATNG--and their interaction with KARST, are shown in Figure 4.4.

The data from each of the climatic stations was punched up onto cards, then read and checked by the program REEDAT. The climatic data was then preconverted by the program PRECON which generates weighted mean climatic data over the basin being simulated. Each of these programs generates a binary file of data which can be stored on a temporary disk, on a permanent file, or on a tape. The two-hourly stage readings at the streamflow stations were punched onto cards. The program RATNG converted the stage readings to daily discharge values, which were also written onto a binary file.

The two files containing the converted climatic and streamflow data were used by the main simulation program. This program contained subroutines performing the algorithms described in Section 4.2, as well as control and input and output subroutines.

The full listings for the four programs are given in Appendix I. A brief description of the four programs REEDAT, PRECON, RATNG and

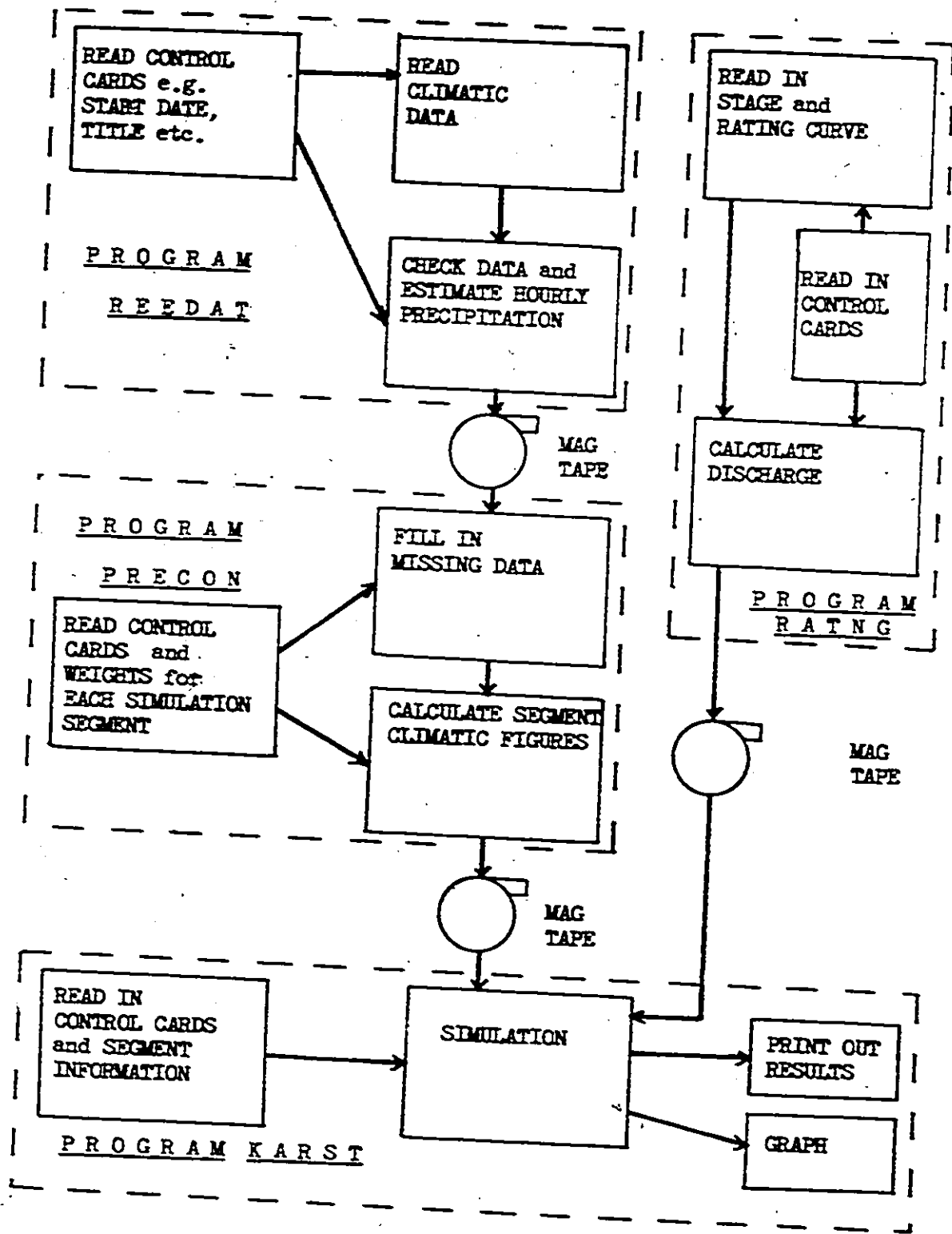


Figure 4.4 Flow chart for the data input and program divisions.

KARST, and the data input, are given in the following subsections.

4.4.1 Climatic Data Input

Climatic data were obtained from the five climatic stations described in Section 3.1. Hourly precipitation data were used from the Marlinton station, daily precipitation data from the Buckeye and Renick stations, potential evaporation data from the Wardensville farm and Bluestone Dam stations, and maximum and minimum temperature data from the Buckeye station (Figure 3.1). The data showing daily precipitation, maximum and minimum temperatures, and potential evaporation were punched onto computer cards. Three cards per month were used. Published figures showing total monthly precipitation and evaporation, and mean temperature, were also punched onto the cards and used for checking.

Hourly precipitation figures were punched onto cards using two cards per day for any day on which there was precipitation. Thus a maximum of 62 cards could be used for one month's data. Usually only about 20 cards were needed each month as precipitation only falls about one day in three. The published figures of total monthly precipitation were also put onto the cards for checking purposes.

4.4.2 Description of Program REEDAT

REEDAT reads and checks the climatic data cards and writes a binary tape of these data. The daily precipitation, potential evapora-

tion, maximum and minimum temperatures, and hourly precipitation figures are checked against the monthly total or mean values, and messages printed out if there are errors.

The daily precipitation is distributed to hourly figures using an average diurnal precipitation distribution (Crawford and Linsley, 1966), taking into account the reading time during the day for the precipitation readings. The mean daily temperature is calculated from the maximum and minimum temperature figures.

Throughout the simulation the time was calculated as the number of days from an arbitrarily chosen datum date (picked as January 1st, 1950). This was easier than carrying the date through the simulation. By using this "day number", alignment of streamflow and climatic records and calculations of the mean parameters in a certain period could be easily and quickly carried out. It would have been slower and more difficult if the calculations had had to be done based on the date. The subroutine DAYM converts the date into the day number, even during leap years. An entry DATEM can be used to convert the day number back to the calendar date. DAYM is used both by REEDAT and by RATNG, which generates the streamflow data.

4.4.3 Description of Program PRECON

This program calculates weighted mean climatic data for use by the simulation program KARST. During simulation by KARST the basin is split up into a number of segments and streamflow generated from each segment. The program PRECON can generate different climatic data for

each segment, using different weights from the climatic stations.

PRECON also fills in missing data. This is done by reading in mean monthly data for the precipitation, potential evaporation and temperature figures, and filling in any data gaps using these mean figures. The climatic data for each segment are written out as a binary file on disk or tape.

PRECON was originally written to give daily temperature and evaporation figures and hourly precipitation output for use with a simulation program with a time interval of one hour. However a simplified version of PRECON was used for most of this study, which produced daily precipitation figures instead of hourly data. In this way the output binary file was shortened, and the climatic data reading in the simulation program KARST was speeded up.

4.4.4 Description of the Streamflow Data and the Program RATNG

The streamflow data at Swago, Locust and Spring Creeks were obtained from the stage recorders set up on each creek. These recorders produced a punched paper tape of stage data, taking a reading every fifteen minutes. The paper tape was two inches wide; unfortunately a reader for the tape could not easily be obtained, therefore the paper tape was read by eye and the data punched onto computer cards. Generally two-hourly stage readings were used, although when the stage was changing rapidly the average stage was estimated from the fifteen minute readings. During periods when the stage was changing slowly, daily

stage readings were taken.

Whenever the stage recorders were serviced and the tape changed, the time and date of the change were written on the tape and compared to the length of the punched tape. Errors of up to a day were sometimes found on the tapes due to the clocks being fast or slow. In these cases the timing errors were assumed to be constant throughout the period and the reading corrected by a proportionate amount.

The rating curves for the three sites were also determined (see Section 3.2) and these rating curves were digitized and punched onto cards.

Program RATNG reads the stage data and the rating curves, and generates a binary file of streamflow at two-hourly intervals. The date is converted to the day number and also written onto the output file for use by the simulation program. Checks are made in the program for missing data, although no provision was included for filling in the missing data. During periods when stage records were not available, zeros were written on the output file in order to maintain the data sequence. RATNG can also produce printer plot hydrographs of the streamflow, and listings of the mean daily and mean monthly streamflows.

4.4.5 Description of Program KARST

The hydrological simulation was performed by a program called KARST, which is listed in Appendix I. A listing and description of the input data cards required by KARST are given in Appendix III. A simpli-

fied flow chart for the program, which includes the names and purposes of the major subroutines in the program, is shown in Figure 4.5. A large proportion of the program performs control, reading, writing and accounting functions for the model. The routines called EVAPW, INTERC, INFLTR, GRNDW, PRECIP, SNOW and OVERFL calculate the algorithms described in Section 4.3.

KARST was written as a subroutine oriented program with each major function or job being contained in a separate subroutine. In this way different subroutines could be changed to perform different functions in a part of the program. Usually the rest of the program did not need to be modified when a subroutine was changed, and therefore the effect of the new subroutine could easily and quickly be seen. Splitting the program into subroutines also aided in the testing of the model, as subroutines were tested and verified separately, using a short driving program, and then combined into the complete program.

The program KARST (and several other programs) were maintained as an UPDATE file (CDC 1971), which is a utility routine for maintaining computer libraries on magnetic tapes. Additions, modifications and corrections to the program were generally made on the UPDATE file, and compilation of the routines was performed directly from the UPDATE program. The subroutines SNOW and PRECIP, however, were developed and tested using INTERCOM, the real time interactive system using the McMaster CDC 6400 computer. INTERCOM was found to be useful and efficient at program development, although the system was not readily available when the other routines were being written.

The program was set up as a single level overlay program so that a load module was produced on a named file. This overlay file was recalled several times in one job, so that the model could be run several times with different data during each job submission. Usually the overlay file, the file containing the climatic data produced by PRECON, and the streamflow file or files produced by RATNG, were all stored on a magnetic tape. The control and segment data for the model were inserted on cards while the program and the climatic and streamflow data were accessed off the computer tape by a suitable set of control cards. The job therefore consisted of only about 100 computer cards which were used to run the model six times with different data. The small physical size of the job and the multiple running of the model during each job submission expedited the simulation, particularly during optimization.

4.4.5.1 Descriptions of the Subroutines Used in KARST

The complete program KARST is a subroutine oriented program, containing a total of 24 subprograms, each of which performs one main function. The inter-relations and calling sequence of the subprograms are shown in Figure 4.5. For clarity the overall program will be described in the approximate order of the computation scheme with the sections which are computed first being described first. Subsidiary and accounting routines will be described at the end of this section.

The total simulation proceeds in four major stages, all of which are controlled by the main program in KARST. The first stage is

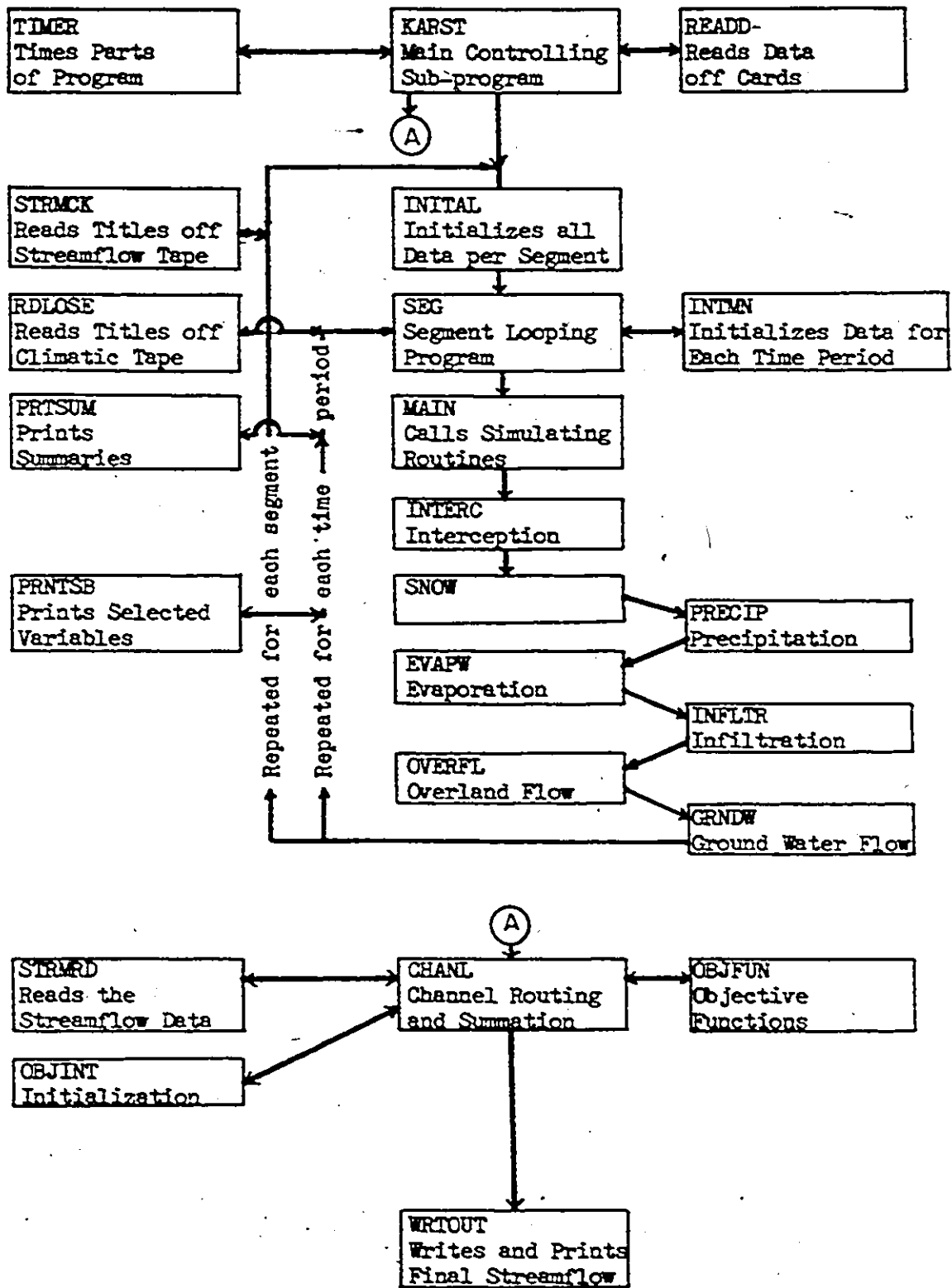


Figure 4.5 Flow chart for the simulation program KARST.

the data reading, the second is the segmental simulation, the third is segmental streamflow routing and summation, and the final stage is the printout of the results.

The segmental data are read in by the subroutine READD, which is the first major subroutine called by KARST. READD reads in and writes out the control data and the data for each segment. In addition, the titles and length of the binary climatic data are read in and printed out, and if the simulation is not to start on the first day that climatic data is available the number of days of climatic data that need to be skipped over is calculated.

The second and most important stage in the program is the calculation of the segmental streamflows. The streamflows are generated by the subroutine SEG and the variables and parameters for each segment are initialized by the subroutine INITAL. These two subroutines are called one or more times by KARST, depending on the number of segments being simulated.

SEG reads in the climatic data each day, calls INTMN, which initializes the variables at each time step and also extracts the correct precipitation, temperature and evaporation figures for the simulation, and then calls MAIN which is the main calling subprogram for the simulation algorithms described in Section 4.2.

Subprogram MAIN calls in six "core" subroutines that carry out the algorithms described in Section 4.2 in addition to subroutines that print out the intermediate data and model variables during the simulation. The subroutines SNOW, INTERC, INFILTR, GRNDW, OVERFL, and EVAPW perform the calculations for snow, interception, infiltration, ground

water, overland flow (which is not used here), and evaporation of water, respectively. The calculations of the algorithms are relatively simple. A major part of the routines is to maintain the water balance and to check for negative flows and storages during the calculation. Thus all water that enters the model basin must leave by either evaporation or by streamflow, or increase the storage in one or more of the storage areas. During testing of each routine, checks were performed to ensure that the water was conserved, under all possible conditions. Checks are also made throughout all six of these subroutines for impending negative flows or storages, and counteraction taken.

Before, between and after the calls to the core subroutines, MAIN calls PRNTSB to store and print out important variables in the model. In addition PRTSUM is called in to calculate a water balance summary over a specified period. At the end of each time step, MAIN writes the segmental simulated streamflow onto a disk file for use later in the program.

The third major section of the simulation is the channel routing and segmental streamflow summation section which is performed in subroutine CHANEL. This subroutine reads in the streamflows for all the segments, and routes and sums the streamflows according to the specified time-delay histograms and time-delay summation method described in Section 4.2.5. CHANEL also reads in the real streamflow from the streamflow file, and then writes the real and simulated streamflows out on a disk for use by WRTOUT. In addition CHANEL calls in OBJFUN which calculates the objective functions. The functions can be calculated for a number of specified periods.

The fourth and last major stage in the simulation is the writing out of the data, which is carried out by the subroutine WRTOUT. This subprogram produces a printer plot and a listing of the simulated and real streamflows. The precipitation is included on the graph and listing for comparison.

As well as the "main line" subroutines described above, a number of other routines are included in the complete program to perform other accounting or control functions.

STRMCK, which is called by KARST, reads off and prints out the titles from the streamflow file. This subroutine also positions the streamflow file at the record for the first day that is being simulated. STRMRD, which is called in by CHANEL at each time step, reads in the streamflow data.

RDLOSE positions the climatic data file. This routine is called in by KARST before each segmental simulation. The routine reads in and rejects the titles on the climatic file and then positions the file at the record for the first day that is being simulated.

OBJINT initializes the objective function calculations. TIMER is used as a checking program to time various parts of the program, and was used in early development to investigate and speed up slow parts of the program.

4.5 Optimization of the Simulation Program

Optimization during simulation is the process of modifying the parameters and possibly also the algorithms of a model to obtain the "best fit" between the real system and the model responses. The "best fit" is obtained by minimizing the objective function. This function gives a measure of the difference between the two responses. When manually optimizing a model by visually minimizing the difference between the real and simulated hydrographs, the objective function is implicit and is very subjective. Optimization can be carried out by manual (trial and error) methods, or automatically by using a program or system to objectively find a good set of parameters for the model. The advantages and disadvantages of the two methods are discussed below.

4.5.1 Automatic Methods of Optimization

Automatic optimization of streamflow generator simulations is not common but has been used for simple parametric hydrological models, for example by O'Connell (1970) using the steepest ascent method, and by James (L.D. James, 1972) using a more complicated model. James used a program called OPSET to determine the optimum set of parameters for the Kentucky version of the Stanford model. Thirteen parameters were determined by four different methods. Two baseflow parameters were calculated directly from the real hydrograph recession. Four parameters were optimized by considering the mean monthly flow volumes, and six other parameters were optimized on hourly flows. The final parameter

was calculated by considering the runoff after storms. The program OPSET did not optimize any snow parameters.

The results from OPSET are not very good, as considerable discrepancies between the real and simulated flows occur, particularly at the intermediate flow rates. As the baseflow parameters are optimized using the real hydrography recessions, low flows are modelled well. As the other parameters are optimized using a sum-of-squares-of-deviations objective function, the peak flows are also modelled well, as described in Section 4.3. However intermediate flows can be 3000% in error, or more, as shown in Table 4.2.

In Table 4.2 the published results (L.D. James, 1972) are shown at the top, and the same quantities shown below for the water year 1963-4. It can be seen that the low and the peak day and month agree reasonably well between the recorded and simulated flows for both years. Some selected figures for the 1963-4 year, however, are shown at the bottom of the table. It can be seen that the simulated flow during September is almost 10 times the recorded flow, on September 28th it is 38 times the recorded flow, and large errors occur on other days throughout the year. Thus OPSET does not give a set of parameters which can model the real system satisfactorily.

James (L.D. James, 1972) indicates that there were problems in writing and running the program, and that ridiculous parameter values were often obtained. Because of the difficulties in running an automatic optimizing program that would give satisfactory results, automatic optimization was not used in this study.

Table 4.2

Comparison of Recorded and Simulated Flows Using OPSET
on the Elkhorn Creek, Kentucky

Results from Table (2), page 295 of James (1972)

"First" Year *	Recorded Flow (flow in cfs-days)	Simulated Flow
Annual	280,000	238,000
Peak Month	99,000	84,100
Low Month	258	175
Peak Day	17,200	16,900
Low Day	2	0

*The year was not stated in the paper.

Results of Water Year 1963-4 (S. Singer, personal communication, 1973)

	Recorded Flow (flow in cfs-days)	Simulated Flow
Annual	191,538	232,130
Peak Month	133,587	128,993
Low Month	615	615
Peak Day	22,100	19,219
Low Day	9.0*	10.7*

*Different dates.

Selected Flows, Water Year 1963-4 (S. Singer, personal communication, 1973)

	Recorded Flow (flow in cfs-days)	Simulated Flow
Month of September	1,307	12,563
September 28	54	2,066
April 23	440	1,385
January 7	2,510	929
June 21	120	540

4.5.2 Manual Methods of Optimization

For manual optimization the model is run using an estimated initial set of parameters. The objective functions and the recorded and/or simulated hydrographs are then inspected and changes made to one or possibly more parameters. The model is then rerun. This process is repeated until the hydrologist is satisfied with the model (or until time and money run out), possibly for several hundred trials. Manual optimization was used in this study.

For this study the "goodness of fit" of the model was based both on the objective functions (Section 4.3) and on inspection of the real and the simulated hydrographs. It was found that the effect of a change in one particular parameter on the simulated hydrograph could be estimated reasonably well from experience and from the results of the sensitivity analysis (Section 4.6). Thus, parameter adjustment to improve the simulated hydrograph was found to be a fairly efficient process, although it was commonly found that an improvement at one part of the hydrograph resulted in a degradation at some other part.

Parameter optimization was carried out in three major stages. The ground water and interflow parameters were optimized by considering the mean monthly flows and the mean objective function during the summer period. Interception, infiltration and channel routing parameters were optimized by considering the daily flows and the peak and temporal objective functions, again in the summer. Finally the snow parameters were optimized during the winter and early spring periods.

The optimization was carried out by running batch jobs on the

McMaster computer. Although time sharing was considered for optimization, the slow printing speed on terminals available reduced the advantage of the real time interaction.

4.6 Sensitivity Analysis

A sensitivity analysis was carried out to determine which model parameters had a significant effect of the objective functions and on the simulation. The results of the sensitivity analysis were used to assist in the optimization of the model. By using Table 4.3 it was possible to estimate which parameters should be changed, and the approximate direction and magnitude of the change, in order to correct an error in the response of the model.

The sensitivity analysis was carried out on the Swago Creek basin for a 71 day period during September, October and November of 1970. Three 19 day subperiods were chosen from the 71 day period, in order to determine the sensitivity of the parameters during different conditions. The subperiods were from the 1st to the 19th day, from the 34th to the 52nd day, and from the 53rd to the 71st day. The first period was chosen in order to test initial conditions, the second to test for modeling during a period when there was no snow, and the third to determine sensitivity during a period when some snow fell.

The parameters for the sensitivity run were initially estimated from other simulation studies or from physical reasoning. A few runs were made and the parameters adjusted by trial and error until a reason-

able simulation was obtained. The base values for the parameters and the values of the objective functions are listed in Table 4.3.

Each parameter which was chosen was then perturbed by a small amount (usually increased by 10% of its value, or by 0.1 if the parameter was a proportion); and the effect on the objective function in the three subperiods was noted. The perturbed value of the parameters and the effect on the objective functions are listed in Table 4.3.

The hydrographs for each run were also obtained and were inspected to determine the effect of each parameter on the hydrographs. The hydrographs were consulted later during optimization of the model, as the effect of some parameters could be more easily seen on the hydrographs than as the change in any objective functions.

Generally the results of the sensitivity analysis are fairly predictable. Thus a change in any of the initial parameters affected the first period considerably more than the last two; the snow parameters only affected the period when snow fell, and the channel routing parameter (TDMET) mainly affected the temporal objective function. However the sensitivity analysis did indicate in a more quantitative way the effects of parameter changes, and did show that several of the parameters have very insensitive effects.

It was found, during several extra runs, that most of the parameters are not orthogonal and that the sensitivity of a parameter is dependant on the values of the other parameters. Thus the numbers in Table 4.3 would not hold for other parameter sets, although parameters found to be sensitive in this analysis were nearly always found to be sensitive in other situations, and vice versa.

INITIAL CONDITIONS, DAY 1-19

123

	PEAK	MEAN	TEMP	TOTAL	SFLW
BASE VALUES	27.6	13.6	10.2	51.5	.03880

PARAMETER:	VALUE:		<u>% Change in Objective Functions</u>				
	BASE	PERTURBED					
SURFACE PARAMETERS							
AREA	12.	13.2	4.0	11.4	3.8	19.1	0.0
SHX	1.	1.1	0.2	-2.5	-0.9	-3.4	-2.3
SIA	.21	.231	0.9	1.8	0.1	2.8	1.5
SAWT	.01	.011	-0.1	-0.2	0.0	-0.4	-0.3
ASM	.15	.165	-0.8	-2.6	-0.9	-4.3	-2.3
ART	.1	.11	0.0	0.1	0.1	0.1	0.0
MAXIMUM STORAGES							
LZSN	2.	2.2	0.1	0.2	0.1	0.3	0.0
UZSN	1.1	1.21	-0.2	-1.3	-0.9	-2.5	-1.3
INITIAL PARAMETERS							
AST INT	.02	.022	0.1	0.2	0.2	0.4	0.3
UZS INT	.1	.11	0.7	1.0	0.5	2.1	0.8
LZS INT	.2	.22	1.6	2.8	1.6	5.8	2.3
GWS INT	.5	.55	0.8	2.5	1.2	4.4	2.0
WE INT	0.0	1.0	4.8	13.1	1.2	19.1	7.3
SOIL AND GROUND WATER PARAMETERS							
BZK	.15	.165	0.8	1.4	1.5	3.5	1.3
GWRRT	50.	55.	-0.8	-1.8	-0.9	-3.6	-1.6
GWEA	.05	.055	0.1	-0.1	0.0	-0.2	-0.3
TIMET(1)	.5,.5	1.,0.	-0.1	1.5	-12.4	-6.6	1.3
TIMET(2)	.5,.5	.6,.6	9.8	22.7	6.5	38.9	18.1
INFMX	2.	2.2	-0.2	-0.3	0.0	-0.5	-0.3
INFMN	.3	.33	0.0	0.0	0.0	-0.1	0.0
INFRT	.1	.11	0.0	0.0	0.0	-0.1	0.0
SOILE	1.	1.1	0.1	-0.3	-0.1	-0.4	-0.3
UBCOF	.5	.55	0.2	1.7	1.1	2.9	1.5
BGCOF	.1	.11	-0.1	-0.2	0.0	-0.4	-0.3
SNOW PARAMETERS							
GM	.02	.022	0.0	0.0	0.0	0.0	0.0
TCOEF	.08	.088	0.0	0.0	0.0	0.0	0.0
HTSTA	2150.	3150.	0.0	0.0	0.0	0.0	0.0
HTSEG	3500.	4500.	0.0	0.0	0.0	0.0	0.0
LPSRT	3.5	3.85	0.0	0.0	0.0	0.0	0.0

Table 4.3 Results of Sensitivity Analysis

	PEAK	MEAN	TEMP	TOTAL	SFLW
BASE VALUES	71.5	-47.3	-16.2	135.0	.01010

PARAMETER:	VALUE:		<u>% Change in Objective Function</u>				
	BASE	PERTURBED					
SURFACE PARAMETERS							
AREA	12.	13.2	-9.5	5.3	0.0	-15.0	0.0
SHX	1.	1.1	9.0	-4.3	-0.2	14.0	-8.9
SIA	.21	.231	1.8	-1.1	0.1	3.0	-2.4
SAWT	.01	.011	1.1	-0.4	-0.1	2.0	-1.2
ASM	.15	.165	1.5	-0.9	0.1	2.0	-2.0
ART	.1	.11	-0.5	0.2	0.0	-1.0	0.0
MAXIMUM STORAGES							
LZSN	2.	2.2	0.0	0.0	0.0	0.0	0.0
UZSN	1.1	1.21	0.7	-0.4	0.2	1.0	-1.1
INITIAL PARAMETERS							
AST INT	.02	.022	0.0	0.0	0.0	0.0	0.0
UZS INT	.1	.11	-0.3	0.2	0.0	0.0	0.0
LZS INT	.2	.22	-0.7	0.4	0.0	-1.0	0.0
GWS INT	.5	.55	-6.6	3.1	0.6	-10.0	5.8
WE INT	0.0	1.0	-2.0	1.1	0.0	-3.1	1.9
SOIL AND GROUND WATER PARAMETERS							
BZK	.15	.165	4.8	-1.9	-0.7	7.0	-3.9
GWRRT	50.	55.	1.8	-0.9	0.1	3.0	-2.1
GWEA	.05	.055	1.9	-0.8	-0.2	3.0	-1.8
TIMET(1)	.5,.5	1.,0.	6.0	-2.8	0.2	9.0	-5.9
TIMET(2)	.5,.5	.6,.6	-18.2	10.6	0.0	-29.0	18.0
INFNX	2.	2.2	-0.4	0.3	0.0	-1.0	0.0
INFMN	.3	.33	-0.1	0.1	0.0	0.0	0.0
INFRT	.1	.11	-0.1	0.1	0.0	0.0	0.0
SOILE	1.	1.1	2.2	-1.2	0.1	3.0	-2.7
UBCOF	.5	.55	-3.2	1.9	-0.1	-5.0	2.9
BGCOF	.1	.11	-0.1	0.0	0.1	0.0	0.0
SNOW PARAMETERS							
GM	.02	.022	0.0	0.0	0.0	0.0	0.0
TCOEF	.08	.088	0.0	0.0	0.0	0.0	0.0
HTSTA	2150.	3150.	0.0	0.0	0.0	0.0	0.0
HTSEG	3500.	4500.	0.0	0.0	0.0	0.0	0.0
LPSRT	3.5	3.85	0.0	0.0	0.0	0.0	0.0

Table 4.3 (cont'd)

	PEAK	MEAN	TEMP	TOTAL	SFLW
BASE VALUES	25.8	-18.0	-12.5	56.3	.03390

PARAMETER:	VALUE:		<u>% Change in Objective Functions</u>				
	BASE	PERTURBED					
SURFACE PARAMETERS							
AREA	12.	13.2	1.7	8.2	2.0	-8.4	0.0
SHX	1.	1.1	-0.3	-3.4	-0.9	3.9	-4.2
SIA	.21	.231	-0.1	0.0	-2.0	1.9	0.0
SAWT	.01	.011	0.0	0.0	0.0	0.0	0.0
ASM	.15	.165	0.0	-0.4	-0.5	0.9	-0.6
ART	.1	.11	-0.1	0.0	0.1	-0.2	0.0
MAXIMUM STORAGEES							
LZSN	2.	2.2	0.0	0.1	0.1	-0.2	0.0
UZSN	1.1	1.21	0.3	-0.3	-0.2	0.8	-0.3
INITIAL PARAMETERS							
AST INT	.02	.022	0.0	0.0	0.0	0.0	0.0
UZS INT	.1	.11	0.0	0.0	0.0	0.0	0.0
LZS INT	.2	.22	0.0	0.0	0.0	-0.1	0.0
GWS INT	.5	.55	0.0	0.7	0.5	-1.1	0.9
WE INT	0.0	1.0	0.0	0.1	0.1	-0.2	0.1
SOIL AND GROUND WATER PARAMETERS							
BZK	.15	.165	-0.5	0.6	0.3	-1.4	0.6
GWRRT	50.	55.	0.0	0.1	0.1	-0.3	0.0
GMEA	.05	.055	0.0	-0.4	-0.3	0.7	-0.6
TIMET(1)	.5,.5	1.,0.	4.4	0.0	-8.5	12.9	0.0
TIMET(2)	.5,.5	.6,.6	5.7	16.3	3.4	-14.1	18.0
INFMX	2.	2.2	0.0	0.0	0.3	-0.3	0.0
INFMN	.3	.33	0.0	0.0	0.1	-0.1	0.0
INFRT	.1	.11	0.0	0.0	0.1	-0.1	0.0
SOILE	1.	1.1	0.0	0.0	0.0	0.0	0.0
UBCOF	.5	.55	-0.4	0.2	0.1	-0.7	0.3
BGCOF	.1	.11	-0.1	-0.2	-0.1	0.2	-0.3
SNOW PARAMETERS							
GM	.02	.022	0.7	1.4	0.5	-1.1	1.8
TCOEF	.08	.088	0.4	0.3	0.0	0.1	0.3
HTSTA	2150.	3150.	22.2	23.5	9.1	0.6	25.0
HTSEG	3500.	4500.	-10.0	-2.6	8.9	-16.3	-3.3
LPSRT	3.5	3.85	-3.2	-2.2	0.9	-1.9	-2.7

Table 4.3 (cont'd)

The absence of orthogonal parameters hindered optimization. With orthogonal parameters, each parameter can be optimized independently, and the optimum solution for the whole system can be found by using the optimum values found for each parameter. If the parameters are not orthogonal, as in most simulation models, the optimum solution for the system has to be found by optimizing all the parameters in the model simultaneously. With non-orthogonal parameters, optimization is considerably more difficult than with orthogonal parameters.

With the present model it was unfortunate that the few parameters that were orthogonal (for example, with respect to the streamflow, the segment area and the second TIMET parameter) were easy to determine by other means. The majority of the parameters, including all the parameters that were hard to estimate, had to be found by simultaneous optimization.

CHAPTER V

THE GENESIS OF THE SWAGO CREEK BASIN

The Swago Creek basin is a high relief young basin which has undergone significant karst development. This development has only altered the basin area by a small amount, but has caused considerable diversions inside it. The original surficial flow was centripetal (Figure 5.3), but at present the water is being diverted to the west, thus enlarging the westerly spring of Cave Creek and depleting the Dry Creek area (Figure 5.2).

The karst development in the basin has been relatively simple, with only three major stages being identified. The first stage was that of surficial flow (Section 5.3). The first major karst development was the formation of the Carpenters Cave system which transmitted water from the end of the Dry Creek valley to the Cave Creek resurgence. The third stage is the present conditions of the area, wherein the lower Dry Creek valley water flows down Overholts Cave, and the upper Dry Creek water sinks and flows to Sharps Run (Figure 5.2). A fourth stage, which is the situation that will occur in the future, is also considered below.

5.1 Hydrological Description of the Present Basin

The Swago Creek basin has been briefly described in Section 1.4.1, but the hydrological and morphological features will be described in more

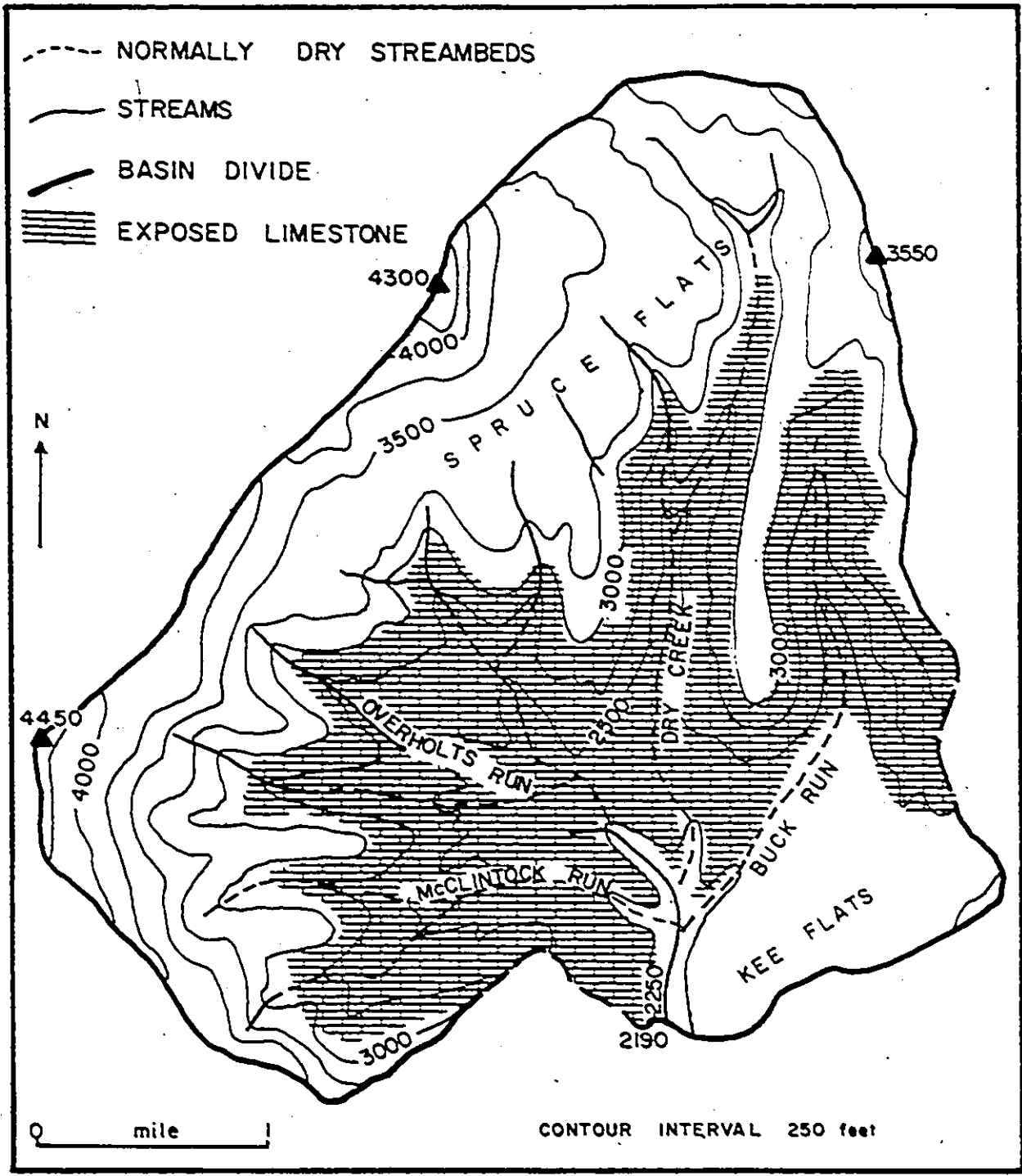


Figure 5.1 Swago Creek basin--topography and drainage.

detail in this section. The basin is roughly pear shaped, with a topographic area above the gauge of 12.0 square miles. The largely ephemeral surficial drainage is approximately centripetal, although in normal water conditions no streams flow across the limestone (Figure 5.2). There are a large number of sinks in the basin, and several major resurgences near the base of the limestone.

The Taggard shale has played an important part in the development of the karst and the caves in the Swago basin. The Taggard is thicker and more resistant in this area than further south, and acts as an aquiclude in the Greenbrier limestone. Several streams flow underground through the upper part of the Greenbrier limestone, resurge at the upper contact of the Taggard shale, and flow over the surface until they sink again in the Patton limestone, just below the shale. These features have been termed "lost waterfalls" (White and Schmidt, 1966), and include Barnes Pit, described in Section 5.2.2, and Hause Waterfall described below. In some flow routes the shale has been breached underground, but its presence is evident in the caves as long galleries above the shale, followed by a series of pitches through the shale into the underlying limestone.

The streams in the west of the basin, which include McClintocks Run (Figure 5.1) and the unnamed stream just to the north, both flow down off the clastic hills and in dry weather sink on reaching the upper part of the Greenbrier limestone. The sinks on McClintocks Run resurge at McClintocks Resurgences, while the northerly stream resurges at Cave Creek Cave (Figure 5.1). In wet weather the streams flow overland to the main Swago Creek channel.

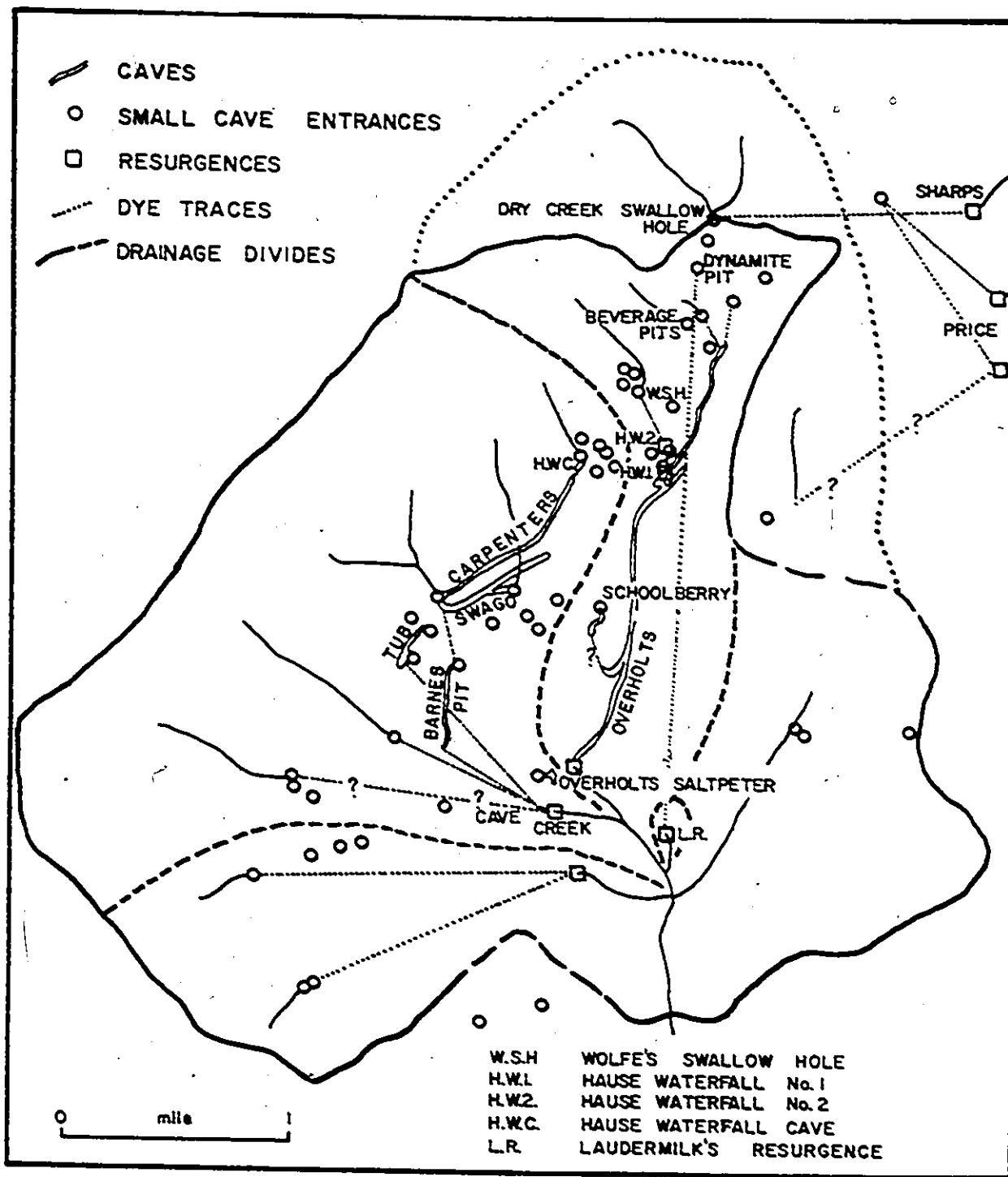


Figure 5.2 Swago Creek basin—caves, underground drainage and present flow routes.

A small stream running off Spruce Flats flows into Swago Cave which is described in Section 5.2.4. This water is known to flow to Barnes Pit and on to Cave Creek Cave. Another small stream sinks at Carpenters Pit which similarly flows to Barnes Pit.

On the east side of the basin, Buck Run does not flow in the upper part of the valley during dry weather, and any runoff appears to flow out of the basin as the lower part of the stream does not carry much water. However no successful dye tracings have been carried out on the creek, as during dry weather there are no obvious sinks to dye, and during wet weather the stream flows on the surface to Swago Creek. From the geological information, consideration of the hydraulic gradient and by comparison with the Dry Creek sink, it is believed that the runoff in the upper part of Buck Run flows to Price resurgence (Figure 5.2) during dry weather, with the high stage water flowing to Swago Creek, as does the lower part of Buck Run under all conditions. No significant caves are known in the Buck Run valley.

5.1.1 Sinks Along Dry Creek

Dry Creek is hydrologically interesting, as it has a complex hydrological history. In the space of a mile along the valley, several streams disappear into caves or sinkholes and flow to four completely different risings which are all almost two miles from the sink points (Zotter, 1963). The upper mile of the creek flows on the Lillydale shale, but sinks at the foot of a large cliff face near the upper contact

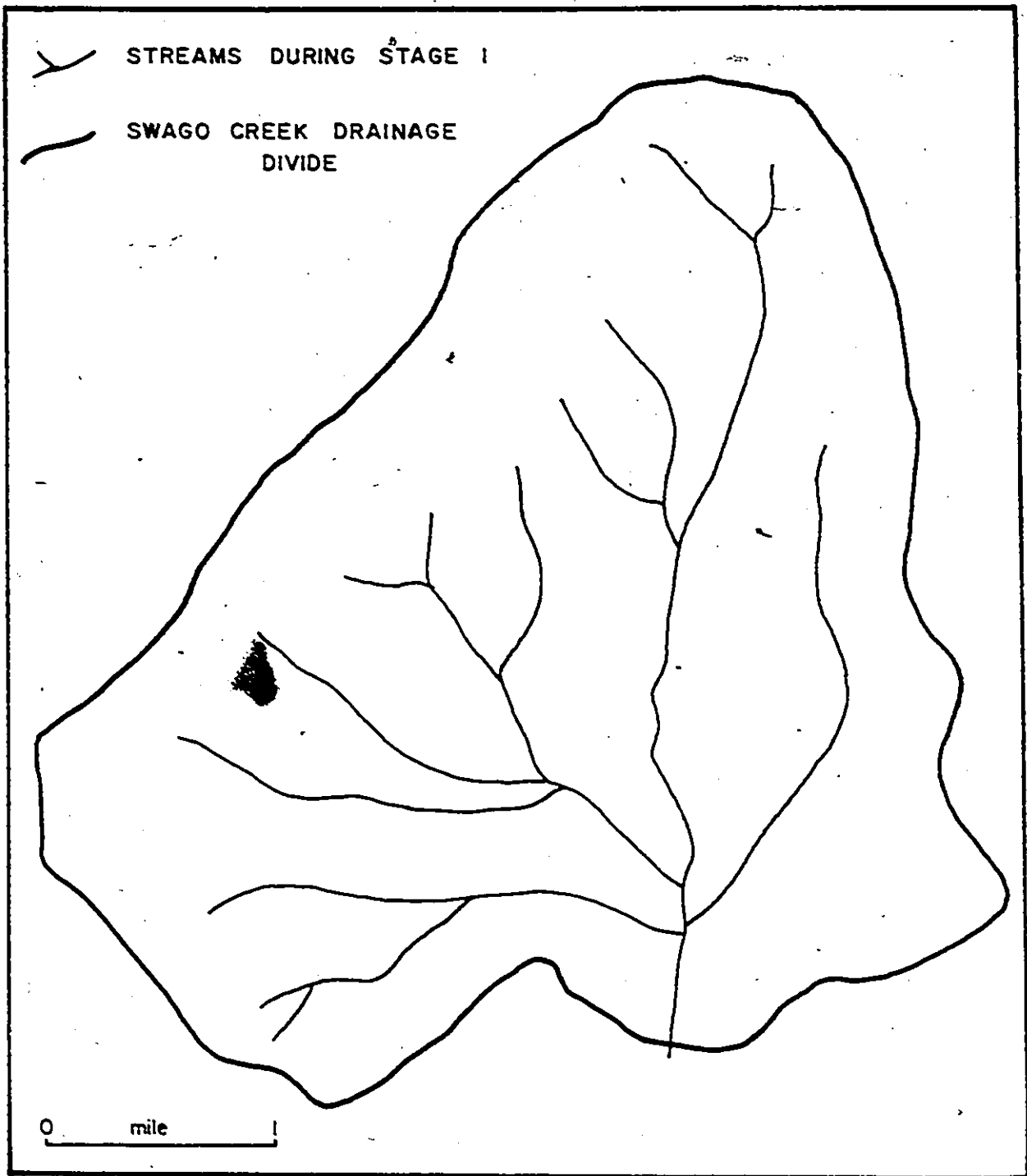


Figure 5.3 Swago Creek basin--surficial flow during Stage 1.

of the Union limestone (Figure 5.2). This stream drains out of the basin and flows to a resurgence on Sharps Run near Campbelltown. During floods, however, the sink is inundated, and the excess water flows down Dry Creek and into the Swago basin.

Further down the valley, Dynamite Pit (Figure 5.2), which is a domepit carrying a small stream, flows two miles underground to the Laudermilk resurgence at the mouth of Dry Creek. Dynamite Pit, however, can only be explored for about 100 feet.

Continuing on down Dry Creek, there are two small streams which run off Spruce Flats, sink into Beveridge Pit and Beveridge Domepit, and flow to Overholts Cave. The known end of Overholts Cave is only a few hundred feet horizontally from them, and is at about the same elevation. Farther south another stream at Hause Waterfall No. 1, which is a "lost waterfall" (White and Schmidt, 1966), resurges out of the Pickaway limestone just above the sink point. This water has been tested from a nearby lost waterfall called Hause Waterfall No. 2, which in turn has been traced from Wolfes Swallow Hole (Zotter, 1963).

Fifteen hundred feet to the west of these lost waterfalls is the Hause Waterfall Cave described in Section 5.2.5. The water flowing through this cave goes through Carpenters Cave to Barnes Pit, and finally resurges at Cave Creek Cave (Section 5.2.1).

One noticeable feature in the Dry Creek valley is a prominent lineation across the valley near Hause Waterfall, oriented at about 110° , which is visible on air photos. On field checking, no fault could be found across the lineation, and the feature was considered to be a major joint. The joint has had a marked effect on the hydrology, as Hause

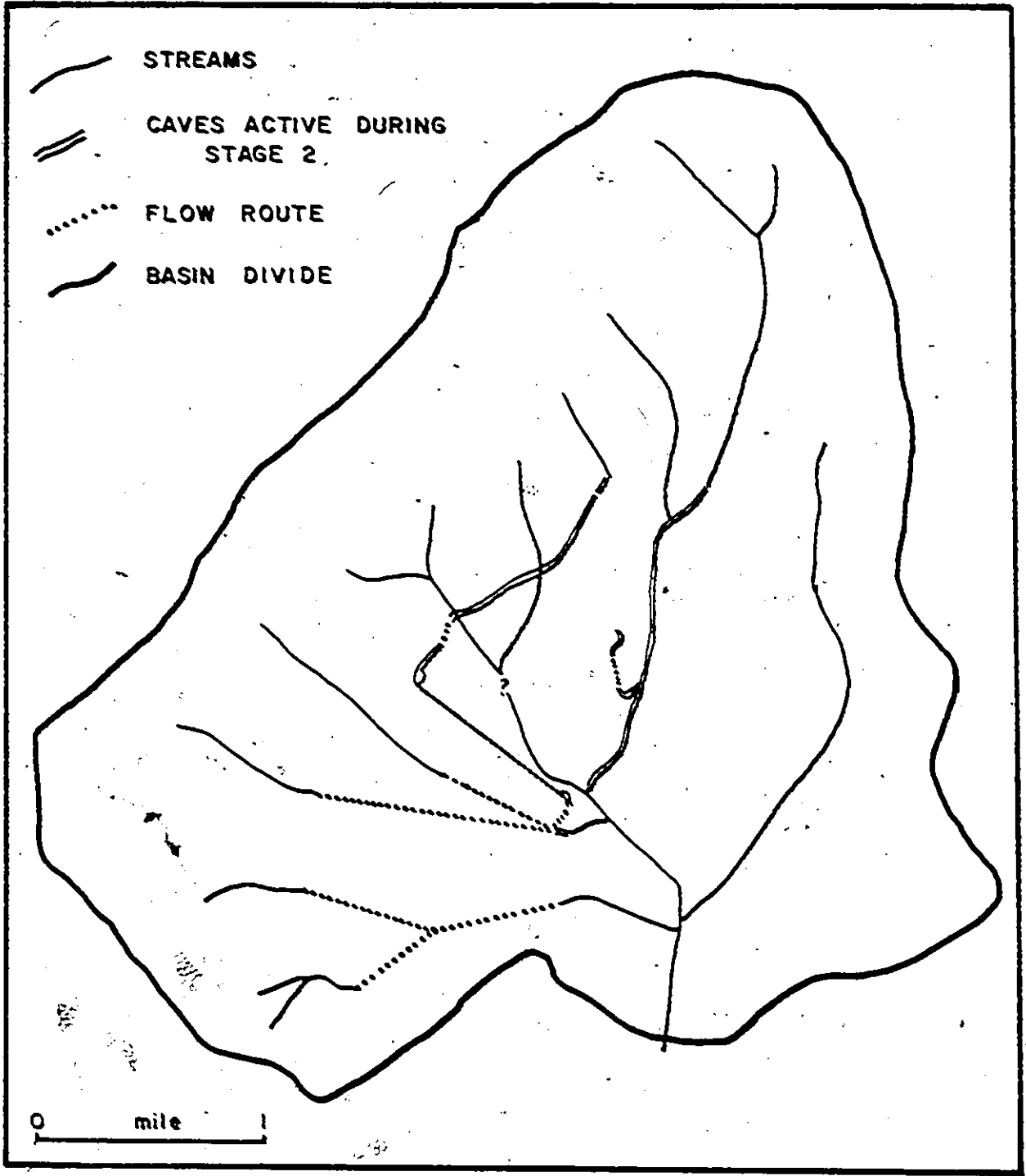


Figure 5.4 Swago Creek basin—karst development during Stage 2.

Waterfall No. 1, Hause Waterfall Cave, and the first two waterfalls in Overholts are all aligned on it. It is a substantial line of weakness in the limestone. In addition, the major sinks of Dry Creek and Hause Run are postulated to sink on this joint during Stage 2.

5.2 Description of the Caves in the Swago Creek Basin

Much of the evidence for the karst development of the basin can be inferred from a study of the caves. Caves are a three dimensional network, and as the basin develops they are often left dry and fossilized as the streams that generated them find new, lower routes. The fossilized caves are more immune to erosion than are surface features, which are usually eroded away or covered by sediment. In addition, inferences can be drawn about the size and type of the stream that generated the caves from a study of the present day cave morphology. It is therefore relevant to look at the size and morphology of caves in order to estimate their mode of formation. Those in the Swago area are described in this section. Many of them were mapped by the members of the McMaster University Caving Club, and all were visited and examined by the author.

The caves are located on Figure 5.2 and include Cave Creek Cave, Barnes Pit, Tub Cave, Swago-Carpenters Cave, Hause Waterfall Cave, and Overholts Cave. Some of the smaller caves, such as Schoolberry and Overholts Saltpeter Cave are described in Section 5.3 on the development of the basin.

5.2.1 Cave Creek Cave

Cave Creek constitutes the principal stream in the Swago Creek basin, as the spring at its head supplies an average of about 8 cfs., which is over half of the discharge from the basin. In spite of the impressive flow and large entrance, Cave Creek Cave cannot be entered for more than 200 feet to a point where the passage is blocked by breakdown.

The cave entrance is about 50 feet wide and 10 feet high, but the passage rapidly reduces to 2 to 4 feet high and 20 feet wide a few feet inside the entrance, where the cave is developed in a bedding plane. Although the roof indicates that the cave was initiated under phreatic conditions, its major enlargement has been by vadose stream action. The stream now flows over gravel on the floor of the cave. The cave is developed in the Hillsdale limestone at the base of the Greenbrier series. It has been reported (Davies, 1958) that the cave continued for several thousand feet, but became blocked in 1957. Inspection of the blockage now confirms that it cannot be passed.

5.2.2 Barnes Pit Cave

About one mile to the north-west of Cave Creek spring (Figure 5.2), there is a "lost waterfall" where water issues from a spring, falls over the Taggart shale, and sinks immediately below the shale. The spring cannot be entered, but the water here has been tested to come from the Swago and Carpenters Caves. The cave at the sink, which is 100 feet downstream, consists of a 2000 foot long simple vadose streamway,

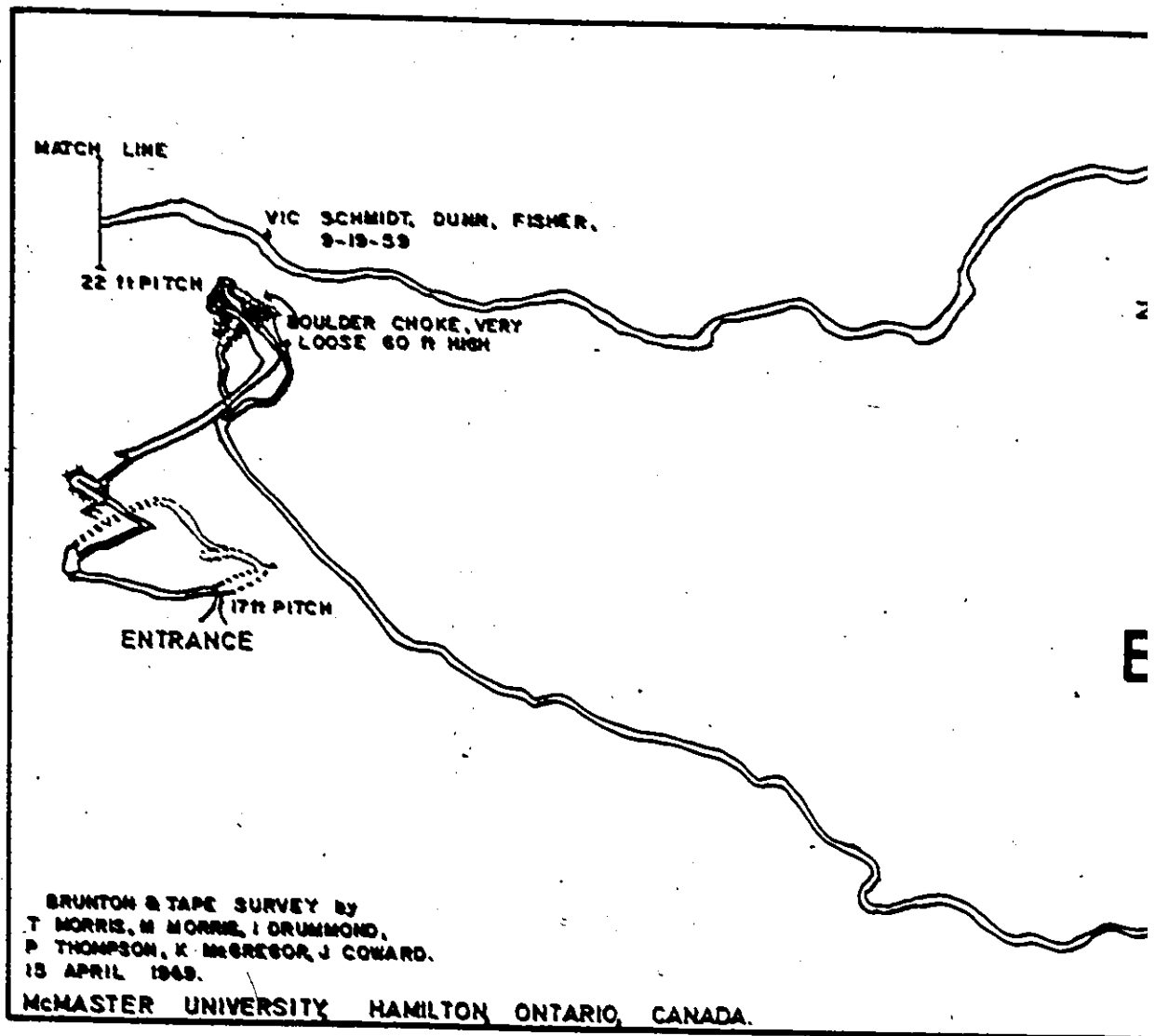
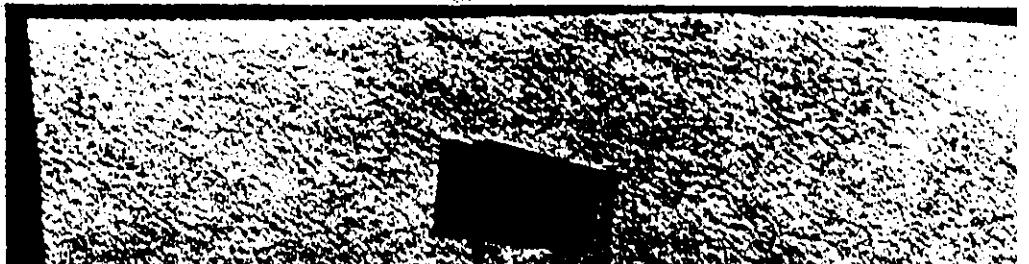
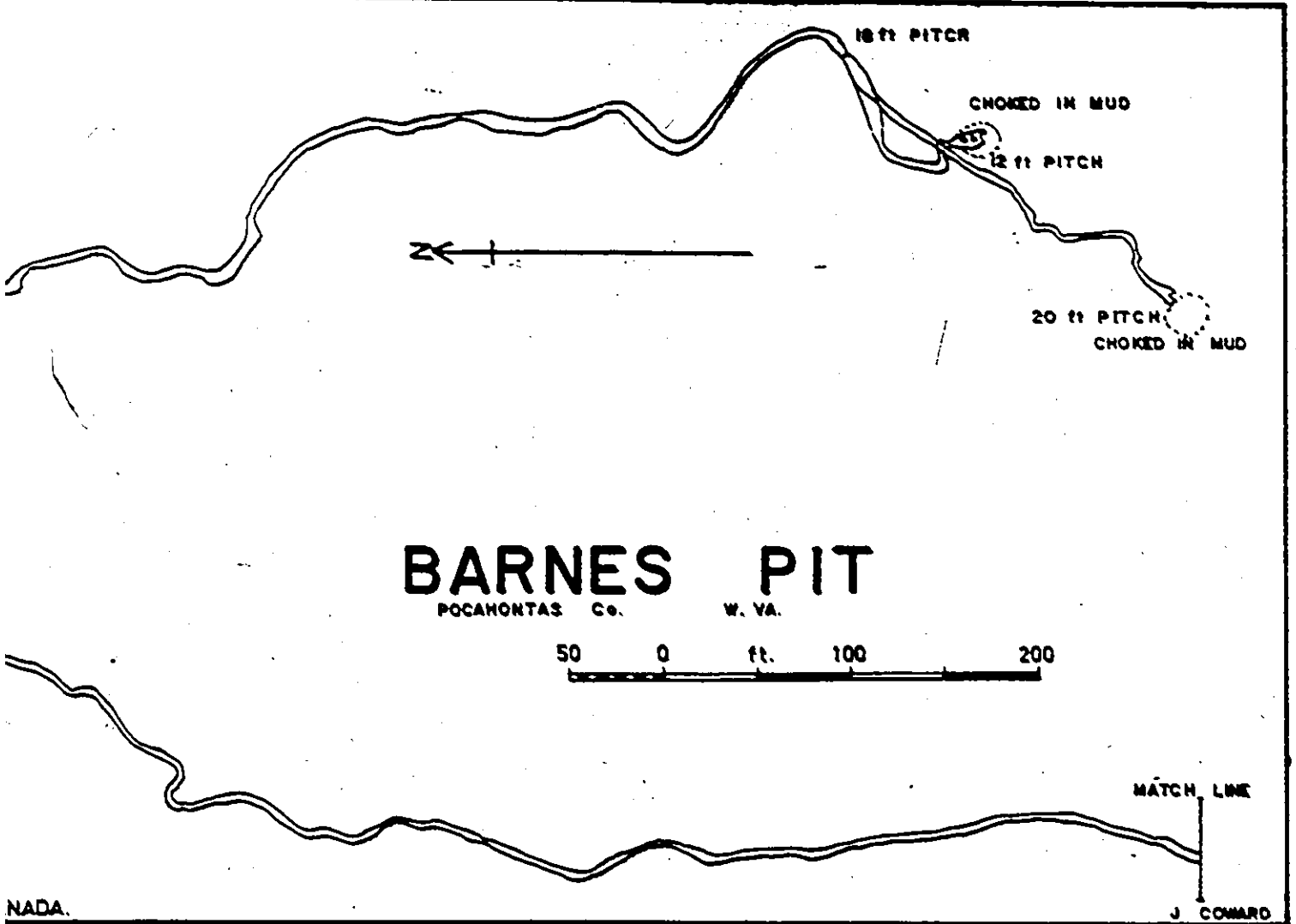


Figure 5.5 Barnes Pit Cave.

137



averaging 30 feet high and 3 feet wide (Figure 5.5). The water disappears at the end of the cave through a 6 foot wide, 3 inch high crack (Drummond, 1969) and has been tested to flow to Cave Creek Cave. From survey data, the lower end of Barnes Pit Cave is only a few feet above the level of the Cave Creek resurgence and about 3000 feet distant from it.

5.2.3 Tub Cave

Tub is a very impressive cave, having a chamber 500 feet long, 200 feet wide, and about 50 feet high, which is larger than any other in a West Virginian cave. Now it plays a minor part in the hydrology of the area. The cave carries a small stream which flows to Cave Creek Cave (Zotter, 1965). Both ends of the chamber are blocked by breakdown, much of which is now covered by flowstone.

In the northern end of Tub Cave a passage can be followed for about 500 feet through the breakdown. This passage appears to have been large, but has now been partially filled in by breakdown. It was formed under phreatic conditions, and scallops indicate that the water that formed the cave was flowing into the present main chamber. The passage is heading towards Carpenters Cave (Figure 5.2). The cave is formed in the Pickaway limestone just above the Taggard shale.

5.2.4 Swago-Carpenters Cave

This cave system consists of two separate caves which are connected underground (Figure 5.6). The two caves are the largely fossilized Carpenters system, and the wet and active Swago stream which has cut down to join the Carpenters passage.

Carpenters Cave includes a large fossilized passage about one mile long, trending to the north-east. The passage is about 40 feet high and 20 feet wide, and is known as the Crumbling Gallery. This passage was formed largely by vadose flow. The Gallery is developed in the Pickaway limestone, immediately above a prominent shale band in the Pickaway, which is visible in the floor at several places. The upper (northeast) end of the Gallery is blocked by mud. Near it are a number of domepits, some with very small streams dripping down them. An underfit stream flows down the Gallery, fed by the domepits and other minor inlets, and has eroded a small trench in much of it.

At the downstream end of Crumbling Gallery, near the present Carpenters entrance (Figure 5.6), the main gallery continues above the Pickaway shale band, finally ending near Beck's Lost Passage in another mud blockage. In this region, however, the shale has been breached, and a considerable vadose development has taken place beneath it.

The Swago stream is a more recent vadose passage containing a number of vertical pitches. The passages average about 10 feet high and 2 feet wide, and are of the typical vadose canyon type. The cave is developed in the Union and Pickaway limestone members, with many of the vertical pitches being held up by shale bands in the limestone. A stream

SWAGO - CARPENTERS CAVE

Based on Surveys by the Pittsburgh Grotto

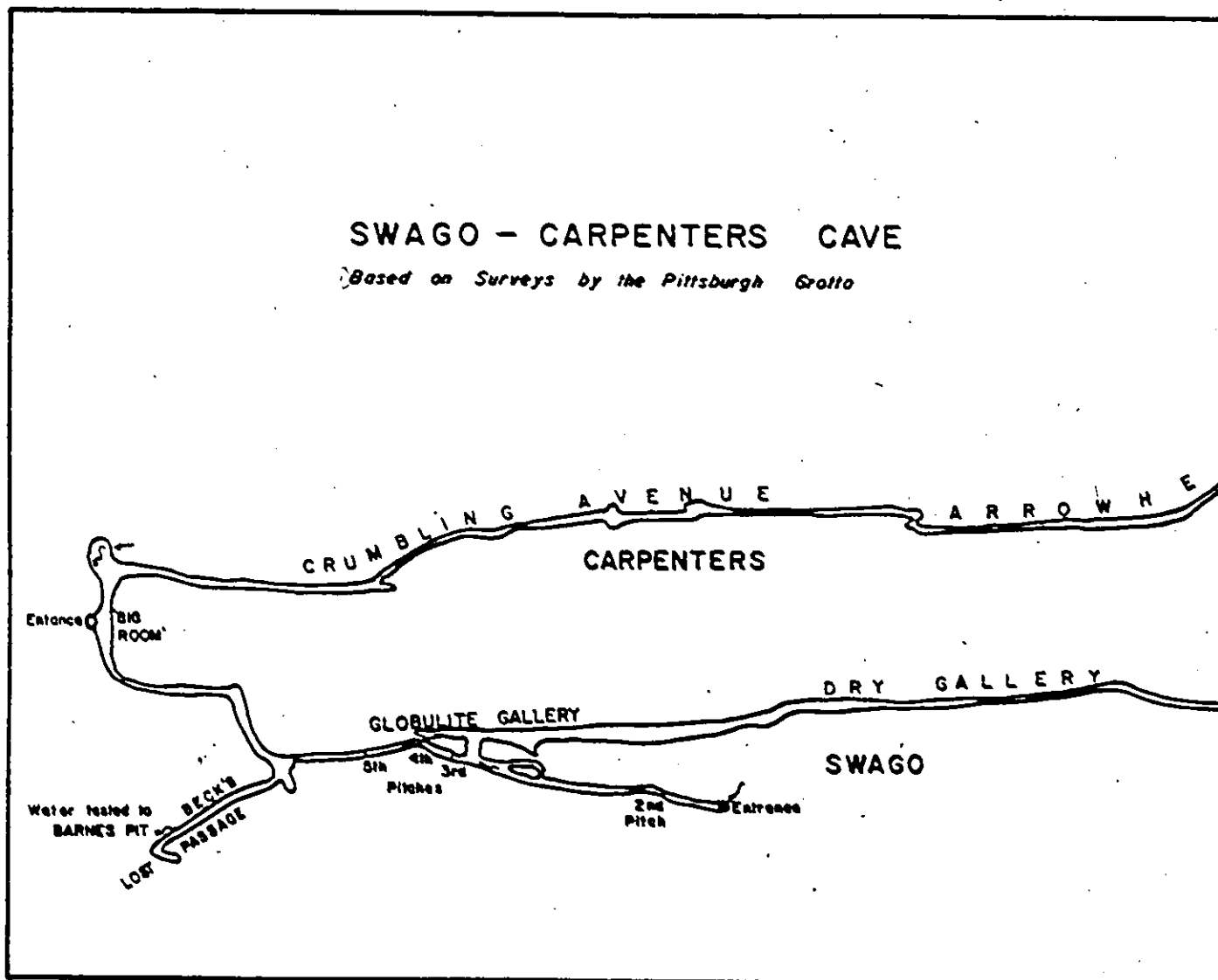
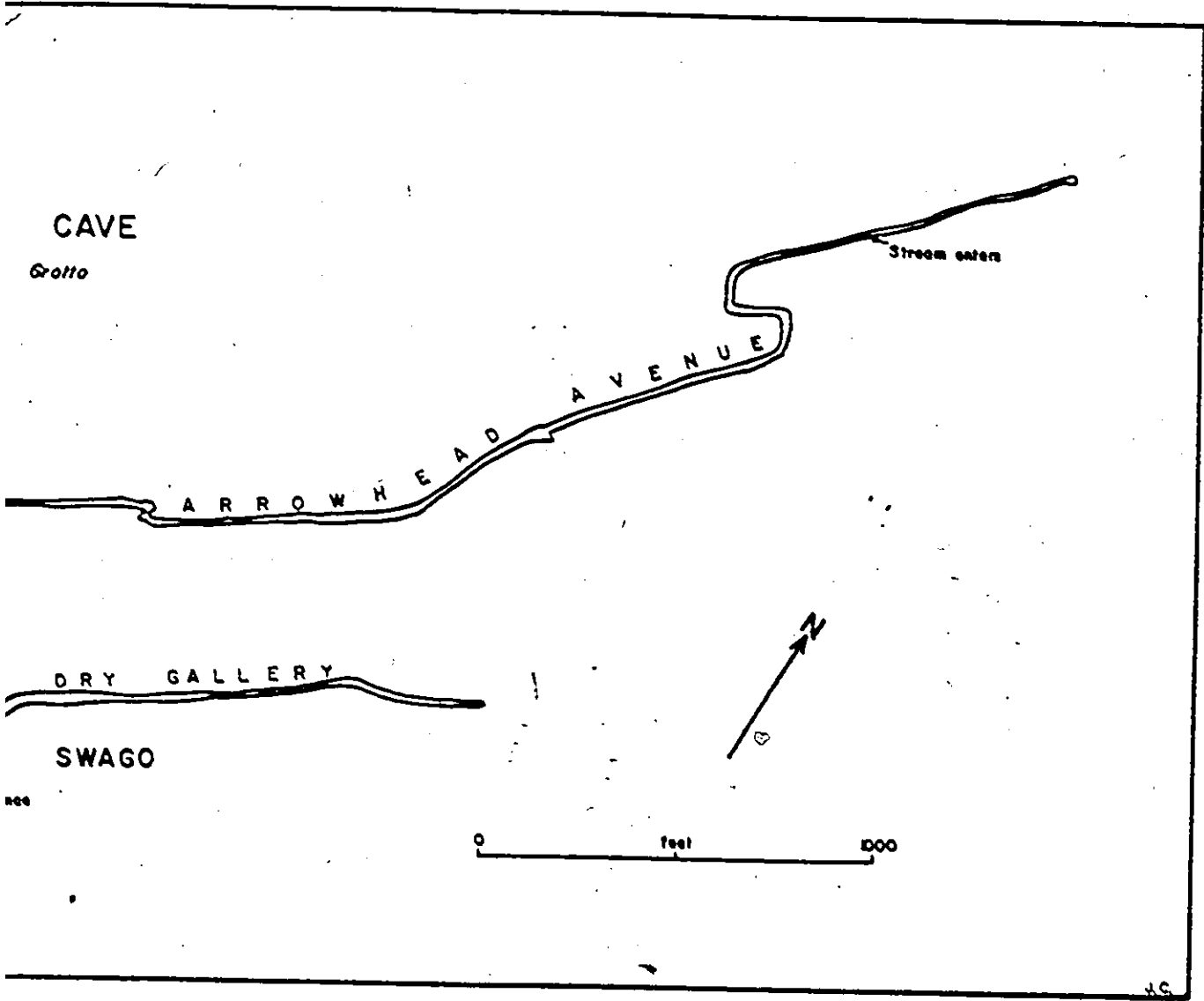


Figure 5.6 Swago-Carpenters Caves.



draining off Spruce Flats runs through the cave, is joined by the Carpenters stream, and disappears in a constricted sump at the base of the Pickaway, immediately above the Taggard shale. This water is next seen at the resurgence above Barnes Pit.

5.2.4.1 The Flood and Dye Test at Swago Creek

As described in Section 2.4, a flood and dye test was carried out in the Swago Cave streamway. The hydrograph is shown in Figure 5.7 along with the modelled flood pulse and the dye pulse.

The flood pulse was modelled using a flow pattern of a series of cascading reservoirs. The cave was assumed to consist of a number of reservoirs of certain surface areas discharging over broad crested rectangular weirs. The discharge, Q , over the weir is given by (Francis, 1958):

$$Q = 3.09 b H^{3/2} \text{ cfs.} \quad (5.1)$$

where b is the weir breadth in feet, and

H is the reservoir head above the level of the weir, in feet.

The routing was carried out by the standard reservoir method (Gray, 1971) using a 2000 cubic feet delta function input to the first reservoir. The error between the real and modelled hydrographs was determined as the sums of squares of the deviations. The number of reservoirs was varied from 1 to 10 and the optimum reservoir areas and spillway widths were found using the hill climbing optimization method developed by

Hooke and Jeeves (1960). A simple computer program was written to perform the calculations which included the optimization routine written by A.A. Smith (personal communication, 1970). This method of modelling is oversimplified as the pools in the cave are known to be connected by sections of streamways which introduces some time delay and dispersion of the flood pulse. Modelling the streamways was not attempted.

The optimum solution consisted of three reservoirs with areas ranging from 1960 to 4760 square feet, and spillway widths ranging from 1.6 to 5.5 feet. By comparison with the real cave the modelled pool areas are too large, but the spillway widths are reasonable (Table 5.1), except at the lower pool. The large modelled pool areas are probably caused by the exclusion of streamway components in the model. In order that a suitable time delay is given by the model to the flood pulse, large pool areas, and so large time delays have to be generated by the model.

The dye pulse was found to take about five times as long as the flood pulse to come through the system (Figure 5.7). This large delay is surprising as the cave is vadose. In vadose caves the flood and dye pulses usually come through close together, while in phreatic caves there is often a large delay in the dye pulse (Ashton, 1966). The delay in Swago Cave is caused by the section of canal and the pools in the streamway which slow up the dye but allow the flood to pass through fairly quickly as a kinematic wave.

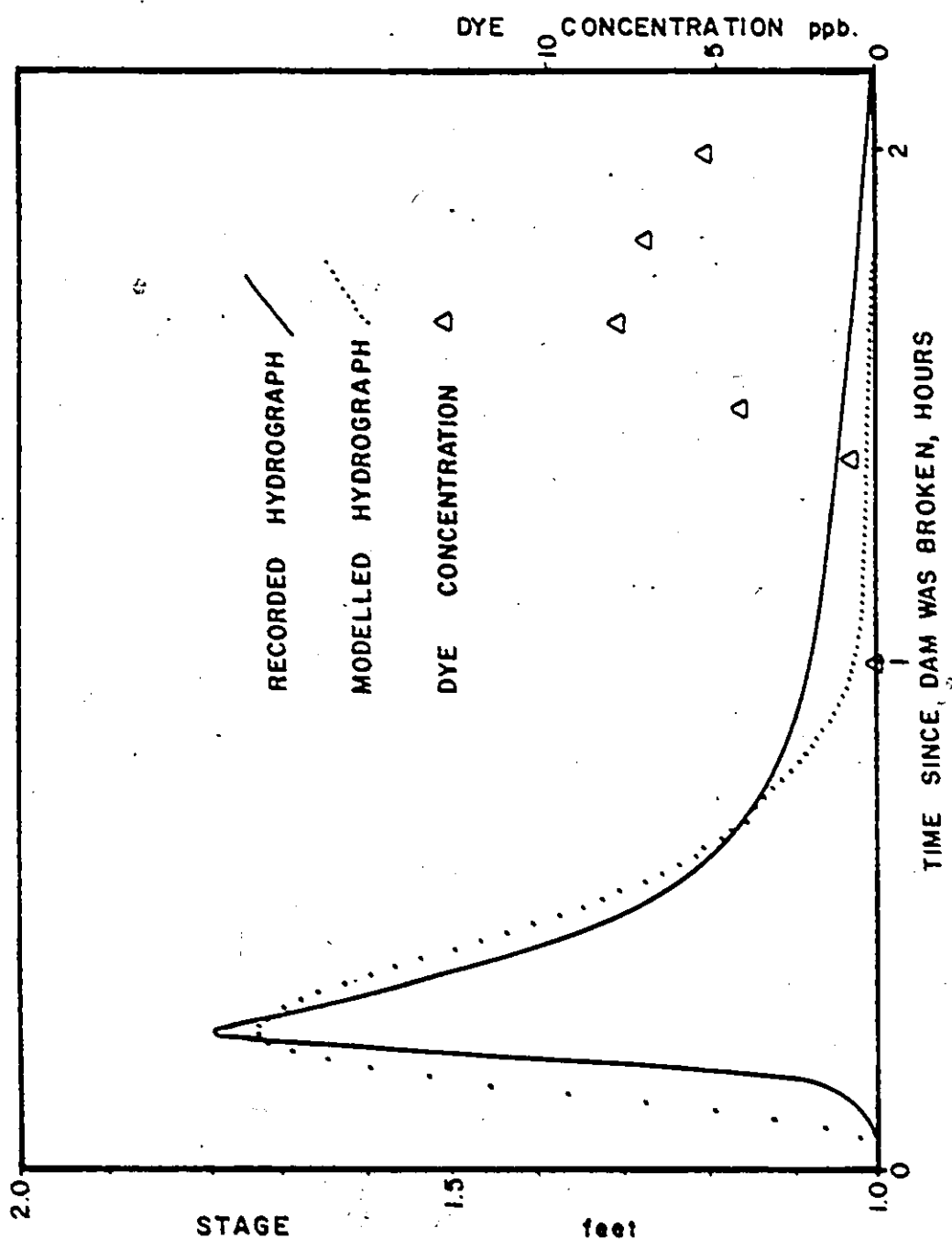


Figure 5.7 Results of the flood and dye test. The real and modelled hydrographs and the real dye concentration are shown.

Table 5.1

Comparison of the Real and Modelled Pool Areas
and Spillway Widths in Swago Cave

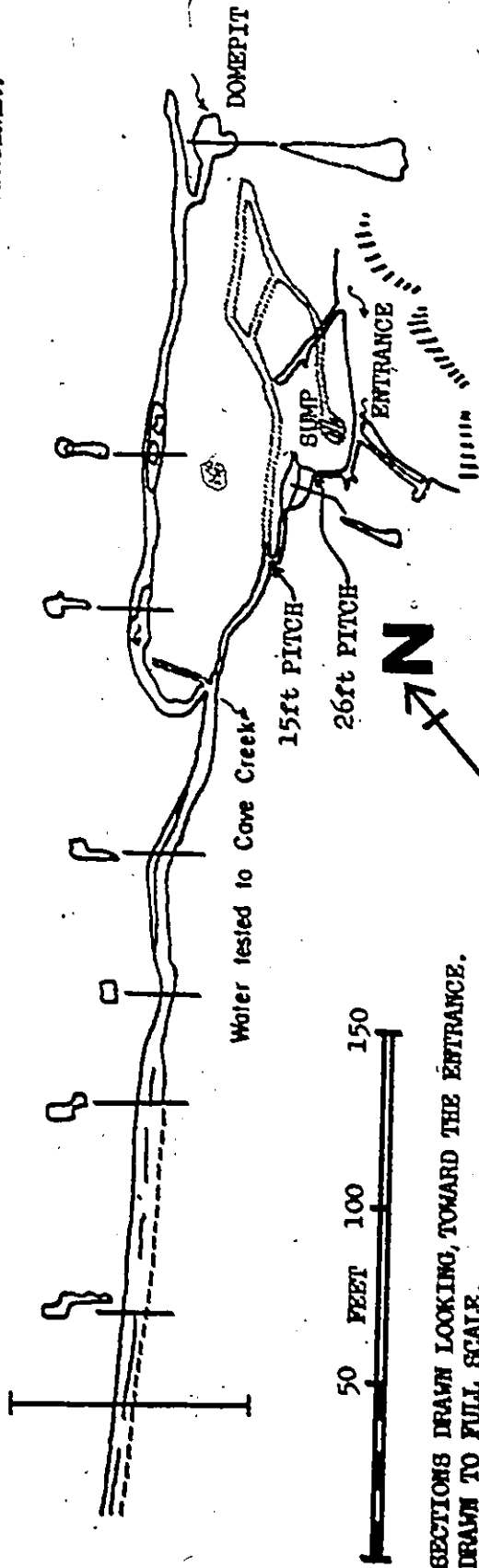
<u>Pool Number</u>	<u>Modelled Pool Area (sq. ft.)</u>	<u>Modelled Spill-Width (feet)</u>	<u>Measured Pool Area (sq. ft.)</u>	<u>Measured Spill-Width (feet)</u>
1	2240	5.2	750	6
2	1960	5.5	1000	4
3	4760	1.8	600	4

5.2.5 Hause Waterfall Cave

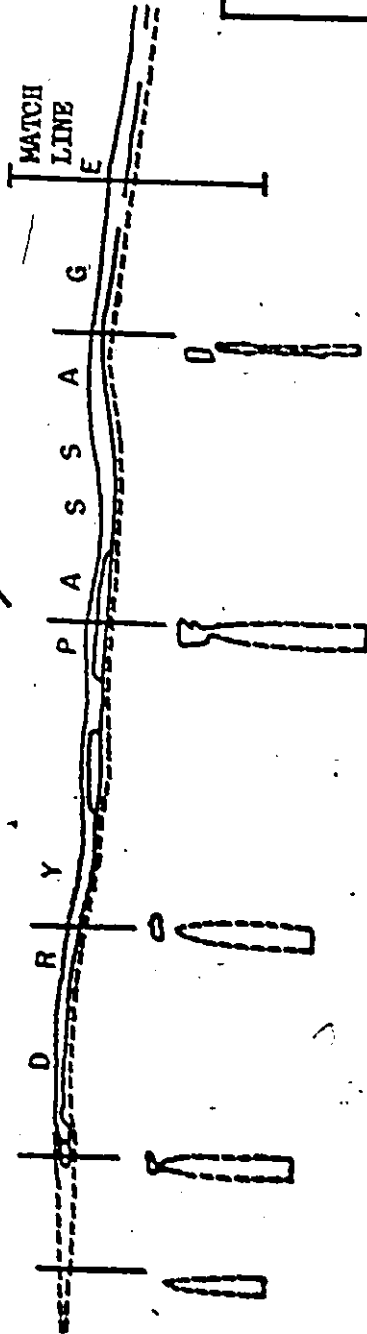
This cave is located on a small tributary of Dry Creek (Figure 5.2) about half a mile from the main Dry Creek channel. The cave consists of a small vadose stream passage, which after 50 feet and two awkward pitches (Figure 5.8) joins a large fossilized vadose passage which is up to 50 feet high and 10 feet wide, and extends for 500 feet to the south-west (MacGregor, 1969). The lower end of the passage is blocked by mud, while the upper part ends in a dome-pit. The cave is developed in the Union and Pickaway limestones.

HAUSE WATERFALL CAVE

SHAGO CREEK AREA, FOCAHONTAS COUNTY, WEST VIRGINIA.



SECTIONS DRAWN LOOKING TOWARD THE ENTRANCE.
DRAWN TO FULL SCALE.



BRUNTON AND TAPE SURVEY.
BRUNTON AND PACED.
EXPLORED ONLY.

SURVEY MADE 7 JUNE 1969

J Coward

Figure 5.8

McMASTER UNIVERSITY HAMILTON, ONTARIO, CANADA.

5.2.6 Overholts Blowing Cave

Overholts Blowing Cave is a major resurgence cave in the Swago Creek area, with a total length of 3 miles and a mean annual discharge of 4 cfs. The cave is developed through the majority of the Greenbrier limestone, with its upper end being in the Union limestone whilst the exit is near the Hillsdale-Sinks Grove contact. The cave has a total fall of about 500 feet (Figure 5.9).

The cave consists of a water passage that may be divided into three major sections separated by waterfalls, plus a number of side passages. The lower section is developed in the Patton and Sinks Grove limestone, and consists of one mile of stream passage averaging 10 feet high and 8 feet wide which extends back from the entrance. This passage was developed under phreatic conditions (Figure 5.11), but has been modified by more recent vadose flow, as can be seen in Figure 5.12. In historic times the cave had two entrances, but the larger passage has been filled in by quarrying operations (Dallas McKeever, personal communication, 1969). The present smaller entrance was developed by vadose flow (Figure 5.10).

The lower section has three major side passages: a) Ann's Avenue, which is a largely fossilized vadose high level passage going off 3000 feet from the entrance; b) Alcoa Avenue, which is also a fossilized passage about 8 feet wide and high, but is at the same general level as the main passage and was developed by phreatic flow. This passage extends for 1000 feet from the end of the lower section of the main passage (Figure 5.9); and c) Waterfall 1B (Figure 5.9) which is a

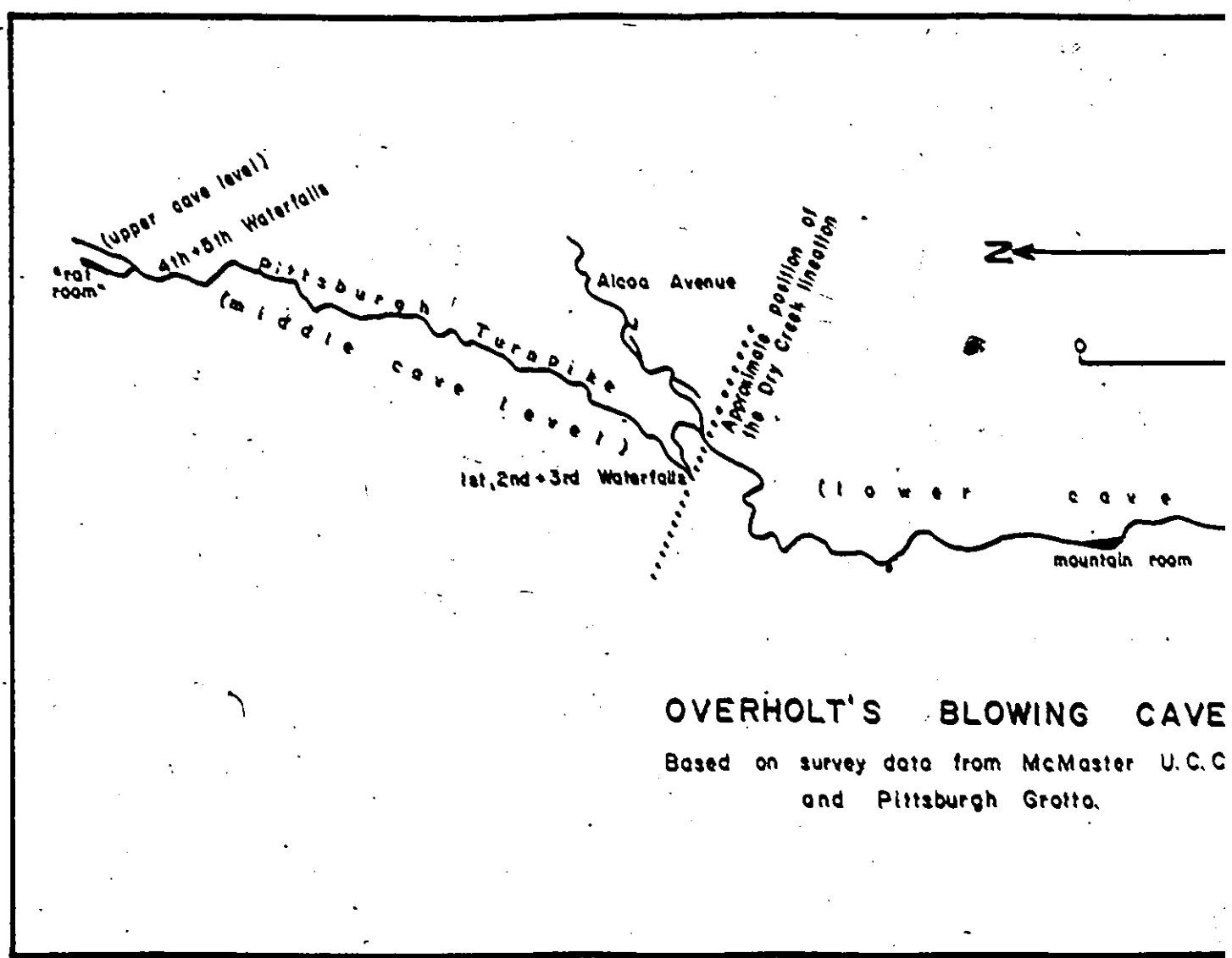
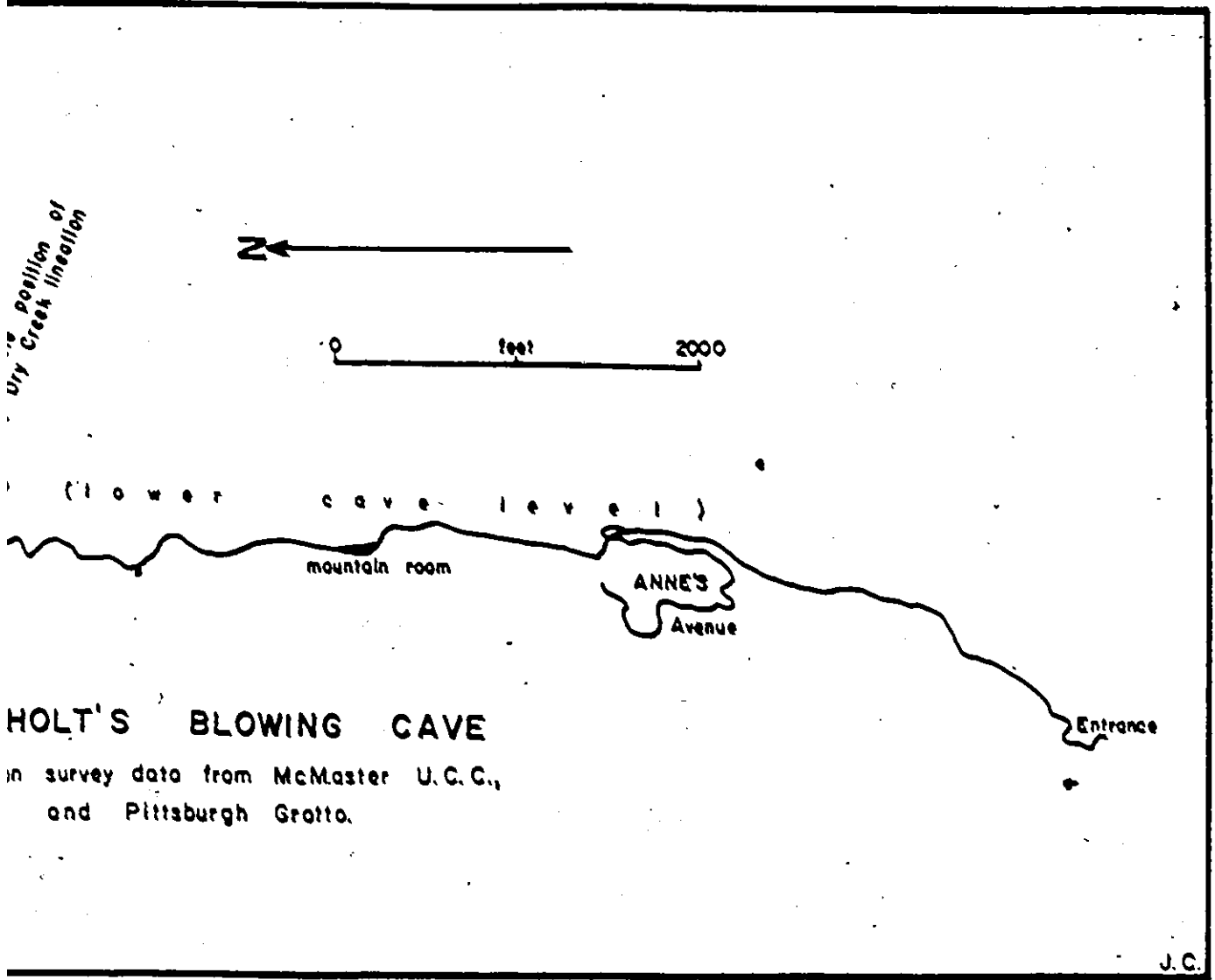


Figure 5.9 Overholts Blowing Cave.



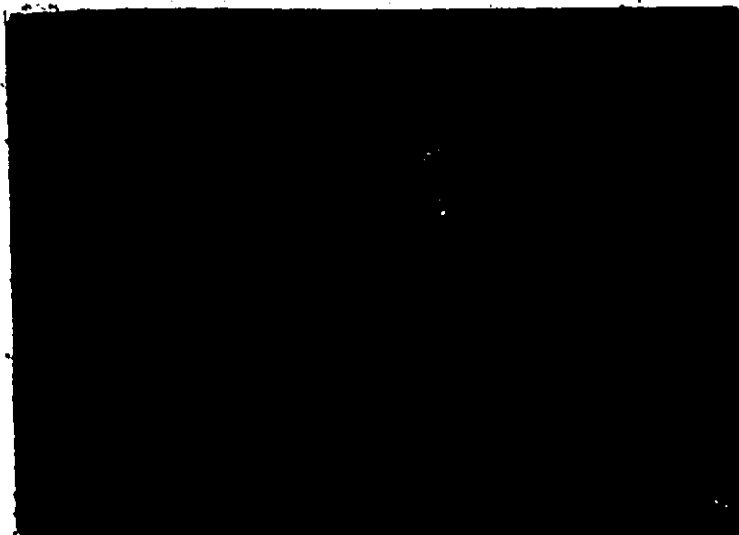


Figure 5.10 The stream passage near the entrance of Overholts Cave. During floods the water rises to the roof. The bed of the stream is on cobbles and gravel, and the passage has been partially filled in by sediments of this calibre.



Figure 5.11. The bypass passage near the entrance to Overholts Cave. The phreatic form of the passage is evident, and although there is sediment on the passage floor, the bedrock is exposed in places, indicating that the sediment is thin, a mere veneer.



Figure 5.12 Fine stream passage in Overholts Cave. The phreatic form of the upper part of the passage, and later vadose development of the lower part of the passage are evident, giving a key-hole type passage shape.

donepit at the end of the lower section carrying a stream, which has been tested to come from Hause Waterfall No. 1. This inlet is recent, active, and was developed by vadose flow.

The second level of the cave is developed in the Pickaway limestone. This section is about 3000 feet long, and averages 5 feet wide and 10 feet high, and was developed by vadose flow. It connects to the lower section of the cave by three waterfalls, which have cut through the Taggard shale and shale bands in the Pickaway limestone.

At the far end of the second level of the cave are a couple of waterfalls, which together are almost 100 feet high. Above them the cave splits up into a number of smaller vadose inlet passages developed in the Union limestone, and this section is considered to be the third level of the cave. Several of the inlet passages contain streams, which have been tested from various sinks in the end of the Dry Creek valley. At present it is not possible to explore Overholts through any of these sinks, as the water disappears in boulder chokes or through impassable fissures.

5.3 Description of the Four Stages of Karst Development in the Swago Basin

From dye tracing work and cave exploration and interpretation, the evolution of the Swago Creek basin can be inferred. Although there are many diversions and piracys throughout the basin, three major stages of development have been identified here and are described in this

section. The initial stage was the original surficial flow, while the second and third stages are the underground development up to the present. A fourth stage is described, which is the situation that should occur in the near future as the karst matures.

5.3.1 Stage 1: Surficial Flow

Initial development of the basin was the wholly surficial flow. The streams were flowing above the limestone in a dendritic pattern which is preserved in the pattern of dry streambeds that exists today (Figure 5.3). As the surface was eroded, the limestone was exposed in the lower end of the basin and some caves may well have developed there. However all evidence for any such caves has been destroyed. Stage 1 is considered here to have ended when the earliest karst that has been preserved was formed.

5.3.2 Stage 2: Initial Karst Development

During Stage 2 a number of streams sank and flowed underground. The underground routes were generally strike controlled and tended to flow in a southwesterly direction, controlled by the northwesterly geologic dip and the generalized southerly topographic slope.

As the clastics were eroded off the limestone in the valley floor, Dry Creek sank progressively upstream. The first suspected sink was in the streambed near Hause Waterfall Cave, when the stream initiated

Overholts Cave (Figure 5.4). The stream sank at the prominent lineation in the Dry Creek valley (Section 5.1.1), flowed along the now fossilized Alcoa Avenue, and then along the presently active lower section of the Overholts Cave to resurge in the Swago valley.

At present the position of the sink in the Dry Creek valley cannot be found, as the streambed is covered by a veneer of cobbles and gravel which would hide any open cave or sinks. There are, however, several pieces of evidence which lead one to suspect that a sink must have occurred in this area:-

- a) The prominent joint in this area (Section 5.1.1) is known to allow water to percolate downwards, as shown at Hause Waterfall Cave and at the first two waterfalls in Overholts Cave. As the lineation allowed water to flow downwards in other caves, it is likely that the Dry Creek stream used this lineation to sink through from the surface to Overholts Cave.
- b) Alcoa Avenue in Overholts Cave is a prominent trunk passage that is now fossilized and almost dry. The passage leads along the trend of Overholts Cave, and the upstream end of Alcoa Avenue ends in a series of domepits just at the lineation. The most probable source for the water that generated Alcoa Avenue is the Dry Creek stream.
- c) The Taggard shale was probably exposed in the valley floor near Hause Waterfall during Stage 2. At present the Taggard is 50 feet above the valley floor, but in the time since Stage 2 this 50 feet of material is believed to have eroded away. Hause Waterfall No. 1 (Section 5.1.1) attests to the difficulty of breaching the Taggard

in this area, and the sink in the Dry Creek streambed probably formed when the Taggard was eroded from the valley floor.

About one mile up the Dry Creek valley is a small tributary stream which sinks and has developed Schoolberry Cave (Figure 5.2). This stream was probably responsible for the development of Ann's Avenue in Overholts Cave during Stage 2.

Farther to the west, Hause Run sank near Hause Waterfall Cave and flowed along Carpenters Crumbling Passage, through Tub Cave and on to the Cave Creek resurgence. The Hause Run was not only pirated away from Dry Creek, but crossed underneath Swago Creek to resurge at Cave Creek (Figure 5.4).

The present Hause Waterfall Cave entrance is small and vadose, unlike the large, fossilized canyon passage at the end of the cave (Section 5.2.5). The present entrance is clearly a recent, Stage 3 addition to the main part of the cave, which was generated during Stage 2. The sink point for the water during this stage, however, cannot be seen now. It is probably in the streambed near the present cave entrance.

The Hause Run water developed the Crumbling Gallery in Carpenters and almost certainly flowed into Tub Cave. The passage in Tub Cave extending to the north-east lines up with the trend in Carpenters Cave (Figure 5.2) and the ends of the passages are only 2000 feet apart. The Carpenters Cave is also the only large stream that can be envisaged to have flowed near Tub Cave and developed the large chamber.

Tub Cave is considerably larger (200 feet wide and 50 feet high) than is Carpenters Cave (which is not larger than 35 feet wide and 40 feet

high), and it is difficult to account for the discrepancy in sizes. There are two possible explanations:-

- a) The water in Tub Cave, while it was being formed, probably flowed out over the Taggard to the south-east of the cave. As the dip of the beds is to the north-west, the cave would have been formed under phreatic conditions and so could be larger than Carpenters because the water was in contact with the walls for longer than in the vadose streamway.
- b) The drainage behind Tub, with an area of about one square mile, drains into the cave. When the cave was being formed the mixed water may have had a greater erosional power than the Carpenters water, due to mixture corrosion (Bogli, 1964).

Either or both effects may have caused the enlargement of Tub Cave.

As the Taggard is not easily breached (see, for example, Barnes Pit and Hause Waterfall), particularly during the early stages of development, the water that developed Tub probably resurged near the cave. By analogy with the other nearby caves, this resurged water probably sank below the Taggard and flowed underground and through Overholts Saltpeter Cave, and resurged at or near Cave Creek Cave.

In the south-west, McClintocks Run and the unnamed stream to the north are believed to have sunk and developed underground routes. Little is known of these routes, however, as there are no significant caves near these streams, and little evidence of flow routes.

5.3.3 Stage 3: Present Conditions

During Stage 3, the Dry Creek stream sank progressively upstream, and finally sank right at the northern end of the basin and flowed out of the Swago basin. The Carpenters and Swago Caves were developed and the Carpenters water flowed through and developed Barnes Pit Cave.

Dry Creek sank farther upstream, sinking for a long time near the Beveridge Pit (Figure 5.2). The exact location of the sink point in the Dry Creek bed is not known, as no indication of the sink point can be seen on the surface. Underground, however, near the end of Overholts Cave, there is a large chamber which has been called the Rat Room, and which is a probable entry point for the Dry Creek streams as the end of the chamber is blocked by boulders and the chamber is near the Dry Creek stream. Inside the cave the stream was held up by the Taggard shale, and developed a long gallery (the Pittsburgh Turnpike) before being able to penetrate the Taggard at the Hause lineation near Hause Waterfall (Figure 5.8).

Dry Creek later sank even farther up the stream at the present sink point, Dry Creek Swallow Hole. This sink is in the upper part of the Union limestone, just below the Grenville shale. The water flows to Sharps Run (Figure 5.2). It appears to flow to this resurgence because from the Dry Creek sink, Sharps Run has a higher hydraulic gradient (320 feet per mile) than to the end of Overholts (125 feet per mile) or to the Overholts entrance (230 feet per mile). At present the flow route from Dry Creek to Sharps Run is unexplorable as both ends of the route are too small to enter.

Overholts Cave is still supplied by a number of small streams flowing off the sides of the Dry Creek valley and sinking in a number of caves and pits in the Beveridge Pit area (Figure 5.2). Dynamite Pit, however, was able to generate a route down the Dry Creek valley to the Laudermilk resurgence (Figure 5.2), although the reason why this route developed is not known. The hydraulic gradients to Overholts resurgence (280 feet/mile), Laudermilk resurgence (300 feet/mile), and to Sharps Run (320 feet/mile) are all similar; some other control must have affected the route that the water in Dynamite Pit took.

Hause Waterfall Cave developed almost vertically from the Big Run stream down to the Carpenters trunk passage. The cave has developed from the Union limestone down to the Pickaway at the Carpenters trunk passage.

The stream to the north of Big Run (Figure 5.2) sank in the Union at Wolfe's Swallow Hole and flowed to Hause Waterfall No. 2, where the water flowed over a shale band in the Pickaway on the surface. The water then flows almost along the strike to Hause Waterfall No. 1 where the Taggard shale is overcome by means of a "lost waterfall". This water then flows into Overholts Cave.

The streams at Swago and Carpenters Pits sank and developed the two caves. The entrances to both Swago and Carpenters Caves are in the Union limestone, and the subsequent pitches in both caves are held up by shale bands, predominantly in the Pickaway limestone. The caves intercepted the Carpenters trunk passage, and due to the increased erosional power of the combined Swago and Carpenters streams, were able to breach the prominent shale band in the Pickaway limestone that had held up Crumbling Gallery in the old Carpenters Cave.

The stream eroded down to the top of the Taggard shale, but was then unable to penetrate this shale underground. It therefore flowed to the Barnes Pit resurgence, ran over the surface and sank immediately below the Taggard shale. Due to the northwesterly dip of the limestone, Barnes Pit, which is located near the most northwesterly exposure of the Taggard shale, represents the lowest spill point for water above the Taggard shale. Barnes Pit Cave, which is in the Patton limestone immediately below the shale, is a recent development along an approximate straight line from the sink to the assumed position of the Cave Creek master channel (Figure 5.2).

On McClintocks Run and Overholts Run further development took place as the streams sank near the top of the limestone, breached the Taggard, and then resurged near the base of the limestone. The only significant cave in this area is Friels Cave, which has developed just below the Taggard shale near Cave Creek Cave. The flow paths at McClintocks Run underdrain the valley, while the two tributaries farther north drain into Cave Creek Cave (Figure 5.2).

5.3.4 Stage 4: Future Conditions

Major changes anticipated in Stage 4 are the enlargement and maturing of flow routes developed in Stage 3. Also the Taggard shale will be breached more often underground, and the lost waterfalls which now exist will disappear.

The Dry Creek sink should enlarge to form an explorable cave,

and will mature until it can take all of the flow, even during floods. To the south Overholts will not change significantly, except that the waterfalls will erode back towards the head of the cave. The feeders to Overholts however, should change, as several of the caves near the Beveridge Pits will enlarge. Wolfe's Swallow Hole will find a more direct route to Overholts, drying up the Hause Waterfalls.

Carpenters Cave should breach the Taggard underground and flow directly to Cave Creek Cave. Also, the unexplorable routes along Overholts and McClintocks Run, and the nearby streams should develop and enlarge.

5.4 Simulation of the Swago Creek Basin

The streamflow of the Swago Creek basin was simulated for the 710 day period from September 20, 1969 to August 31, 1971. The model was started 30 days in advance of the real record (on August 2nd, 1969), to reduce the effect of the initial conditions (which could not be easily defined) on the actual simulation. A plot of the real and simulated flows on a logarithmic scale, along with the basin precipitation for the complete period, is shown in Appendix II. Figure 5.14 shows a linear plot of the simulation results for the period October 26, 1970 to April 30, 1971, which brings out most of the features of the complete record. The measured, estimated and optimized parameter values used at Swago are shown in Table 5.2, and the parameter values that were the same for all the basins are shown in Table 8.4.

In the Swago basin there are a number of different geomorphologic areas, particularly the karsted limestone area and the overlying clastic area. The simulation results, however, were not markedly better than those obtained using one segment, and so further modelling was performed using a single segment. This led, however, to some problems in estimating certain parameter values, such as the soil storages or baseflow recession constants, as these parameter values are markedly different over the limestone and clastic areas. In the single segment model the parameter values were estimated as the mean between the limestone and clastic values, and corrected by optimisation.

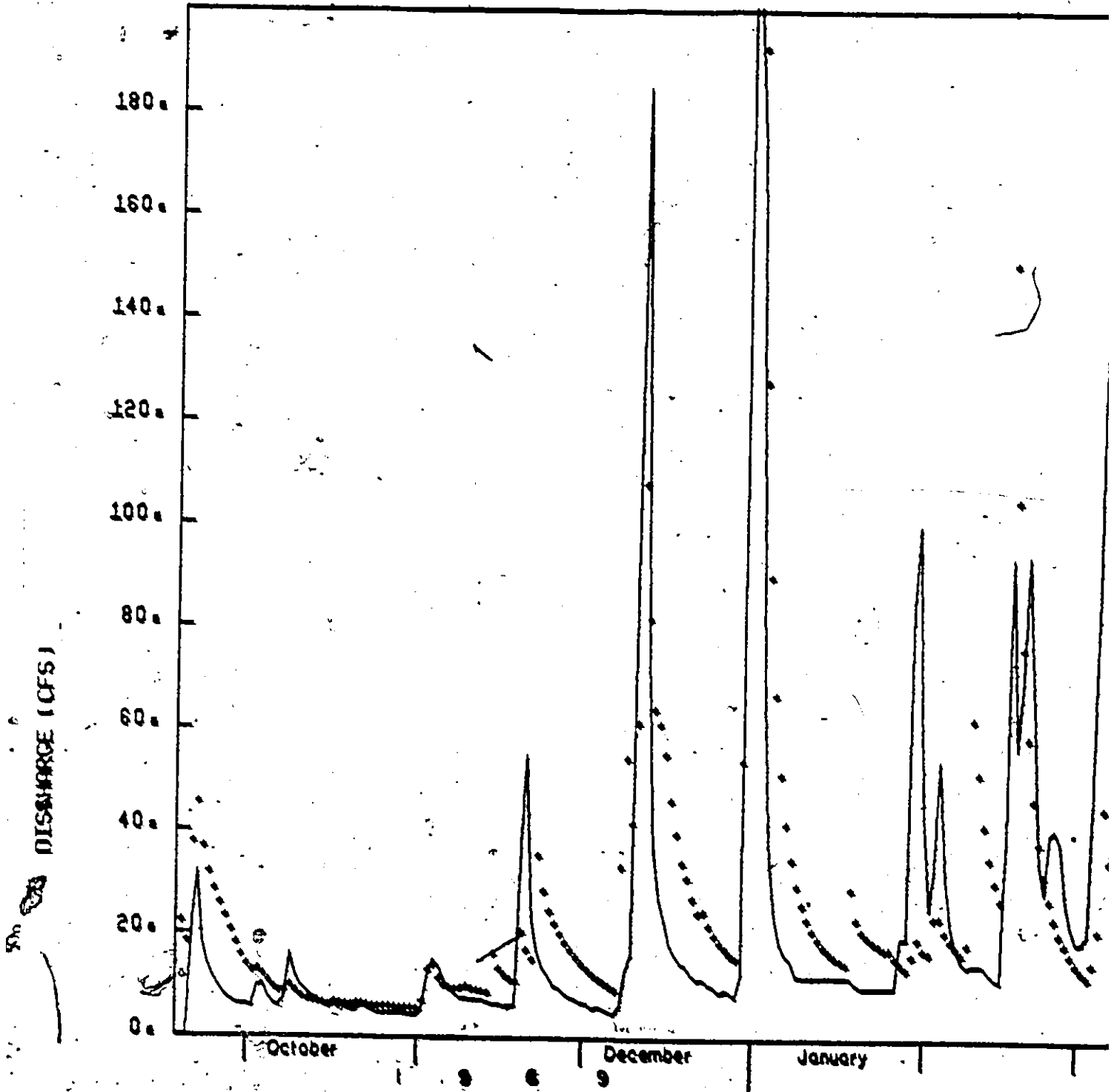
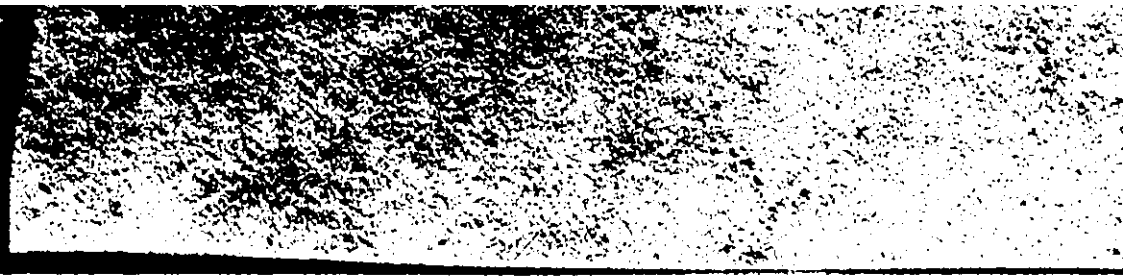
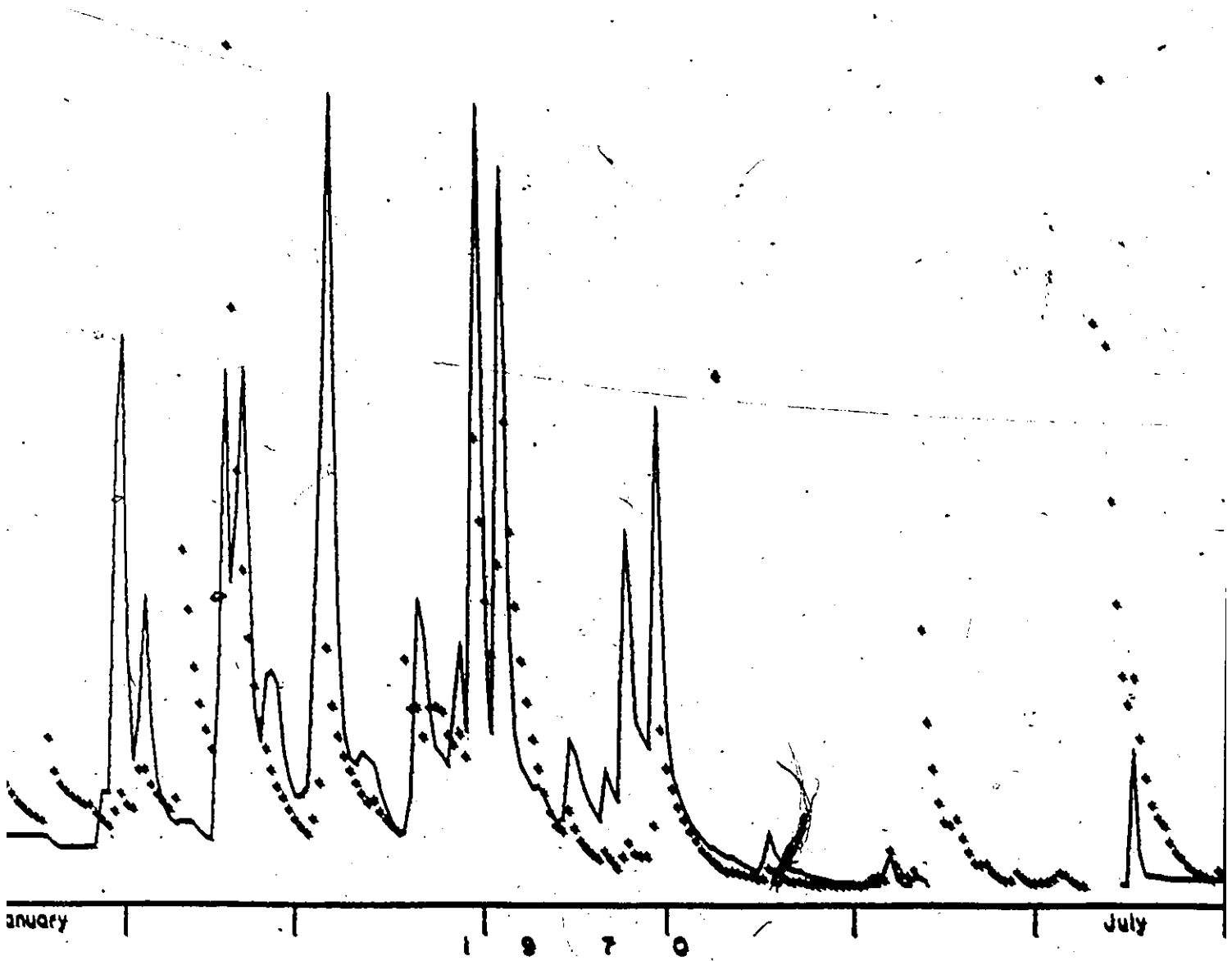


Figure 5.13 The real and modelled hydrographs for Swago Creek.



▲ RECORDED
• SIMULATED



5.4.1 Description of the Real and Simulated Streamflows

The full streamflow hydrograph at Swago can be seen in Appendix II. There are a number of places where the real streamflow record is unreliable. These are:-

- a) During an 18 day period in January, 1970 the float became frozen in the recorder and the streamflow data were lost.
- b) Throughout most of the summer of 1970 the float bottomed in the tube and gave unreliable stage figures. Unfortunately, this fault was not detected until the end of the summer. During this period storms did occur which raised the float and gave some readings, but flows below about 4 cfs. were not recorded. The slight variation in the minimum level is due to the varying amounts of sediment in the down pipe.
- c) The recording chart for a 31 day period in June and July 1970 was lost. Also, the clock on the recorder stopped for 14 days during January 1971, preventing readings from being obtained in these periods.

Throughout the simulation period there are several times when the model response does not match the real data very well. The peak heights are sometimes 50% or more in error: for example, the simulated flow is larger during the peaks in September and October 1969, and in October 1970, but smaller in March and December 1970 (Appendix II). The simulated flood peak recession rates are also in error at different times, for example being too slow in September 1969 and January 1970, and too fast in May 1970 and April 1971. It appears that the real recession is slower during

Table 2.2

Sensitive Parameter Values Used at Swagg Creek

PARAMETER	DESCRIPTION AND UNITS	VALUE
<u>Measured Parameters</u>		
AREA	Segment area (square miles)	12.0
HTSTA	Mean elevation of the climatic stations (feet)	2150
HTSEG	Mean segment elevation (feet)	3500
<u>Estimated Parameters</u>		
LPSRT	Lapse Rate ($^{\circ}$ F/1000 feet)	.5
GRWRT	Ground water recession rate (days)	200
BZK	Interflow recession rate (1/days)	0.2
TDDET	Time delay histogram (1/days)	0.5 0.5
OWSINT	Initial ground water storage	5
IADD	Time delay between this segment and the outlet (days)	-
<u>Optimized Parameters</u>		
INFMAX	Maximum infiltration rate (inches/day)	2
INFMIN	Minimum infiltration rate (inches/day)	0.3
INFRT	Infiltration coefficient	.1
UBCOF	Upper to lower zone percolation coefficient	.5
BCCOF	Lower to ground water percolation coefficient	.2
LESN	Nominal lower zone storage (inches)	2
UESN	Nominal upper zone storage (inches)	1.1

the spring snowmelt period than at other times of the year. This could be due to extra water being held in storage in the snowpack. No account¹⁻ was taken in the model of any seasonal changes in recession rates although such a factor may well improve the model response.

One of the major areas of errors in the model was during the summer of 1970. At this time the float was often bottoming, and the recorders were giving an apparent reading which was too large. However during this period, particularly during July and August (Appendix II), the simulated flows were usually well above the recorded flows. On August 10th, for example, after 1.14 inches of rain fell, the simulated flow was 86 cfs. (equivalent to 0.27 inches/day of runoff over the basin) while the real flow was only 14 cfs. (= 0.044 inches/day). The model was not evaporating enough of the precipitation during this period. Efforts to improve the 1970 summer simulation by increasing the interception storage, evaporation correction coefficient, upper zone storage or infiltration rates always led to degradation of the simulation at other times. It is not known why the simulation was so poor during the summer of 1970, and further work needs to be done to improve it.

The snowfall and snowmelt periods also contain several discrepancies. The timing and magnitude of many of the snowmelt events are often in error, as can be seen from an inspection of February and March records for both 1970 and 1971 (Appendix II). The snowmelt routine used is clearly an oversimplification, but most of the data needed to implement a more sophisticated routine (such as radiation, humidity and wind speed) are not available. When the model was initially run, an excessively large

modelled snowpack built up in the winter and melted in the spring, giving small winter flows and large spring floods. To counteract this the modelled basin temperature was increased to give a better snowmelt distribution. This was done by inputting a negative lapse rate of $-5^{\circ}\text{F}/1000$ feet instead of the accepted figure of $3\frac{1}{2}^{\circ}\text{F}/1000$ feet, which increased the mean basin temperature by about 11°F . This allowed some melt to take place even if the mean temperature was just below freezing, as the maximum temperature in these cases may well be above freezing.

A better method of modelling the snowmelt would be to shorten the time increment and use a diurnal temperature distribution to calculate the temperature throughout each day. Melt could then be satisfactorily modelled in the afternoon even though the true mean basin temperature could be below freezing. In addition calculations of the form of the precipitation would be improved if hourly precipitation data were used along with the short term temperature information. This scheme was not pursued due to lack of time.

5.4.2 Geomorphic Significance of the Model Parameters

The parameters used in the simulation of the Swago basin allowed some estimates to be made of the geomorphic characteristics of the basin. The major implications include:-

- a) The low value of the lower zone nominal storage which is 2 inches, indicates the thinness of the soil in the karst area. In clastic regions the lower zone nominal storage is often about 14 inches

(Crawford and Linsley, 1966), and the value of this constant is related to the maximum storage of water in the lower soil zone.

b) The value of the interflow recession constant is very fast at 5 days. This low value is due to the quick draining of the unsaturated limestone. The long baseflow recession constant of 200 days is related to the draining of the clastic material in the basin headwaters. The 200 day baseflow recession is comparable to the values often encountered in clastic basins (Crawford and Linsley, 1966).

c) The time delay histogram was set at two steps, with 0.5 of the flow each day. Thus the simulated streamflow on any day consists of the sum of one-half of the same day's, and one-half of the previous day's modelled runoff. This is equivalent to a channel delay of 12 hours. The basin is about 4 miles in diameter and thus the "average" flow rate in the channels is about 1000 feet an hour. From the flood and dye test (Section 5.2.4.1), it was found that the Swago stream flowed at a rate of 3000 feet an hour. As the flow rate of the Swago stream was estimated to be typical of the large streams seen in the basin, the unknown portions of the flow routes must have some sections where the flow is delayed compared to the speed of the flow along the Swago streamway section. The unknown flow routes probably contain vadose streams and pools and are unlikely to contain long or direct phreatic sections of flow, as this would give a very fast pulse response.

CHAPTER VI

THE GENESIS OF THE LOCUST CREEK BASIN

The Locust Creek basin has undergone a complex and varied history of karst development. The stream channel pattern has developed from an original, wholly surficial flow to the present situation, where the majority of the streams flow underground for a large part of their journey to the Greenbrier River. The karst development has had a significant effect on the drainage areas in the Locust Creek and adjacent basins. The surficial and original drainage area to Locust Creek was only 5.5 square miles; at present the drainage area to Locust Creek is about 37 square miles. Locust Creek is thus far larger now than it was previously.

Karst development of the basin took place in a number of stages as flow paths for the various streams were diverted or pirated to new routes. The major diversion was the capture of the Hills and Bruffey Creeks from the Spring Creek drainage basin to Locust Creek (Figure 6.21). This diversion was not a simple one-step process, however, but occurred in several steps, as described in Section 6.3.3 to 6.3.5. Other streams in the basin were similarly diverted; their captures and modes of development are described in Section 6.3.

It appears that there were five major stages of development, although each could be divided into a number of sub-stages. The initial stage was the wholly surficial or non-karstic flow. The second stage was the underdraining of several of the surface streams. No piracy took

place at this stage. The third and most significant stage of development (Section 6.3.3) is the diversion of the Hills stream through Outlip Cave and into Locust Spring (away from the Spring Creek valley), and the diversion of the Bruffey stream to Upper Hughes Cave. The fourth stage (Section 6.3.5) is further shortening of the flow path to Locust Creek. The modern situation is one of transition between the fourth and fifth stages of development.

Evidence for recent events in the basin is widespread, thus the recent stages of development can be postulated in detail and with a good degree of certainty. Evidence for the earlier stages of development has, in many cases, been destroyed by subsequent erosion or sedimentation. Thus knowledge of the earlier stages of development is less detailed although it is suspected that they span a far longer time period than the later stages. It is also probable that minor sub-stages and diversions of the streams occurred in the early stages of development for which no evidence now exists. However if these diversions and sub-stages occurred they would not alter the total picture of the karst development very much.

The development time for each stage cannot be accurately assessed, but estimates have been made based on the use of a number of techniques. Estimates of the development time have been assessed for the later stages based on the rate of erosion. Geochemical methods can be used for estimates of the time for the earlier stages. The exact temporal relationship for the various sub-stages is even more difficult to assess, and the sub-stages described as occurring contemporaneously or in a particular order may well have occurred in some other order. However the exact

order of the sub-stages is usually not vital to the overall mode of development, and it is believed that the order of development of the major stages relative to each other is correct.

6.1 Hydrological Description of the Surficial Basin

The Locust Creek basin has been briefly summarised in Section 1.4.2, but the hydrological and morphological features will be described in more detail in this section. The present hydrological basin is roughly oval in shape (Figure 6.1), and is about 10 miles long and 6 miles wide. The elevations in the basin range from approximately 2070 feet at Locust Creek to the 4525 foot Kennison Mountain. The surface and underground hydrology of the basin is shown in Figure 6.2 during flood conditions, and in Figure 6.3 during dry conditions.

The most prominent feature in the basin is the Hills Creek valley which runs down off Kennison Mountain to the north, across the center of the basin, and out to the west of the basin (Figure 6.1). The valley is drained by Hills Creek in the north, but becomes a broad undulating and predominantly dry valley in the south-west of the basin. During high water Hills Creek sinks in the Hills Creek Cave (described in Section 6.2.1), but during dry weather the stream sinks in some small joints in the limestone streambed about 300 yards above the cave entrance.

The water flowing into Hills Creek Cave has been tested to Upper Hughes Creek Cave, but the water sinking in the streambed has been tested to Outlip Cave. However both routes finally lead to Locust Creek.

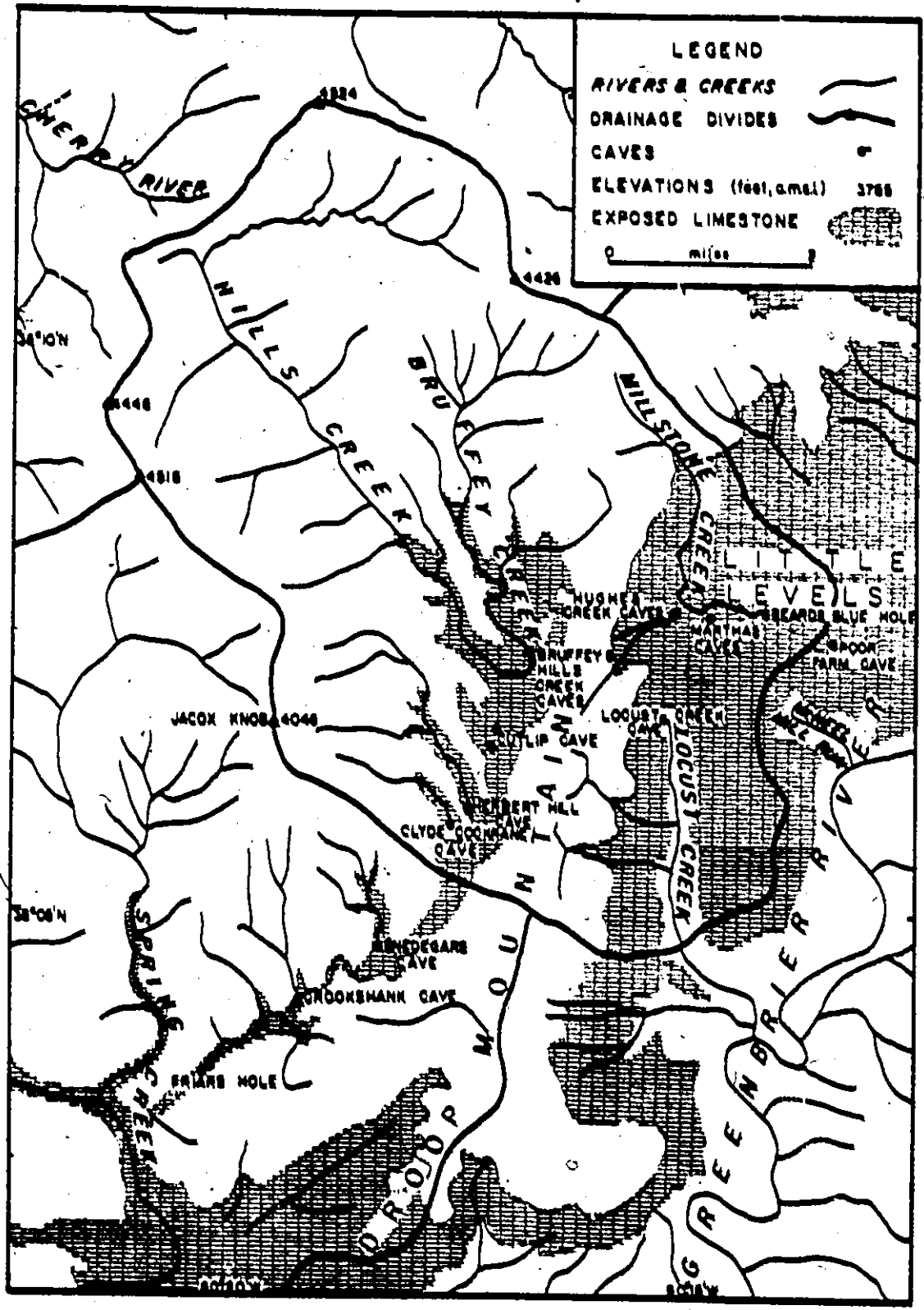


Figure 6.1 Locust Creek basin--topography, surficial drainage and location of caves.

Three-quarters of a mile farther down the dry valley is a prominent sink in which there is a small cave entrance leading into Cutlip Cave. During extreme floods Hills Creek inundates the Hills Creek Cave and floods the valley, to form a lake one mile long and several hundred yards wide. The southern end of the lake drains into Cutlip Cave. In historic times Hills Creek has never flowed beyond the Cutlip sink.

To the north of Hills Creek a smaller stream called Bruffey Creek drains part of Spruce Mountain and flows over the Alderson limestone and Greenville shale and onto the Union limestone near Lobelia (Figure 6.1). During high water the stream flows into the Bruffey Creek Cave entrance, just 200 yards north of Hills Creek Cave. During floods the Bruffey Creek Cave is inundated and the creek flows down the valley to Cutlip Cave (Figure 6.2). During dry weather Bruffey Creek sinks in gravel and stones in the streambed. At this stage, it has been tested to Upper Hughes Creek Cave, as has the water which enters Bruffey Creek Cave.

Farther down the Hills Creek valley, small tributaries run off the adjoining hills and sink in the valley floor. One stream runs into Herbert Hill Cave, which can only be followed for 100 feet, and another runs into Clyde Cochran Cave (described in Section 6.2.3). Farther south a small unnamed stream, shown in Figure 6.2, sinks in its streambed. It was tested to drain to Locust Spring. The next southerly stream drains into Snedegars Cave (Figure 6.1) and this has been tested to Spring Creek. Thus the drainage divide for the basins is between these two streams.

The Hills Creek valley continues on past Snedegars Cave right down to the Spring Creek valley, but the lower part is known as the

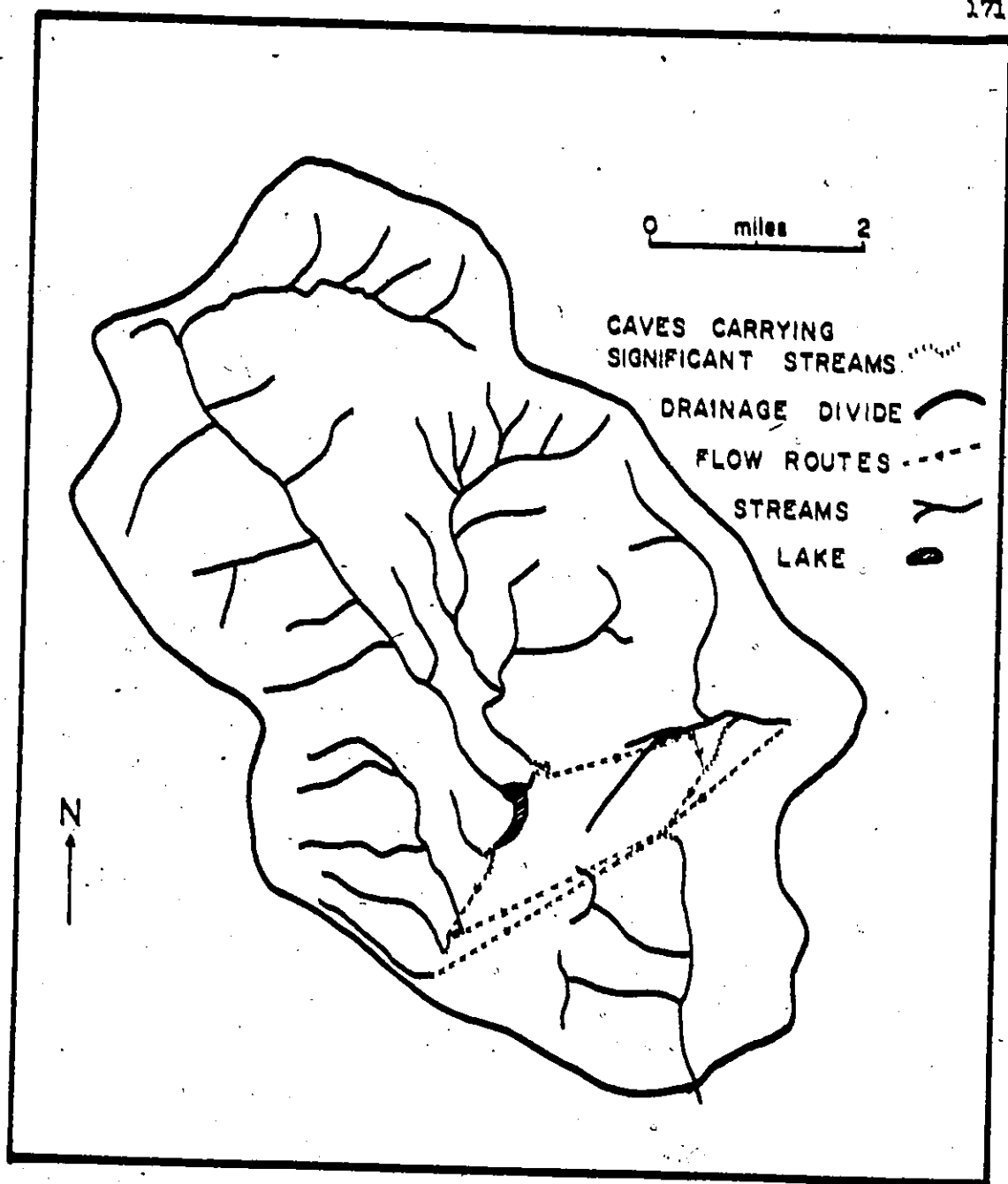


Figure 6.2 Loquat Creek basin--high water sink points.

Friars Hole valley. In the lower reaches, several streams flow off the adjoining hills and sink in caves, such as Friars Hole or Rolling Stones Caves, or in sinkholes. The Friars Hole valley forms a hanging valley approximately 150 feet above the floor of the Spring Creek Valley.

To the north-east of the basin is another complex of caves and sinking streams. Millstone Creek runs off Viney Mountain and flows onto a large depression in a broad, rolling karst plain known as the Little Levels (Figure 6.1). Millstone Creek usually sinks as soon as it reaches the limestone, but in flood flows down to the sink at Beards Blue Hole (Figure 6.2). Beyond Beards Blue Hole a dry valley continues on down to the Greenbrier River via McNeels Mill Run. The valley floor rises, however, beyond Beards Blue Hole, by about 150 feet above the elevation of the present Millstone Creek. It then drops off towards the Greenbrier River.

About a mile to the west of Beards Blue Hole (Figure 6.1) are three prominent cave entrances--Upper and Lower Hughes Creek Caves, and Marthas Cave. Normally none of these caves has a stream in the entrance, but in high water a stream flows out of Upper Hughes Creek Cave, runs for 100 yards to the Lower Hughes Cave, then sinks. In extreme floods, such as after Hurricane Camille in 1969, Lower Hughes Creek Cave cannot take all the water from the Upper Cave, and the excess flows overland to Beards Blue Hole. In these conditions water also flows out of Marthas Cave and runs over the surface to Beards Blue Hole.

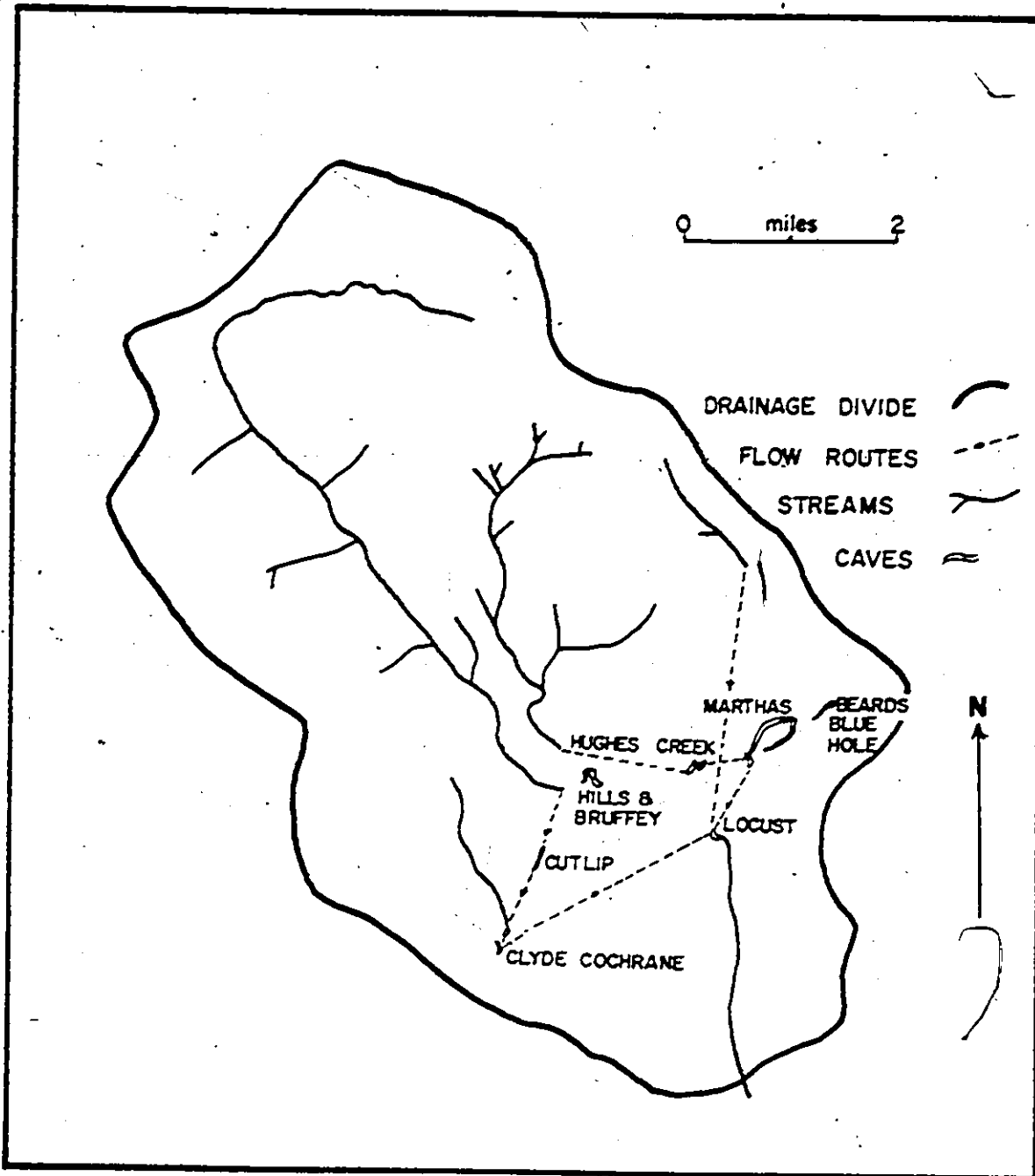


Figure 6.3 Locust Creek basin--low water sink points and caves.

6.2 Description of the Caves and Major Flow Routes in the Locust Creek Basin

In the Locust Creek area there are a number of significant caves which were mapped or explored by the author. They are shown in Figure 6.3, and include the following: Hills-Bruffey Cave, Cutlip Cave, Clyde Cochran Cave, Soedegars Cave, Friars Hole, Hughes Creek Cave, Marthas Cave, Beards Blue Hole, Poor Farm Cave, and Locust Creek Cave.

The caves or water conduits are not always explorable. Streams often sink and rise in gravel or boulders, or through impenetrable cracks, or through sumps, which are water-filled passages. Fossilized caves or conduits can also be filled in with sediments or can collapse, preventing exploration. These inaccessible conduits, either active or fossilized, are important in the understanding of the karst development, and are also described in this section. The active conduits were inferred by dye tests, and the fossilized conduits from evidence in the caves. The major conduits are: Bruffey to Upper Hughes Creek Cave, Hills to Locust Creek route, and the lower Friars Hole route.

6.2.1 Hills-Bruffey Cave

The Hills-Bruffey Cave system is a major trunk passage in the process of abandonment that has played an important part in the development of the Locust basin. The cave has had a varied history, as at one time it carried the entire flow of the Hills and Bruffey streams, but now it only carries a significant stream during high water, i.e. it is

Hills Creek and Bruffeys Creek Cave

POCAHONTAS CO W.VA.

SURVEYED BY M.U.C.C.C. 1969-70.

C.R.G. GRADE 4.

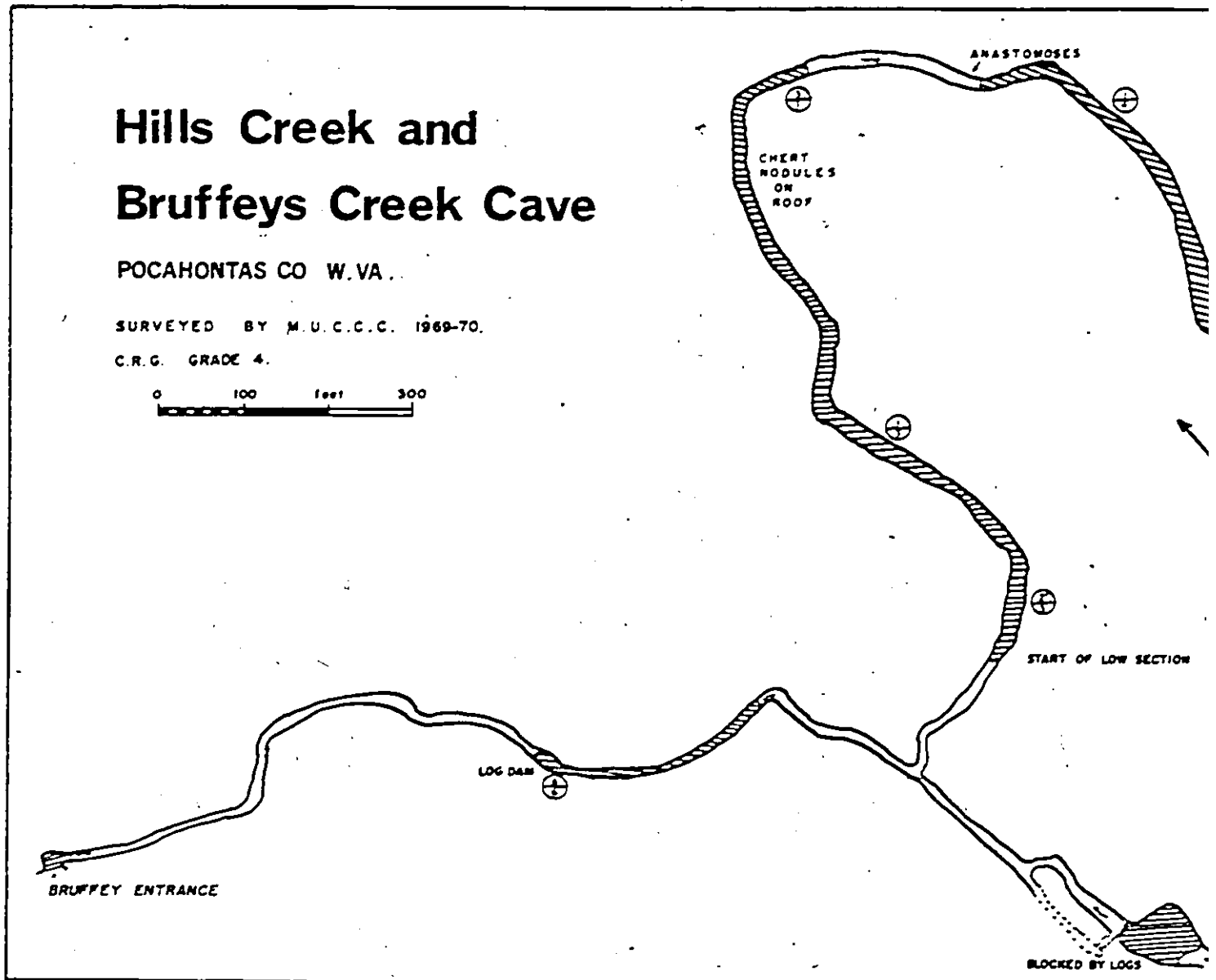
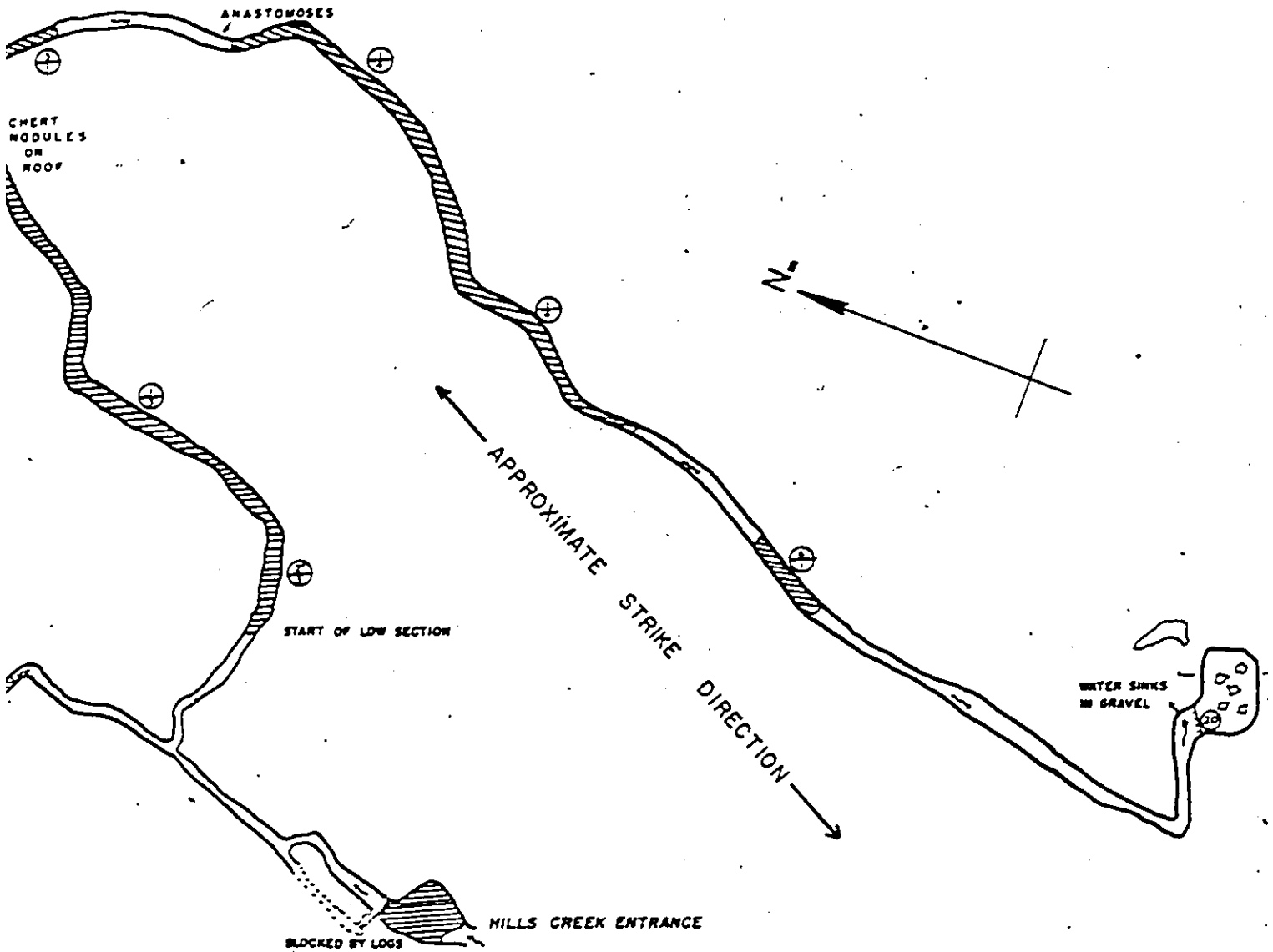


Figure 6.4 Hills-Bruffey Cave.



an overflow route.

The Bruffey entrance is about 20 feet by 20 feet, and the cave continues at this size for 500 feet, then gradually reduces to about 8 feet wide and 10 feet high near the junction with the Hills Creek Cave (Figure 6.4). Beyond the junction the passage continues at about 20 feet wide and 10 feet high for 2500 feet through several pools to a large chamber containing a large number of boulders.

The Hills Creek Cave averages only 6 feet wide and 15 feet high, and the cave is about 300 feet long to the junction with Bruffey Creek Cave. At the junction, Hills Creek Cave is considerably smaller than Bruffey Creek Cave, being only 6 feet wide and 8 feet high. The roof level in Hills is lower than in Bruffey, indicating that the Hills Cave is younger than the Bruffey Cave.

During dry conditions neither the Hills nor the Bruffey streams reach the cave (Coward, 1971) and there is no significant stream in the cave. The cave does, however, contain several deep pools, and some local drips and seepages maintain the levels in these pools and drain to the chamber at the end of the cave. The water disappears in the boulders, and further exploration is not possible. A number of logs jammed in the roof of the chamber and cave passage indicate that the cave now floods to the roof.

The cave was formed partly phreatically and partly under vadose conditions. The entrance and end of the cave have been developed under vadose conditions, and although the initiation of the cave was probably phreatic, no evidence for this could be seen. The middle section of the

cave, near the pools, was developed under phreatic conditions. The roof in this section is lower than the rest of the cave, with the roof being only a few feet above the water surface over most of the pools. The cave is nearly horizontal, with the end being only about 20 feet below the entrance.

The water that flows through the Hills and Bruffey Caves drains to Hughes Creek Cave. Hughes Creek Cave is just north of east (80°) from the Hills-Bruffey Cave (Figure 6.1), and yet the end of the cave is well to the south of east from either entrance. Although the Hills Cave is joint controlled, much of Bruffey Cave is strike oriented with the dip direction being north-west. The drainage direction is up dip, which probably accounts for some of the deep pools in the cave and its devious route towards the resurgence.

Hills Creek has a catchment area which is double the size of the Bruffey catchment at the caves, and there is no evidence that major differences in the sizes of the Hills and Bruffey catchments have occurred recently. As the Bruffey Cave is larger than the Hills Cave, we can infer that the Bruffey Cave must be older, or have carried water for a longer time, than the Hills Cave.

6.2.2 Cutlip Cave

Cutlip Cave is in the dry valley below Hills Creek and is about one mile from Hills Creek Cave (Figure 6.1). It has been described by Louch (1971). The cave is short, the main passage being only 1200 feet

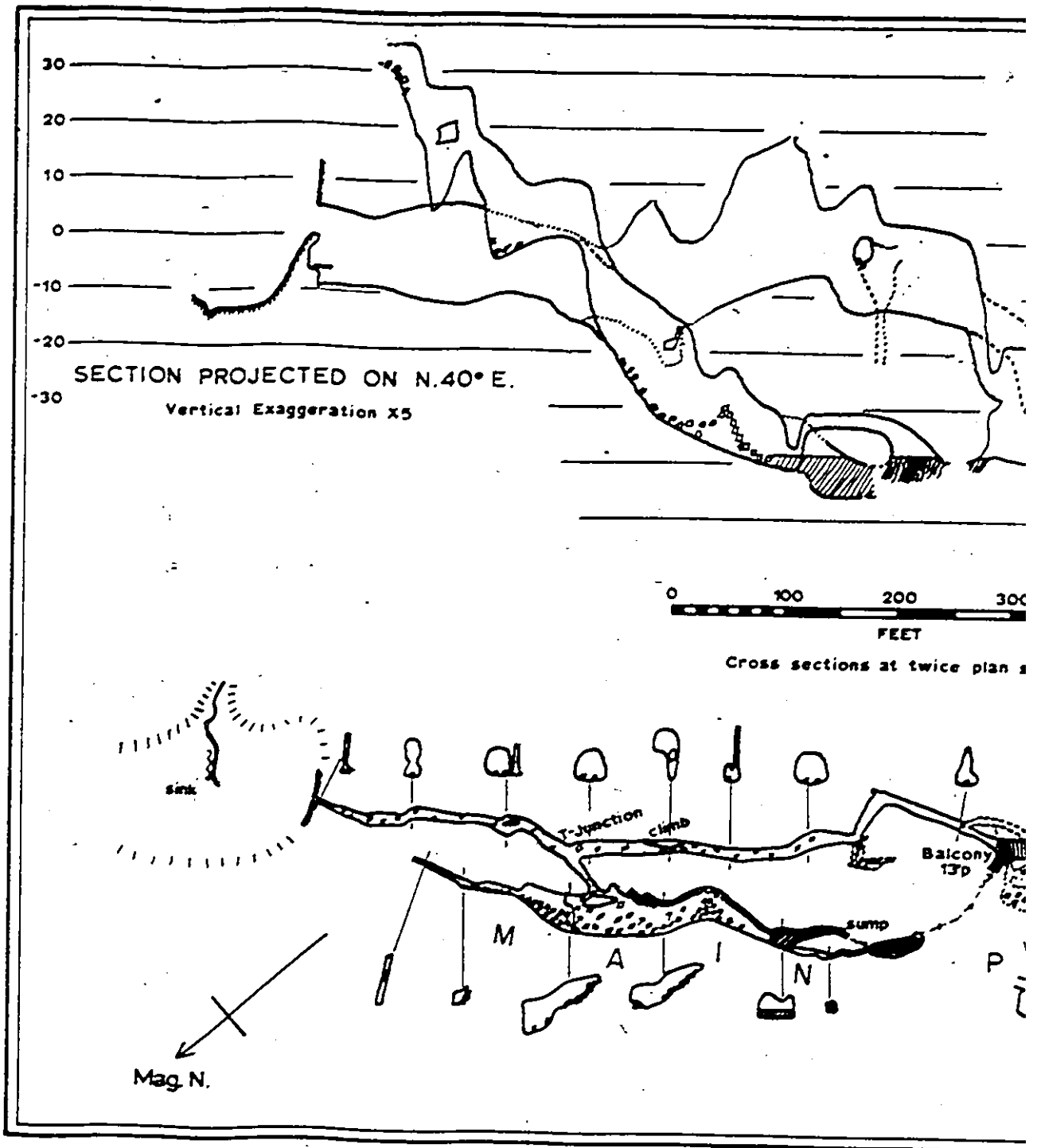


Figure 6.5 Cutlip Cave.

CUTLIP CAVE

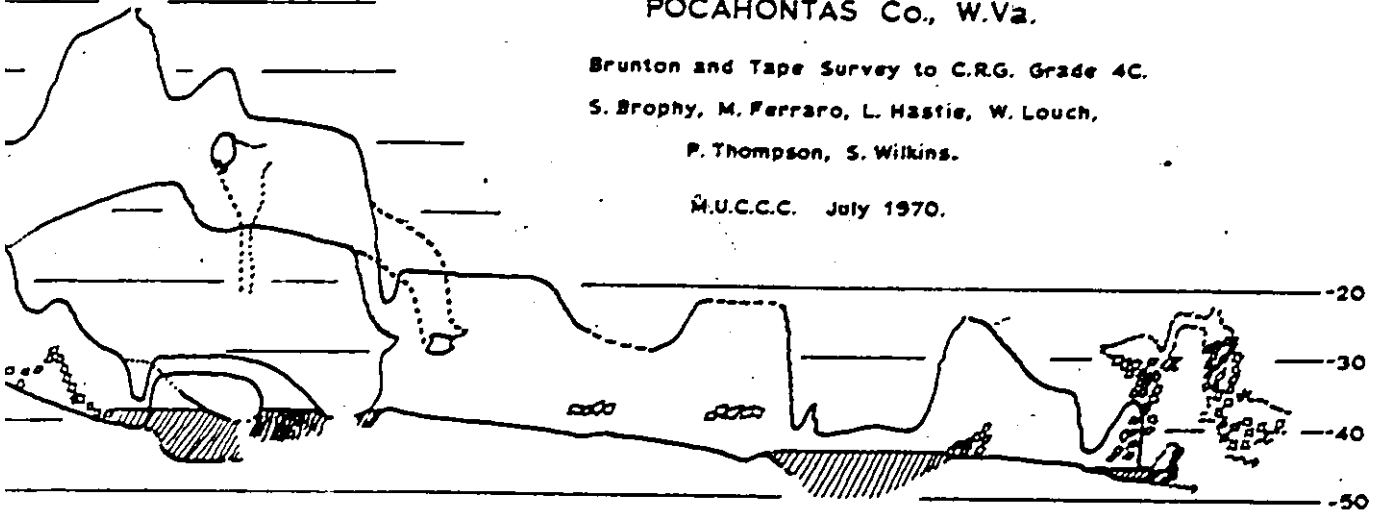
POCAHONTAS Co., W.Va.

Brunton and Tape Survey to C.R.G. Grade 4C.

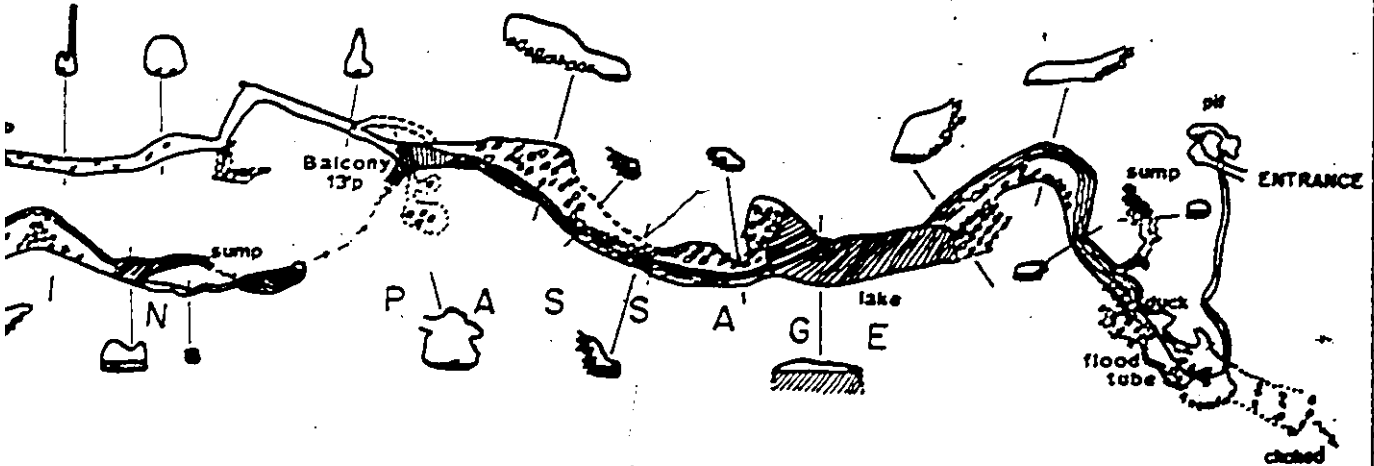
S. Brophy, M. Ferraro, L. Hastie, W. Louch,

P. Thompson, S. Wilkins.

M.U.C.C.C. July 1970.



Cross sections at twice plan scale.



Drawn by M. Ferraro.

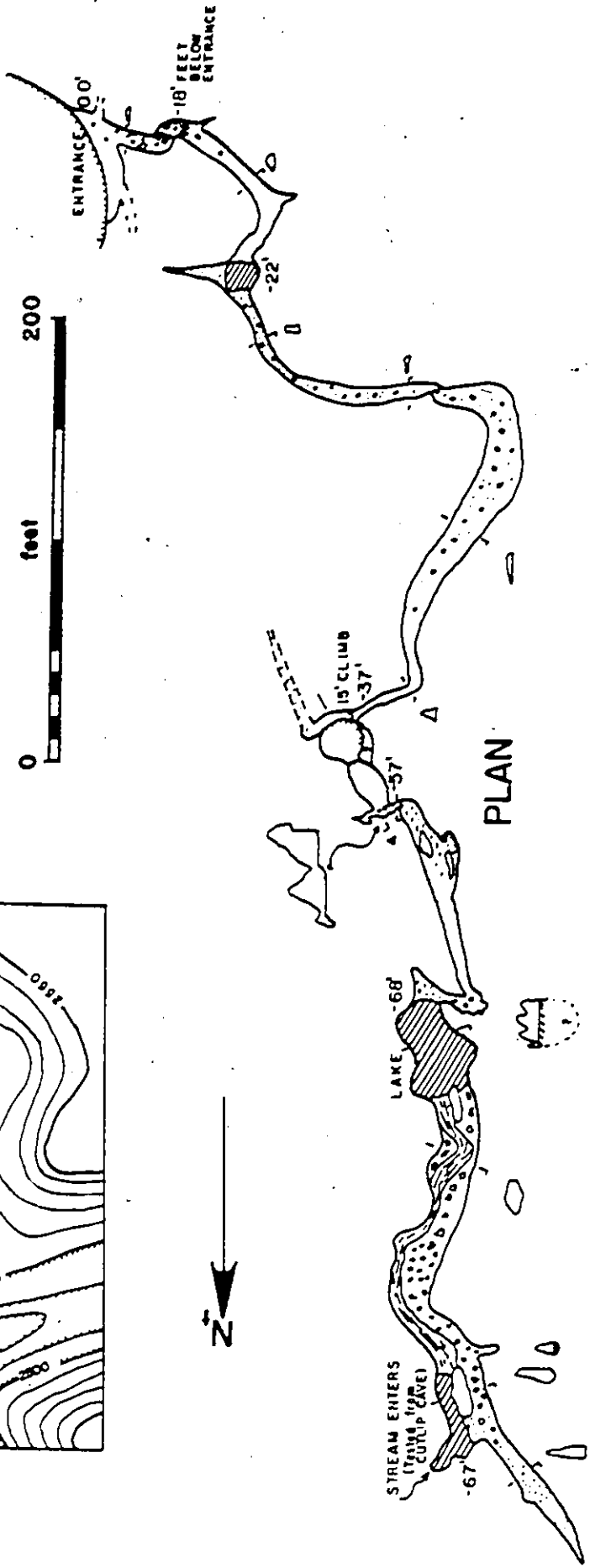
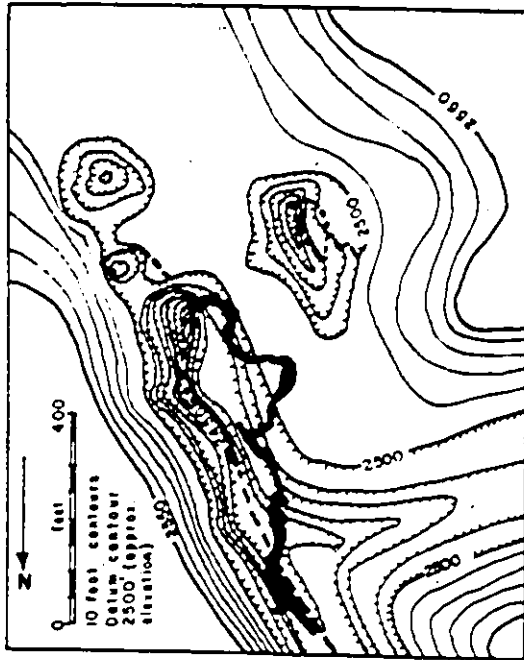
long (Figure 6.5). However it is large, averaging 30 feet wide and 20 feet high, but containing in places some breakdown and infilling. At present small surface streams enter the two entrances of the cave and a large stream enters the main passage inside the cave through boulders, flows through a lake and along a short section of streamway to disappear in boulders at the lowest point. The main stream disappears and resurges through sumps in two places along the cave (Figure 6.5). The stream has been tested to come from the sink of Hills Creek, and flows to Locust Cave via Clyde Cochrane Cave without draining through the Hughes or Marthas Caves. The cave was formed in the Union limestone by phreatic flow, with some recent vadose modification. The cave orientation is controlled by the strike direction. The hydraulic gradient from Cutlip to Locust is just north of east and yet the cave is formed in a southwesterly direction. The cave is oriented, however, towards Clyde Cochrane Cave through which the Cutlip stream flows.

There have been several stages in the development of Cutlip Cave (Figure 6.5). The first major route to form was from a high level entrance above the present sink, which has since been blocked off, and along the main passage. Later the present entrance was used and the water flowed along the entrance passage to the balcony and on through the lower part of the cave. The water was then diverted through the T-junction (Figure 6.5) into the main passage. Recently, when Hills Creek no longer flowed to Cutlip over the surface, the upper levels of the cave became fossilized. The downstream entrance is a late vadose addition to the cave.

Figure 6.6

CLYDE COCHRANE SINKS POCAHONTAS COUNTY WEST VIRGINIA.

C.R.G. GRADE 4d



TOTAL LENGTH 971 FEET.

M.U. C.C.C.

6.2.3 Clyde Cochran's Cave

Clyde Cochran's is the lowest cave along the valley below Hills Creek that drains to Locust Creek. The cave entrance is at the end of a stream valley (Figure 6.6) and the cave can be followed down past a few climbs for 800 feet to a large deep pool of water (Coward, 1972). A larger streamway on the far side of the pool can be followed up for 150 feet to a sump. The water flowing out of this sump has been tested from Cutlip Cave, which is 6000 feet up valley, although Herbert Hill Cave which is 1000 feet up valley almost certainly drains to here as well.

6.2.4 Snedegars and Friars Hole Caves

In the large, predominantly dry valley below Hills and Bruffey Creeks are two large caves--Snedegars and Friars Hole (Figure 6.1). Although these caves are outside the present Locust Creek basin, they played an important part in the paleohydrology of the Locust basin.

The Snedegars system is a complex of caves, with a total length of over two miles, containing a major trunk passage (Figure 6.7), one end of which forms the main entrance, and a number of tributary inlets, three of which can be followed out to known entrances. Three entrances are close together and are known as Snedegars "Wet", Snedegars "Dry", and Snedegars "Staircase" Entrances. The fourth entrance, and the associated cave, is Crookshank Cave.

The main trunk passage of the cave can be followed past a low

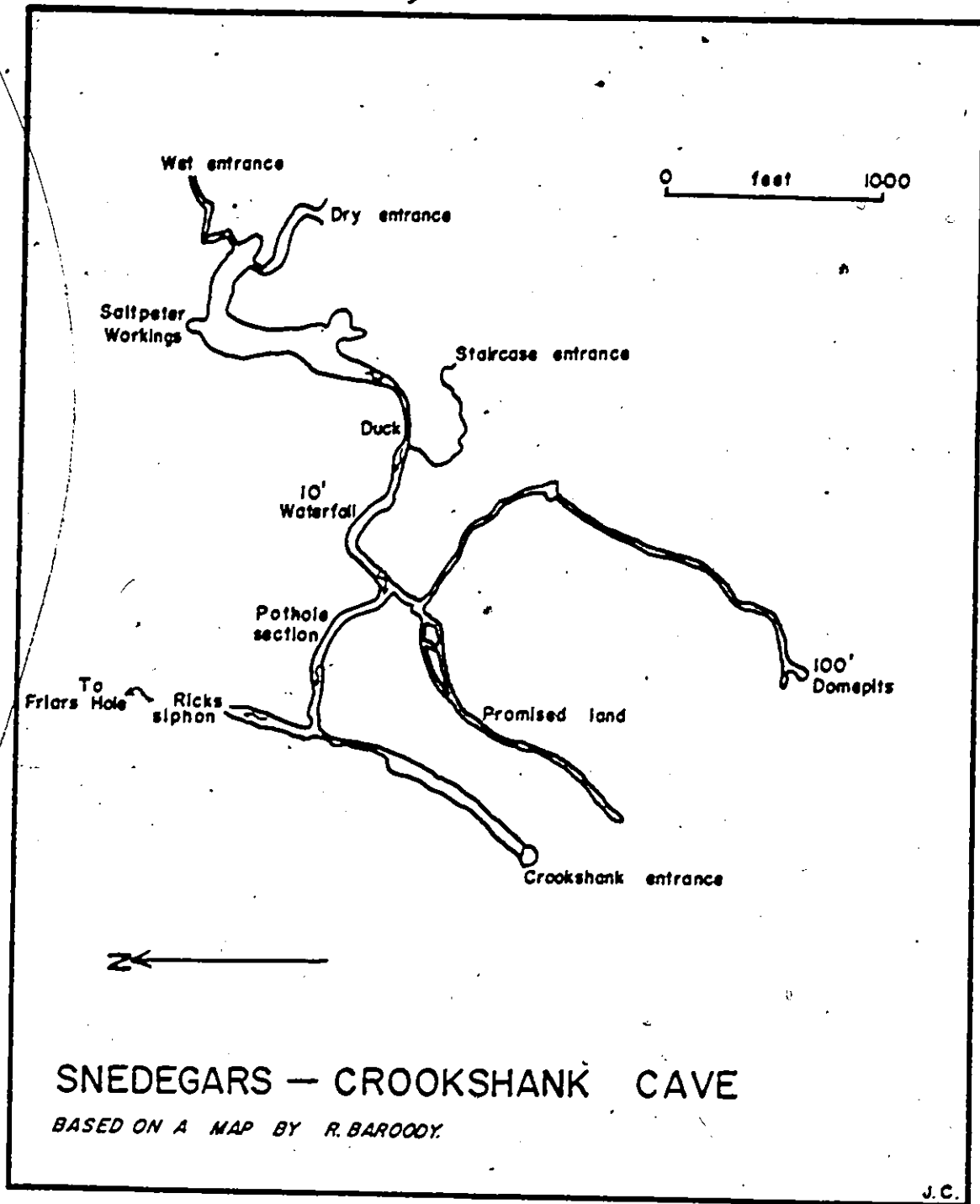


Figure 6.7 Snedegars Cave.

duck for about a mile, at which point exploration ends in a constricted sump, Rick's Siphon. Near the entrance the passage averages 30 feet high and 50 feet wide, but further down the passage becomes smaller (about 20 feet square after 1000 feet). The large size of the entrance passage can be attributed to development by aggressive water entering into this entrance, and dropping steeply down the passage to the level of the present duck. Near the duck there has been considerable infilling, since the passage now is only 4 feet high and about 20 feet wide. The depth of the infilling is unknown. Beyond the duck the passage continues for several thousand feet, mostly about 20 feet high and 10 feet wide, although there are several lower sections only 10 or 15 feet high. At the end of the main passage (Rick's Siphon) the passage reduces in height to less than a foot over gravel and cobbles, and further exploration is not possible.

The cave is developed in the Union and upper part of the Pickaway members of the Greenbrier limestone. The Pickaway member contains several shale bands which are shown in Table 6.1. This is part of a section mapped by Price (1939) near the village of Julia, which is about two miles to the south of Snedegars. Although the top of the Union is not exposed at the Julia section (Table 6.1), the Union is about 185 feet thick in this area (Price, 1939), indicating that the contact is at an elevation of 2550 feet at Julia. The elevation of the top of the Union was estimated to be about 40 feet above the Snedegars Cave entrance (2440 feet), giving the contact an elevation of 2480 feet. The Greenbrier limestone, therefore, has an apparent dip of about 40 feet per mile ($\sim \frac{1}{2}^\circ$) to the north in this region. The duck area (Figure 6.7) which is 150 feet

Table 6.1

Geological Section of the Upper Part of the Greenbrier Limestone at Julia,
and Comparison with the Passages in the Snedegars and Friars Hole Systems

<u>Description</u>	<u>Thickness (feet)*</u>	<u>Elevation at Julia (feet)*</u>	<u>Elevation at Snedegars & Friars Hole (feet)</u>	<u>Cave Passages in Snedegars and Friars Hole and Approximate Elevation (feet)</u>
<u>Union Limestone</u>		2565	2480**	
A) Union limestone and concealed	171			Creek Entrance to Snedegars (2440) Dry Section of Snedegars (2350-2490)
		2384	2324	
B) Union limestone, blue, massive	29			Crookshank Shaft (2290-2390) Snedegars Staircase (2300-2470)
		2365	2295	
<u>Pickaway Limestone</u>				
C) Limestone, grey to yellow, shaley	5			
		2360	2290	Duck (2290)
D) Limestone, light grey	10			
		2350	2280	Friars Hole Entrance (2280)
E) Limestone, yellow	20			
		2330	2260	18' Waterfall Base (~2260)
F) Limestone, dark grey, argillaceous	10			
		2320	2250	Pothole Section
G) Limestone, bluish grey, hard, massive	30			
		2290	2220	Rick's Siphon (~2220)

(cont'd...)

Table 6.1 (cont'd)

<u>Description</u>	<u>Thickness</u> <u>(feet)*</u>	<u>Elevation</u> <u>at Julia</u> <u>(feet)*</u>	<u>Elevation at</u> <u>Snedegars &</u> <u>Friars Hole</u>	<u>Cave Passages in Snedegars</u> <u>and Friars Hole, and</u> <u>Approximate Elevation (feet)</u>
<u>Pickaway Limestone</u>				
H) Limestone, blue-grey, shaley	25	2265	2195	1st Pitch (2190-2210)
I) Limestone, yellow argillaceous	2	2263	2193	Top of 2nd Pitch (2180)
J) Limestone, light grey with clay seams	28	2235	2165	Trunk Passage (2150-2170)
<u>Taggard Limestone</u>				
K) Red and shaley limestone	25	2210	2140	
<u>Patton Limestone</u>				
L) Various fairly pure limestones	125	2085	2015	Lower Passages in Friars Hole (2080) (base level at Spring Creek, 2050)
(continues)				

*Data from Price (1939), pp. 187 - 188.

**Elevation of the top of the Union Limestone

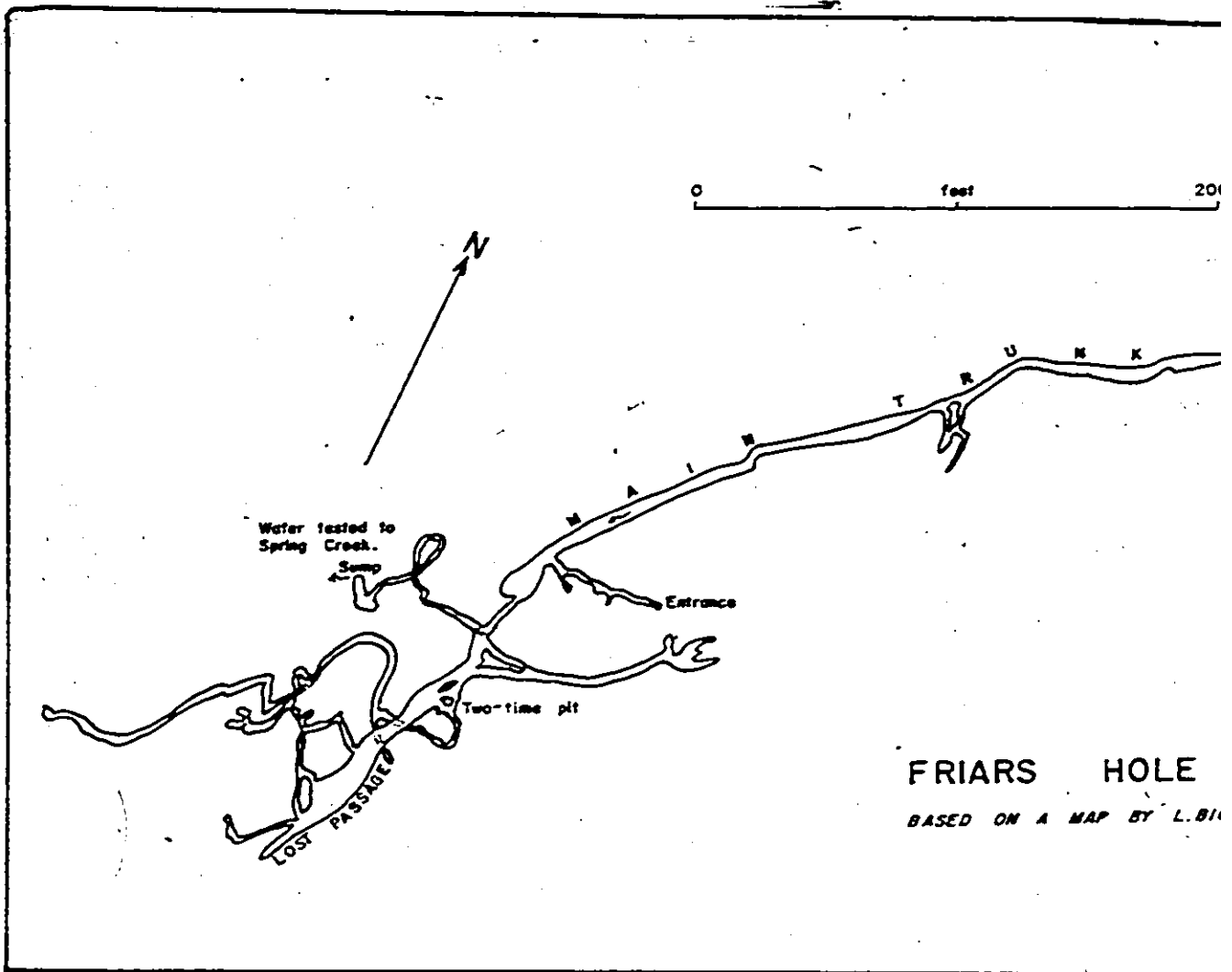
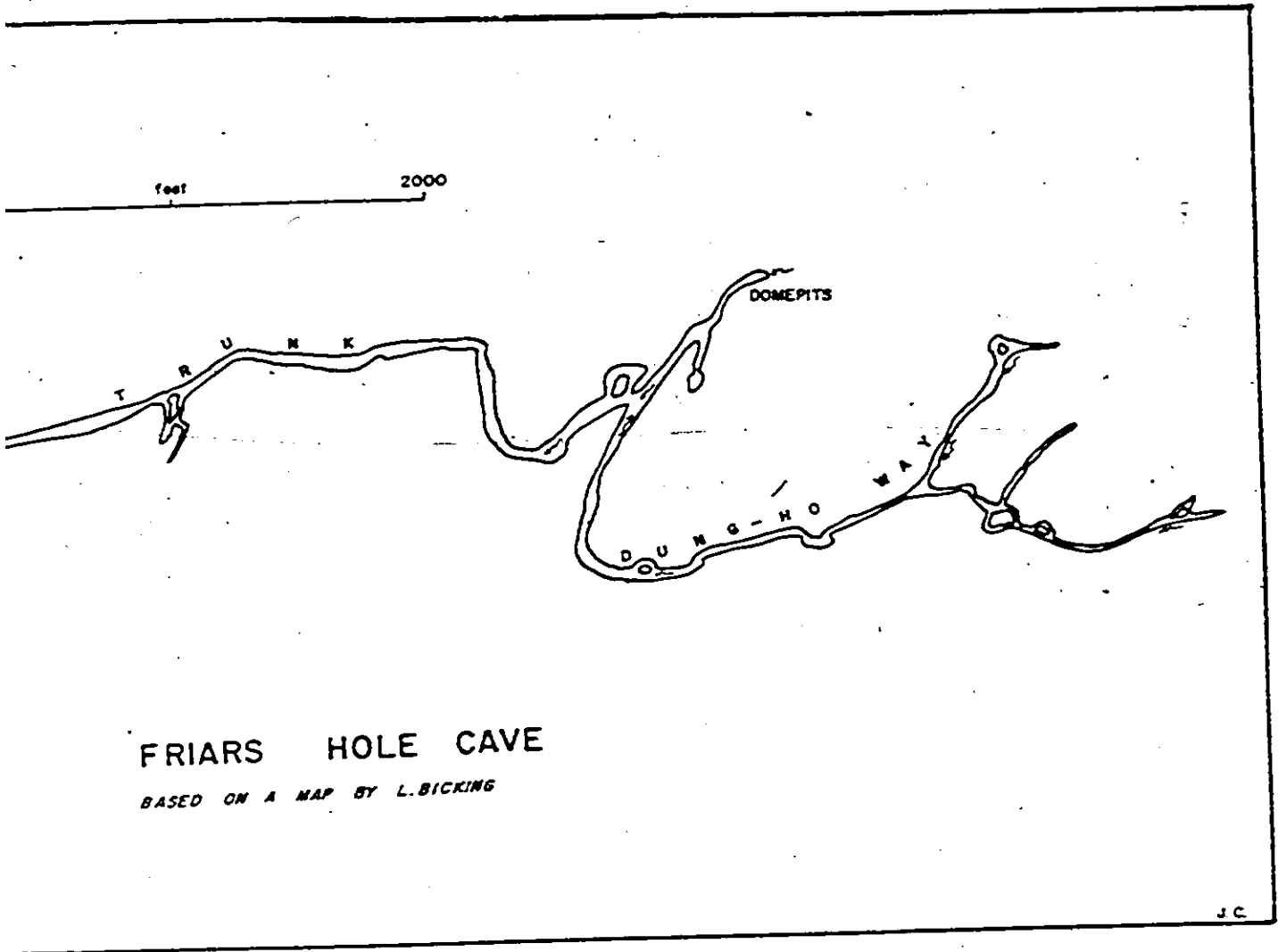


Figure 6.8 Friars Hole.



below the entrance (W. Skinner, personal communication, 1974), corresponds to the top of the Pickaway limestone, while the 18 foot waterfall and pothole section of the streamway are developed in the purer limestone members (marked as E and G in Table 6.1). It can be seen that the large parts of the cave are developed in the purer limestone, while the smaller passages (such as the Duck and Rick's Siphon) are developed in the more shaley limestone beds.

The main streamway was formed under phreatic conditions, but has been enlarged and modified by vadose action. The main chamber in the entrance series is now dry and fossilized, but the stream that enters the wet entrance appears from boulders just above the duck and flows through the lower part of the cave to Rick's Siphon. This stream now drains 1.8 square miles to the south of Jacox Knob.

A number of tributary inlets enter the main passage (Figure 6.7). The Staircase, Crookshanks, and 100 foot Domepit passages all carry streams and are small recent vadose passages. The Promised Land section is a phreatic, fossilized passage network that forms a maze between the Crookshank area and the Snedegars streamway. A number of the passages in Snedegars are controlled by a prominent joint set in a part of the Pickaway limestone (Price, 1939). The joints are oriented at 45° East of north, which is the predominant direction of the Promised Land and 100 foot Domepit inlets and parts of the main streamway.

Friars Hole cave is an important trunk cave that is interpreted to have carried the entire flow of Hills, Bruffey and Snedegars streams during Stage 2 of the basin development. The cave has a surveyed length of 4 miles, and has been mapped and described by Bicking (1966).



Figure 6.9 Friars Hole Cave: the main trunk passage near the downstream end of the cave. The domed shape of the passage and the phreatic pockets in the roof attest to the phreatic origin of this passage. The large scallops, from 2 to 3 feet long, which can be seen on the left hand wall of the photo, indicate that the cave was developed by very slow flow of about 0.02 feet per second (Goodchild, 1970)

The present entrance is a small constricted vadose passage (Figure 6.8) which carries a small stream draining about one square mile of the Friars Hole valley. After 300 feet it joins the main trunk passage near the downstream end. The main trunk passage is about 30 feet wide and from 20 to 50 feet high, and extends in a northeasterly direction for over a mile. The main trunk was developed phreatically, with later vadose entrenchment. There are a number of recent vadose inlets, such as the entrance series and the inlet from the domepits.

The cave has been surveyed (Figure 6.8), but unfortunately no elevations were taken during the survey. However the entrance elevation is 2280 feet, and the entrance series has a drop of 130 feet to the main trunk passage. This passage, with a floor elevation of about 2150 feet, is running on the Taggard shale. From Table 6.1 it can be seen that the Taggard at Snedegars (2 miles to the northeast of Friars Hole) is at an elevation of 2165 feet, indicating that the Snedegars-Friars Hole valley is almost exactly strike oriented. Below the entrance series junction, the trunk passage continues for 200 feet to a large dome room containing a large pile of boulders on the floor. From here a small stream passage can be followed, dropping down a climb where the Taggard shale (Table 6.1) can be seen, and on down a number of climbs till the stream finally disappears in breakdown. This lower stream passage is small, recent, and vadose. The total elevation drop is estimated to be about 70 feet, giving an elevation at the end of 2080 feet, which is only 30 feet above the elevation of Spring Creek at the end of the Friars Hole valley. Another passage leading off from below Dome Chamber leads into the Lost Passage

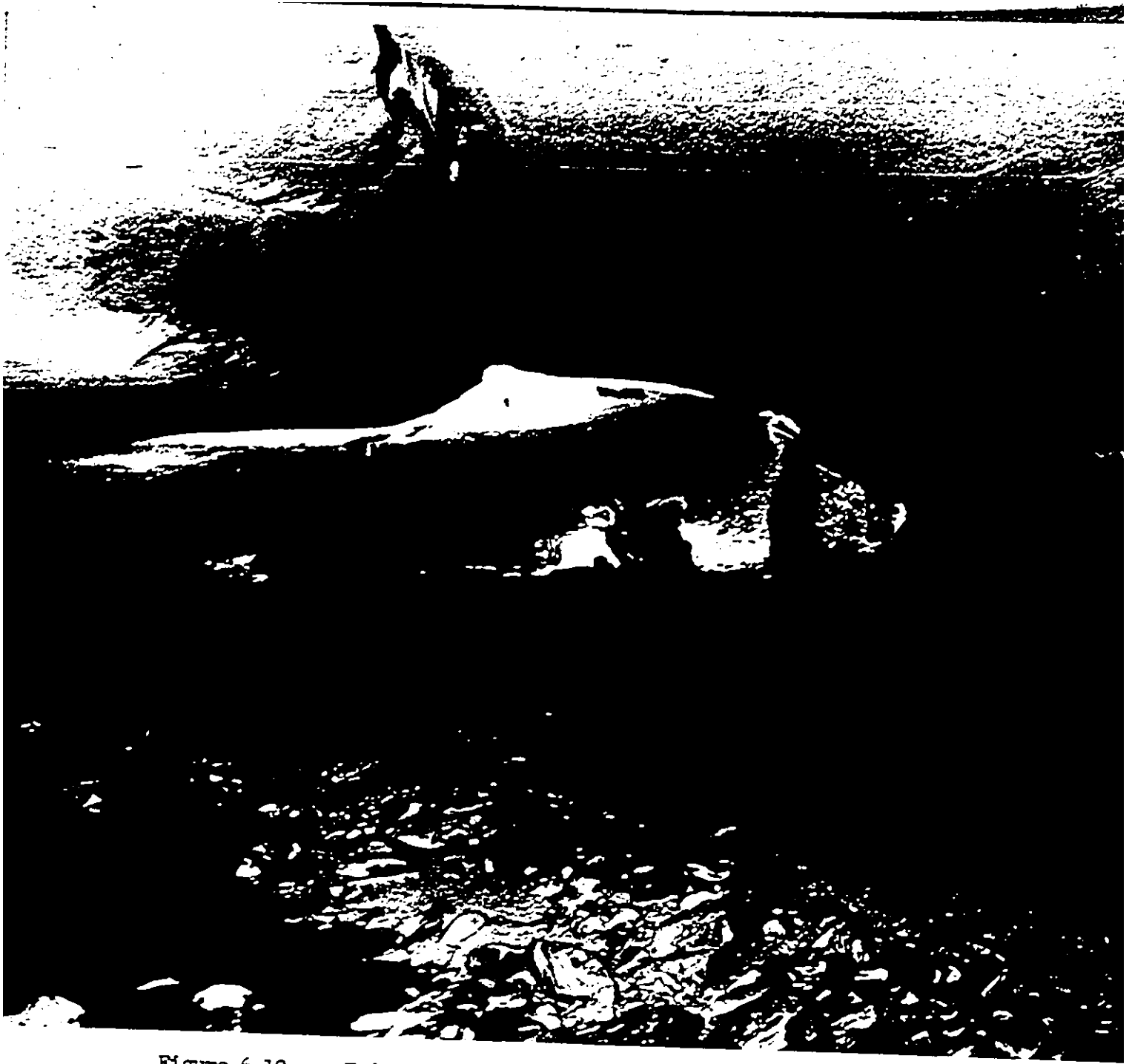


Figure 6.10

Friars Hole Cave: near the upstream end of the main trunk passage. The joint in the roof that initiated development can be seen, as well as the wide and low phreatic passage shape. The cobbles in the floor are the result of recent infilling by the present vadose streamway.

190

(Figure 6.8) which is the continuation of the trunk passage. Both ends of the Lost Passage are blocked by boulders. The Lost Passage was the former route of the main cave during Stage 2, on its way to Spring Creek.

As Friars Hole was developed under phreatic conditions it is probable that the cave was developed when Spring Creek was at a higher elevation than the trunk passage. If this was so, Spring Creek must have eroded at least 100 feet since Friars Hole Cave was formed (from Table 6.1). At present any outlet for the Friars Hole conduit along Spring Creek has been blocked by sediments.

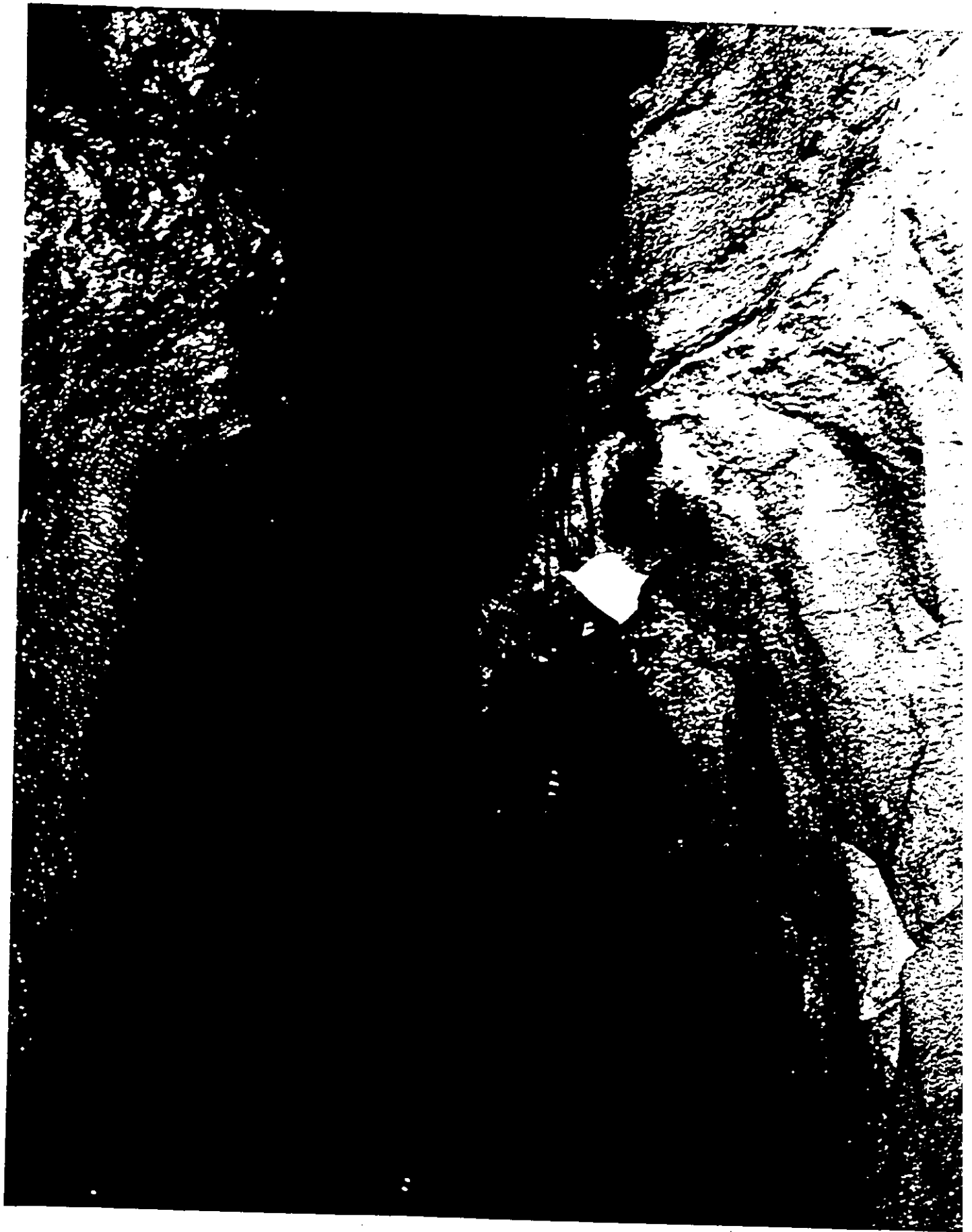
Upstream, the trunk does not gain much elevation. The Broken Room, where the stream is first seen, is only about 20 feet above the lower end of the trunk passage, and so still about 50 feet below the elevation of Rick's Siphon in Snedegars, which is about 3000 feet away. The water in Friars Hole has not been tested from Snedegars, but it is virtually certain that the Snedegars water does flow to Friars Hole, as both drain to Spring Creek, and Snedegars is the only stream large enough to account for the flow in Friars Hole.

A number of other smaller streams enter the top end of the cave. The stream entering to the south of the Broken Room, and the water entering the Domepits to the north of the Broken Room, are suspected to be from the streams that sink in the Friars Hole valley.

Along the course of the dry valley from Hills Creek to Spring Creek there are two rather small caves (Hills-Bruffey and Cutlip) that now carry large streams, and down valley are two large caves (Snedegars and Friars Hole) that carry relatively small streams. The down valley

Figure 6.11 Friars Hole Cave entrance series. (Opposite)

The second pitch in the entrance series. As a comparison to Figures 6.9 and 6.10 this shows the small constricted nature of the entrance series. The rift-type passage and frequent climbs and ladder pitches indicate the vadose nature of this part of the cave, and the small size as compared to the passage shown in Figure 6.9 attest to the youth of this passage.



caves are interpreted to have carried the combined flow of Hills and Bruffey Creeks during Stage 2.

6.2.5 Hughes Creek Caves

Hughes Creek Caves consist of two separate systems a few hundred feet apart in the Little Levels district (Figure 6.1), but with entirely different characteristics. The Upper cave consists of two large (about 50 feet wide and 20 feet high) parallel phreatic passages about 500 feet long (Figure 6.12), one being at a higher level than the other. The cave is developed in the base of the Pickaway limestone. A stream in the lower passage has eroded through the underlying Taggard shale and sinks, to reappear later in Lower Hughes Creek Cave. The upstream ends of both passages terminate in breakdown, and the downstream end of the Upper passage ends in breakdown very close to the cliff face.

The Lower cave is a small constricted maze cave, with evidence of some joint control, that has been developed by vadose flow. The cave is developed in the Patton limestone immediately below the Taggard shale. During low flow, the stream sinking in the Upper cave appears in the Lower cave (Figure 6.12), but during high water, a stream flows out of the Upper cave, runs for 300 feet over the surface, and sinks at the Lower cave entrance. During floods the Lower cave is inundated and the stream from the Upper cave flows past it to join Millstone Creek.

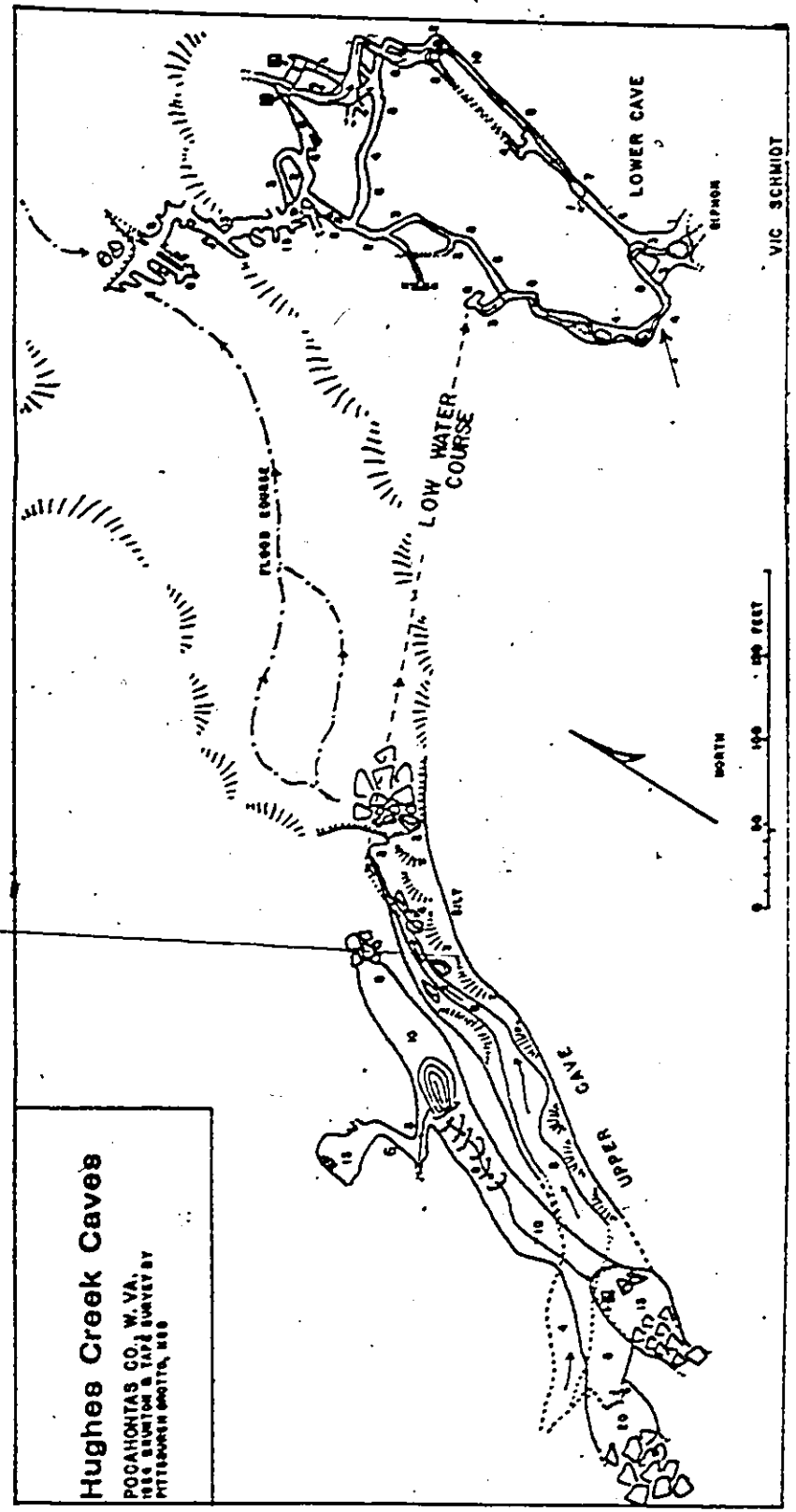


Figure 6.12 Hughes Creek Caves.

6.2.6 Marthas Caves

The Marthas Caves consist of two large cave passages in the Little Levels district (Figure 6.1), with their entrances a few feet apart. The caves are known as Upper and Lower Marthas.

The Upper cave, as its name implies, is a few feet above the Lower cave, and is developed in the base of the Patton limestone just above the Patton shale. The cave consists of a phreatic passage about 2000 feet long and averaging 20 feet square (Figure 6.13), although in places there has been some infilling and recent vadose entrenchment to alter the passage dimensions. The cave ends in a sand and silt blockage. The Upper cave is now fossilized, but carries some small streams derived from local runoff, which have eroded the Patton shale, and disappear in small cracks and sumps in the cave.

The Lower cave is developed in the Sinks Grove limestone just below the Patton shale. The entrance series was developed by phreatic flow, but has been considerably enlarged and modified by vadose entrenchment. The passage is about 2000 feet long and 20 feet square, and runs down to join a large phreatic passage 1500 feet long, the end of which carries a large stream (Schmidt, 1962). Near the stream the passage is up to 80 feet wide and 50 feet high. The stream appears and sinks in large boulder chokes. It has been tested from Hughes Cave, and flows to the Locust spring.

The whole of Lower Marthas Cave has evidence of flooding, as there are many large mud banks, and logs and branches in the roof. The flood characteristics are interesting. During moderate floods (which occur at

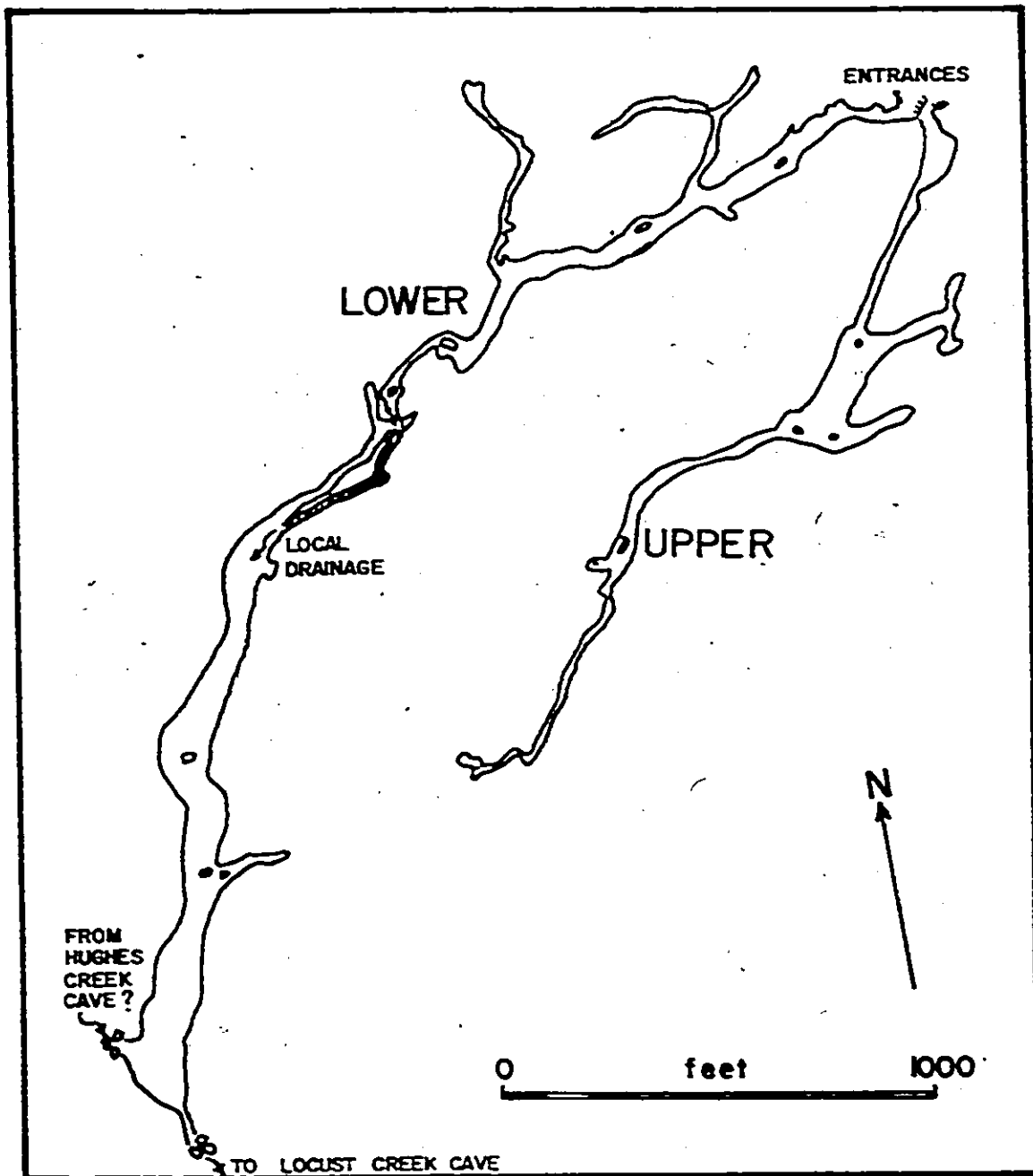


Figure 6.13 Marthas Caves.

about a one year interval), Millstone Creek floods its banks and flows into Marthas Cave. However during extreme floods (recurrence interval of many years), such as during Hurricane Camille in 1969, water flows out of Lower Marthas Cave entrance and down Millstone Creek to sink at Beards Blue Hole (Mr. McNeel, 1969, personal communication).

6.2.7 Beards Blue Hole

This is a short but hydrologically important cave at the end of the Millstone Creek streambed. During low and moderate water conditions the cave carries very little water, but during floods it carries the majority of the flow of Millstone Creek, as well as the outflow from the Hughes and Marthas Caves. The cave consists basically of a large sink developed in the Sinks Grove limestone (Figure 6.14), but also contains some small, recent inlet passages, which are largely joint controlled (Coward, 1971).

6.2.8 Poor Farm Cave

This cave is on the eastern side of the Locust Creek basin, at an altitude of 2360 feet, and does not now drain to Locust Creek. The cave was, however, involved in the early development of the Locust basin.

The cave consists (Figure 6.15) of two roughly parallel passages, one about 10 feet above the other (Wolfe, 1970). Both passages are now

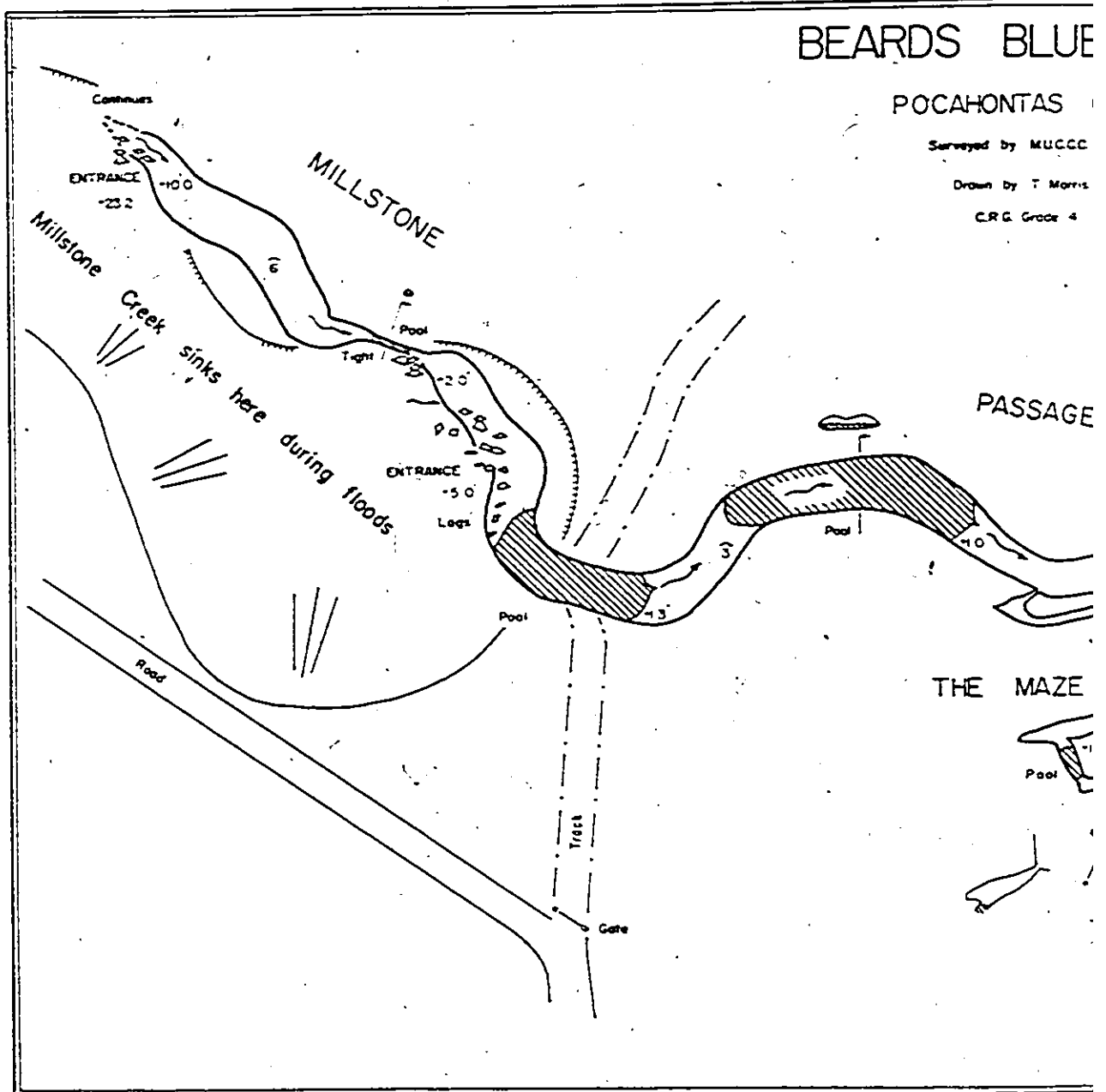


Figure 6.14 Beards Blue Hole.

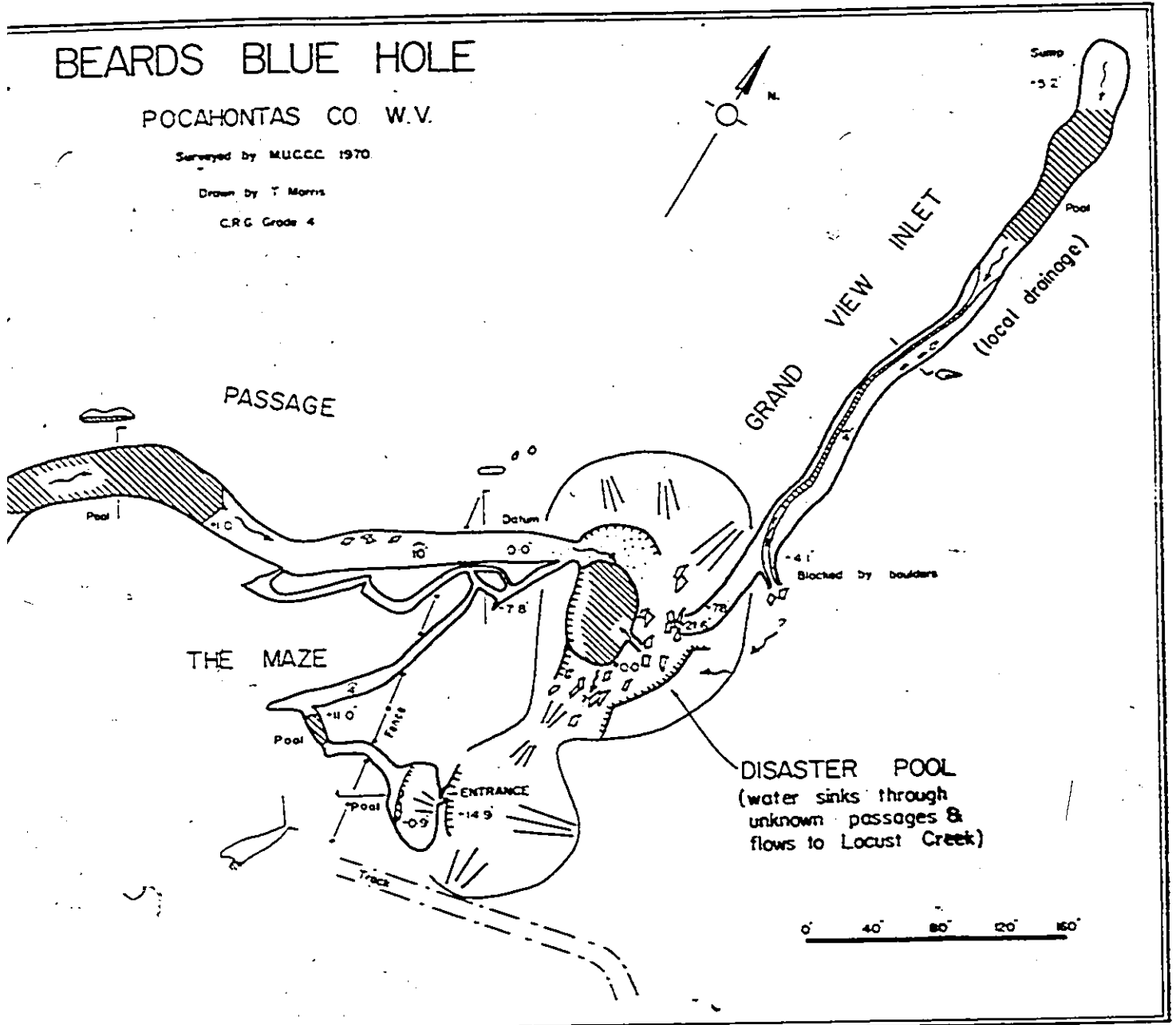
BEARDS BLUE HOLE

POCAHONTAS CO W.V.

Surveyed by M.U.C.C.C. 1970

Drawn by T. Morris

C.R.G. Grade 4



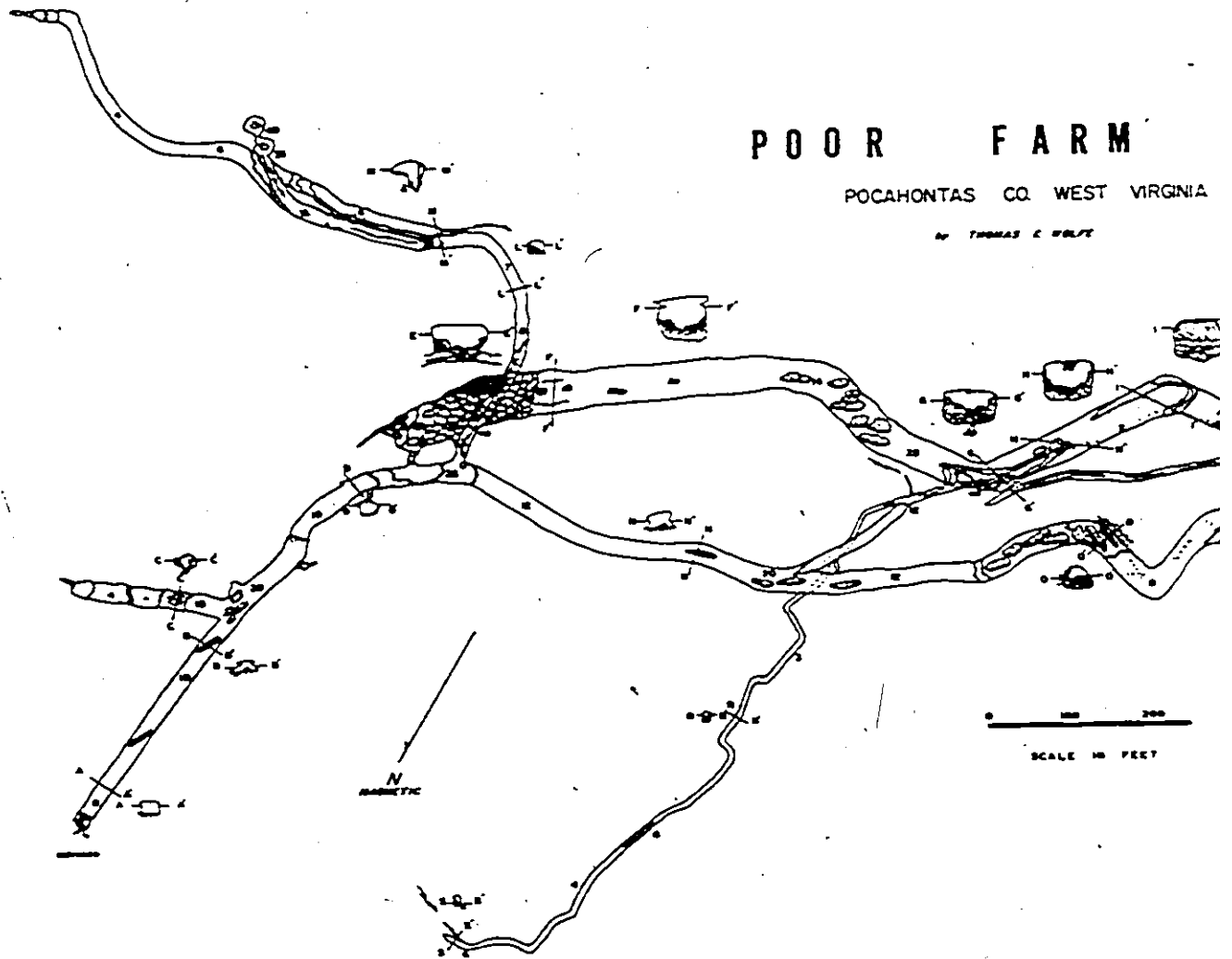


Figure 6.15 Poor Farm Cave.

fossilized, although a small, lower and active passage contains a stream. The high level passage is the larger, being about 50 feet wide and 30 feet high, and contains scallops in the roof which are from 25 to 30 inches long (Wolfe, 1973). Scallops of this size are formed by a flow velocity of about 0.015 to 0.02 feet per second (Goodchild and Ford, 1971), indicating that the cave was formed by water which had a discharge of about 25 cfs. Poor Farm Cave is developed in the Sinks Grove limestone near the bottom of the Greenbrier limestone series.

6.2.9 Locust Creek Cave

The Locust spring, although discharging a considerable amount of water, is small and constricted. The water issues from cracks and sumps inside the cave which is only about 1000 feet long, 30 feet wide, and from 5 to 15 feet high (Figure 6.16). The cave is developed by phreatic flow in the base of the Hillsdale limestone, which is the lowest member of the Greenbrier limestone. The cave and streamway below the cave are manifestly underfit, due to the piracy of the Hills and Bruffey streams to Locust Creek.

6.2.10 Description of the Bruffey to Upper Hughes Creek Cave and to Locust Creek Flow Routes

This active flow route has been proved by dye tests between the Hills-Bruffey Cave and Upper Hughes Cave. Both ends of the route are

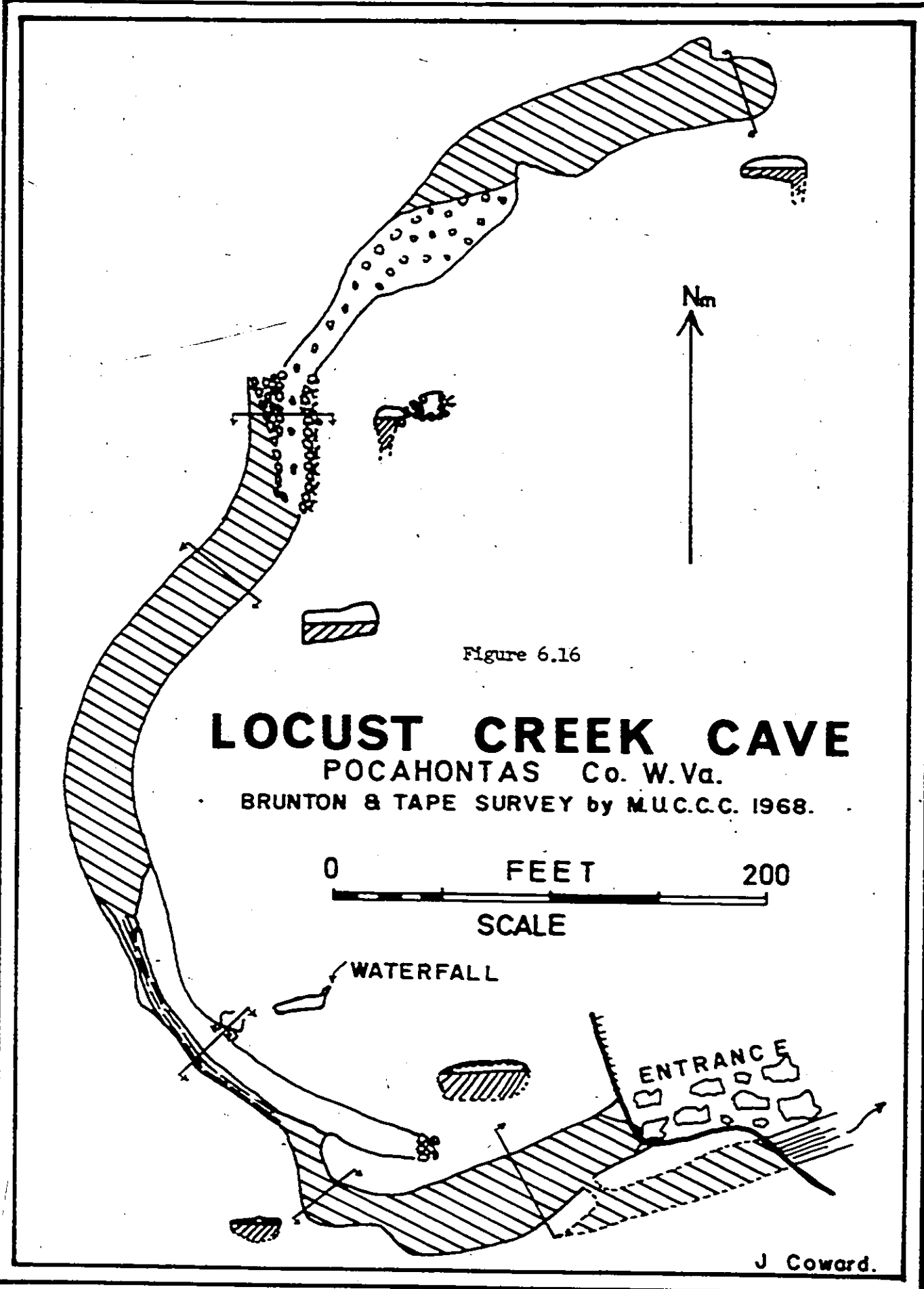


Figure 6.16

LOCUST CREEK CAVE

POCAHONTAS Co. W. Va.

BRUNTON & TAPE SURVEY by M.U.C.C.C. 1968.

0 FEET 200

SCALE

WATERFALL

ENTRANCE

J Coward.

now blocked by boulder chokes, but there is an approximate 7000 feet of straight-line conduit between these two caves. At present during low flows the Bruffey stream sinks in the streambed several hundred feet from Bruffey Cave, and the water is not seen in the cave. The Bruffey water, however, even during low flows still flows to Upper Hughes and in high water conditions the Hills Creek stream also flows through this route to the Upper Hughes Cave.

The Taggard shale has played an important part in the development of this system and of the outlet at Hughes Cave. The limestone is exposed above Locust Creek Cave, which is nearer to Bruffey Creek than is Hughes Cave, but due to the northwesterly dip of the Greenbrier series the elevation of the beds around Locust Creek is higher than at Hughes Creek Cave. The top of the Taggard above Locust is at an elevation of 2420 feet, while the Taggard at Hughes Creek Cave is at 2229 feet, giving the Bruffey-Hughes Creek route a considerably higher gradient than any more direct routes to the Taggard above Locust Creek.

The direct Hills Creek to Locust Creek route is one of the most recent routes to form in the basin and is the major route which has breached the Taggard shale. The upstream end of the route is in the lower end of Cutlip Cave, and the water is not seen again for 8000 feet until it resurges at Locust Cave. The route traverses the majority of the Greenbrier limestone, dropping 300 feet, but due to the dip of the beds about 450 feet of limestone section is traversed.

A chemical pulse test was carried out on this system to estimate the characteristics of the conduit behind the cave. The test was carried

out in July, 1971 during a period when the streams were low, but just after a heavy rain. Just before the test it was seen that Hills Creek stream was not flowing to the Hills Creek Cave, but was sinking and flowing into Cutlip Cave. As Hills Creek is about twice the size of Bruffey, the major single source of the Locust spring during the test was Hills Creek, flowing through the unexplorable Hills Creek to Locust route.

At Locust Creek resurgence twenty samples were taken and analysed for calcium, magnesium and alkalinity (Section 2.6), and the temperature, pH and the stage of the water measured, during a two day period. The results of the analyses are presented in Figure 6.17 which shows the variations in the calcium, pH, saturation level with respect to calcite, stage at the cave, and discharge at the gauging site two miles downstream.

Generally after a rain the composition of the water will change due to the dilution effect of the relatively unmineralized rainwater (Smith and Mead, 1962). The ionic concentration will generally decrease, the pH decrease, as the rainwater will tend to be more acidic due to the solution of carbon dioxide in the water, and the degree of saturation towards calcite will be less due to lower concentrations of calcium and bicarbonate ions and lower pH.

Immediately after a rain the initial flash of water is often observed to have characteristics opposite to those described above (Ashton, 1966), as stagnant water is swept out of the system by the flood pulse. The stagnant water will be nearly saturated, higher in minerals, and have a relatively high pH. This effect can be seen in Figure 6.17, particularly in the curves of calcium and degree of saturation. From these

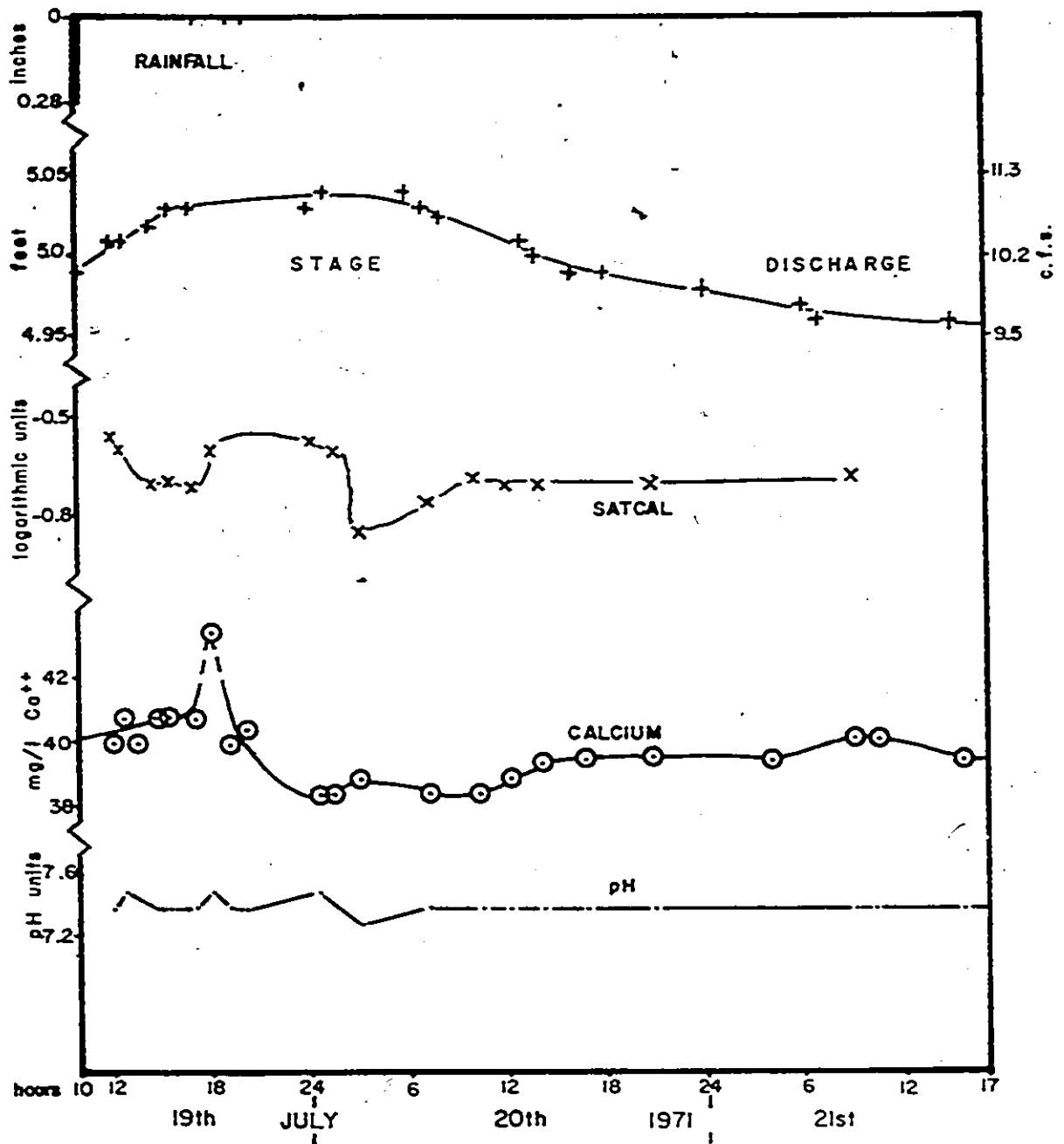


Figure 6.17 Chemical characteristics during the flood pulse test at Locust Creek Cave. The SATCAL figures are the logarithmic ratios of the ion product (Ca^{++}) and (CO_3^{--}) over the equilibrium constant for calcite.

curves it is possible to estimate the volume of stagnant water behind the spring. From Figure 6.17 it can be seen that the pulse of stagnant water came through for approximately 5 hours, with the discharge averaging 10.3 cfs. The volume of water is thus 0.19×10^6 cubic feet, which if averaged out over an assumed 2 miles of conduit gives a conduit area of 18 square feet.

From the stage figures it can be seen that the water started to rise four hours after the rain and peaked after about 15 hours. The pulse took a further six hours to travel down to the gauge, which is about 2 miles farther down stream. The relatively long time that the pulse took to come through the system indicates that the conduit is vadose in moderate flood conditions, as a phreatic channel tends to have a very quick response to flood pulses.

6.3 Description of the Five Stages of Development

From evidence from the caves, their sediments, dye tracing and other techniques, the evolution of the Locust Creek basin can be inferred. The development took place in a number of stages, as various streams were diverted or pirated away from their former courses. It is semantic to consider the exact number of stages in the development, as there were many, and some of the changes are insignificant. Five major stages of development can be determined, and these are described in this section. The initial stage is the surficial flow, while the last stage is the conditions that will occur in a few years time.

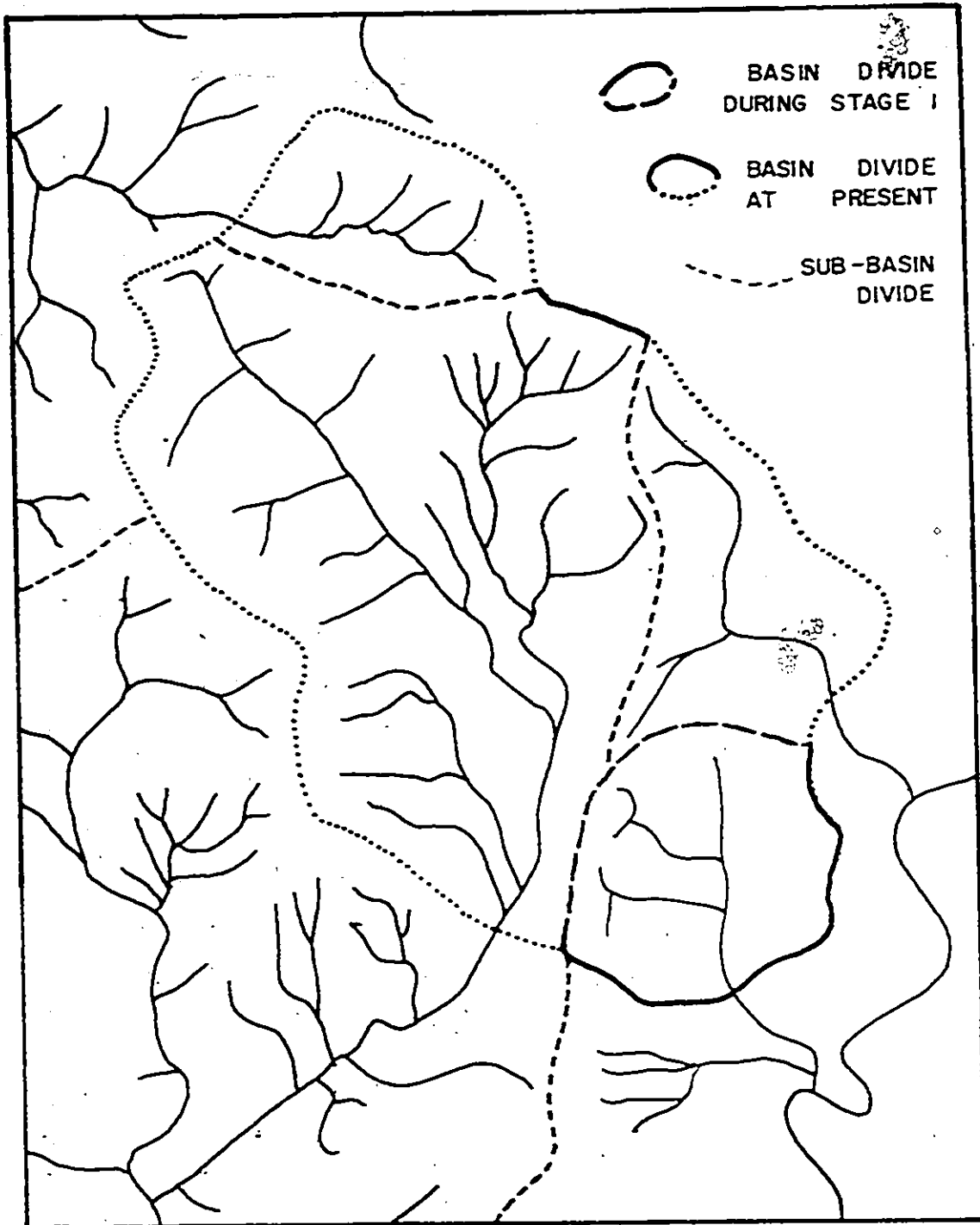


Figure 6.18 Locust Creek basin--surficial flow during Stage 1.

6.3.1 Stage 1: Surficial Flow

The initial stage of development is shown in Figure 6.18. It is the situation that existed before the land surface had eroded down to the limestone and before any karst development had taken place.

In the extreme north of the basin there is some evidence to suggest that the upper part of Hills Creek originally flowed to the Cherry River, which is to the west of the Locust basin. The gradient of the present Hills Creek near the Falls of Hills Creek is considerably higher (600 feet per mile) than the gradient of the Cherry River (80 feet per mile), as seen on the long profile, Figure 6.19. Thus Hills Creek would probably have a far higher rate of headward erosion than the Cherry River and be very liable to pirate the end of the Cherry River. The orientation of the top part of Hills Creek also supports this idea, as does the marked elbow of capture in the modern stream.

Farther down Hills Creek, this stream, joined by Bruffey Creek, flowed down past the present Hills and Bruffey Caves, along the Friars Hole valley to Spring Creek. This stream carved out the prominent Friars Hole and Suedegars valleys, which are now virtually dry and undrained.

Farther to the east, Millstone Creek flowed off Viney Mountain across what is now the Little Levels, and flowed down the valley of McNeels Mill Run into the Greenbrier River. The end of the present Millstone Creek (at Beards Blue Hole) and McNeels Mill Run are now joined by a prominent dry valley.

Locust Creek during Stage 1 was small and only drained about 5 square miles, compared to the present drainage area of 40 square miles.

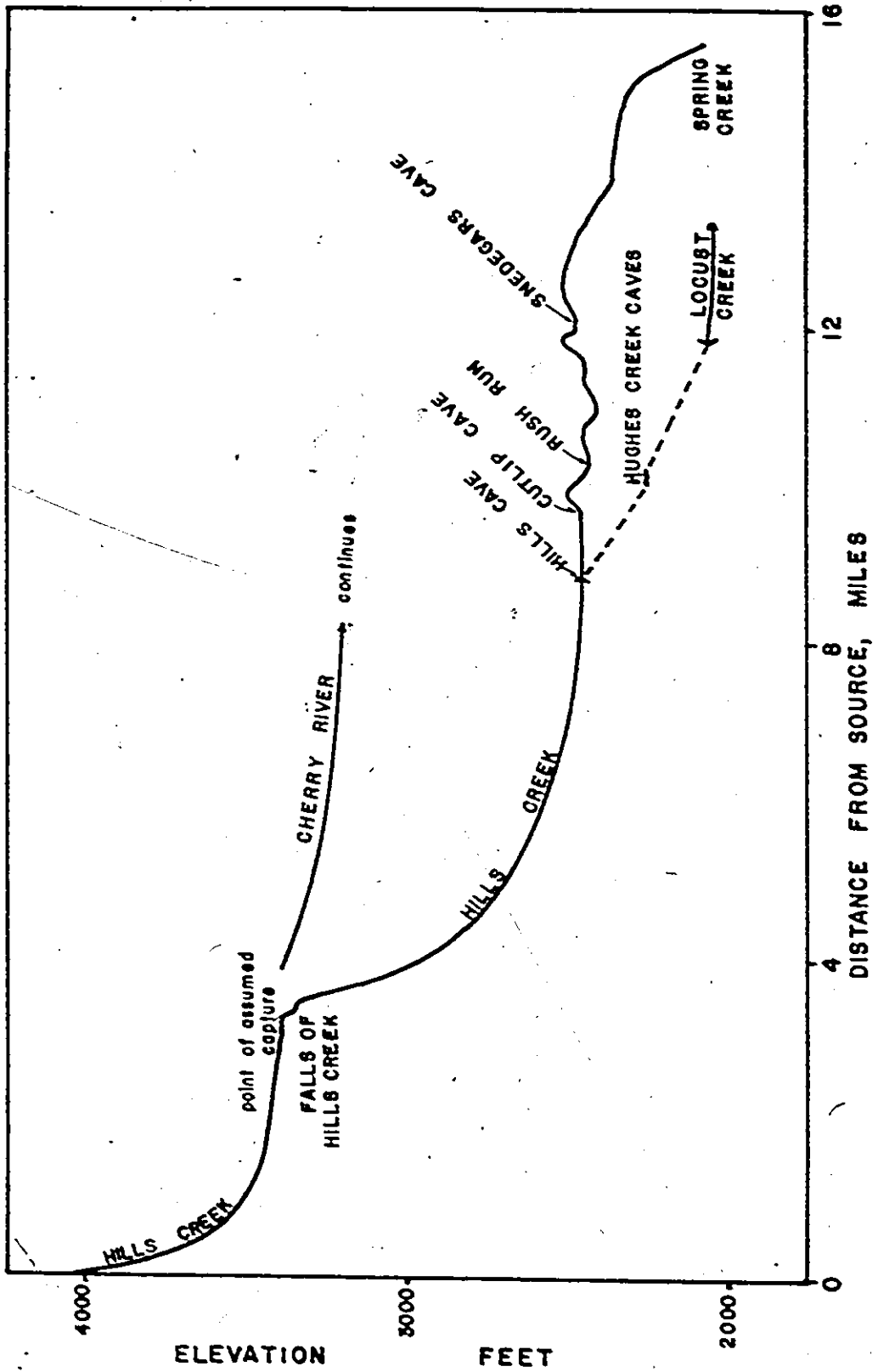


Figure 6.19 Long profile of Hills Creek, the Cherry River and the Friars Hole valley.

The creek was limited to draining the local topographic divide before flowing into the Greenbrier River.

The present basin was composed of four sub-basins during Stage 1 that drained in different directions. The basins were:

- a) the northern part of Hills Creek draining to the Cherry River,
- b) the present lower part of Hills Creek draining to Spring Creek,
- c) Millstone Creek draining to the Greenbrier River via McNeels Mill Run, and
- d) the embryonic Locust Creek.

6.3.2 Stage 2: Initial Karst Development

In the second stage of development the surface streams eroded down the limestone beds and cavern development was initiated. Generally the initial tendency of the caves and conduits was to underdrain the valleys (Figure 6.20): no major piracy took place from one creek to another. As this is the oldest stage of cave development, much of the evidence of the caves has been lost, and the development of this stage is considerably less detailed than later stages.

The Greenbrier River is on the south-east or up-dip side of the Locust Creek basin, and so will have been flowing on beds which are stratigraphically lower than the beds that other streams in the basin were passing over. The river, therefore, must have been the first stream to reach the limestone during the cutting down from Stage 1 to Stage 2. However, there is no evidence now of any of the karst development that

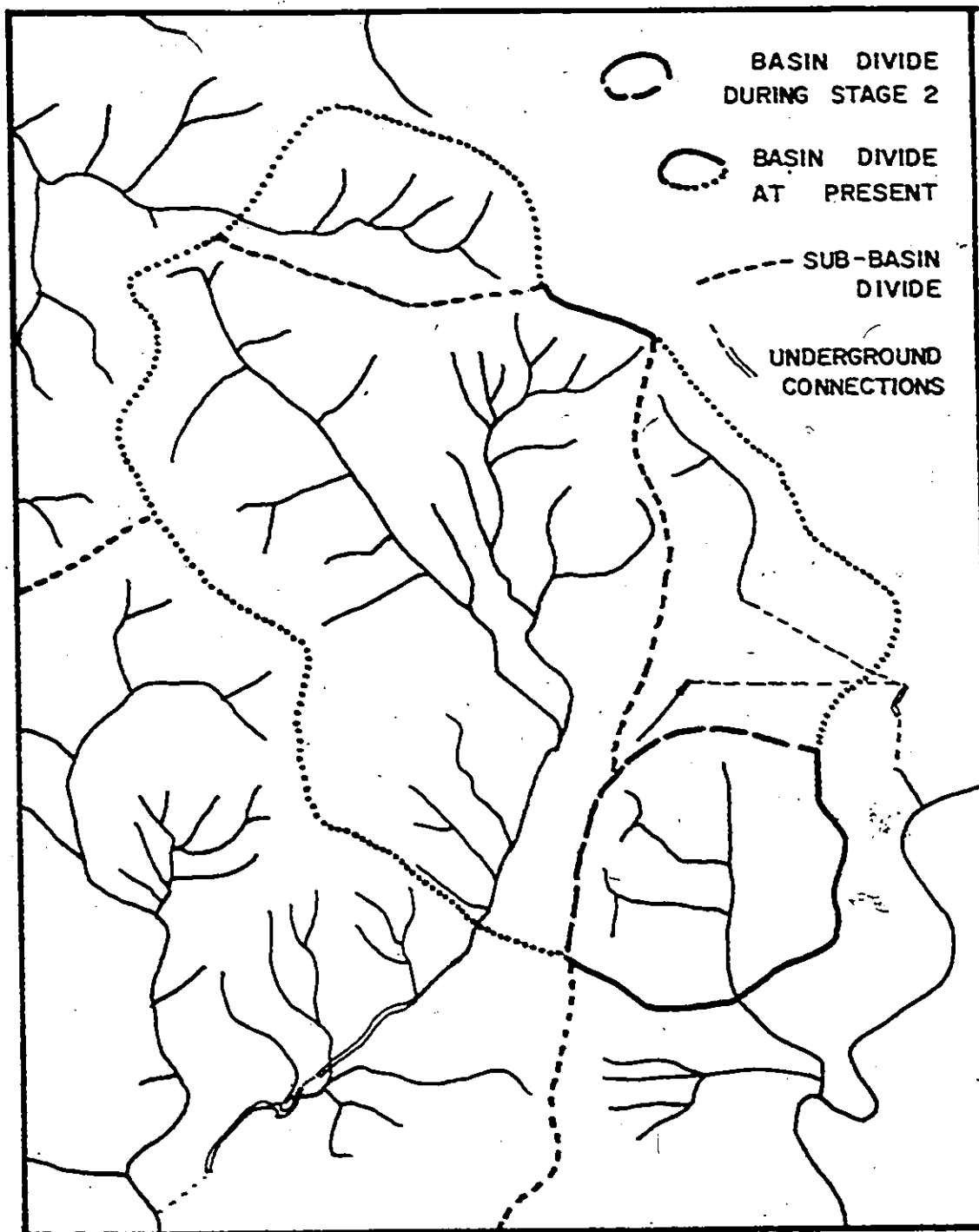


Figure 6.20 Locust Creek basin—initial underdraining of the valleys during Stage 2.

that may have occurred along or underneath the Greenbrier River.

Just to the east of the Locust Creek basin and nearer to the Greenbrier River, is Poor Farm Cave, which is certainly one of the oldest caves in the area. Although Poor Farm Cave is not in the present basin, it was formed from water draining from the basin. Wolfe (1973), noted milky quartz pebbles derived from the Pottsville or Princeton formations in Poor Farm and Upper Hughes Caves, but not in the upper reaches of Millstone Creek. Wolfe postulated that the Poor Farm Cave was developed by the Hills and Bruffey streams flowing through Hills-Bruffey and Upper Hughes Caves, and along a now destroyed conduit from Upper Hughes to Poor Farm Cave and thence to the Greenbrier River.

From several pieces of evidence, however, it seems unlikely that Poor Farm Cave could have been formed from water travelling through the Hills-Bruffey Cave system:-

a) The Poor Farm passage is considerably larger than the Hills-Bruffey Cave. Poor Farm's main passage is 50 feet wide and 32 feet high (Wolfe, 1973) while the Hills-Bruffey passage is only one-fourth of the size, at 20 feet square (Section 6.2.1). Poor Farm was developed by a stream discharging 25 cfs. (Section 6.2.9): the Hills and Bruffey streams are now discharging a combined 20 cfs. Even though the climatic conditions and so the stream discharges would not be the same as today, it is likely that the Hills and Bruffey streams would have been the major source of the Poor Farm water if Poor Farm developed from the Hills-Bruffey stream. In this case the Hills-Bruffey Cave would be considerably larger than the Poor Farm passage, as the water would be more aggressive near the sink point than

further downstream.

b) Poor Farm Cave is a fossilized cave in a "remnant limestone hill that stands 200 feet above the sinkhole plain" (Wolfe, 1973). The cave is at least 200,000 years old, based on isotopic dating of flowstone in the cave (Thompson, 1972, personal communication). Hills-Bruffey Cave, however, is semi-active now, and stands on the edge of the Hills and Bruffey streams. It is unlikely that while the area around Poor Farm Cave eroded 200 feet, the area around Hills Creek could only have eroded about 10 to 20 feet, particularly as there are no large active streams near Poor Farm now, and as the Hills and Bruffey streams have been active in the past 200,000 years while Poor Farm has been inactive for this period.

c) The source material for the milky quartz pebbles found in Poor Farm and Upper Hughes Caves is the Princeton or the Pottsville formation. Millstone Creek drains off Viney Mountain, and at present only a very few acres of the Millstone Creek basin have the Princeton conglomerate exposed, which would explain the sparsity of quartz pebbles in the stream today. However, in the past, when Poor Farm Cave was being formed, the exposure of the Princeton in the Millstone Creek basin would be larger and could account for the quartz pebbles in Poor Farm Cave.

For these reasons it is postulated that Poor Farm Cave was developed by water from the Millstone Creek basin. The water passing through Poor Farm Cave probably resurged along the Greenbrier River near the present McNeels Mill Run. At this stage, which was at least 200,000 years

ago, the Hills-Bruffey, Upper Hughes and other caves in the Little Levels district had not formed.

On the northwest side of Droop Mountain the Hills and Bruffey streams flowed over the surface to Spring Creek. As they cut down to the Union limestone, the streams sank underground and underdrained the Friars Hole valley. The most important sink was at the present day entrance to Snedegars Cave, although other and shorter lived sinks may have occurred farther down the valley. The reason for the sink at Snedegars Cave is unclear, but it could be due to a minor upwarping of the limestone which would expose the Union limestone to the stream, or to jointing or weakening of the limestone at this point. At Snedegars Cave the Hills-Bruffey stream enlarged the cave down to the top of the Pickaway limestone (described in Section 6.2.4) and the water then flowed in the Pickaway to the end of Friars Hole Cave. From here the water flowed through an unexplorable conduit to resurge in the Spring Creek valley.

At the end of the development of Stage 2, a minor diversion occurred in the course of Millstone Creek. The creek abandoned Poor Farm Cave and, flowing on the Patton shale, developed Upper Marthas Cave (Figure 6.13). The cave is developed in the Patton limestone just above the shale. The end of the cave is blocked by flowstone, and it is not known where the water went from the end of the cave. However, on the basis of the hydraulic gradient, the water probably flowed to Locust Creek with a gradient of 100 feet per mile, rather than to McNeels Mill Run where the gradient is only 60 feet per mile. In addition the orientation of the present explorable Upper Marthas Cave indicates that the

water was heading towards Locust Creek.

The present Locust Creek resurgence however, is too young to be equivalent to the obvious age of the Upper Marthas passage, and an older resurgence at the head of the Locust Creek valley seems likely. Such a resurgence could have been covered by hill waste (the hill slopes are very steep (1 in 3) at the head of the valley) and the present Locust Creek Cave could have drained any former resurgence. The marked elbow of the stream 200 yards from the present resurgence further supports this contention. There is, however, no directed evidence for a fossilized resurgence.

6.3.3 Stage 3: Major Piracies

This is the most significant stage in the development of the Locust Creek basin, as the Hills and Bruffey streams were diverted away from Spring Creek to the Locust Creek drainage (Figure 6.21).

The combined Hills and Bruffey streams sank upstream as limestone was exposed farther up the streambed. A major sink point was at Cutlip Cave and the water then flowed through Clyde Cochrane and into Snedegars Cave. Two major inlet passages are present in Cutlip (Section 6.2.2) and these were formed in turn as the route matured.

Bruffey Creek then sank at the present entrance to the Bruffey Creek Cave and flowed under Droop Mountain, creating Upper Hughes Creek Cave. The Taggard played an important part in the development of this route as the water could not penetrate the shale underground. It

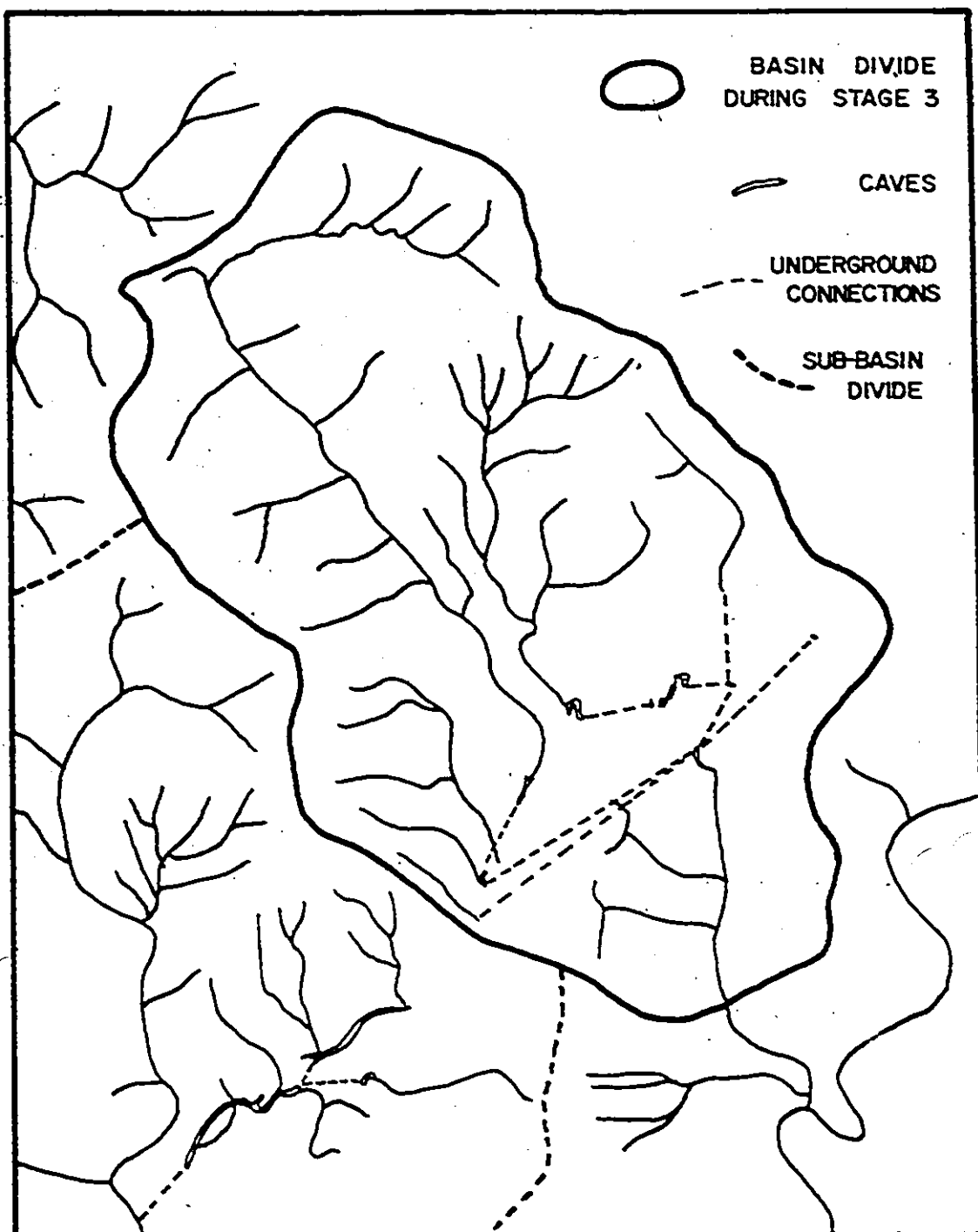


Figure 6.21 Locust Creek basin--piracy of the Hills drainage to Locust Creek during Stage 3.

therefore developed the course in the upper portion of the Greenbrier limestone that offered the highest hydraulic gradient between sink point and spring.

Bruffey Cave is at an elevation of 2432 feet, while Upper Hughes Creek is at 2229 feet and is 2 miles away. The duck in Snedegars is at 2290 feet (Table 6.1) and is about 3 miles distant. The gradient to Hughes is therefore about 100 feet per mile, while it is only 50 feet per mile to the duck in Snedegars. Although the Pickaway limestone outcrops directly above Locust Creek Cave, just under 2 miles from Bruffey Cave, due to the northwesterly dip the outcrop is at about 2270 feet, and so the gradient to this exposure is 80 feet per mile. Thus Upper Hughes Cave is located at that point along the Pickaway outcrop which has the highest gradient from the Bruffey Cave sink.

Hills Creek, however, did not join Bruffey in its path to Locust, and continued to flow through Cutlip, Clyde Cochrane, Snedegars and Friars Hole Caves down to Spring Creek. The stream flows underground for six miles, held up by the Taggard shale. At some point, for reasons that are not clear, the stream was able to breach the shale and flow directly to the Locust Creek area. This is a far more efficient route, having a hydraulic gradient of 170 feet/mile compared to 40 feet/mile to the end of Friars Hole. The water from Hills flowed through the present Lower Marthas, developing the large passage at the end of this cave.

In the Little Levels area the Bruffey stream flowed out of Upper Hughes Creek Cave and joined Millstone Creek, which was flowing down to Upper Marthas Cave (Section 6.4.2). The Millstone Creek was able to

erode through the Patton shale just in front of Marthas Cave, and was then able to sink through the relatively pure Sinks Grove limestone, developing Lower Marthas Cave. The Lower Marthas route was able to develop towards the Clyde Cochrane-Locust route, and the combined Millstone Creek and Hills water enlarged the lower part of Marthas Cave. From here the water flowed to Locust Spring. Later on, Millstone Creek abandoned Marthas Cave and sank at Beards Blue Hole, developing the large phreatic passage which runs to the west of the present shakehole (Figure 6.14). It is not known why Marthas was abandoned in preference to Beards Blue Hole.

6.3.4 Stage 4: Shortening of the Flow Routes

As the Hills streambed became more eroded and the limestone was exposed farther upstream, the creek was able to sink before Cutlip Cave, and developed the Hills Creek Cave (Figure 6.22). This cave joined the Bruffey Creek Cave, and the combined water flowed to Upper Hughes Creek Cave.

Down the Friars Hole valley, Snedegars and Friars Hole Caves had been abandoned by the Hills Creek and Bruffey streams, but were fed by local streams. In particular, streams flowing off the local hills developed Snedegars Staircase, Crookshanks and Rolling Stones Caves, all of which drain into the Snedegars Cave. To the south-west a small stream flowed down the now almost dry Friars Hole valley, and developed the present entrance to Friars Hole Cave.

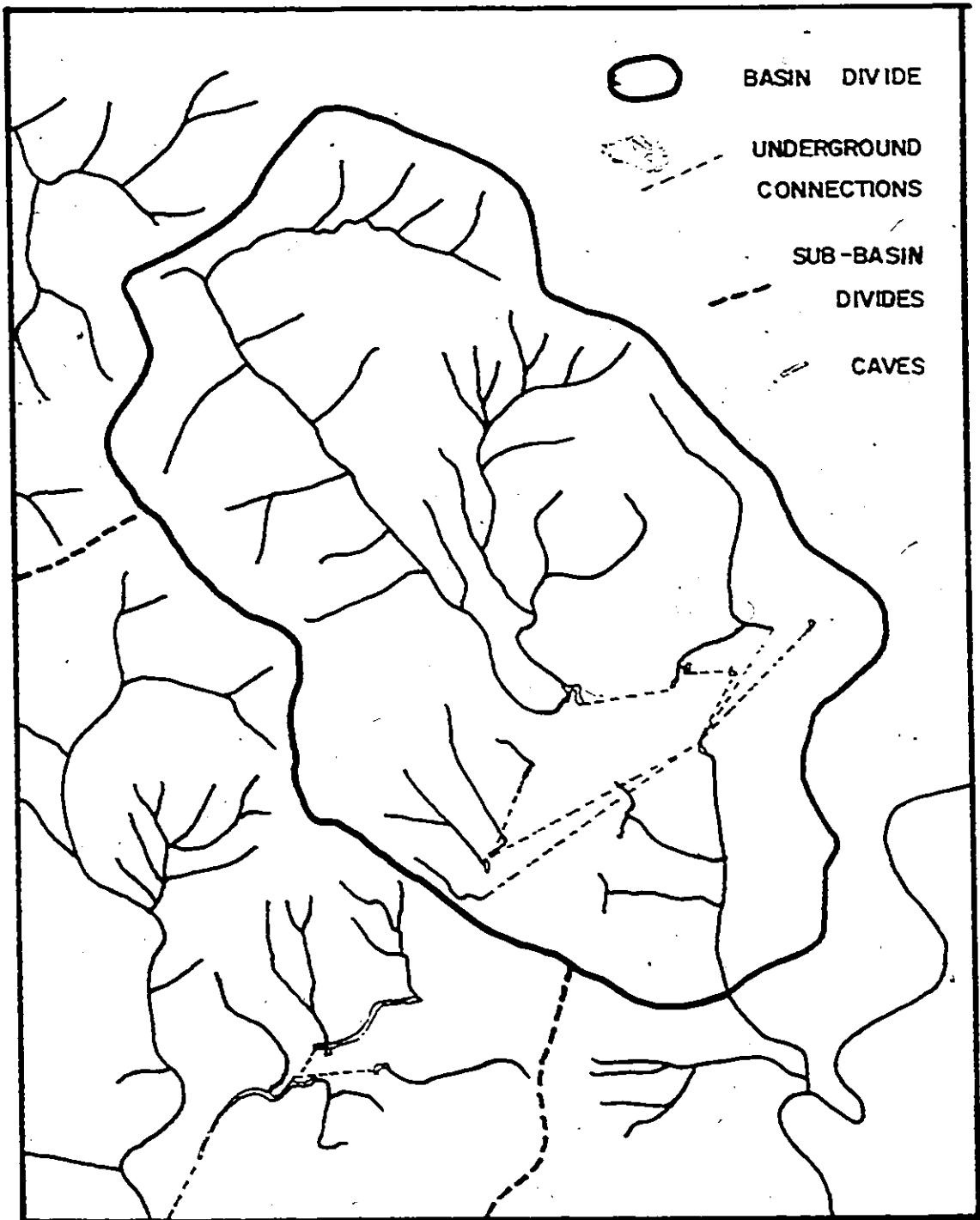


Figure 6.22 Locust Creek basin--capture of the Clyde Cochrane and Rush Run drainage during Stage 1.

During this stage the present Locust Creek Cave formed, draining the older and probably higher level resurgence at the head of the valley. The old resurgence became hidden by hill waste.

6.3.5 Stage 5: Further Shortening of the Flow Routes

Stage 5 represents present and future conditions, as illustrated in Figure 6.2. In the Hills Creek valley an interesting reversal is taking place. During Stage 3 Hills Creek sank at Cutlip and flowed into Clyde Cochrane Cave. During Stage 4 Cutlip was abandoned and the creek flowed through the Hills Creek Cave. Now, however, Hills Creek is sinking in the streambed before reaching Hills Creek Cave, and the water is flowing once again to Cutlip and Clyde Cochrane Caves. From here the water flowed to Locust, but has shortened the route and now no longer flows through Marthas Cave. Hills Creek Cave will be abandoned, although at present the cave is used during flood conditions. Similarly, Bruffey Cave has been abandoned except during floods, as the creek sinks in the streambed some way from the cave. At present the sink point is in cobbles and boulders, but in time a sizable conduit should develop. Although the Bruffey water sinking in the streambed is not seen in Bruffey Cave, the water still flows to Upper Hughes Creek Cave.

The stream emerging from Upper Hughes Cave sank during this stage at Lower Hughes Cave, which is about 100 yards from the upper cave. Lower Hughes Cave is developed in the Patton limestone immediately below the Taggard shale, and the Upper and Lower Caves form a lost waterfall

(White and Schmidt, 1966) which is a mechanism for breaching the impervious Taggard shale that is common in the Swago Creek basin (Chapter V). Lower Hughes is a small constricted cave that has not fully developed into a mature cave. Even at present the cave cannot take all the water issuing from the upper cave during floods, and the excess water flows on the surface to join Millstone Creek.

In Upper Hughes Cave the stream which was flowing on the Taggard shale has eroded through the shale, probably by mechanical erosion on the vadose streambed. The Hughes stream now usually sinks inside the cave and flows by an underground route to a rise in the lower cave. The stream is now seen for a few hundred feet before sinking in a constricted sump and flowing to Marthas Cave, and from there to the Locust spring. In future the underground Upper to Lower Hughes Cave route will enlarge until it is capable of taking all flows. Under natural conditions the entrances to both caves would probably become blocked—the upper cave by breakdown from the cliff-face above the cave, and the lower cave by sedimentation.

Millstone Creek now sinks in cobbles and gravel along its streambed about one mile above Beards Blue Hole, and only enters this cave during floods. In time a significant cave should develop along this route and become mature enough to carry all flows of Millstone Creek. When this happens, the Little Levels area will be devoid of any significant surface streams under any flow conditions.

6.4 The Simulation of Locust Creek

Locust Creek was simulated for the 647 day period from November 20th, 1969 to August 31st, 1971 with an additional 50 day run-in period. The full results are presented on a logarithmic scale in Appendix II and a typical portion shown on a linear scale in Figure 6.24.

The Locust Creek basin contains areas of differing hydrologic characteristics. For this reason the basin was divided up into three segments during modelling (Figure 6.23). These were:-

- a) Segment 1. The Hills Creek and Jacox Knob streams draining a total of 18.4 square miles of clastic hills. This segment drains underground to Locust Creek without passing through Hughes Cave and the Little Levels area.
- b) Segment 2. Bruffey Creek draining 6.4 square miles of clastic hills. The creek sinks and flows across the Little Levels area before flowing to Locust Creek.
- c) Segment 3. The Little Levels and lower Locust Creek basin draining 12.6 square miles of which about 50% has limestone exposed on the surface. The first two segments drain into this lower area.

The parameters for each segment were estimated and then corrected by simulation. The final parameter values for the three segments are shown in Tables 6.2 and 8.4.

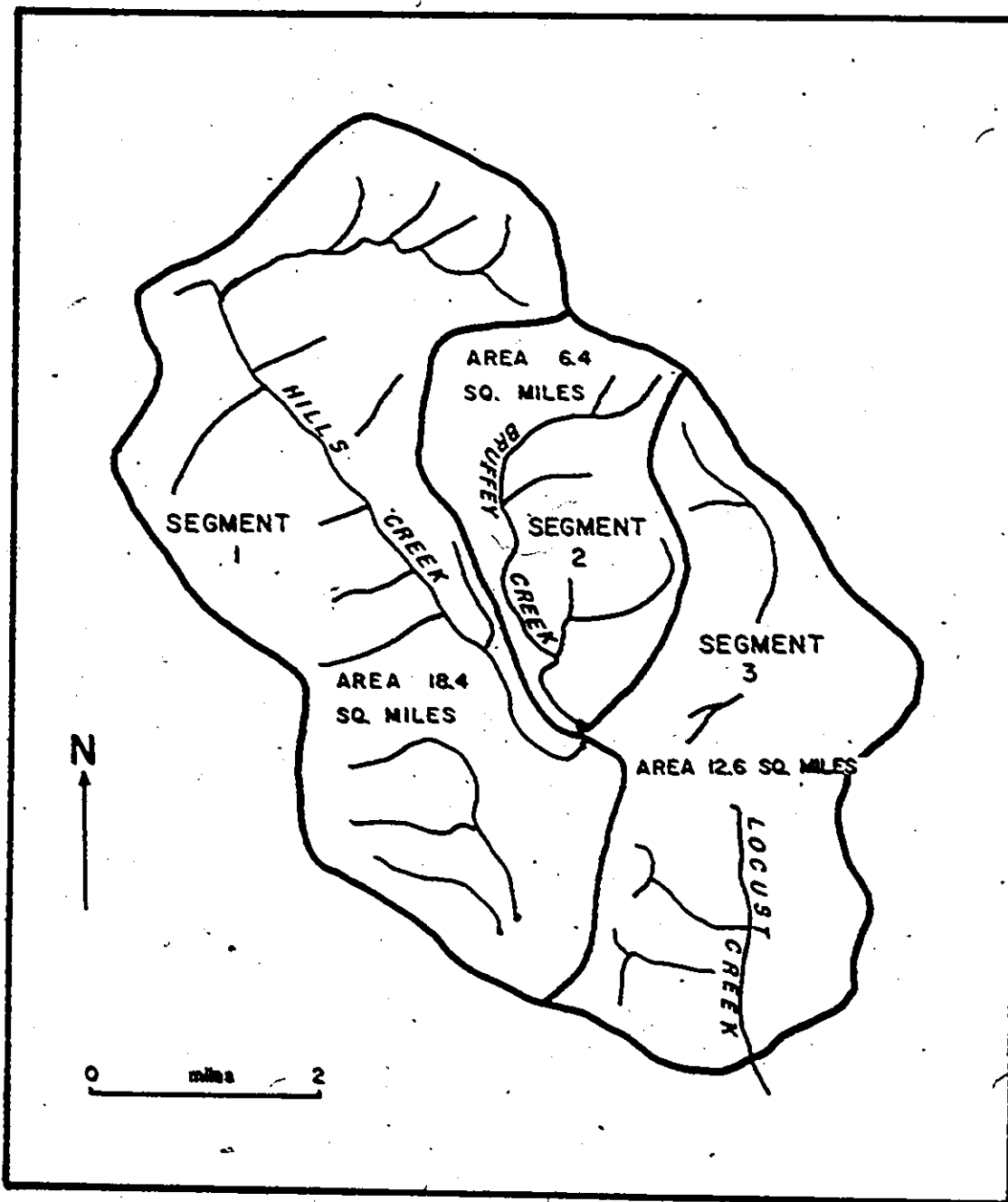


Figure 6.23 Locust Creek basin--the three segments used in the model.

6.4.1 Comparison Between the Real and Simulated Streamflows

The real streamflow hydrograph can be seen in Appendix II, but there are two areas where records are missing or unreliable. These are during parts of December 1969 and January 1970 where the float became frozen in place, and during parts of June and July 1970 when the stage recorder records were lost.

Overall the response of the model was generally reasonable on a long term basis, but many of the detailed responses were in error. Thus the simulated and real flows differ by only 3% on a long term basis, but the daily flow values are often about 200% or more in error. The major periods of error include the following:-

a). During December 1969 and January 1970 heavy precipitation occurred without significantly affecting the real streamflow. For example, on December 11th, 1.17 inches of precipitation fell when the minimum and maximum temperatures at Buckeye were 33° and 39°F. Although 1.17 inches a day is equivalent to 1200 cfs. of basin runoff, the real discharge rose only 1 cfs. while the model gave 161 cfs. on that day. Further study showed that the precipitation fell at 4 a.m. and must have fallen as snow, particularly in the higher parts of the basin, and did not significantly increase the runoff. Similarly 3.3 inches of precipitation fell on December 30th and 31st (equivalent to a daily runoff of 1700 cfs.), but this only increased the real discharge by 12 cfs. and must have fallen as snow, although it was modelled as rain on the basis of the mean temperature.

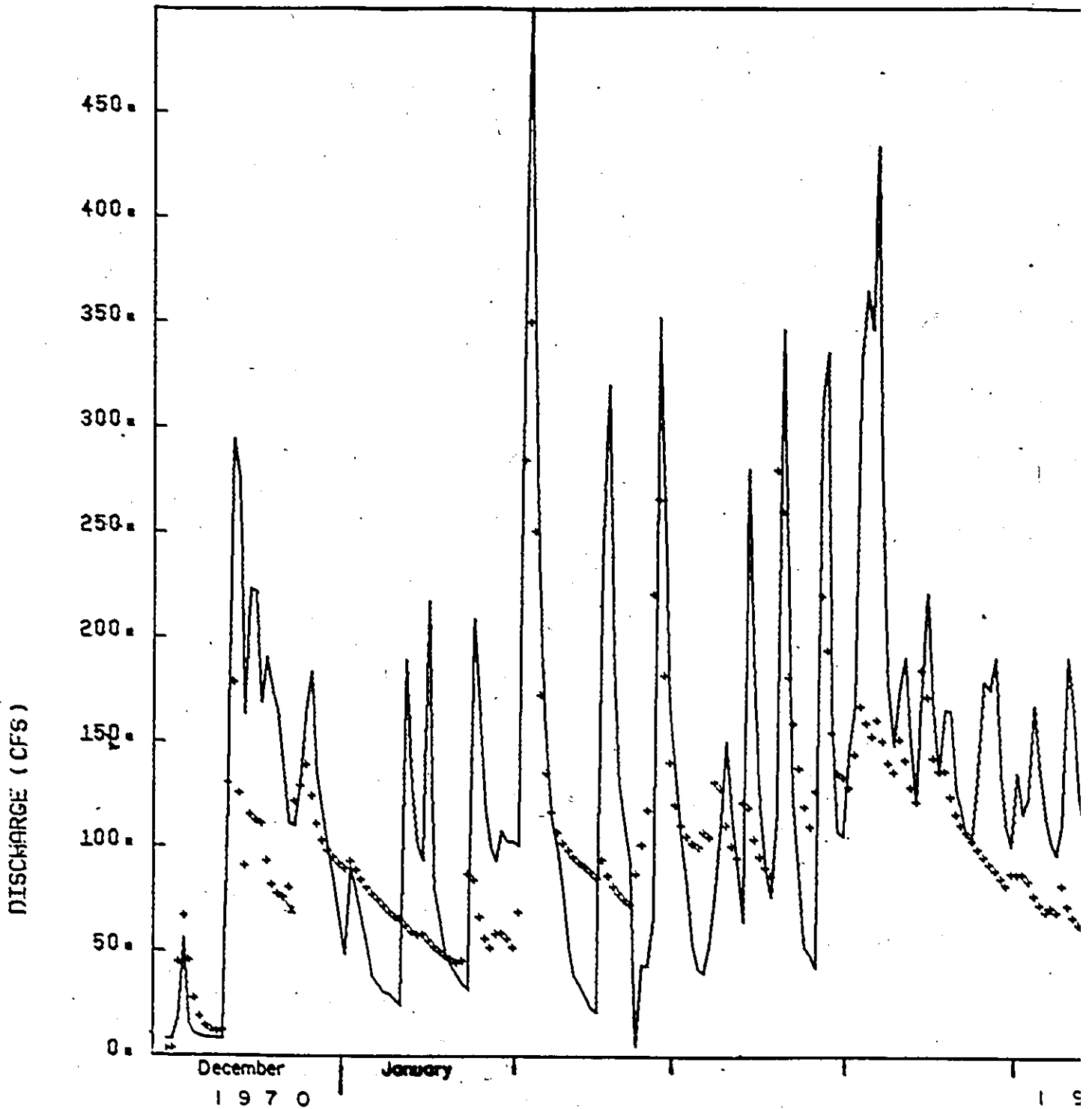
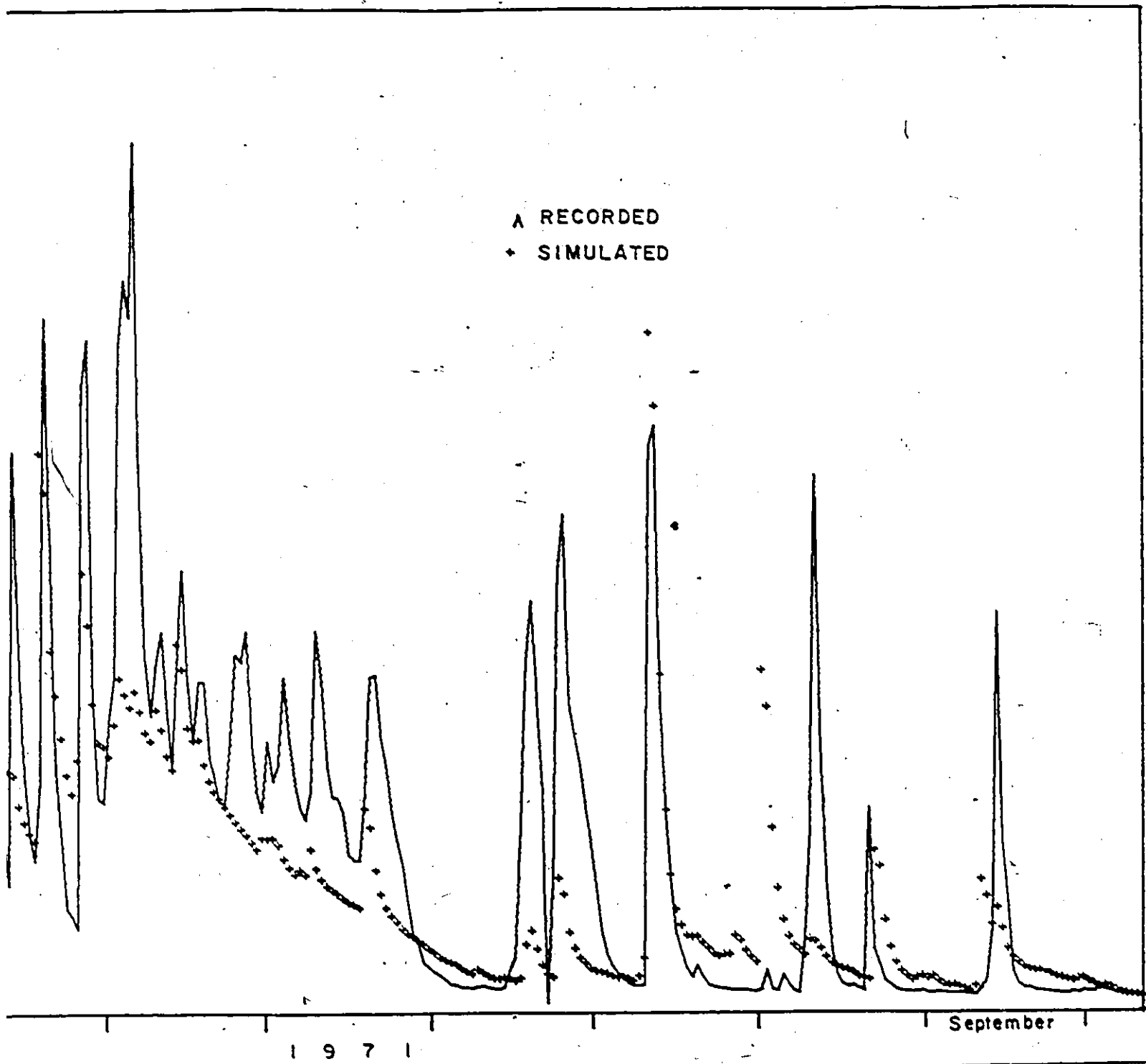


Figure 6.24 The real and modelled hydrographs for Locust Creek.



cust Creek.

- b) In December 1970 and January 1971 the modelled snowmelt is often in error. The timing and size of the real and simulated snowmelt peaks differ, and some real peaks, such as the ones on January 5th and 27th, are missed completely. The mean temperature that is used in the model causes this error, as warm afternoons can be missed, and the temperature during rainfalls or snow cannot be exactly determined from the mean temperature figures.
- c) The recession rates often differ. Thus the model response in May 1970 and November 1970 is too slow but in July 1970 and August 1971 the response is too fast. Effects to correct these recessions by changing the baseflow or interflow constants did not improve the responses.
- d) The modelled streamflow in July 1970 is about four times higher than the real, and daily response is often in error. Thus on July 9th and 10th 3.06 inches of rain fell (equivalent to a mean discharge of 1500 cfs. from the basin) and the streamflow only rose by 14 cfs., while the model gave a discharge of 219 cfs., recessing rapidly to about 40 cfs.

6.4.2 Geomorphic Significance of the Model Parameters

From the model parameters a number of geomorphic implications were drawn. These include:-

- a) The lower value of the lower zone storage (2 inches) and quick ground water and interflow recession rates (100 and 5 days respec-

Table 6.2

Sensitive Parameter Values Used at Locust Creek

PARAMETER	DESCRIPTION AND UNITS	VALUE AT SEGMENT		
		1	2	3
<u>Measured Parameters</u>				
AREA	Segment area (square miles)	18.4	6.4	12.6
HTSTA	Mean elevation of the climatic stations (feet)	2150	2150	2150
HTSEG	Mean segment elevation (feet)	3500	3100	2400
<u>Estimated Parameters</u>				
LPSRT	Lapse rate ($^{\circ}$ F/1000 feet)	-5	-5	0
GWRRT	Ground water recession rate (days)	500	500	100
BZK	Interflow recession rate (1/days)	.1	.1	.2
TIMET	Time delay histogram (1/days)	.5 .5	.5 .5	.5 .5
GWSINT	Initial ground water storage	1.	1.	1.
LADD	Time delay between this segment and the outlet (days)	0	1	
<u>Optimized Parameters</u>				
INFMX	Maximum infiltration rate (inches/day)	2	1	4
INFMN	Minimum infiltration rate (inches/day)	.3	.3	.3
INFRT	Infiltration coefficient	.1	.1	.1
UBCOF	Upper to lower zone percolation coefficient	.1	.1	.1
BGCOF	Lower to ground water percolation coefficient	.1	.1	.1
LZSN	Nominal lower zone storage (inches)	4	4	2
UZSN	Nominal upper zone storage (inches)	5	5	3

- tively) in Segment 3 indicate the karstic nature of this segment.
- b) The higher values of the lower and upper zone storages (4 and 5 inches) and the longer ground water and interflow recession rates (500 and 10 days respectively) in Segments 1 and 2 reflect the thicker soil cover over those segments.
- c) The time delay histogram had a value of 0.5, 0.5 for all segments representing a 12 hour delay in the channel of each segment. Segment 2 (Bruffey Creek) was modelled as flowing to Locust with a one day delay corresponding to the delay in the flow through the Little Levels area. Segment 1 (Hills Creek) however was modelled as having no time delay into Locust as this route does not flow through the Little Levels area.

CHAPTER VII

THE SPRING CREEK BASIN

The Spring Creek basin is the largest and most southerly basin in this study. It was studied in cooperation with Tom Wolfe, who has used sediment and morphological analysis to determine the paleohydrology of the basin, particularly of the Culverson Creek sub-basin. Although the basin is larger, the detailed paleohydrology can be determined more exactly than in the Locust or Swago basins because it is somewhat simpler. The description given here is briefer than for the other basins, and the doctoral thesis of Tom Wolfe (1973) was used as the basis for much of the analysis in the Culverson Creek area.

7.1 Description of the Spring Creek Basin

Spring Creek is the largest and most southerly of the three basins considered in this study (Figure 7.1). It has an area of 129 square miles (Table 1.1) and although the relief is similar to that of the other basins, the ruggedness is less because the basin is larger.

The basin can be divided into four major sub-basins--the Culverson Creek drainage to the west, the upper Spring Creek basins to the north, and the lower Spring Creek basin to the east, and also the Great Savanna area to the south (Figure 7.2). Hydrologically, these are very different

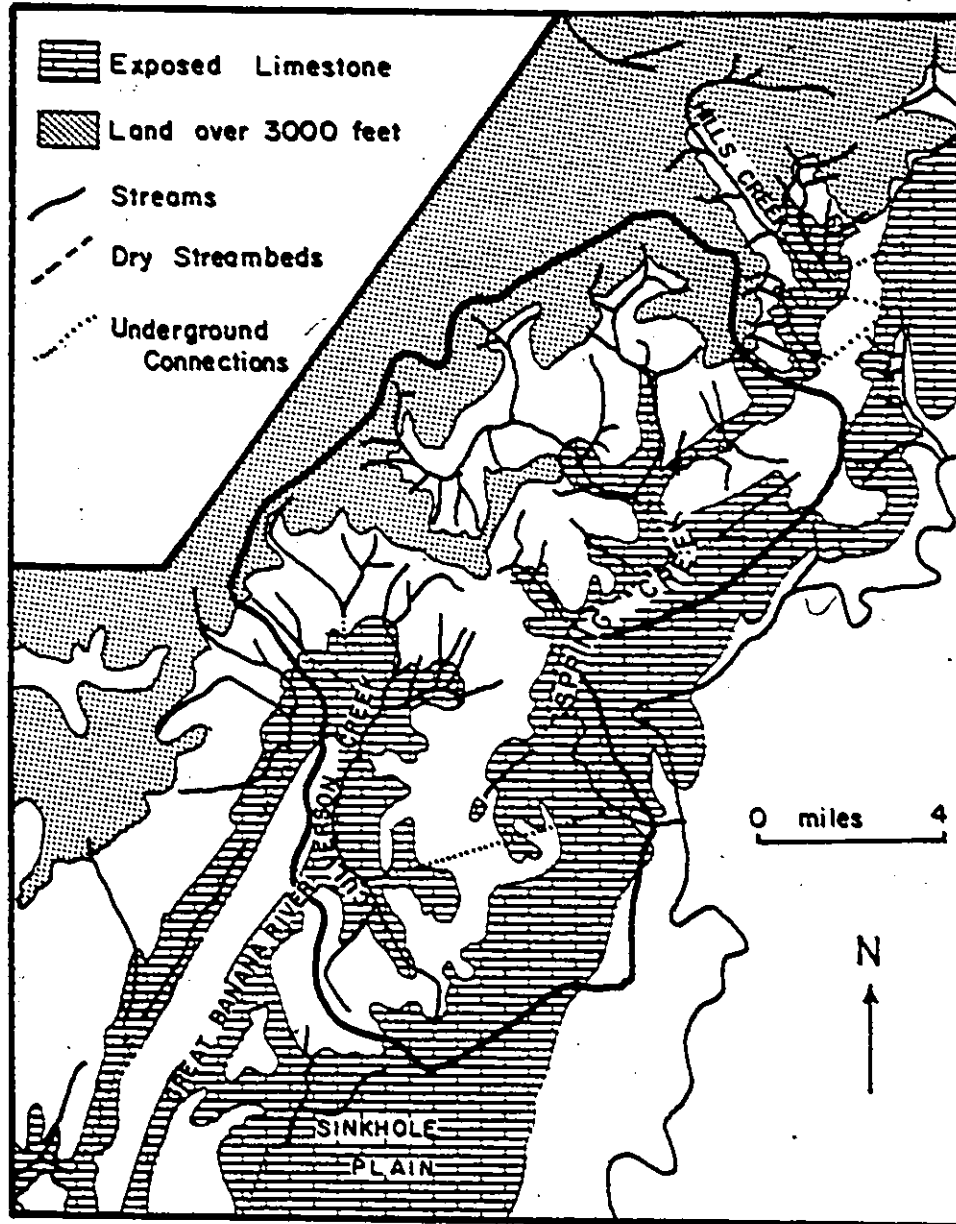


Figure 7.1 The Spring Creek basin--topography and drainage.

from one another. Culverson Creek drains 39 square miles and flows mainly on the surface until the stream sinks at a large cave mouth near Unus (Figure 7.2). This water then flows underground for at least 5.7 miles before resurging near Spring Creek. The upper Spring Creek is a large stream draining 38 square miles which, during low and moderate flows, sinks in the streambed north of Esty. During high water it flows over the surface to lower Spring Creek. The Great Savanna has an area of 18 square miles in the Spring Creek basin and is a classic sinkhole plain (White et al., 1970) developed on the Greenbrier limestone and containing no major surface streams. The lower Spring Creek basin includes the Friars Hole and Renicks valleys, and drains 34 square miles, mainly of exposed limestone.

7.1.1 The Culverson Creek Sub-basin

The northerly part of Culverson Creek is fed by a number of tributaries, some of which sink through the Alderson limestone. Roaring Creek and Charley Run both sink when they reach the Alderson limestone, flow for just over a mile underground, and resurge along the valley of Culverson Creek over the Greenville shale. The Indian Run and other tributaries to the upper part of Culverson Creek do not sink through the Alderson, and are supported on a thin veneer of alluvium (Wolfe, 1973). Culverson Creek then flows for a further 6.5 miles on the Greenville shale and upper part of the Union limestone before sinking at Culverson Creek Cave.

Culverson Creek Cave is a large cave with 10.73 miles of mapped

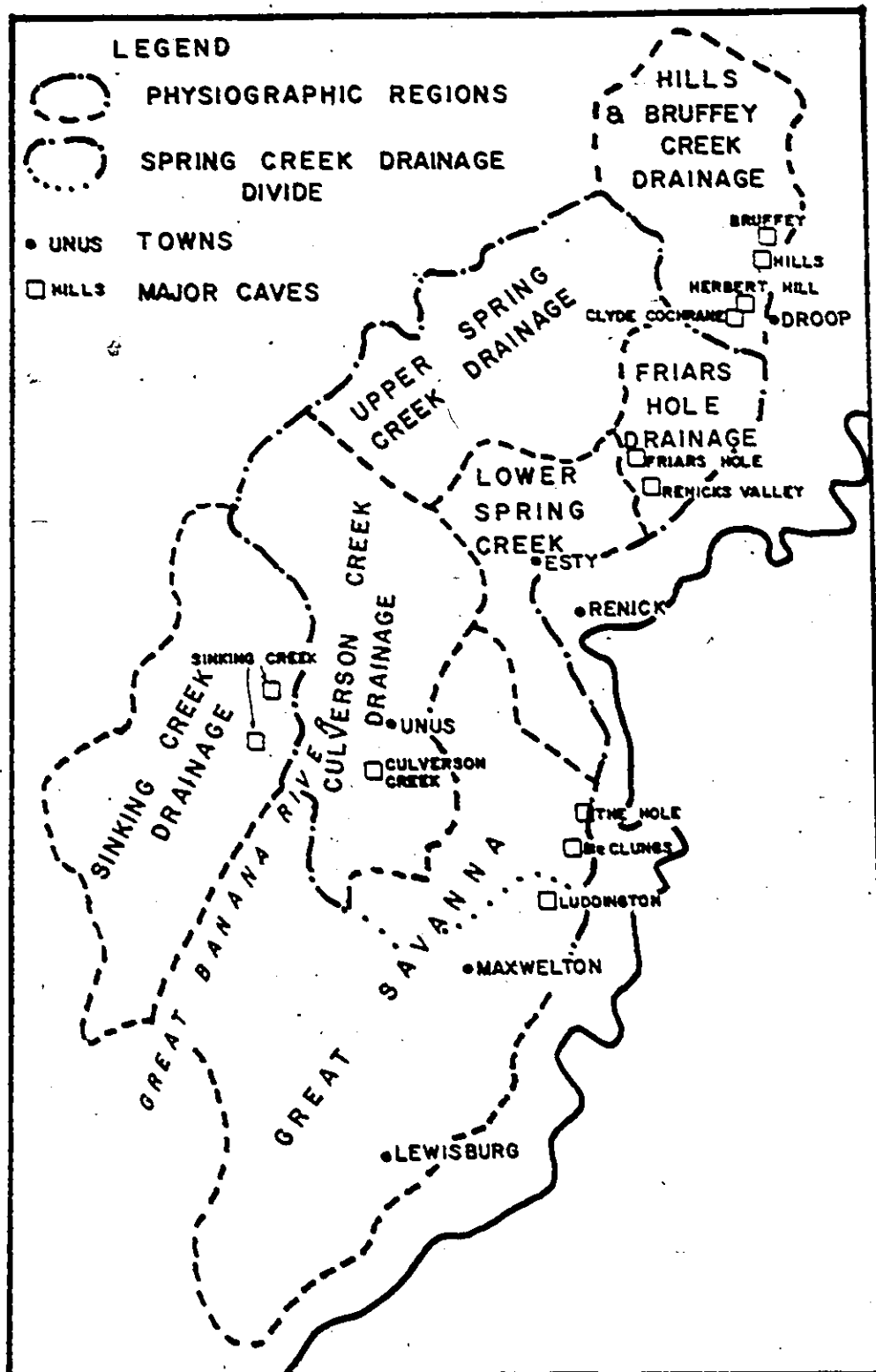


Figure 7.2 Spring Creek basin--major sub-basins, towns and cave locations.

passages (WVACS, 1971). It consists of three sections of active stream passage with a total length of two miles, plus a number of fossil passages above the sections of streamway. The cave has five entrances and the whole of it can be traversed underground (although in 1970 a passage near one entrance collapsed, cutting off the upper streamway from the rest of the cave). From the lowest sump in the system the stream flows for a straight line distance of 4.7 miles to a resurgence on Spring Creek.

Wolfe (1973) has argued that a stream used to flow out of the Culverson Creek Cave entrance (in the reverse direction to that at present) to join Culverson Creek when it was flowing down the Great Banana River (Figure 7.2). The major pieces of evidence for this are the presence of scallops in some of the upper passages of Culverson Creek indicating the reversed flow, and the sharp bend at Spruce where it joins the lower part of Culverson Creek. This will be discussed further in Section 7.2.2.

7.1.2 The Upper Spring Creek Sub-basin

This sub-basin drains the clastic rocks in the northern part of the Spring Creek basin. The two main tributaries join north of Esty (Figure 7.2) and just below this point the stream usually sinks through the cobbles in the streambed. During most conditions the stream flows underground for six miles before resurging near the Greenbrier River. During high water however, the upper Spring Creek stream inundates the sink and the excess water flows on the surface to the river, down what is usually a dry streambed.

7.1.3 The Great Savanna Sub-basin

The Great Savanna is a term used by Rutherford (1971) to describe the large sinkhole plain that exists in Greenbrier County. This area is characterized as a gently rolling limestone plain, with a relief of about 150 feet, dissected by a large number of uvalas, dolinas, shakeholes and caves.

The Great Savanna is bordered by small hills rising about 100 feet above the plain to the east, and by Bushy Ridge which has 300 feet of relief to the west (Figure 7.3). Both of these ridges are composed of McCrady shale. Running along near the western side of the Great Savanna is a ridge composed of the Bluestone Formation which overlies the limestone. These three ridges are a consequence of three sub-parallel folds in the Mississippian rocks (Figure 7.3), creating a limestone basin with no natural drainage to the east or the west. The Greenbrier River cuts across and drains the southern part of the Great Savanna. In the north the Spring Creek valley crosses the limestone and forms the natural ground water outlet for the northern part of the sinkhole plain.

The infiltration is high in this area, with most of the precipitation sinking into the limestone as soon as it falls. No major surface streams cross the limestone, although a number of small streams are supported on alluvium and do flow across the sinkhole plain for short distances.

Due to the generally diffuse runoff on the Great Savanna, few caves have formed in the central region of the plain. The majority of the caves form at the edges of the area, where streams concentrate on

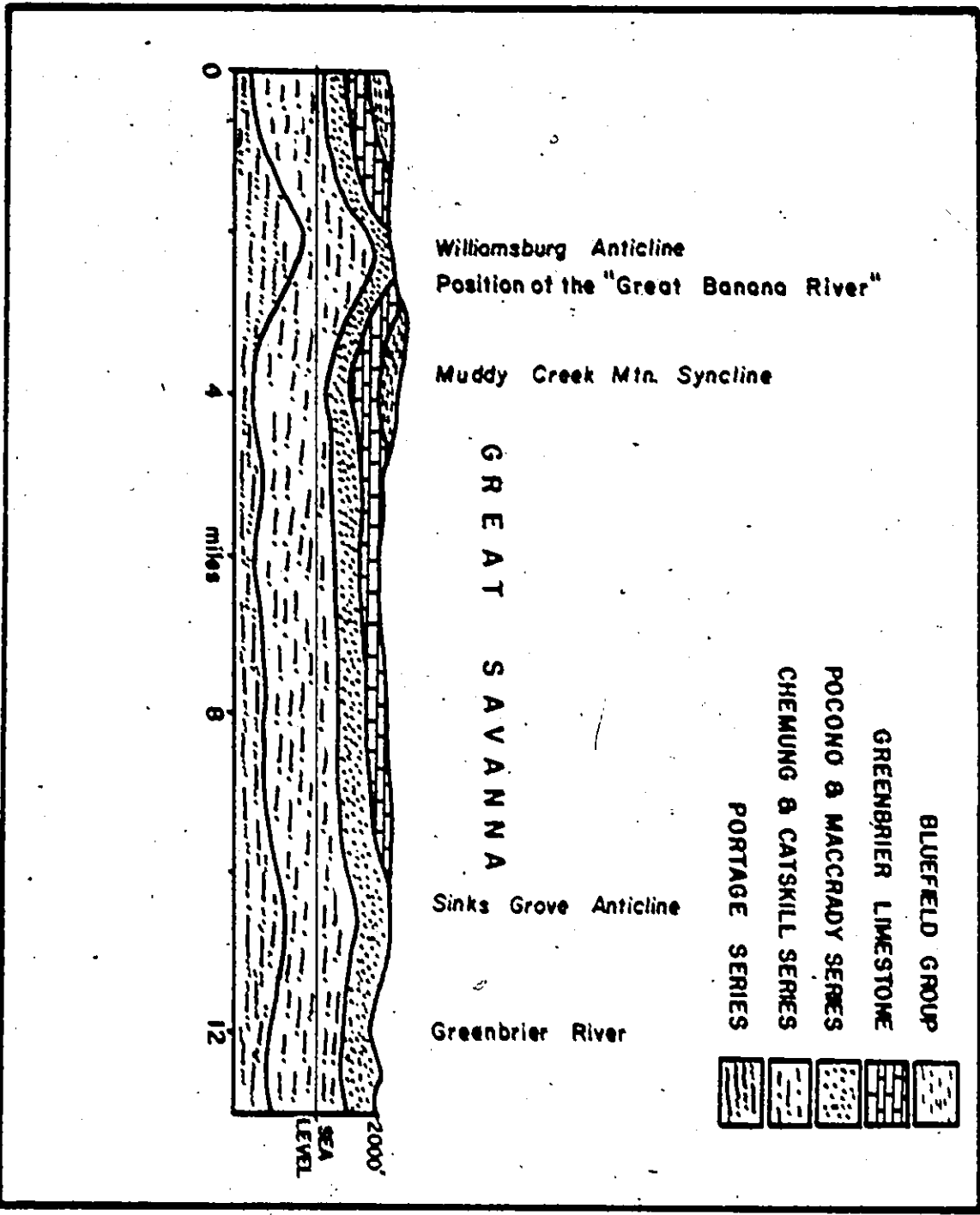


Figure 7.3 Cross section across the "Great Savanna" region.

the clastic rocks and, due to the increased erosional power, develop caves near the margins of the limestone. There are a number of such "contact" caves on the eastern side of the plain, where streams running off the McCrady hills have developed McClungs Cave, Luddingtons Cave and The Hole. All three caves are several miles long and each is formed in the Hillsdale limestone immediately above the McCrady shale.

The water in Luddingtons is known to flow to McClungs, and Luddingtons Cave was tested to flow to the southerly resurgence of Fort Spring (Section 2.5.1). The Hole, however, drains north to Spring Creek (Rutherford, personal communication, 1970). The drainage divide for Spring Creek must therefore be between these caves. Due to the number of dolinas and depressions, and the lack of surface streams on the sinkhole plain, difficulty was had in establishing the position of the drainage divide in this region. The divide was estimated, however, to run along the approximate topographic divide between Luddingtons Cave and The Hole. The Great Savanna has an area of about 90 square miles, of which 18 square miles drain to Spring Creek.

7.1.4 The Lower Spring Creek Sub-basin

The lower Spring Creek sub-basin includes the Friars Hole and Renicks valley drainage. Both valleys are underdrained and the water in each flows underground for about six miles, to resurge near the Greenbrier River. The rest of the sub-basin is similarly underdrained and contains few surface streams.

Near the Greenbrier River, Spring Creek displays some large entrenched meanders through the limestone and onto the underlying McCrady shale. The shale is now exposed in the streambed for about three miles above the junction of the river. Near the McCrady shale-limestone contact there are over ten springs, from whence the creek derived its name, which are fed from the upper Spring Creek, the Culverson Creek and the Great Savanna sub-basins.

7.2 The Development of the Spring Creek Basin

Development of the Spring Creek basin, particularly in the Culverson Creek sub-basin, has been investigated by Wolfe (1973). His analysis is briefly described here, with the addition of the proposed development of the other sub-basins, in order to obtain a total picture of the basin genesis.

The development has included a large number of distinct events, but four major stages can be identified. These are:

- a) the original surficial flow,
- b) the initial underdraining of the valleys,
- c) major diversions, and
- d) shortening of the flow routes.

These four stages are described in the following sub-sections.

7.2.1 Stage 1: Surficial Flow

The initial surficial flow conditions are shown in Figure 7.4. The major differences in the surficial flow conditions to those today are the loss of the Culverson Creek drainage and the addition of the Hills and Bruffey streams. Thus, although the basin during Stage 1 was of different shape than today, its area was similar (115 square miles compared to 129 square miles today).

Culverson Creek and its tributaries flowed down the "Great Banana River" (Wolfe, 1973), parallel to the present Sinking Creek flow route. It then joined Mill Creek, a tributary of the Greenbrier River near Alderson. The Hills and Bruffey drainage flowed down the Friars Hole valley, as described in Section 6.3.1, to join Spring Creek. At the northern end of the basin, the upper reaches of Hills Creek drained away from Spring into the Cherry River, as described in Section 6.3.1.

In the "Great Savanna" area a surface stream almost certainly flowed north to Spring Creek. However at present there is no indication of the position of such a stream or even for the position of the southerly drainage divide. In Figure 7.4 the drainage divide is placed in its present position, and the surficial stream on the Great Savanna is along the thalweg of the area. However both positions could be considerably in error.

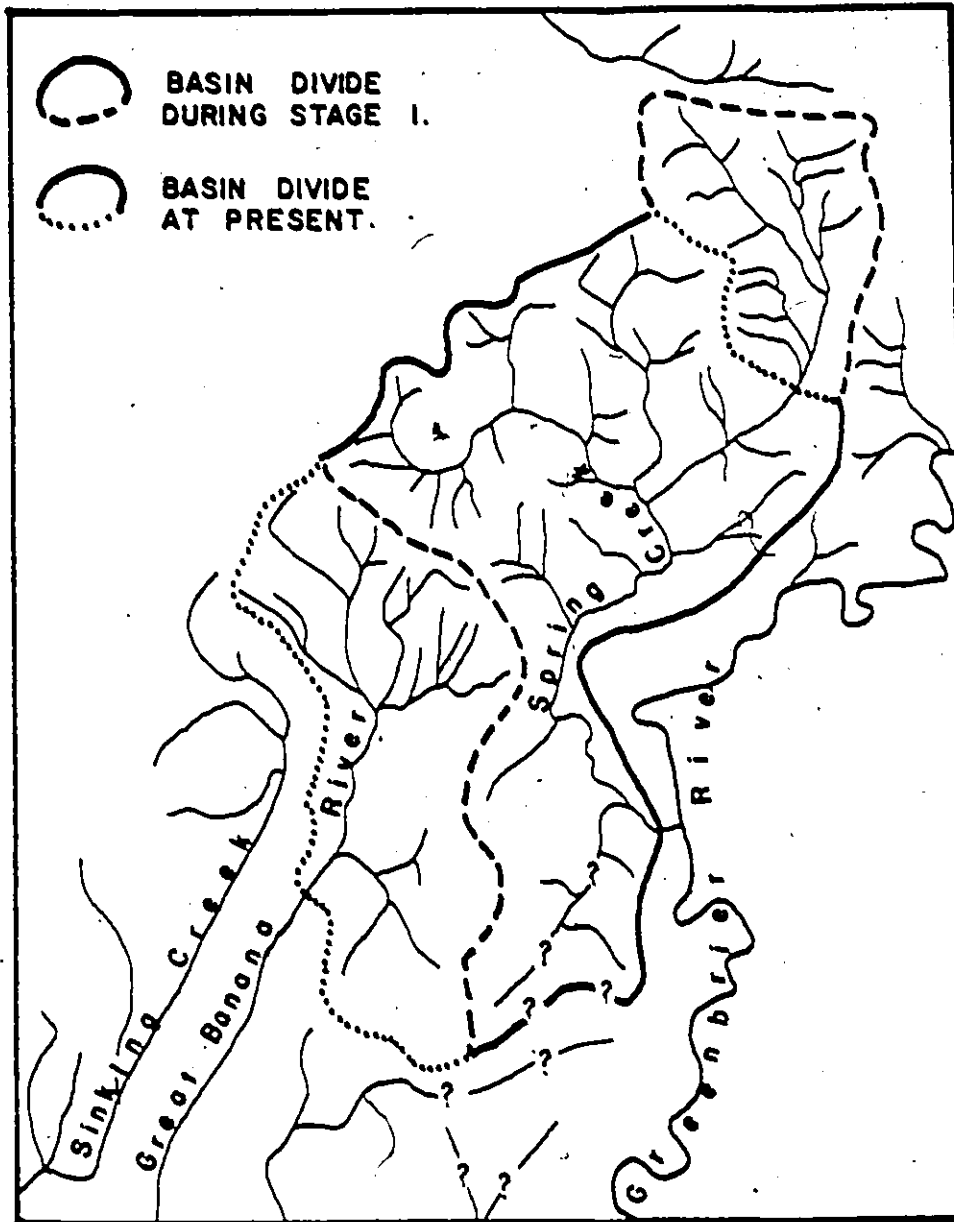


Figure 7.4 Spring Creek basin--surficial flow during Stage 1.

7.2.2 Stage 2: Underdraining of the Valleys

As the overlying clastic rocks were entrenched by the streams, underdraining of the surface valleys into the limestone commenced. Underdraining achieved considerable dimensions in the Friars Hole valley, along the Great Banana River and along Spring Creek.

The Hills and Bruffey streams flowed down together to Snedegars Cave and thence underground to Spring Creek (Section 6.3.2), through Snedegars and Friars Hole Caves (Figure 7.5). Spring Creek similarly sank and underdrained the valley. The position of any of the sinks is unclear as the stream disappears in cobbles and boulders along the streambed. It is probable that the position of the sink point for Spring Creek has changed as the basin has developed, moving upstream as more limestone was exposed. The positions of the sinks are not known as no sinks or significant caves are visible along the streambed. The present sink is just downstream of the junction with the Friars Hole valley and the stream flows underground for a straight line distance of 6 miles at a gradient of 30 feet/mile. There are no major discontinuities in the stream gradient below the sink so that groundwater from any downstream sinks would flow at similar gradients to the resurgence.

The reason that the sinks are not exposed appears to be related to the competence of the streams to move the bedload. Competence of a stream is roughly proportional to the stream discharge and the stream gradient (Leopold, Wolman and Miller, 1964). Referring to Figure 7.6, it can be seen that although Spring Creek has an intermediate gradient between Hills Creek and Culverson Creek, its competence is larger since

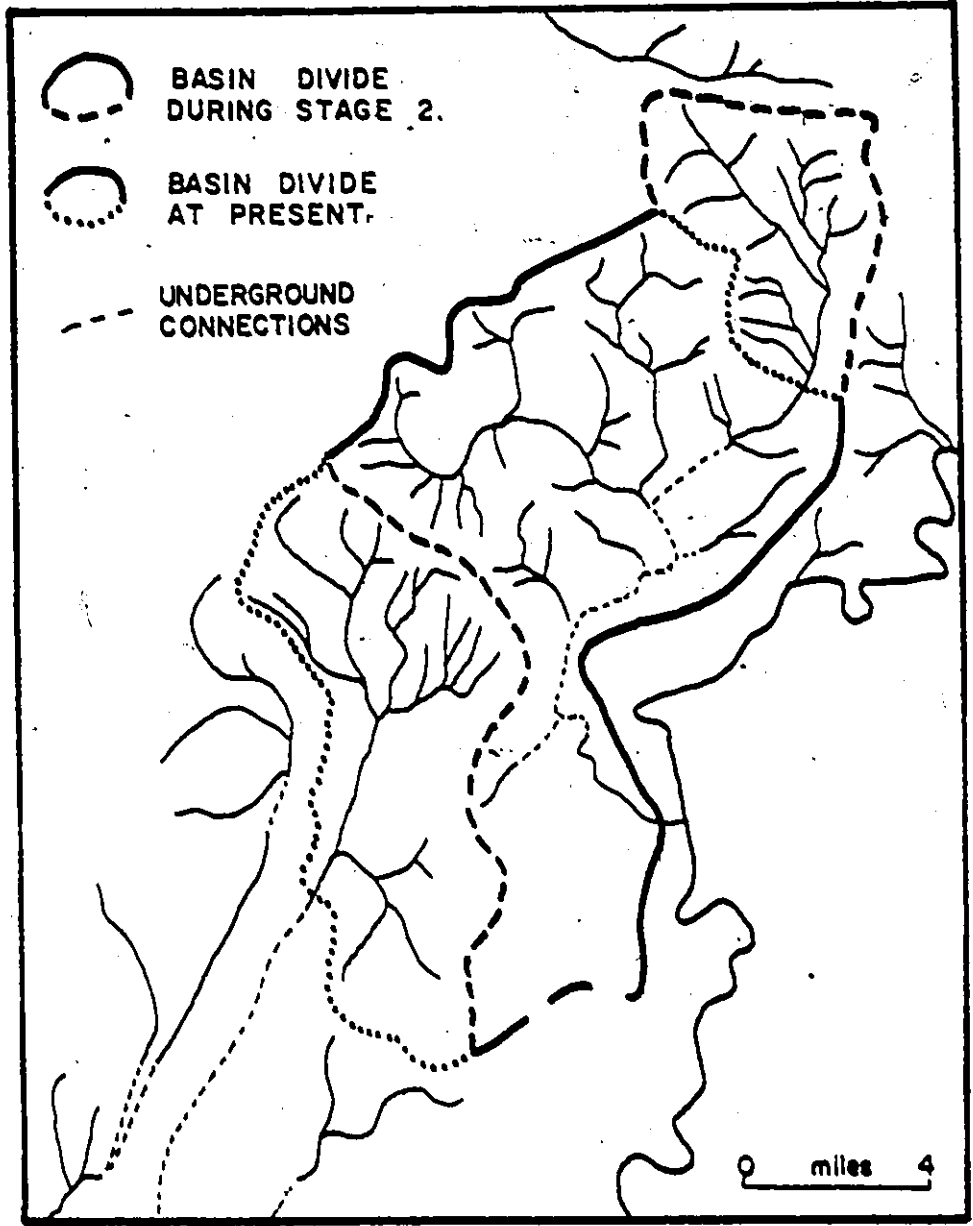


Figure 7.5 Spring Creek basin--initial underdrainage of the valleys during Stage 2.

the drainage area is larger than that of Hills Creek. Thus the bedload material which is moved may be expected to be larger in Spring Creek than in the other streams. This is apparent when the streams are inspected. Figure 7.7 shows the size and extent of boulders that were moved by Spring Creek during the Camille flood of August 1969. Although flooding occurred in Culverson and Hills Creeks during the same storm, neither stream was moving boulders as large as the ones indicated in Figure 7.7. Any caves or conduits that do form along the Spring Creek channel would quickly be filled up with boulders. The smaller size of bedload moved by Hills and Culverson Creeks allows open caves to remain at the sink points.

Cave development also took place in other areas of the basin. The small streams that drained off the hills near the village of Unus sank and flowed out of a passage just above the present Culverson Creek entrance (Wolfe, 1973). The evidence for this is based on scallop directions in the upper levels of Culverson Creek Cave and from sedimentary evidence (Wolfe, 1973). From the Culverson Creek Cave area the stream flowed westward to join the Great Banana River (Figure 7.5).

It is probable that the Great Banana River sank along the lower part of the valley during Stage 2. The major pieces of evidence for this are:-

- a) By comparison with the present Sinking Creek drainage. Sinking Creek is the stream just to the north-west of the Great Banana River (Figure 7.1). Due to the northwesterly dip of the limestone, Sinking Creek is stratigraphically higher than the Great Banana River, and so in a more youthful stage. Sinking Creek now flows for about

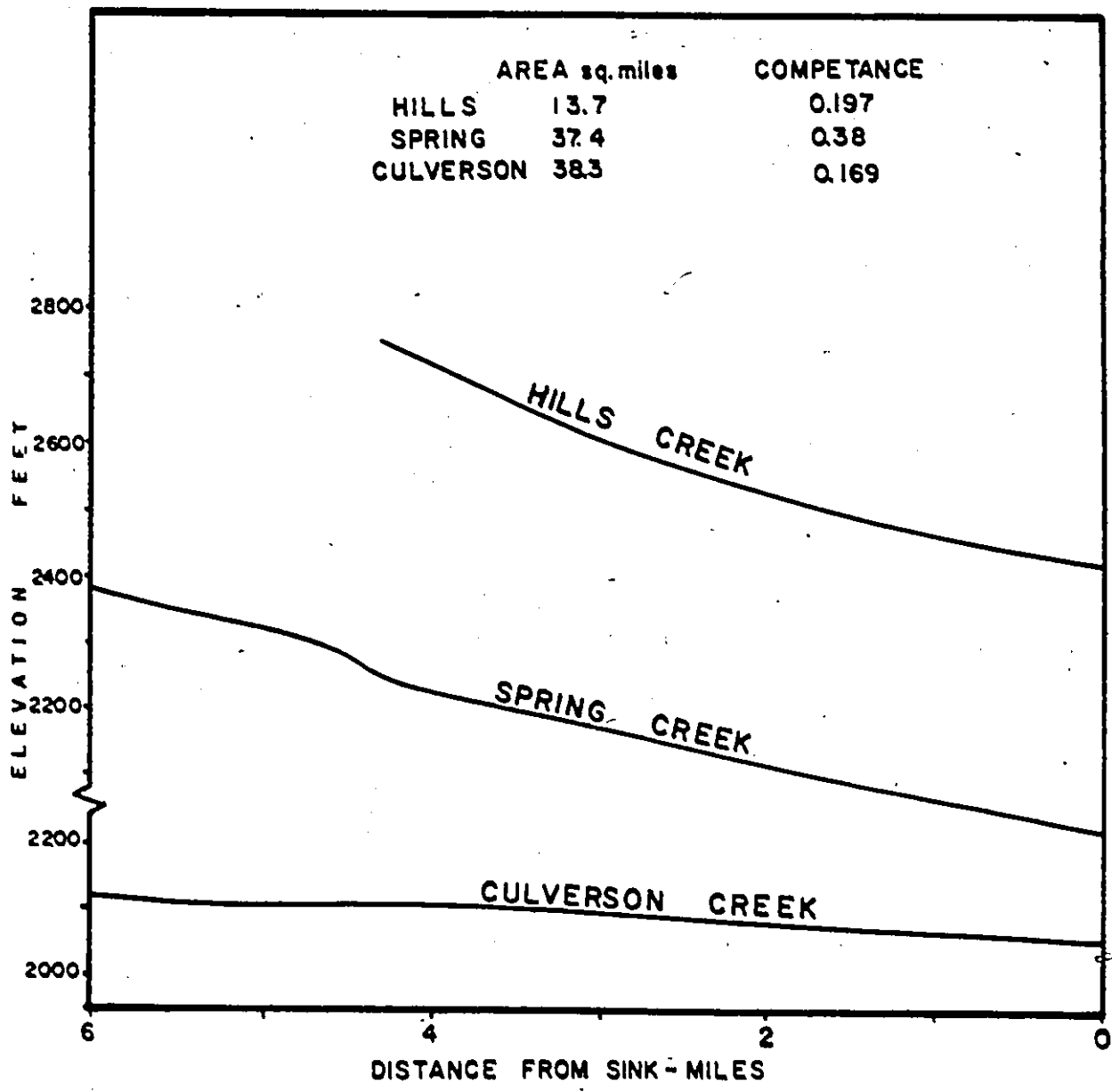


Figure 7.6 Stream profiles and competence of Hills, Spring and Culverson Creeks near the sink points.

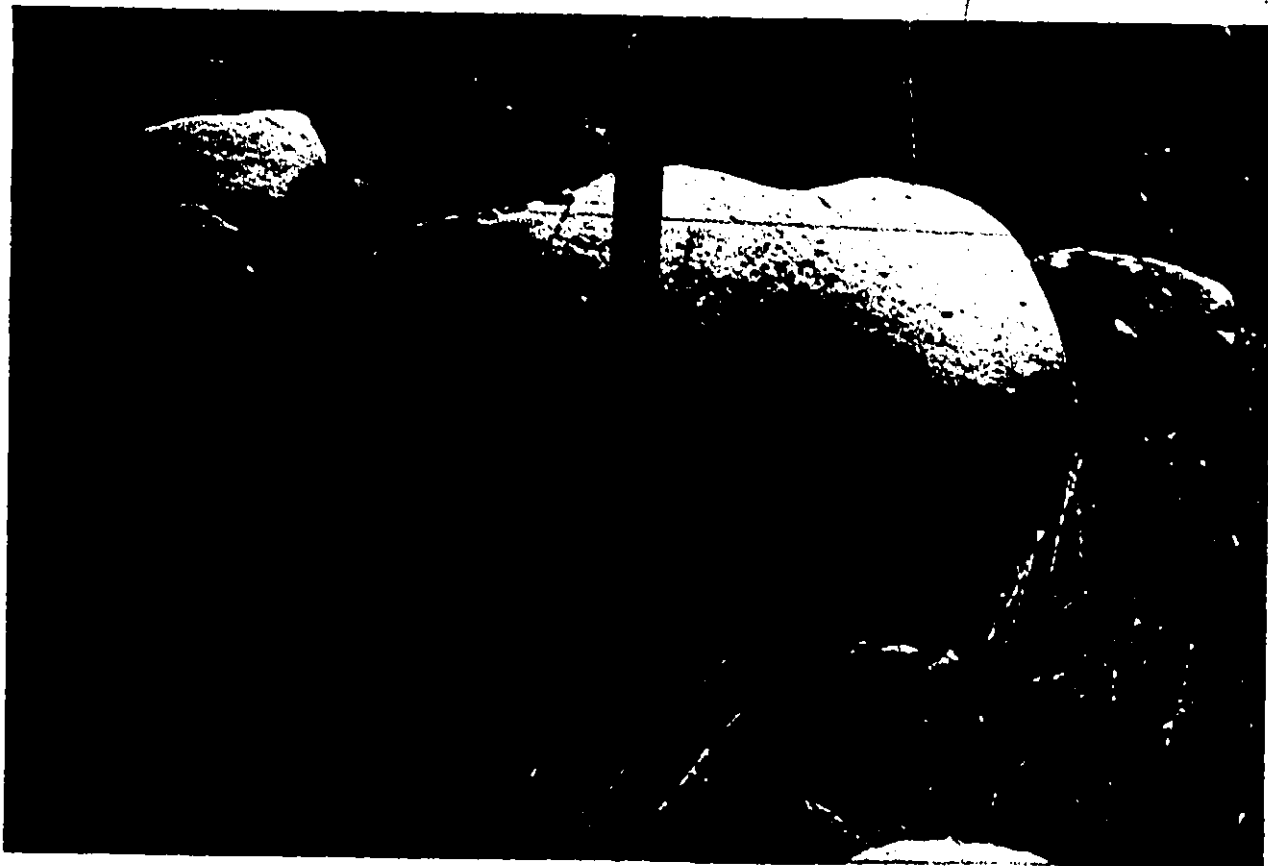


Figure 7.7 Boulders moved during the Camille Flood in August 1969.
The scale is three feet long.

2 3/4 miles (straight line distance) underground, down to the resurgence at Pierce's Mill. It is probable that the Great Banana River also sank underground for some of its course down to Mill Creek.

b) Caves along the valley. There are a number of caves in the Great Banana River valley, such as Jarretts Water, Ashbury and McFerrins Caves (Davis, 1965). Although the total length of trunk passage in these caves adds up to only about 1000 feet, they do indicate that cave development has taken place.

c) Sedimentary evidence. Wolfe (1973) has shown that the Kaolinite/Illinite clay ratio in McFerrins Cave sediments is lower than in active streamways. This lower clay ratio supports the evidence that McFerrins Cave was part of the Great Banana paleodrainage, as low clay ratios are associated with fossilized caves (Wolfe, 1973).

For these reasons it is probable that the Great Banana River sank for at least part of its course during Stage 2.

At the northern end of the Culverson basin, Roaring Creek developed Bob Gee Cave, which is in the Alderson limestone near Trout (Wolfe, 1973). It is probable that Bob Gee Cave was part of a long cave conduit active during Stage 2, continuing on down the Great Savanna.

In the south of the basin it is probable that the streams flowing on the Great Savanna also sank in a similar fashion to the northern streams. The evidence for such conduits includes a number of caves such as Rapps and Spencer Caves, both of which are short phreatic systems. No long conduit can be discerned now. It may be supposed that erosion and sedimentation have destroyed many of those envisaged during Stage 2.

7.2.3 Stage 3: Major Piracies of the Streams

Between the second and third stages of development major diversions of the streams occurred. Culverson Creek was captured by Spring Creek away from the Muddy Creek drainage; the Hills and Bruffey streams were captured away from the Spring Creek drainage into Locust Creek (Figure 7.8). Other caves developed in the Great Savanna area.

One interesting feature of the development from Stage 2 to 3 was the reversal of the flow direction outside Culverson Creek Cave (Wolfe, 1973). During Stage 2 the small streams around the Culverson Creek Cave flowed through the cave and out of a resurgence above the Culverson Creek entrance. However, an underground route formed from the cave to Spring Creek and this route captured the cave drainage. The cave then also was able to capture the whole Culverson Creek drainage of 37 square miles and drain this basin to Spring Creek. The route from Culverson to Spring took place along the highest hydraulic gradient route to any possible resurgences at 39 feet/mile. The gradients to Mill Creek and Fort Spring, which are the other possible flow routes, are only 22 and 26 feet/mile respectively, as shown on Table 7.1.

The Hills and Bruffey streams were captured by Locust Creek and drained away from the Spring Creek basin. This capture has been described in Section 6.3.3. The Friars Hole and Snedegars drainage still flowed into the Spring Creek basin, also described in Section 6.3.3.

Several caves developed on the eastern edge of the Great Savanna. In this area the dip of the beds is about 3° to the north-west. Near the Greenbrier River there are some hills of the McCrady shale, and the streams

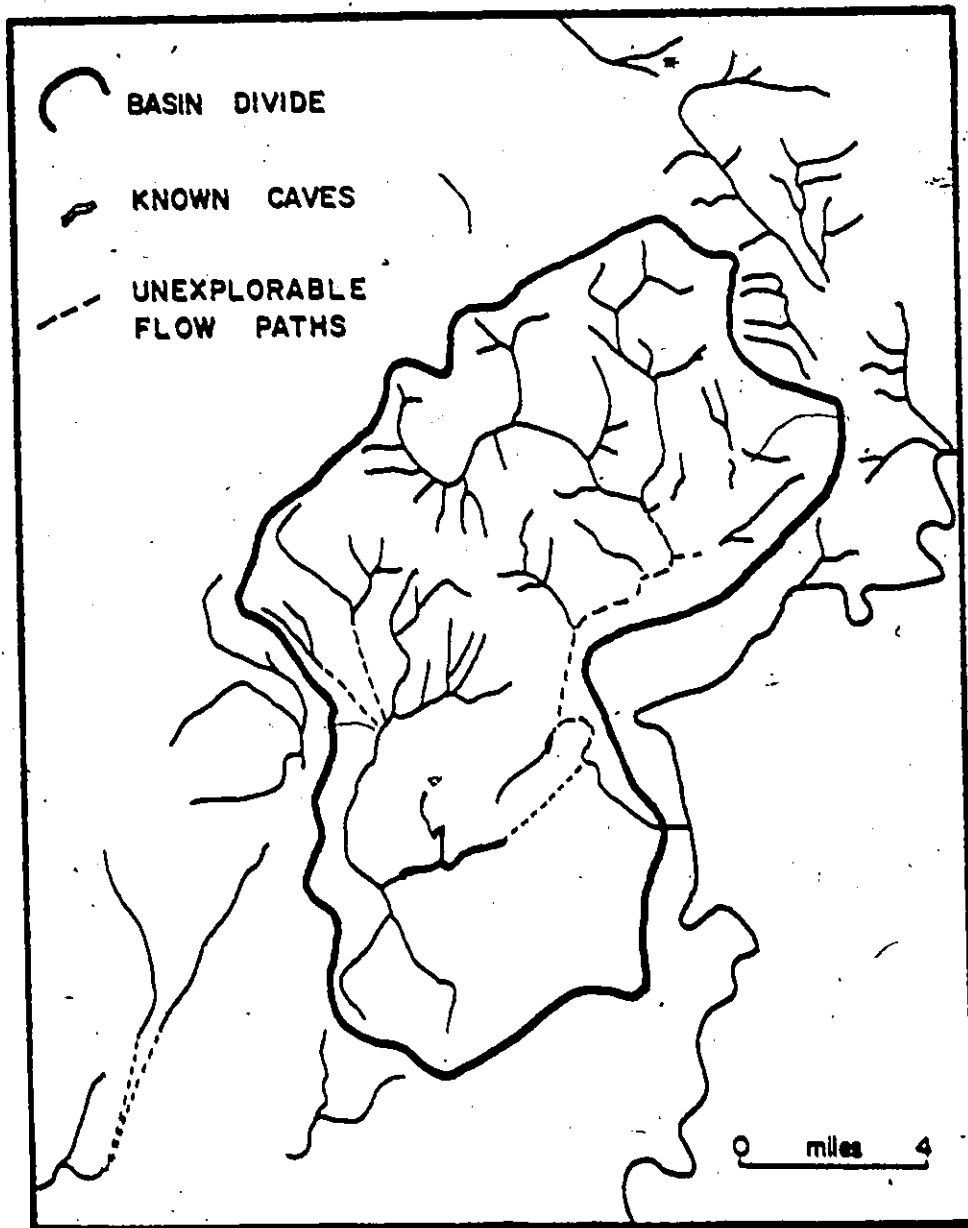


Figure 7.8 Spring Creek basin--major diversions during Stage 3.

on the western side of these hills run off onto the Hillsdale limestone where they have developed a number of "contact" caves. The Hole drains to Spring Creek, and Luddingtons and McClungs drain south to Fort Spring. These caves do not fit the pattern of developing along the highest hydraulic gradient, as can be seen from Table 7.1.

For the contact caves the development situation is different than for most of the other caves. They are developed at the Hillsdale-McCrady contact, and the development and drainage direction is intimately tied up with the dip and topography of the McCrady shale. Thus, although the gradient to Spring Creek is higher than to Fort Spring, some other factor must have controlled the drainage direction of Luddingtons and McClungs Caves.

Near Trout a number of streams have developed underground flow routes through the Alderson limestone. Roaring Creek and Charley Run both sink on reaching the Alderson limestone (Wolfe, 1973), but no active caves can be entered now as the sinks are covered by thick layers of alluvium. The streams flow underground for just over a mile before resurging and joining Culverson Creek.

Buckeye Creek Cave is another route that developed during Stage 3. The cave is in the Alderson limestone, is almost a mile long, up to 60 feet high and 20 feet wide. The cave was largely developed by vadose flow and carries a stream which runs off Butlers Mountain towards Spring Creek. Higginbothams Cave similarly carries a stream running off the Bluefield Hills through the Alderson limestone. The cave is 4000 feet long and up to 30 feet wide and 15 feet high and formed by phreatic flow.

Table 7.1

Hydraulic Straight Line Gradients from Various Caves
to Spring Creek, Fort Spring and Mill Creek

<u>Cave</u>	<u>Gradient of Cave to:</u>		
	<u>Spring Creek</u>	<u>Fort Spring</u>	<u>Mill Creek</u>
The Hole	<u>200</u>	30	
Luddingtons	60	<u>45</u>	
McClunge	70	<u>20</u>	
Culverson Creek	<u>39</u>	22	26
Coffmans	<u>71</u>	<u>35</u>	39

The underlined values indicate the actual flow routes.

The stream in Higginbothams resurges at the base of the Alderson, flows over the Greenville shale and sinks to flow through Coffman Cave which is in the Union limestone. Coffmans is only 300 feet long but averages 6 feet high and 12 feet wide and was largely developed by vadose flow.

7.2.4 Stage 4: Shortening of the Flow Routes

The development from Stage 3 to 4 was not very significant. No major drainage patterns were altered, but a number of drainage routes were shortened or slightly modified.

In Culverson Creek Cave, Wolfe (1973) has described the shortening of, and modifications to the main channel route down to the final siphon once inside the cave. In addition, a small surface stream developed Fullers Cave, which is a recent vadose passage that joins the lower section of the Culverson streamway.

At the lower end of Friars Hole Cave, recent vadose development has taken place (see Figure 6.9). This downcutting at the end of the cave has breached the Taggard shale due to mechanical erosion in the cave.

During Stage 4 the sink point for the upper Spring Creek drainage has moved further upstream as the stream eroded the overlying shales. It is probable that the underground conduit will open up as time goes on and as the stream gradient decreases, thus reducing the bedload movement along Spring Creek. If this does occur, a significant cave should develop and the frequency of flooding along the normally dry lower Spring Creek streambed will decrease.

7.3 The Simulation of Spring Creek

Spring Creek was simulated for the 413 day period from July 13, 1970 to August 31, 1971 and for an additional 50 day run in period. The full simulation results are presented on a logarithmic scale in Appendix II and a portion shown in a linear scale in Figure 7.9.

In addition, the Culverson Creek basin was modelled for the area above the Wildcat gauge for the 157 days that streamflow records were available. These results are shown in Figure 7.10.

The Spring Creek basin contains a number of areas of differing hydrological characteristics (Figure 7.1). Simulation was initially tried using one segment, and later four segments corresponding to the four areas described in Section 7.1. However, as the streamflow record was so short the four segments could not be uniquely optimized and further runs were made using two segments. These were:

- a) Segment 1. The upper Spring Creek and Culverson Creek sub-basins, draining 77 square miles of primarily elastic hills.
- b) Segment 2. The lower Spring Creek and Great Savanna areas, draining 52 square miles, of which 80% is exposed limestones.

The parameter values for the two segments plus the Wildcat segment are shown in Table 7.2 for the measured, estimated and optimized parameters, and in Table 8.4 for the parameters which did not vary from basin to basin.

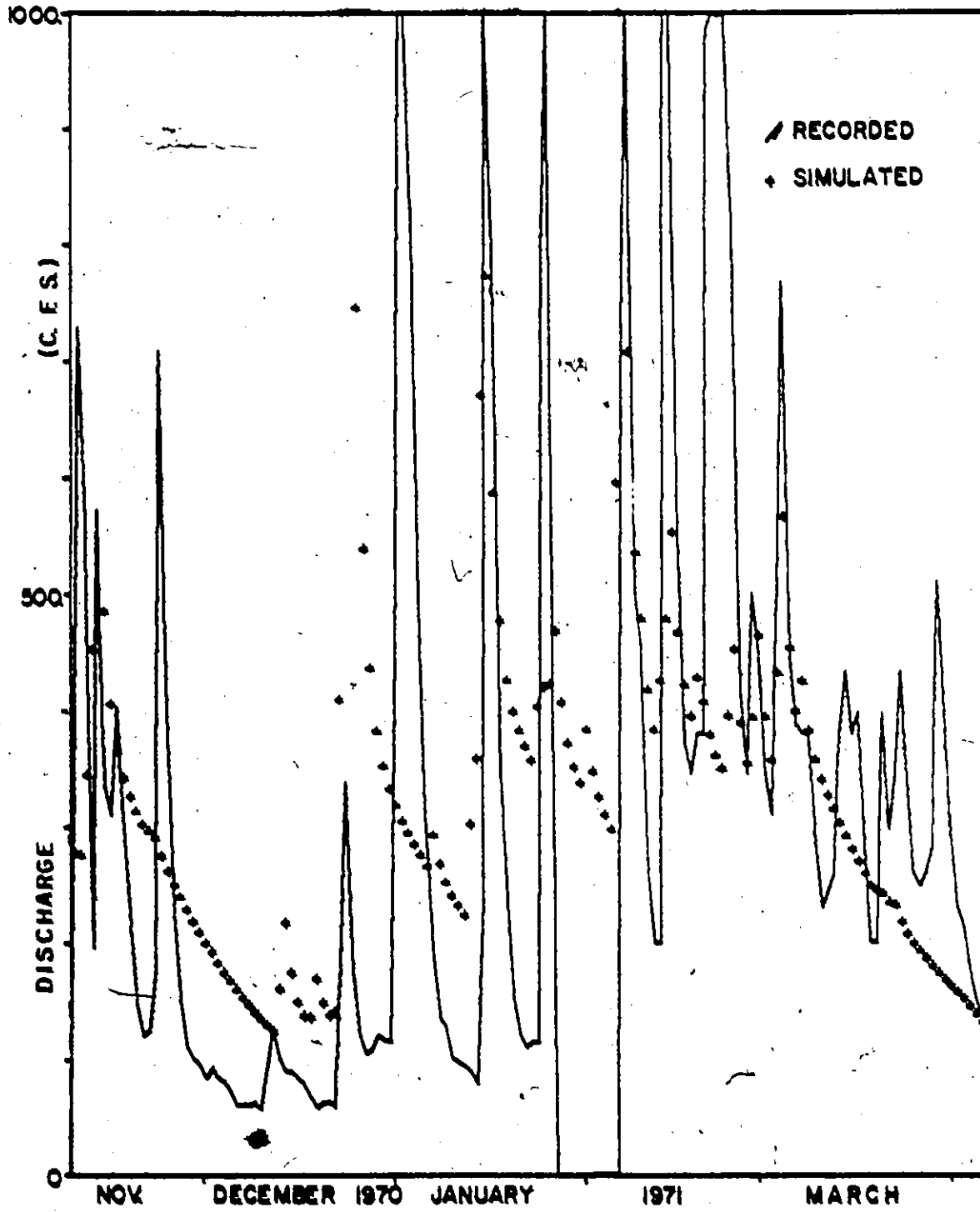


Figure 7.9 The real and modelled hydrographs for Spring Creek.

Table 7.2

Sensitive Parameter Values Used at Spring and Wildcat Creeks

PARAMETER	DESCRIPTION AND UNITS	VALUE AT:		
		Spring, 1	Segment 2	Wildcat
<u>Measured Parameters</u>				
AREA	Segment area (square miles)	77	51	38
HTSTA	Mean elevation of the climatic stations (feet)	2050	2050	2150
HTSEG	Mean segment elevation (feet)	3500	2450	3500
<u>Estimated Parameters</u>				
LPSRT	Lapse rate ($^{\circ}\text{F}/1000$ feet)	-5	-5	0
GWRRT	Ground water recession rate (days)	200	100	200
BZK	Interflow recession rate (1/days)	.2	.3	.2
TDMT	Time delay histogram (1/days)	0.5 0.5	0.5 0.5	0.5 0.5
GWSINT	Initial ground water storage	1.	1.	1.
IADD	Time delay between this segment and the outlet (days)	1	-	-
<u>Optimized Parameters</u>				
INFMX	Maximum infiltration rate (inches/day)	2	4	4
INFMN	Minimum infiltration rate (inches/day)	.3	.3	.3
INFRT	Infiltration coefficient	.1	.1	.1
UBCOF	Upper to lower zone percolation coefficient	.1	.1	.1
BQCOF	Lower to ground water percolation coefficient	.1	.1	.1
LZSN	Nominal lower zone storage (inches)	4	2	4
UZSN	Nominal upper zone storage (inches)	5	1	5

7.3.1 Comparison Between the Real and Simulated Flows

In the Spring Creek record, data were lost during parts of February, May and June 1971 because the clock in the recorder stopped.

The monthly mean simulated and real streamflow values for this basin agree fairly well for most of the period. Daily values, however, tend to have more errors, as was found at the other basins. The major areas of error include:

- a) In November 1970 the simulated flow was far higher than the real flow due to the precipitation being modelled as rain when it must have fallen as snow.
- b) The snowmelt period in December 1970 and January 1971 has several errors, with the snowmelt peaks being misplaced or of incorrect magnitude. These two errors are caused by the oversimplification of the temperature input data: this error has been discussed in Section 6.4.1.

7.3.2 Geomorphic Significance of the Model Parameters

The implications that were drawn from the model parameters about the geomorphic characteristics of the Spring Creek basin are similar to those described in Sections 6.4.2 for Locust Creek and 6.4.2 for Snake Creek. Briefly the implications are:

- a) The quick recession, high infiltration rates and small soil storages in Segment 2 (Table 7.2) all characterize karst segments.

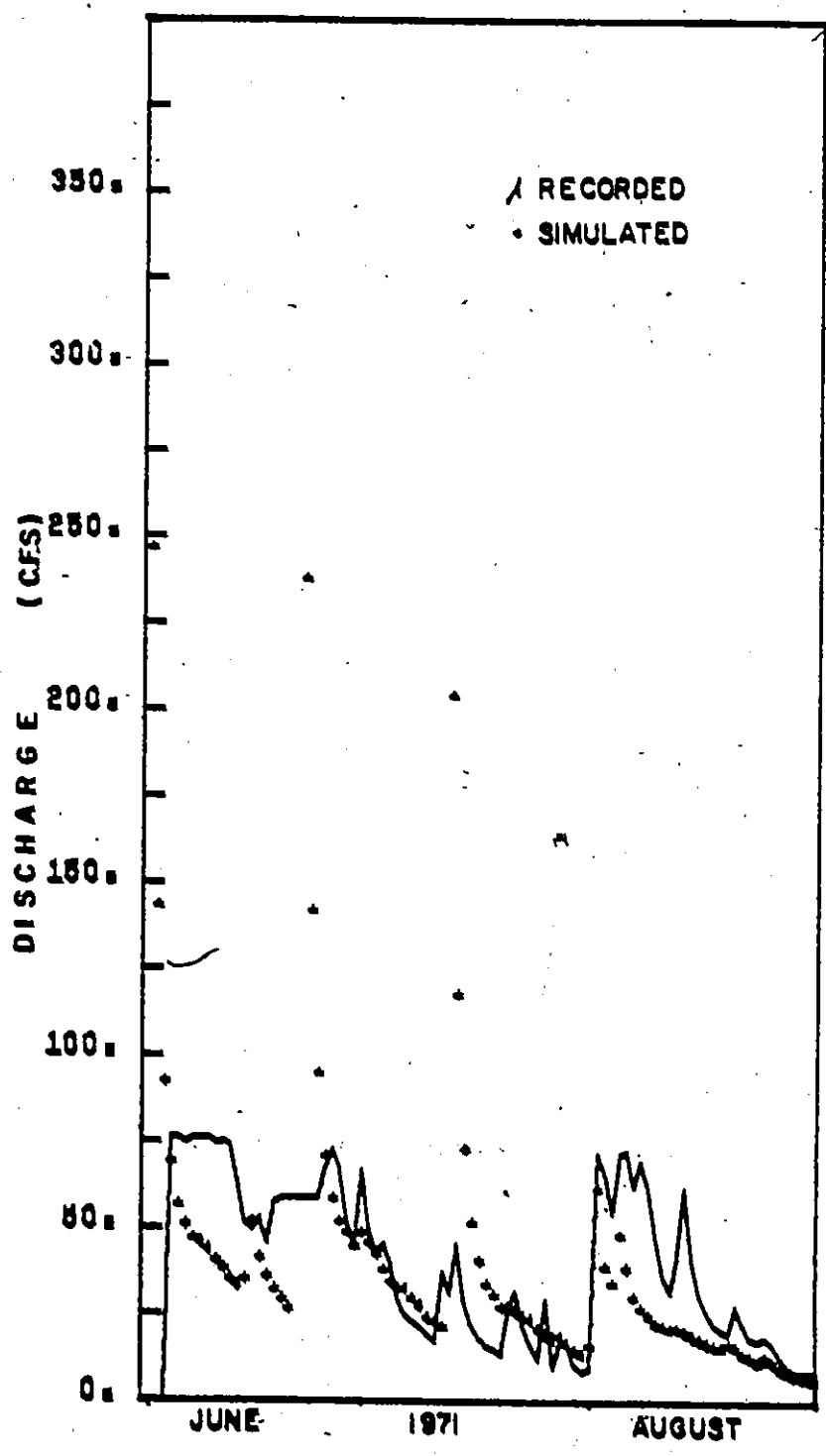


Figure 7.10 The real and modelled hydrographs for Wildcat Cave.

b) The slower recession and higher soil storages in Segment 1 (Table 7.2) indicate the thicker soil in the Culverson Creek and upper Spring Creek segment.

c) The one day time delay between the upper segment and the outlet models the delay in Culverson Creek Cave and in the underground Spring Creek channel.

CHAPTER VIII

DISCUSSION AND CONCLUSIONS

From the mode of formation of the three drainage basins studied, a model for the generalised development of karst basins in this region of West Virginia can be formulated. In this chapter the pertinent features of the real basins are reviewed and the generalised model presented. In addition, comparisons of the simulations for the three basins are presented and discussed. The final parts of the chapter are concerned with the conclusions of the study.

8.1 Summary of the Basin Genesis

In spite of large differences in the basin characteristics, particularly the drainage areas, the three basins of Swago, Locust and Spring Creeks developed in a similar fashion. In each, the first stage was the surficial flow. The second was initial strike-oriented sub-surface flow, often manifested as underdraining of the valleys, and the third the major piracy into or out of the basins. A fourth stage of development (and in the Locust Creek basin a fifth stage) can be identified, which consists of recent and usually minor modifications to the flow patterns.

8.1.1 Development of the Swago Creek Basin

The Swago basin is the most rugged and youthful of the three basins being studied (Table 8.1). The hydrological development is not as far advanced as in Locust and Spring Creeks. The final stage of recent development that has been identified in the other basins is not complete in the Swago basin, and will be completed in the future as the basin matures.

In the Swago basin the second stage of development consists of the sinking of the Dry Creek stream to resurge at the Overholts Spring, and the sinking of Big Run to resurge at Tub Cave. Both of these diversions are developed along the approximate strike directions and consist of piracy from one sub-basin to another. The third stage of development was various minor piracies, shortening of the flow routes, and opening up of a number of recent vadose streamways. Because the karst is not mature, flooding of the sinks and high water diversions are common in the Swago basin. A fourth stage, of future development, has been suggested when the immature flow routes will be enlarged and the "lost waterfalls" eliminated.

The Taggard formation has played a major role in the development of the basin. Many of the caves, such as the upper part of Overholts, Carpenters and Tub Caves are formed above the Taggard, and a number of flow routes are controlled by this shale. The whole karst development of the basins has been significantly modified by this shale.

Table 8.1Characteristics of the Basin Development

	<u>Swago</u>	<u>Locust</u>	<u>Spring</u>
Basin Area During Stage 1 (sq. mi.)	12.0	5.65	115
Basin Area at Present (sq. mi.)	10.1	37.4	129
Basin Relief (feet)	2550	2455	2663
Basin Ruggedness (relief/max. diam., %)	12	6.5	3.8
Total Length of Major Channels (miles)	5.5	16	35
Length of Major Sub-surface Channel (straight line distance, miles)	2.2	1.4	4.5
Number of Major Stages of Development to the Present	3	5	4
Stage of the First Major Piracy	2	3	3
Present Generalized Stage of Development at Present (described in Section 8.2)	C	between C and D	D

8.1.2 Development of the Locust Creek Basin

The Locust Creek basin is the intermediate basin in position, ruggedness and area (Table 8.1). The basin has developed into its maximum relief, and also has the largest proportion of its flow on the overlying Mauch Chunk rocks. It has the best preserved and most complex history of development in the sample.

The basin's second stage of development was the underdraining of the Snedegars-Friars Hole valley where major caves were formed. Poor Farm Cave was also developed during Stage 2 by Millstone Creek. The third stage consisted of major piracy of the Hills and Bruffey Creeks, which were captured to the Locust Creek basin. Along with the capture of Millstone Creek, the Hills and Bruffey capture increased the drainage area of Locust Creek more than five times (Table 8.1). Later development, identified as Stages 4 and 5, functioned to shorten the flow routes. In the Locust Creek basin the Taggard shale has had a significant effect on the basin development and many of the caves and flow routes are controlled by it.

8.1.3 Development of the Spring Creek Basin

This is the largest and most southerly basin. It has passed the point of maximum relief (Wolfe, 1973), because the hills are now eroding faster than the valleys. In spite of this, the basin has a higher relief than either of the other basins (Table 8.1), but a low ruggedness. The

basin has developed the most mature karst, with little or no high water diversion occurring as in the other basins.

Spring Creek now has four major sub-basins draining to it, all of comparable size. These are: an underdrained surficial flow sub-basin; Culverson Creek, which is a major sinking stream; a karst sinkhole plain which has no integrated surficial drainage network; and the lower part of Spring Creek.

Initial development of the basin was the underdraining of the Great Banana and Hills-Bruffey valleys, which occurred during Stage 2. The major development occurred during Stage 3 when the Culverson Creek drainage was captured to Spring Creek and the Hills and Bruffey drainages were lost to Locust Creek. Later development consisted of enlargement or shortening of the flow routes and formation of small vadose caves, by lesser tributary streams.

8.2 Generalized Development of the Karst Basins

In the three basins being studied, four major stages of development can be identified. The stages are: A) the surficial flow conditions, B) strike-oriented drainage and underdraining of the valleys, C) major piracy, and D) enlargement and shortening of the flow routes.

In the descriptions of the genesis of the Locust and Spring Creek basins in Chapters 6 and 7, Stages A, B, C and D above correspond to Stages 1, 2, 3 and 4 respectively of the individual basins. In Locust, a further stage (Stage 5) was identified, which also corresponds to Stage D

above. The development in the Swago basin was slightly different. Stages 1 and 4 do correspond to Stages A and D respectively, but Stage 2 in the Swago basin must be split up between Stages B and C, and Stage 3 is split between Stages C and D above.

In all basins the original basin area is of different size and shape to the present basin. The major change in the drainage to the streams occurred between Stages B and C when the major piracy of the streams took place, and this must be considered to be the most significant period of development.

8.2.1 Stage A: Surficial Flow

The first stage in the development of the basins was the entirely surficial flow. Drainage was controlled in the Spring and Locust areas by the geology. The dip of the beds is northwesterly, and many of the streams, including the Greenbrier River, are oriented along the strike in a northeasterly to southwesterly direction. The Swago basin, however, initially had a nearly centripetal drainage.

8.2.2 Stage B: Strike Oriented Drainage and Underdraining of the Valleys

During this stage, which can be identified in all of the basins, strike oriented drainage took place. In addition, the major valleys were underdrained. The orientation of the valleys and flow routes can be seen

in Table 8.2. It can be seen from this table that during Stage B the first five routes listed were strike oriented, while the last four listed underdrained the valleys. As the Great Banana and Friars Hole valleys are strike oriented, these routes are both underdrained and strike oriented.

The development of the conduits beneath the valleys was initiated when the limestone became exposed due to erosion of the overlying clastic rocks. Because the limestone would become exposed progressively upstream as the clastics were eroded, it is probable that the conduits underdraining the valleys developed from a number of sink points. These sink points would gradually move up the valley as the basin matured. Evidence for a progression of sink points is not widespread, mainly because Stage B was relatively early and any inactive sink points have collapsed or been filled in by sediments, or the cave has been eroded away. The progressive sink points are more easily identified in the caves and can be seen in the following areas:

- a) The Friars Hole - Snedegars system, where the sink point has moved from the Friars Hole Cave to the old Snedegars entrance up to the present Snedegars stream entrance.
- b) The Overholts Cave. The sink point has moved from the Alcoa Avenue area to the present end of the cave.
- c) The Great Banana valley. The sink point appears to have moved up from Ashbury to Jarretts Water to McFerrin Cave.

Table 8.2

Orientation of Drainage Routes During Stages B to D

<u>Route</u>	<u>Orientation of the Surficial Valley Near the Sink (to North)</u>	<u>Orientation of the Flow Route (to North)</u>	<u>Re-orientation Affected by Underground Drainage</u>	<u>Strike Controll- ed Drainage</u>	<u>Under- draining of the Valleys</u>
<u>Stage B</u>					
Dry Creek to Overholts	160	190	30W	•	
Big Run to Carpenters	160	230	70W	•	
Carpenters to Tub	130	240	110W	•	
Friars Hole and Soedegars	230	230	0	•	•
Great Banana	210	210	0	•	•
Spring Creek	180*	180	0		•
Millstone Creek to Poor Farm	120**	120	0		•
<u>Stages C and D</u>					
Dry Creek to Sharps Run	180	100	80E		
Carpenters to Barnes Pit	130	180	50W		
Barnes Pit to Cave Creek	120	140	20W		
Bock Run to Price Run	180	80	100E		
McClintocks Run	90	90	0		•
Hills Creek to Hughes	200	70	130E		
Beards Blue to Locust	110	210	100W		
Lower Hughes to Locust	60	180	120W		
Glyde Cochrane to Locust	220	70	150E		
Roaring to Culverson	170	170	0		•
Culverson to Spring Creek	300***	60	120W		
Buckeye Creek	60	20	40E		
Coffmans to Spring Creek	180	20	120E		
The Hole (Boggs Entrance) to Spring Creek	320	350	30W		

*Mean orientation of lower part of Spring Creek.

**Assumed.

***Original flow direction of Culverson out of cave mouth.

Note: regional strike direction is about 220° to the north.

8.2.3 Stage C: Major Piracies and Diversions

This is the most important stage in the basin genesis as the drainage area changed considerably in the period from Stage B to Stage C. The following major piracies took place in the three basins:

- a) Dry Creek to Sharps Run,
- b) Big Run via Carpenters Cave to Cave Creek Cave,
- c) Hills and Bruffey Creeks to Upper Hughes,
- d) Great Banana to Culverson Creek, and
- e) Millstone Creek to Locust.

In addition to altering the basin drainages the piracies usually affected the resurgence and lower stream valleys. Thus the Locust Spring now discharges considerably more than previously, and Locust Creek is therefore an overfit stream in a relatively small stream valley. Conversely the stream valleys below the diversions are now either dry or carry underfit streams. Milligan Creek, for example, drains the Great Banana valley and is a small stream in a major valley.

The orientation of the flow routes and of the corresponding valleys near the sink points can be seen in Table 8.2. It can be seen that very few of the flow routes are controlled either by the valley direction or by the regional strike. The major control on the flow route direction appears to be the direction of the highest hydraulic gradient. This is discussed in more detail in Section 8.3.

8.2.4 Stage D: Opening Up and Development of the Flow Routes

During Stage C a number of new routes were opened up which pirated the water from one basin or sub-basin to another. However during floods the new routes were not mature enough to carry all the water and the excess followed the old routes of Stage B. During Stage D the new routes opened up sufficiently to take all possible floods and the original route dropped from a dormant state to one of total inactivity. In addition the routes generated during Stage C became shortened and simplified as development took place up to Stage D.

Other changes that occurred in Stage D were the development of small vadose streamways, which drained small streams underground. These small caves are almost certainly not unique to Stage D, but most that formed during earlier stages were either enlarged to form major flow routes or have been eroded away, filled in or have collapsed, and so are not now evident.

In all of the basins the karst is in a state of flux, with changes still occurring to the drainage pattern. None of them can be considered now to be wholly in Stage D. In the Swago Creek basin in particular the present situation is only a short way beyond Stage C; considerable development will occur in the future. At Locust some development has to occur to bring the basin to Stage D, but at Spring the development appears to be nearly complete at Stage D.

8.3 Major Controlling Factors in the Development of the Basins

On a casual inspection of the flow routes they appear to be formed in a willy-nilly fashion. On closer inspection, however, the factors which control the formation of the flow routes can be discerned. The major factors are: A) the Taggard shale, B) strike direction, and C) hydraulic gradient.

8.3.1 The Taggard Shale

The Taggard formation consists of two shales separated by a thin limestone band (Price and Heck, 1938), located in the middle of the Greenbrier limestone. In the northern part of the basin the shale is very impervious and has had a major influence on the flow of water through the Greenbrier limestone. In the Spring Creek basin, however, the shale is thinner and less disruptive to the hydrology. In the Swago and Locust basins, the shale caused a number of "lost waterfalls" (White and Schmidt, 1966) to be formed where the water flowing through the upper part of the Greenbrier limestone resurges over the impervious shale, flows across the shale and sinks on reaching the underlying limestone (Figure 8.1). This occurs, or has occurred, at:

- a) Hause Waterfall,
- b) Barnes Pit,
- c) Tub Cave, and
- d) Hughes Creek Caves,

and at a number of seeps and smaller streams, particularly in the Swago

Creek basin.

The Taggard has played a major role in the development of the caves in the Locust and Swago basins. In general the underground water flowed down through the top part of the limestone but was then unable, initially, to penetrate the Taggard. The water became perched by the shale, flowed out at resurgences near the top of the shale, and developed long galleries in the base of the Pickaway limestone (Figure 8.1). The following caves were developed by water perched above the shale:

- a) Pittsburg Turnpike in Overholts,
- b) Tub,
- c) Upper Hughes Creek,
- d) Carpenters, and
- e) Friars Hole.

The water, after flowing across the surface over the shale, sank in the top of the Patton limestone (Figure 8.1) and developed caves. These caves are usually of vadose form, and descend steeply through the Patton limestone. Caves that are active now include:

- a) Barnes Pit,
- b) Lower Hughes Creek,
- c) Beards Blue Hole.

In addition some fossilized old caves were probably formed by water flowing over the Taggard. One such cave is:

- d) Overholts Saltpeter.

Many of the flow routes have also been controlled by the shale. The Taggard often disrupts the route of the underground drainage, forcing

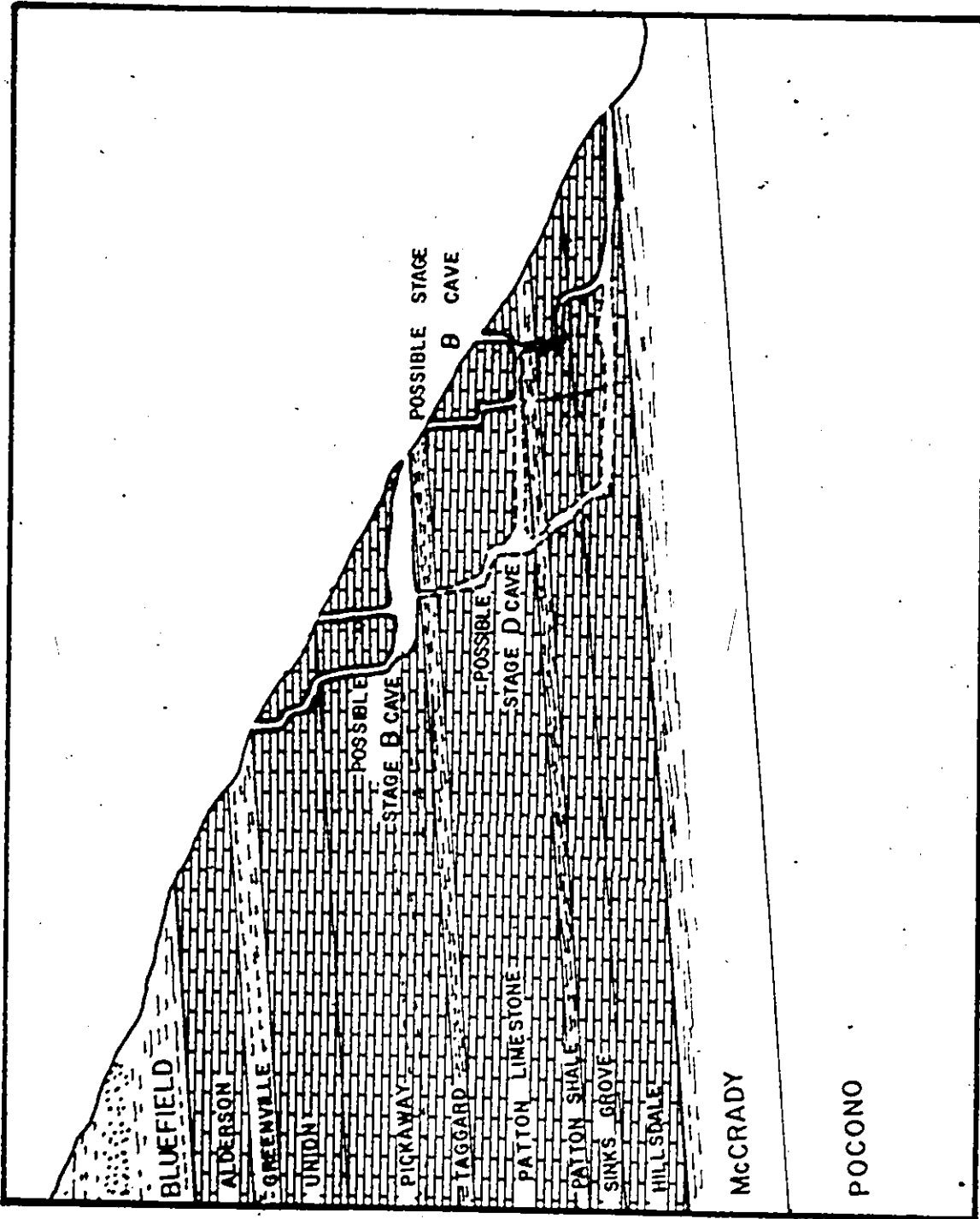


Figure 8.1 The caves developed above and below the Taggard shale.

the water to flow along paths that are considerably longer and so less efficient than the direct sink to rising route. Such disrupted routes include:

- a) Big Run to Carpenters,
- b) Initial Dry Creek to Overholts,
- c) Barnes Pit to Cave Creek,
- d) Hills and Bruffey to Upper Hughes,
- e) Beards Blue Hole to Locust, and
- f) Marthas to Locust.

There are a number of other shales in the limestone. The upper shale is the Greenville, with the Alderson limestone overlying it. The Greenville shale is thick and very impervious, and no significant flow routes or caves breach it. In the Swago and Locust areas, the Alderson is thin and does not disrupt the surface stream significantly. However in the Trout area of the Spring Creek basin a number of flow paths have developed through the Alderson (Section 7.1).

The Pickaway limestone, which lies on top of the Taggard shale, also contains a number of shale bands. These shale bands have controlled the development of Snedegars and Carpenters Caves, as explained in Sections 6.2.4 and 5.2.4.

The Patton shale which lies between the Patton and Sinks Grove limestones is thin and usually easily breached without significantly affecting the caves or flow routes. However in the Locust Creek basin the shale has influenced the Marthas Caves. Upper Marthas is a perched cave above the shale while the entrance series of Lower Marthas is immediately below the shale band.

8.3.2 Strike Direction

During the early development of the basins, the strike direction played an important part in controlling the direction of the flow paths. The strike controlled routes are listed in Table 8.2, and it can be seen that five of the seven routes developed during Stage B are strike controlled. Wolfe (1973) found similar strike control in the Trout Run basin, which is 22 miles to the north-east of the Swago Creek basin.

The reason for the strike control is tied up with the predominant drainage and dip directions. These are in opposite directions with the drainage trend (to the south-east) running up dip. Cave or conduit initiation along the drainage trend, where the water would have to flow across the limestone bedding, is therefore difficult, as most conduit initiation has been observed to occur along the bedding planes (Ford, 1965; White, 1960; Sweeting, 1973). Due to the opposing dip and hill slope directions the only bedding plane route that has a hydraulic gradient is the strike direction and this was the route of the first major underground drainage.

The strike control is only important during the early development of the basins. After caves had been initiated other controls became more important in the cave directions, as can be seen from Table 8.2.

8.3.3 Hydraulic Gradients

During the later development of the basins, the main control of the flow route direction is the hydraulic gradient. The routes developed

along the path that offered the greatest gradient from the sink point to the resurgence, often, however, being influenced as well by the Taggard shale. This control can be observed in all three basins. Table 8.3 shows the hydraulic gradients of the possible routes from various sinkholes, with the active route being shown.

It can be seen from Table 8.3 that the first five routes shown (developed during Stage B) do not flow along the route with the highest hydraulic gradient. The early routes are not, therefore, controlled by the highest hydraulic gradient. However all routes, except one, developed during Stages C and D do flow along the highest hydraulic gradient route (Table 8.3). The exception is the Dynamite Pit route which flows to Laudermilks resurgence on a gradient of 300 feet/mile, while to Sharps Run the gradient is 320 feet/mile. As stated in Section 5.3.3, other factors must have controlled this route. In addition, the contact caves of McClungs and Luddingtons do not fit this pattern as shown in Table 7.1. These caves, however, are controlled by the underlying McCrady shale, as explained in Section 7.2.3, and not by the highest hydraulic gradient.

With the exception of these above routes, the conduits developed during Stages C and D appear to be controlled by the highest straight line hydraulic gradient between the sink and any possible resurgences.

Table 8.3

Hydraulic Straight-Line Gradients of the Routes in the Swago, Locust and Spring Creek Basins, from Various Sinks to Nearby Resurgences

<u>Sink</u>	<u>Actual Resurgence</u>	<u>Hydraulic Gradient</u> (ft./mi.)	<u>Other Nearby Resurgences</u>	<u>Hydraulic Gradient</u> (ft./mi.)
<u>Stage B Routes</u>				
Dry Creek (near Hause)	Overholts	140	Laudermilks Sharps	180 70
Big Run	Carpenters	63	Hause No. 1 Overholts	500 240
Carpenters	Tub	50	Cave Creek Overholts	330 ^a 310 ^a
Snedegars	Spring Creek (near Friars Hole)	64	Locust	80 ^a
Culverson	'Great Banana' on Muddy Creek	30	Spring	39 ^a
Upper Spring	Spring	25	Greenbrier River (near Renick)	40
Millstone Creek (assumed sink)	Poor Farm	145	Locust McNeels	240 ^a 150
<u>Stage C Routes</u>				
Bruffey	Upper Hughes	200*	Top of Taggard above Locust Snedegars	80* 80*
Dry Creek	Sharps Run	320	Overholts Ent- rance Top end of Overholts	230 125
Hills Creek	Locust Creek	300	Spring Creek (near Friars Hole valley)	60

(cont'd...)

Table 8.3 (cont'd)

<u>Sink</u>	<u>Actual Resurgence</u>	<u>Hydraulic Gradient</u> (ft./mi.)	<u>Other Nearby Resurgences</u>	<u>Hydraulic Gradient</u> (ft./mi.)
<u>Stage C Routes (cont'd)</u>				
The Hole	Spring Creek	200	Fort Spring	30
Culverson Creek	Spring Creek	39	Fort Spring Mill Creek	22 26
Beards Blue	Locust Creek	125	McNeels Mill Run	105
Clyde Cochrane	Locust Creek	170	Spring Creek (near Friars Hole valley)	40
Buck Run Sink	Price Run	400	Overholts Lower Buck Run	350 300
<u>Stage D Routes</u>				
Lower Hughes	Locust Creek	180	McNeels Mill Run	60
Coffmans	Spring Creek	71	Fort Spring Mill Creek	35 39
Dynamite Pit	Laudermilks	300	Overholts Ent- rance Sharps Run	280 320

^a These assumed routes would have to penetrate the Taggard.

* These routes are also controlled by the Taggard shale.

8.4 Simulation Results

The Swago, Locust, Spring and Wildcat basins were simulated for 710, 647, 413 and 89 days respectively up to August 31, 1971. During data preparation and optimization the values for the 29 parameters in each segment were assigned. The parameters can be split up into four types: A) insensitive or constant, B) measured, C) estimated and D) optimized parameters. The insensitive and constant parameters have been listed in Table 8.4 and although found to be constant in this study may take different values in other situations. The measured, estimated and optimized parameters have been listed in the appropriate chapters in Tables 5.2, 6.2 and 7.2, and the estimated and optimized parameters that varied between segments are compared in Table 8.5.

The objective functions were determined for selected periods for all four basins. These functions are listed in Table 8.6. In addition the objective functions and the water balances (corrected for the annual rate) for the four basins are compared in Table 8.7 for the total period of record.

In this section the simulated results for the three major basins will be compared and reasons for any differences between the real and modelled streamflows given. The geomorphic significance of the model parameters will also be discussed.

Table 8.4

Parameter Values Used in the Model which were Constant
for all Segments in all the Basins

<u>Parameter</u>	<u>Description</u>	<u>Value</u>	<u>Units</u>
SLA	Proportion of impervious area in segment	0.1	--
SAWT	Proportion of lakes, channels and open water in segment	0.01	--
AFT	Proportion of segment where interception does not occur	0.1	--
GWEA	Ground water evaporation coefficient	0.0	--
GM	Snow ground melt	0.02	inches/day
TCOFF	Temperature index for snow melt	0.08	inches/day/°F
ASTINT	Initial interception storage	0.02	inches
UZSINT	Initial upper zone storage	0.1	inches
LZSINT	Initial lower zone storage	0.2	inches
WEINT	Initial snow pack storage	0.0	inches
SOILE	Soil evaporation coefficient	0.8	--
EVAPC	Evaporation constant	1.5	--
ASM	Interception storage	0.5	inches
TIMET	Time delay histogram	0.5/0.5	--
INFMN	Minimum infiltration rate	0.3	inches/day
INFRT	Infiltration coefficient	0.1	--

Liab rasu

Table 8.5

Comparison of the Sensitive Parameter Values at the Four Basins

(See Table 4.1 for a description of the parameters and their units.)

	<u>Swago</u>	<u>Locust, Segment</u>			<u>Spring, Segment</u>		<u>Wildcat</u>
		(1)	(2)	(3)	(1)	(2)	
LPSRT	-5	-5	0	0	-5	-5	0
GWERT	200	500	500	100	200	100	200
BZK	0.2	0.1	0.1	0.2	0.2	0.3	0.2
GWSINT	5.0	1.0	1.0	1.0	1.0	1.0	1.0
IADD	-	0	1	-	1	-	-
INFMX	2	2	1	4	2	4	4
UBCOF	.5	.1	.1	.1	.1	.1	.1
BGCOF	.2	.1	.1	.1	.1	.1	.1
LZSN	2	4	4	2	4	2	4
UZSN	1.1	5	5	3	5	1	5
% of Exposed Limestone in Segment	42	8	15	61	11	80	21

8.4.1 The Objective Functions for the Basins

The objective functions for selected periods (usually 3 monthly) are compared in Table 8.6 for the four basins. The Wildcat figures are listed in Table 8.6, but as the record length is so short and did not include a snowmelt period, they were not used for detailed comparisons with the other basin figures.

The objective functions for different periods allow an objective comparison to be made of the simulation results from the basins. Four objective functions were calculated and each value is sensitive to different errors in the simulated and real responses.

When any of the objective functions are small the modelled and real streamflows match closely and the simulation is "good". The significance of each of the objective functions and their values at the three basins are described below.

8.4.1.1 Peak Objective Function

The peak objective function gives a measure of the mean ratio between the real and simulated flow (with the higher value being the numerator). The relationship between the peak objective function and the ratio between the flows is shown in Figure 8.2. For example a peak objective function of 50 indicates (from Figure 8.2) that the ratio of the real and simulated flows averages 1.65, or that the simulated flows are an average of +65% in error.

Table 8.6

Comparison of the Objective Functions for Selected Periods in the Four Basins

	<u>Swago</u>	<u>Locust</u>	<u>Spring</u>	<u>Wildcat</u>
<u>Peak Objective Function</u>				
Sept. 10 - Dec. 31, 1969	52.4			
Nov. 22 - Dec. 31, 1969		128.1		
Jan. 1 - March 31, 1970	55.1	74.7		
April 1 - June 11, 1970	48.9	50.3		
July 14 - Oct. 31, 1970	67.8	69.5	88.8	
Nov. 1 - Dec. 31, 1970	38.5	49.1	97.8	
Jan. 1 - March 31, 1971	67.2	50.7	63.6	
April 1 - May 31, 1971	62.1	66.6	82.6	
June 1 - Aug. 31, 1971	72.7	67.1	166	
June 3 - Aug. 31, 1971				48.1
Average for the Total Period	58.1	69.5	99.6	48.1
Mean Ratio Between the Daily Flows (using Figure 8.2)	1.80	2.01	2.73	1.65
<u>Mean Objective Function</u>				
Sept. 10 - Dec. 31, 1969	8.9			
Nov. 22 - Dec. 31, 1969		232		
Jan. 1 - March 31, 1970	3.5	-19.3		
April 1 - June 11, 1970	-24.2	-48.1		
July 14 - Oct. 31, 1970	84.2	7.3	110.7	
Nov. 1 - Dec. 31, 1970	13.3	-24.7	88.2	
Jan. 1 - March 31, 1971	-23.4	-17.9	21.5	
April 1 - May 31, 1971	-50.7	-43.2	-40.1	
June 1 - Aug. 31, 1971	110.7	22.9	173.2	
June 3 - Aug. 31, 1971				4.6
For the Total Period	2.0	-18.1	10.1	4.6

(cont'd...)

Table 8.6 (cont'd)

	<u>Swago</u>	<u>Locust</u>	<u>Spring</u>	<u>Wildcat</u>
<u>Temporal Objective Function</u>				
Sept. 10 - Dec. 31, 1969	0.8			
Nov. 27 - Dec. 31, 1969		-16.2		
Jan. 1 - March 31, 1970	-2.2	-2.3		
April 1 - June 11, 1970	-1.0	-4.5		
July 14 - Oct. 31, 1970	4.8	6.2	3.4	
Nov. 1 - Dec. 31, 1970	5.1	-3.9	-0.5	
Jan. 1 - March 31, 1971	.4	-10.1	-2.4	
April 1 - May 31, 1971	-8.2	-1.8	-2.0	
June 1 - Aug. 31, 1971	10.6	5.5	0.7	
June 3 - Aug. 31, 1971				-3.4
For the Total Period	1.3	-3.5	-0.8	-3.4
<u>Total Objective Function</u>				
Sept. 10 - Dec. 31, 1969	62.0			
Nov. 22 - Dec. 31, 1969		376.8		
Jan. 1 - March 31, 1970	60.7	95.6		
April 1 - June 11, 1970	74.1	102.6		
July 14 - Oct. 31, 1970	156.7	82.7	202.8	
Nov. 1 - Dec. 31, 1970	56.9	77.7	186.4	
Jan. 1 - March 31, 1971	91.0	78.7	87.5	
April 1 - May 31, 1971	120.9	111.7	125.3	
June 1 - Aug. 31, 1971	194.4	95.5	340.1	
June 3 - Aug. 31, 1971				56.1
For the Total Period	61.4	91.1	109.5	56.1

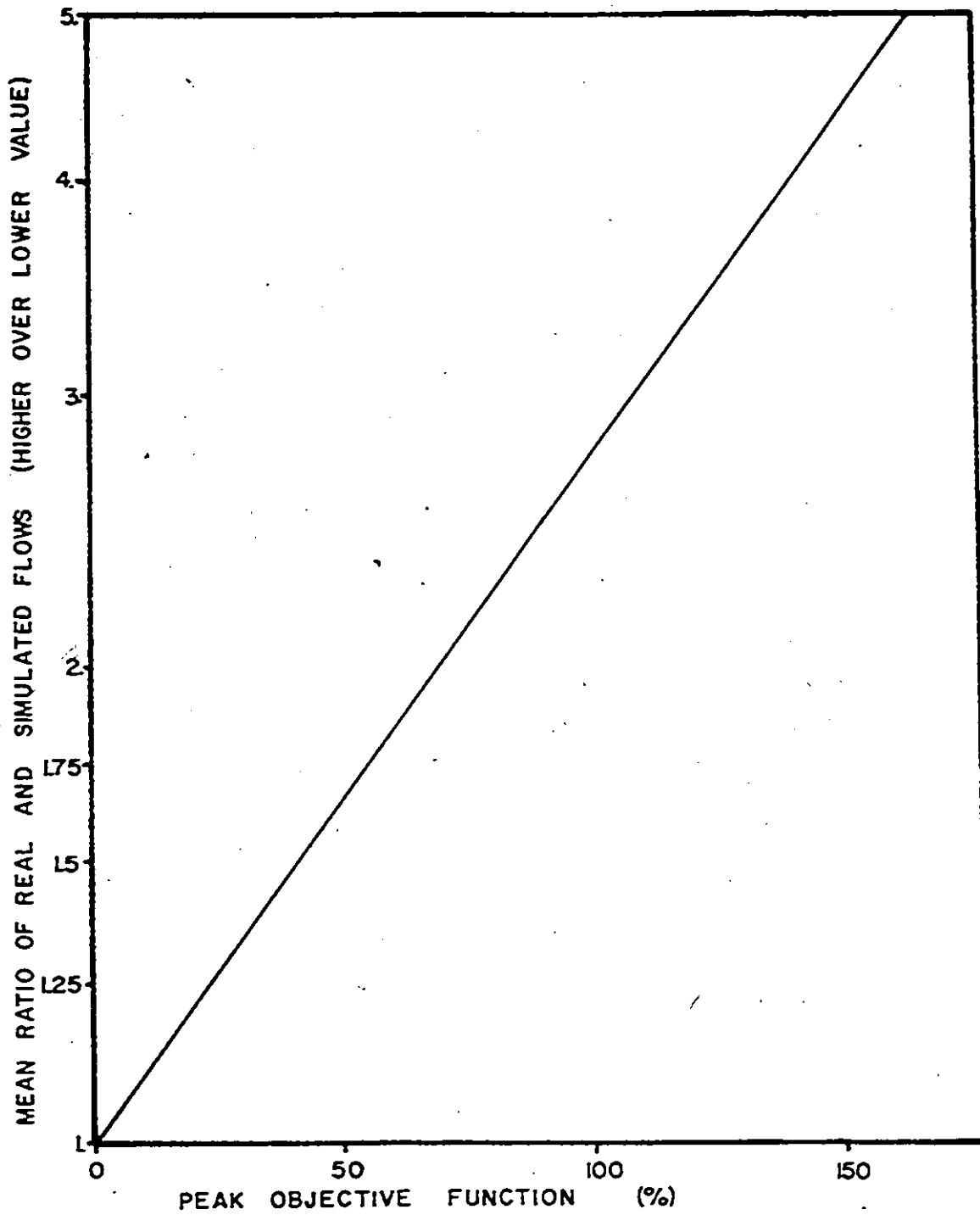


Figure 8.2 Relationship between the peak objective function and the ratio of the flows.

In the Swago basin the peak objective function (Table 8.6) is the highest during the summer months (July 14 - October 31, 1970 and June 1 - August 31, 1971) and low during the fall periods (November and December). There are three major reasons for the poor simulation during the summer: A) summer storms produced heavy localized rainfalls which may not be represented by the climatic stations; B) the summer flows at Swago were sometimes unreliable due to bottoming of the float in the recorder; and C) the model often gave too large a flow in the summer, due to poor representation of the physical processes. The significance of each of the sources of error was not determined.

At Locust Creek the major error in the peak objective function occurred in the initial period (Table 8.6). Comparing the Locust and Swago hydrographs (Appendix II) suggests that the Locust streamflow records in this period are unreliable. Otherwise it was generally found that the summer flows were simulated poorly while the fall and winter flows were modelled better, as was the case at Swago.

At Spring Creek the peak objective function was higher than at the other basins and no obvious seasonal trend could be seen. The poorer simulation at the Spring Creek basin was believed to be due to the larger distances between the climatic stations and the basin, which would cause larger errors in the climatic data.

8.4.1.2 Mean Objective Function

The mean objective function gives the percentage difference between the mean real and mean simulated flows over the stated period.

The value is positive if the simulated flow is larger than the real flow.

In all basins the simulated summer flows are too high while the winter flows were too small (Table 8.6). It was found that the model did not give good low flow simulation and in order to keep the water balance reasonable for the complete period the spring flows had to be underestimated.

At Swago the long term water balance was good (2% difference) but the mean objective function reached 100% during the summer of 1971. The Locust values were poor in the initial period, but the mean flows for the rest of the selected periods (Table 8.6) were generally simulated better than at Swago Creek, although the mean flow for the complete simulated period was 18% less than the recorded flow. Spring Creek was generally simulated less well than the other basins during the selected periods, although for the total period the simulated flow was 10% higher than the recorded.

8.4.1.3 Temporal Objective Function

The temporal objective function gives a measure of the mean temporal relationship between the peak positions. The function is positive if the simulated hydrograph leads, and negative if it lags the real hydrograph.

Generally the function indicates that the simulation lags in winter and spring and leads the real hydrograph in the summer months for all the basins. The reason for this has been mentioned in Section 5.5.1

where the simulated recession rates were found to be too fast in the winter and too slow in the summer months, which would lead to objective function values as found.

8.4.1.4 Total Objective Function

This objective function is the absolute sum of all of the other three objective functions and so gives an overall view of the simulation results.

The Swago Creek basin was simulated the most successfully for the complete period (Table 8.6) and the Spring Creek basin the least successfully as its average total objective function was the highest. The total objective functions can also be used to consider simulation during different periods in the year. Thus the simulation was found to be the best during January to March, then from November to December, then from April to June, and the least successful during July to October for all the basins in all the years when records were available.

8.4.2 The Water Balances for the Basins

The precipitation that enters a basin must leave as runoff, evapotranspiration or possibly by ground water flow, unless there is a change in storage levels in the basin. No ground water loss was modeled in the basins and the water balances for the other quantities are

Table 8.7

Summary of the Objective Functions and
Water Balances for the Four Basins

	<u>Swago</u>	<u>Locust</u>	<u>Spring</u>	<u>Wildcat</u>
No. of Days with Streamflow Records Available	679	615	401	89
<u>Average Objective Function Values</u>				
Peak	58.1	69.5	99.6	48.1
Mean	2.0	-18.1	10.1	4.6
Temporal	1.3	-3.5	-0.8	-3.4
Total	61.4	91.1	109.5	56.1
<u>Water Balances for the Period of Record (inches/year)</u>				
Precipitation	46.7	45.8	44.0	50.5
Potential Evaporation	47.4	48.5	57.3	107.7
Actual Evapotranspiration	20.3	23.4	24.2	47.1
Simulated Runoff	28.2	22.7	20.8	14.9
Change in Storages	-1.9	-0.3	-1.1	-11.5
Recorded Runoff	27.7	27.7	18.9	14.3
Overland Flow	9.4	7.1	6.6	5.7
Interflow	5.0	2.4	2.6	1.2
Baseflow	14.1	13.4	12.0	8.6
Channel Evaporation	0.3	0.3	0.4	0.6

listed in Table 8.7. The higher evaporation and lower runoff figures at Wildcat and Spring Creeks are not due to any intrinsic differences in the values, but due to the larger proportion of summer conditions in these records.

Of the precipitation entering the basins approximately one half contributes to the runoff (Table 8.7) and half is lost as evapotranspiration. No ground water loss or gain outside the basin was modelled and the change in storage levels is small (except at Wildcat, where 2.80 inches of water was removed from storage due to the usual summer recession).

The modelled runoff is composed of overland flow, interflow and baseflow, corrected for a small amount of channel evaporation. The baseflow makes the largest contribution to the runoff, while the interflow is the smallest component. In order to assess the differences that the karst areas make on the components, the percentage of each component to the total runoff was plotted against the limestone area in each segment or basin (Figure 8.3). The overland flow can be seen to be inversely proportional to the amount of limestone in the segment. The limestone has a higher infiltration capacity than the clastic soils and so should produce less overland flow. The interflow is proportional to the limestone area. This is again due to the higher infiltration capacity of the limestone which increases the water in the lower zone storage and so increases the interflow. The baseflow, however, shows no obvious trends against the area of limestone in the basin. The baseflow may be expected to be higher in limestone areas due to the higher infiltration rates, but it appears that the higher limestone infiltration increases the interflow but does not materially increase the baseflow.

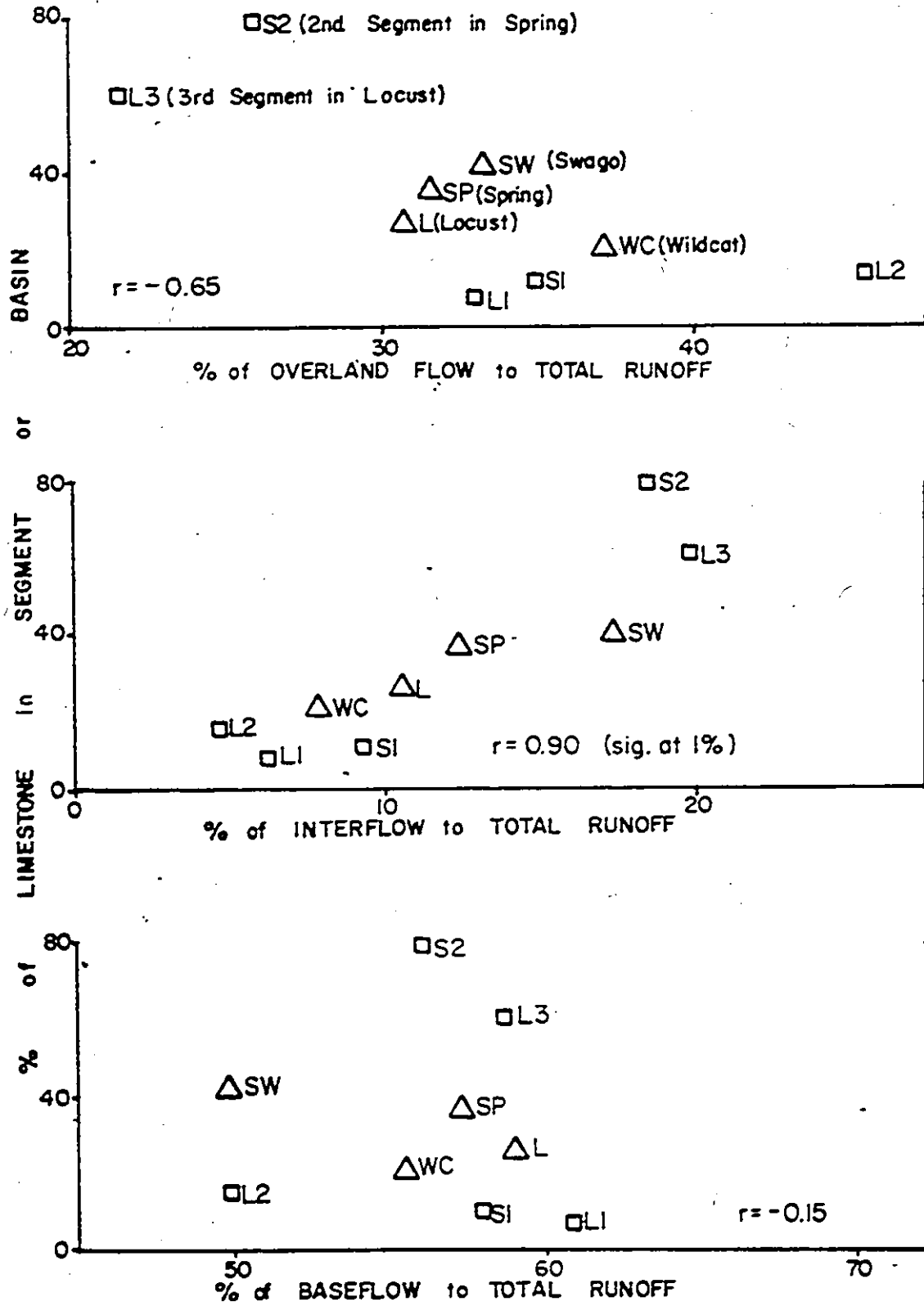


Figure 8.3 Relationship between the percentage overland flow, interflow and baseflow to the limestone area in each segment.

8.4.3 Errors in the Model Responses

The major differences between the real and simulated responses in the model can be attributed to two causes: a) the poor representation in the input data, and b) simplifications in the model.

a) The climatic data were obtained from existing stations near the basins, but the basin climate may have been very different from the climatic data that could be obtained from the stations. The variations in the precipitation figures from the stations have been discussed in Section 3.1, and similar differences between the evaporation figures were noted. In addition the winter evaporation figures, which although small are significant, were obtained from the monthly mean values (Thorntwaite, 1955) and could have considerable errors. The temperature figures are probably more reliable than the precipitation or evaporation figures, although only the mean daily temperature data were used in the snow and snowmelt calculations, which led to some errors. At times the streamflow records were also unreliable, mainly due to freezing in of the stage recorder float in winter, or bottoming of the float in summer.

b) The model contained some simplifications which did not represent the real situation very well. One simplification was to use a daily time period for the analysis, which can cause errors in the snowmelt and infiltration calculations. The snowmelt was determined by using the mean daily temperature, but melt would often occur on warm afternoons even though the mean temperature was below freezing. The snowmelt would be better modelled using hourly temperature data, or

a distribution based on the maximum and minimum daily temperatures.

The infiltration rate of a dry soil is relatively high, but as the soil becomes wet the infiltration rate decreases. If heavy rain occurs the infiltration is modelled at the rate based on the soil conditions at the start of the day, while it would be better to model the infiltration rate on the hourly or even 15 minute soil conditions. Using a short time period for the infiltration and snowmelt calculations would not prevent a longer time period being used for the slower processes, such as interflow and ground water flow.

8.4.4 Geomorphic Significance of the Parameter Values found in the Segments in the Four Basins

It was found during simulation that the parameter values could not be precisely determined due to the errors in the simulation. These errors were caused by the errors in the climatic data input and by the simplifications in the model used. As the parameters could not be precisely determined the values shown in Table 8.5 must be considered approximations. In spite of this, a number of implications can be drawn from the values of some of these parameters.

In the Locust and Spring Creek basins one of the segments selected had a large proportion of limestone exposed while the other segments were largely on the clastic hills. By comparing the lowest Spring and Locust segments, which are karstic, with the other segments, the differences between the parameters on the karst and non-karst areas can be derived.

The major differences are summarized below:

- a) The fast values for the baseflow (GWERT) and interflow (BZK) constants in the karst areas are related to the fast recession and small ground water storages in the karst aquifer. In the clastic areas the recession rates were slower due to the larger ground water storage values and lower ground water transmissivity values. At Swago, where only a single segment was modelled, the ground water recession rate was related to the slow rate in the clastic hills, while the interflow was related to the faster value in the karstic areas.
- b) The nominal lower (LZSN) and upper (UZSN) zone storage levels are related to the maximum storages in the soil. In the karst areas the soils tend to be thin and so the nominal soil storages are small. In the clastic areas thicker soils generate large soil storages in the model. In the Swago basin the soil storages are more closely allied to the karstic values due to the large proportion of exposed limestone (42%) in this segment.
- c) The infiltration rate is higher in karstic areas than in the clastic regions. The higher karst infiltration rate is due to the thinness (or absence) of soil on the limestone areas and the high permeability of the karst areas due to fissuring and solutional channels. The infiltration in the model is controlled by the maximum rate (INFMAX), the minimum rate (INFMIN) and by the infiltration factor (INFRT). It was found that the maximum rate, which is the

rate used when the soil is dry, was more sensitive to the proportionate karstic area than were the other two factors. When the soil is wet the infiltration over all segments was approximately constant.

d) The time delay histogram at all segments was found to be 0.5 and 0.5 for a 2 day delay. Thus the flow on any day consisted of one half of the previous day's flow and one half of the same day's simulated flow. This is equivalent to a channel delay of 12 hours in each segment. Although other values were tried it was found that this proportion gave the optimum temporal objective factor value and also appeared to give the "best looking" simulated hydrograph. The time delay hydrograph had an effect on the peak values in the hydrograph. As this technique is equivalent to a 2 day running mean smoothing method, the peak simulated flows are reduced in height and the peaks broadened out. This effect occurs in the real basins as the channel routing does smooth out the hydrograph. The TRMT parameter does affect the peak flows as well as the temporal relationship between the real and simulated flows.

e) The IADD parameter affects the delay with which the upstream segments are added into the lower segments. Thus an IADD of 0 indicates that the segment is added on without a delay and an IADD of 1 indicates that the upstream flow is lagged by one day before being added on to the downstream segment. This parameter models the delay of water through the stream (on the surface or subsurface) from the upstream areas to the basin outlet. It was found that a one day delay had to be given to the Bruffey Creek segment (No. 2) in the Locust basin and in the Spring Creek upstream segment (No. 1). This factor, coupled to the implied 12 hour routing in each segment, gave an effective 36 hour delay from the

precipitation to the basin outlet for the Bruffey and upper Spring Creek sub-basins. This indicates a relatively slow response (see Section 5.5.2) and suggests that the flow routes are vadose and are not phreatic, which would give a quicker response.

The Hills Creek segment (No. 1) was modelled as coming through without a time delay, except for the 12 hour implied channel routing. It was shown in Section 6.2.10, from the chemical flood pulse data, that the water takes about 15 hours to flow from Hills to Locust Creek under average flow conditions. This time delay is compatible with the implied modelled delay of 12 hours.

8.5 Conclusions

8.5.1 Basin Genesis

1. The development of the basins has taken place in four major stages:
 - a) the surficial flow, b) strike controlled drainage, c) major piracy, and d) opening up and enlargement of the flow routes.
2. The most rugged basin is in the most youthful stage of karst development. The least rugged basin is the maturest basin.
3. The oldest basin has the most extensive karst features developed in it. The karst features developed in the Spring Creek basin include uvalas, dolinas, sinkholes, caves and resurgences. Swago Creek, which is the youngest basin, has a limited variety of karst features. These include only sinkholes, caves and resurgences.

4. The initial control on the cave and conduit orientation is the strike direction. As several of the valleys in the basins are also strike controlled, the strike drainage often manifests itself as underdrain- ing of the valleys.
5. The major control on the flow routes during the third and fourth development stages is the hydraulic gradient. The flow routes are oriented along the direction of the highest hydraulic gradient.
6. The contact caves are controlled by the underlying McCrady shales. They often develop contrary to the highest hydraulic gradient direc- tion, and are predominantly dip caves, at right angles to the strike.
7. The Taggard shale has had an important effect on the development of the conduits and flow routes in the Swago and Locust Creek basins. In the Spring Creek basin however, the shale is thinner, more easily breached, and has had little effect on the conduit development.
8. The Taggard shale cannot easily be breached underground in the Swago and Locust Creek basins.
9. The final stage of basin development is the shortening of the flow routes. This is usually accomplished by the breaching of the Taggard shale underground. In the Swago Creek basin, and partly in the Locust Creek basin, this shortening of the flow routes is incomplete.
10. The presence of sink points along streambeds appears to be related to the competence of the streams. If the stream is competent to move large boulders open sinks do not occur. Sinks occur along relatively small low gradient streams.

8.5.2 Simulation

11. There were two major causes of errors in this simulation: a) the errors in the input data, and b) the simplifications in the model algorithms. In this study both types of errors are significant.
12. Snowmelt and infiltration simulations would be better carried out using hourly or maximum and minimum daily temperatures rather than the mean temperature.
13. Large differences between the precipitation figures from nearby stations were found, and the precipitation was found to increase significantly with altitude. In order to achieve good simulations in this area of West Virginia, a larger number of climatic stations would be needed, with several stations located on the hills of the basins.
14. From the model parameters, the karst segments were found to have thinner soils, higher infiltration rates, and faster baseflow and interflow recession rates, than were found on the clastic segments.
15. The modelled channel delays indicate that the major flow routes occur under vadose conditions in this region.
16. The overland flow was found to be inversely proportional to the limestone area in the segments: the interflow was found to be directly proportional to the limestone area.

BIBLIOGRAPHY

- Aley, T., 1971. The water tracers cookbook. Available from the author at Mark Twain National Forest, Springfield, Missouri. 42 pp.
- _____, 1972. Groundwater contamination from sinkhole dumps. Caves and Karst, 14(3), 17-23.
- American Paulin System, undated. Record of altimeter observations. Available from American Paulin System General Offices, 1524 Flower St., Los Angeles, California.
- Anderson, E.A. and Crawford, N.H., 1964. The synthesis of continuous snowmelt runoff hydrographs on a digital computer. Tech. Rep. 36, Dept. Civil Eng., Stanford Univ.
- Ashton, K., 1966. The analysis of flow data from karst drainage systems. Trans. Cave Research Group of Great Britain, 7(2), 161-203.
- Atkinson, T. and Drew, D.P., with C. High, 1967. Mendip karst hydrology project. Phases one and two. Wessex Cave Club Occasional Publications, 2(1), 38 pp.
- Betson, R.P., 1965. What is watershed runoff? Water Resources Research, 1, 1541-1552.
- Bicking, L., 1966. Friars Hole Cave. Nat. Speleo. Soc. News, 24(2), 24-27.
- Bogli, A., 1964. Mischungskorrosion: ein Beitrag zum Verkarstungsproblem. Erkunde, 18(2), 83-92.
- Boon, M. et al., 1966. The 1965/66 karst hydrology expedition to Jamaica. Obtainable from M.P. Livesey, 84 Crowokes Rd., Lindley, Ruddersfield, Yorks., England. 63 pp.
- Burwell, E.B., Jr., and Moneymaker, B.C., 1950. Geology in dam construction. In: S. Paige, Application of Geology to Engineering Practice, Geol. Soc. America, Berkeley Volume, 11-43.
- Carter, R.W. and Anderson, I.E., 1963. Accuracy of current meter measurements. J. Hydraulics Div., Amer. Soc. Civil Eng., 24(HY4), 105-115.

- Church, M. and Kellerhals, R., 1970. Stream gauging techniques for remote areas using portable equipment. Tech. Bull. 25, Inland Waters Div., Dept. of the Environment, Ottawa, 90 pp.
- Claborn, B.J. and Moore, W.L., 1970. Numerical simulation of watershed hydrology. Lab. Tech. Rep. HYD 14 - 7001, Hydraulic Eng. Dept., Univ. Texas, 225 pp.
- Clark, G.M., 1968. Sorted patterned ground: new Appalachian localities south of the glacial border. Science, 161, 355-356.
- Coward, J., 1971. Hills Bruffey Cave, West Virginia. The Canadian Caver, No. 4, p. 40.
- Coward, J., 1972. Clyde Cochrane Sinks, Pocahontas County, West Virginia. The Canadian Caver, 4(1), 57-59.
- Craig, A.J., 1969. Vegetational history of the Shenandoah Valley, Virginia. Geol. Soc. America Special Paper 123, 283-297.
- Crawford, N.H. and R.K. Linsley, 1966. Digital simulation in hydrology, Stanford Watershed Model IV. Tech. Rep. 39, Dept. Civil Eng., Stanford Univ., 210 pp.
- Darlington, H.C., 1943. Vegetation and substrate of Cranberry Glades, West Virginia. Bot. Gazette, 104(3).
- Davar, K.S., 1970. Peak Flow - Snowmelt. In: D.M. Gray, Principles of Hydrology. The Secretariat, Canadian National Committee for the International Hydrological Decade, Ottawa, 25 pp.
- Davies, W.E., 1958 (with supplement, 1965). Cavern of West Virginia. W. Virginia Geol. and Econ. Survey Rep., 19, 400 pp.
- Davis, S.N., 1966. Initiation of ground water flow in jointed limestone. Bull. Nat. Speleo. Soc., 28(3).
- Dawdy, D.R. and O'Donnell, T., 1965. Mathematical models of catchment behaviour. J. Hydraulics Div., Amer. Soc. Civil Eng., 91(HY4), 123-137.
- Donley, D.E. and Mitchell, R.L., 1939. The relation of rainfall to elevation in the Southern Appalachian Region. Trans. Amer. Geophys. Union, 20, 711-721.
- Drew, D.P. and Smith, D.I., 1969. Techniques for the tracing of subterranean drainage. Tech. Bull. No. 2, British Geomorphological Research Group, 36 pp.

- Drooker, P.B., 1968. Application of the Stanford Watershed Model to a small New England watershed. Unpublished Masters Thesis, Dept. Soil and Water Science, Univ. of New Hampshire, Durham.
- Drummond, I., 1969. Barnes Pit. The Canadian Caver, No. 1, 23-25.
- Duckstein, L., M.M. Fogel, and C.C. Kisiel, 1972. A stochastic model of runoff-producing rainfall for summer type storms. Water Resources Research, 8(2), 410-421.
- Elder, J.W., 1959. The dispersion of marked fluid in turbulent shear flow. J. Fluid Mechanics, 5, 233-257.
- England, C.B. and Coates, J.J., 1971. Component testing within a comprehensive watershed model. Water Resources Bull., 7(3), 421-427.
- Ford, D.C., 1973. Development of the canyons of the South Nahanni River, N.W.T. J. Earth Sciences, 10(3), 366-378.
- Francis, J.R.D., 1962 (2nd ed.). A Textbook of Fluid Mechanics for Engineering Students. Edward, London, 340 pp.
- Glover, R.E., 1964. Dispersion of dissolved and suspended materials in flowing streams. U.S. Geol. Survey, Prof. Paper 433-B.
- Gregory, S., 1963. Statistical Methods and the Geographer. Longmans Green, London, 229 pp.
- Goodchild, M.F., 1970. The generation of small-scale relief features of eroded limestone: a study of erosional scallops. Unpublished Ph.D. dissertation, Dept. of Geography, McMaster Univ.
- Haas, J.L., 1959. Evaluation of ground water tracing methods used in speleology. Bull. Nat. Speleo. Soc., 21(2), 67-76.
- Hamon, W.R., 1971. Reynolds Creek, Idaho. Agricultural Research Service Precipitation Facilities and Related Studies, U.S. Dept. of Agr. ARS 41 - 176, 117 pp.
- Hanna, F.K., 1966. A technique for measuring erosion in cave passages. Proc. Univ. of Bristol Speleo. Soc., 11(1).
- Hantush, M.S. and Jacob, C.E., 1955. Non steady radial flow in an infinite baby aquifer. Trans. Amer. Geophys. Union, 36(1), 95-100.

- Henderson, F.M. and Wooding, R.A., 1964. Overland flow from a steady rainfall of finite duration. J. Geophys. Research, 69(8), 1531-1540.
- High, C. and Hanna, F.K., 1970. A method for the direct measurement of erosion on rock surfaces. Tech. Bull. 5, British Geomorph. Research Group, 24 pp.
- Hooke, R. and Jeeves, T.A., 1961. Direct search solution of numerical and statistical problems. J. Assoc. for Computing Machines, 8(2), 212-229.
- Horton, R.E., 1956. Erosional development of streams and their drainage basins. A hydrophysical approach to quantitative morphology. Bull. Geol. Soc. Amer., 56, 275-370.
- Howarth, J.H., et al., 1900. The underground waters of Northwest Yorkshire, Part I. The sources of the River Aire. Proc. Yorks. Geol. and Polytech. Soc., 14(1), 1-48.
- Rudlow, M.D. and Clark, R.A., 1969. Hydrograph synthesis by digital computer. J. Hydraulics Div., Proc. Amer. Soc. Civil Eng., 95(HY3), 839-860.
- Hull, D.E., 1962. Dispersion and persistence of tracer in river flow measurements. Internat. J. Applied Radiation and Isotopes, 13, 63-74.
- James, I.D., 1966. Use of the digital computer to analyze hydrologic problems. Fifth Annual Sanitary and Water Resources Engineering Conference, Vanderbilt Univ.
- _____, 1970. An evaluation of relationships between streamflow patterns and watershed characteristics through use of OPSET: a self-calibrating version of the Stanford Watershed Model. Research Rep. No. 36, Univ. of Kentucky Water Resources Institute, Lexington.
- _____, 1972. Hydrologic modelling, parameter estimation and watershed characteristics. J. Hydrology, 17(4), 283-306.
- James, W., 1972. Developing simulation models. Water Resources Research, 8(6), 1591-1592.

- Jones, W.K., 1973. Hydrology of limestone karst in Greenbrier County, West Virginia. W. Virginia Geol. and Econ. Survey, Bull. No. 36, 49 pp.
- Leopold, L.B., M.G. Wolman and J.P. Miller, 1964. Fluvial Processes in Geomorphology. W.H. Freeman, San Francisco, 522 pp.
- Lichty, R.W., D.R. Dawdy and J.M. Bergman, 1968. Rainfall-runoff model for small basin flood hydrograph simulation. Extract of Publication No. 81, Symposium of Tucson, Internat. Assoc. of Scientific Hydrology, 356-367.
- Linsley, R.K., Jr., M.A. Kohler and J.L.H. Paulhus, 1949. Applied Hydrology. McGraw-Hill, New York, 689 pp.
- Louch, W., 1971. Cutlip Cave, West Virginia. The Canadian Caver, No. 4, 37-39.
- MacGregor, K., 1969. Hause Waterfall Cave. The Canadian Caver, No. 1, 19-21.
- Malott, C.A., 1939. Karst valleys. Bull. Geol. Soc. Amer., 50, p. 1984.
- Mandeville, A.N., et al., 1970. River flow forecasting through conceptual models. Part III - The Ray catchment at Grendon Underwood. J. Hydrology, 11, 109-128.
- McCue, J.B., et al., 1939. Limestones of West Virginia. W. Virginia Geol. Survey Rep., 12, 560 pp.
- Meinzer, O.E., 1927. Large springs in the United States. U.S. Geol. Survey, Water-Supply Paper 557, 94 pp.
- Meinzer, O.E., 1949. Hydrology. Dover Publications, New York, 712 pp.
- Miller, C.F., 1968. Evaluation of runoff coefficients from small natural drainage areas. Research Rep. No. 14, Univ. of Kentucky Water Resources Institute, Lexington.
- Miller, D.H., 1965. The heat and water budget of the earth's surface. Adv. in Geophysics, 11, 175-302.
- Moitke, F.D. and Palmer, A.N., 1972. Genetic relationship between caves and landforms in the Mammoth Cave National Park area. A preliminary report, 69 pp. Available from A.N. Palmer, Dept. Earth Science, State Univ. College, Oneonta, New York 13820, U.S.A.

- Nash, J.E. and Sutcliffe, J.V., 1970. River flow forecasting through conceptual models. Part I - A discussion of principles. J. Hydrology, 10, 282-290.
- O'Connell, P.E., et al., 1970. River flow forecasting through conceptual models. Part II - The Brosna catchment at Ferbane. J. Hydrology, 10, 317-329.
- Palmer, A.N., 1969. A hydrologic study of the Indiana karst. Unpublished Ph.D. dissertation, Dept. of Hydrology, Indiana Univ., 181 pp.
- Philip, J.R., 1954. An infiltration equation with physical significance. Soil Science, 77(2), 153-157.
- Porter, J.W. and McMahon, T.A., 1971. A model for the simulation of streamflow data from climatic records. J. Hydrology, 13, 297-324.
- Price, P.H., 1929. Pocahontas County. W. Virginia Geol. Survey Rep., 531 pp.
- Price, P.H. and Heck, E.T., 1939. Greenbrier County. W. Virginia Geol. Survey Rep., 846 pp.
- Pysklywec, D.W., 1966. Correlation of snowmelt with the controlling meteorological parameters. Unpublished Masters thesis, Dept. of Civil Eng., Univ. of New Brunswick, Fredericton.
- Rainwater, F.H. and Thatcher, L.L., 1960. Methods for collection and analysis of water samples. U.S. Geol. Survey Water-Supply Paper 1454, 36 pp.
- Rantz, S.E., 1968. Characteristics of logarithmic rating curves. In: Selected techniques in water resource investigations, 1966-67. U.S. Geol. Survey Water-Supply Paper 1892, 142-152.
- Rauch, H.W. and White, W.B., 1970. Lithologic controls on the development of solution porosity in carbonate aquifers. Water Resources Research, 6(4) 1175-1193.
- Reams, M.W., 1968. Cave sediments and the geomorphic history of the Ozarks. Unpublished Ph.D. dissertation, Washington Univ., St. Louis, Mo.
- Rimmar, G.M., 1953. Use of electric conductivity for determination of water discharges by a dilution method. Trudy, Gosudarstvennogo Gidrologicheskogo Instituta, 36(90), 18-48. Translation No. 749, National Engineering Laboratory, Glasgow.

- Ross, G.A., 1970. The Stanford Watershed Model: the correlation of parameter values selected by a computerized procedure with measurable physical characteristics of the watershed. Research Rep. 35, Univ. of Kentucky Water Resources Institute, Lexington.
- Rutherford, J.M., Jr., 1971. Factors affecting cavern development in the Great Savannah, West Virginia. Caves and Karst, 13(6), 48-49.
- Sanders, J.E. and Friedman, G.M., 1967. Origin and occurrence of limestones. In: G.V. Chilingar et al., Developments in Sedimentology, Elsevier, Amsterdam, 169-266.
- Schmidt, V., 1962. Marthas Cave. Netherworld News, 10(1), 14-15.
- Sittner, W.T., C.E. Schauss and J.C. Monro, 1969. Continuous hydrograph synthesis with an API type hydrologic model. Water Resources Research, 5(5), 1007-1022.
- Smith, D.I. and Mead, D.G., 1962. The solution of limestone with special reference to Mendip. Proc. Univ. Bristol Speleo. Soc., 9(3), 188-211.
- Spreen, W.C., 1947. A determination of the effect of topography upon precipitation. Trans. Amer. Geophys. Union, 28, 285-290.
- Strahler, A.N., 1953. Revision of Horton's quantitative factors in erosional terrain. Trans. Amer. Geophys. Union, 34, p. 345.
- Strahler, A.N., 1960. Physical Geography. John Wiley and Sons, New York, 533 pp.
- Sweeting, Marjorie M., 1973. Karst Landforms. Columbia Univ. Press, New York, 362 pp.
- Thiessen, A.H., 1911. Precipitation averages for large areas. Monthly Weather Rev., July 1911, p. 1082.
- Thompson, P., 1973. Speleochronology and late Pleistocene climates inferred from O, C, H, U and Th, isotopic abundances in speleothems. Unpublished Ph.D. dissertation, McMaster Univ., 352 pp.
- Thornthwaite, C.W., 1955. Average climatic water balance data of the continent - America. Lab. of Climatology, 8(1).
- Todd, D.K., 1959. Ground Water Hydrology. John Wiley and Sons, New York, 336 pp.

- Turner, G.K., Associates, 1968. Fluorometry in studies of pollution and movement of fluids. Fluorometry Reviews, Acc. No. 9941, 22 pp. Available from G.K. Turner Associates, 2524 Pulgas Ave., Palo Alto, Calif.
- U.S. Army, Corps of Engineers, 1960. Runoff from snowmelt. EM 1110-2-1406 Washington D.C., Sup. of Documents, 75 pp.
- Vessel, A.J., 1939. Soils of Greenbrier County. In: Price and Heck, Greenbrier County, W. Virginia Geol. Survey Rep., 648-652.
- Villines, J.R., 1968. Economic analysis of flood detention storage by digital computer. Research Rep. No. 9, Univ. of Kentucky Water Resources Institute, Lexington.
- Watson, R.A., 1966. Central Kentucky karst hydrology. Bull. Nat. Speleo. Soc., 28, 159-166.
- White, W.B., 1969. Conceptual models for carbonate aquifers. Ground Water, 7(3), 15-21.
- White, W.B. and Schmidt, V.A., 1966. Hydrology of a karst area in East Central West Virginia. Water Resources Research, 2, 549-560.
- White, W.B., et al., 1970. The Central Kentucky karst. The Geographical Review, 60(1), 88-115.
- Williams, G.P. and Guy, H.P., 1973. Erosional and depositional aspects of Hurricane Camille in Virginia, 1969. U.S. Geol. Survey, Prof. Paper 804, 43 pp.
- Wilson, J.F., Jr., 1968. Fluorometric procedures for dye tracing. U.S. Geol. Sur. Techniques of Water-Resources Investigations. Book 3, Applications of Hydraulics. Chapter A12, 31 pp.
- Wolfe, T.E., 1962. An investigation of the controls of cavern development in the Greenbrier limestone of Southeastern West Virginia. Unpublished Masters thesis, Univ. of Pittsburgh.
- _____, 1964. Cavern development in the Greenbrier series, West Virginia. Bull. Nat. Speleo. Soc., 26(2), 37-60.
- _____, 1970. Poor Farm Cave, West Virginia. The Canadian Caver, No. 3, 30-33.

Wolfe, T.E., 1973. Sedimentation in karst drainage basins along the Allegheny escarpment in Southeastern West Virginia, U.S.A. Unpublished Ph.D. dissertation, McMaster Univ., 454 pp.

Zotter, H., 1963. Stream tracing techniques and results - Pocahontas and Greenbrier Counties, West Virginia. Nat. Speleo. Soc. News, 21(10), 136-142.

_____, 1965. Stream tracing techniques and results - Pocahontas and Greenbrier Counties, West Virginia - Part II. Nat. Speleo. Soc. News, 23(12), 169-176.

APPENDIX I

PROGRAM LISTINGS FOR KARST, PRECON, REEDAT and RATNG

```

OVERLAY(JCO,0,0)
PROGRAM KARST(INPUT,TAPE5=INPUT,OUTPUT,TAPE6=OUTPUT,
2TAPE25,TAPE30,TAPE31,TAPE40,TAPE60)

```

```

C *****
C THE MAIN DRIVING SUBPROGRAM
C IMPORTANT CALL IS CALL SEG
C *****

COMMON/WRTOT/NA,OOMAX,OOMIN
COMMON /NPTSS/NOPT,NOPTS(15),NPT
COMMON/TAPES/NDSK,ITMPA,ITMPB,ISTAPE,ITAPC
COMMON/REEL/OREEL(12),STRNCK,STMFLW,IDYSS,IDYNDS,IDYS
LOGICAL STRNCK,STMFLW
COMMON/LGPRNT/LPLOT,LPRNT,LTEST
LOGICAL LPLOT,LPRNT,LTEST

COMMON/NSEGG/NSEG
WRITE(6,204)
204 FORMAT(20HIKARST START.
ISTAPE=40
ITAPC=41
NDSK=25
ITMPA=30
ITMPB=31
REWIND 25
CALL TIMER
WRITE(6,200)
200 FORMAT(100H ***** PROGRAM KARST *****
2VERSION OF APRIL 18 1972
REWIND NDSK
CALL READD(NSEG,IGSTA,NDSK)
CALL TIMER

100 CONTINUE
REWIND ISTAPE
IF(STMFLW)CALL STRMCK
CALL TIMER

C NS IS SEGMENT NO.
DO 900 NS=1,NSEG

CALL TIMER
REWIND NDSK
CALL RDLOSE(NDSK)
CALL TIMER

C AU973 CORRECTS FOR SHORTER CLIMATIC DATA IN INITAL
CALL INITAL(NS,IGSTA)

REWIND ITMPA

```

```

REWIND ITMPB
I=ITMPA $ ITMPA=ITMPB $ ITMPB=I
CALL TIMER
CALL SEG(NS,NA,IGSTA)

```

```
CALL TIMER
```

```

900 CALL PRNTS8(100,NS,NS)
CONTINUE

```

```

CALL OBJINT
REWIND ITMPB
CALL CHANEL
REWIND ITMPB
IF(LPRNT)CALL WRTOUT
CALL TIMER

```

```

STOP77777
END

```

```
SUBROUTINE TIMER
```

```

C *****
C THIS TIMES PARTS OF THE PROGRAM
C *****

```

```

DATATO/0./
CALL SECOND(T)
TINC=T-TO
TO =T
WRITE(6,100)TINC,T
100 FORMAT(20H INCREMENTAL TIME= F7.3,15H TOTAL TIME= F7.3,
27H SECS )
RETURN
END

```

```
FUNCTION PLUS(X)
```

```

C *****
C FUNCTION TO TO TALE THE POSITIVE VALUE OF X JUST ABOVE ZERO
C *****

```

```

PLUS=1.0E-10
IF(X.GT.1.0E-10)PLUS=X
RETURN
END

```

```

SUBROUTINE STRMCK
COMMON/RDSEG/IDAY, IDYND, IDY

```

```

C *****
C READS TITLES OFF STREAMFLOW TAPE. ALSO CHECKS FOR STREAMFLOW DATA.
C STREAMFLOW TAPE ,TAPE40) IS A BINARY TAPE WRITTEN BY ANOTHER
C PROGRAM CALLED GURLEY.
C *****

COMMON/TAPES/NDISK,ITMPA,ITMPB,ISTAPE,ITAPC
COMMON/REELQ/QREEL(12),STRNCK,STMFLW,IDYSS,IDYNDS,IDYS
LOGICAL STRNCK,STMFLW
DIMENSION TITLE(8)
STRNCK=.F.
READ(ISTAPE)TITLE
WRITE(6,100)TITLE
100 FORMAT(40H TITLE ON RATING CURVE                                8A10)
READ(ISTAPE)TITLE
WRITE(6,101)TITLE
101 FORMAT(40H TITLE ON THE STREAMFLOW RECORDS                    8A10)
READ(ISTAPE)IDYSS,IDYNDS
IDYNDS=IDYNDS-5
WRITE(6,220)IDYSS,IDYNDS
WRITE(6,1)
WRITE(6,1)
1 FORMAT(1H0)
220 FORMAT(40H STREAMFLOW RECORDS FOR DAYS                        2I10)
IF(IDYSS.LT.IDYND.AND.IDYNDS.GT.IDAY)GOTO 110
WRITE(6,111)IDAY, IDYND, IDYSS, IDYNDS
111 FORMAT(40H NO STREAMFLOW COMPARISON ANAL DYS=                2I6,
240H AND STREAMFLOW RECORDS FOR DAYS                             2I5)
WRITE(6,1)
WRITE(6,1)
RETURN
110 CONTINUE
I=IDYSS-1
200 IF(I.GE.IDAY-1) GOTO 201
READ(ISTAPE)I,QREEL
GOTO 200
201 CONTINUE
IDYS=I
RETURN
END

```

SUBROUTINE PRTSUM

```

C      *****
C      PRINTS A SUMMARY OF THE SEGMENTAL WATER BALANCES.
C      *****

COMMON/RDSEG/IDAY, IDYND, IDY
COMMON/SUMSS/SUMS(15), ASTR(5)
COMMON/QRRRL/QREAL
COMMON/EVPA/EGS, EET
COMMON/OVFCC/OVFKA, OVFKB, QFIN
COMMON/CLN /PR(24,10), CLIN(10,10), CLIM(7)
COMMON/VARIA/OVF, GWF, PP, PERC, QCHAN, RRS, GWOUTT, SPR, QOUT
COMMON/TIMAA/TIMA
COMMON/STORA/UZS, LZS, GWS, AST
COMMON /NPTSS/NOPT, NOPTS(15), NPT
COMMON/REELQ/QREEL(12), STRNCK, STMFLW, IDYSS, IDYNDS, IDYS
COMMON/LASTT/LAST
COMMON/SNOW/T, GM, WE, SNWA, SNWB, SNWC, SNWD
LOGICAL STRNCK, STMFLW
REAL LZSC
REAL LZS
C TO PRINT A SUUMMARY OF THE DATA AT DAYS NOPTS.
LOGICAL LAST
200 CONTINUE
IF(NPT.GT.NOPT)LAST=.T.
IF(LAST)RETURN
IF(NOPTS(NPT).LT.IDY.OR.NOPTS(NPT).GT.IDYND)GOTO900
SUMS(1)=SUMS(1)+SPR
SUMS(2)=SUMS(2)+CLIM(2)
SUMS(3)=SUMS(3)+QOUT/QFIN
SUMS(4)=SUMS(4)+GWF
SUMS(5)=SUMS(5)+OVF
SUMS(6)=SUMS(6)+PERC
SUMS(7)=SUMS(7)+PP
SUMS(8)=SUMS(8)+EET
SUMS(9)=SUMS(9)+QREAL
SUMS(10)=SUMS(10)+(QOUT-QREAL)**2
IF(NOPTS(NPT).EQ.IDY) GOTO 300
RETURN
300 CONTINUE
C THIS IS THE PRINTING SECTION
I=IDAY
IF(NPT.NE.1)I=NOPTS(NPT-1)
WRITE(6,1)
WRITE(6,801)I,NOPTS(NPT)
801 FORMAT(40H WATER BALANCE IN INCHES FROM I10,10H
2TO I10)
WRITE(6,802)
802 FORMAT(20X,40H AST UZS LZS GWS SNOW )
WRITE(6,803)AST,UZS,LZS,GWS,WE
803 FORMAT(20H NEW STORAGES 5F7.3)

```

```

WRITE(6,804)(ASTR(I),I=1,5)
804  FORMAT(20H OLD STORAGES                               5F7.3)
      ASTC=AST-ASTR(1)
      ASTR(1)=AST
      UZSC=UZS-ASTR(2)
      ASTR(2)=UZS
      LZSC=LZS-ASTR(3)
      ASTR(3)=LZS
      GWSC=GWS-ASTR(4)
      ASTR(4)=GWS
      WEC=WE-ASTR(5)
      ASTR(5)=WE
      WRITE(6,805)ASTC,UZSC,LZSC,GWSC,WEC
805  FORMAT(20H CHANGE IN STORAGES                               5F7.3)
      WRITE(6,806)
806  FORMAT(130H PRECIP      EVAP      DELTT.S      RUNOFF      BALANCE      ***
2**  GWF          OVF          PERC          PP          POT EVAP
2
      DELTS=ASTC+UZSC+LZSC+GWSC+WEC
      BAL=SUMS(1)-SUMS(2)-SUMS(3)-DELTS
      WRITE(6,808)SUMS(1),SUMS(8),DELTS,SUMS(3),BAL,(SUMS(I),I=4,7)
2SUMS(2)
808  FORMAT(1X,5F10.3,6X,5F10.3)
      I=IDAY
      IF(NPT.NE.1)I=NOPTS(NPT-1)
      YY=NOPTS(NPT)-I
      IF(YY.LT.0.99)YY=1.0
      X=SUMS(3)*QFIN
      Y=SUMS(3)/YY*TIMA/24.0
      Z=Y*QFIN
      WRITE(6,810)SUMS(3),X,Y,Z
810  FORMAT(40H SIMULATED STREAMFLOW TOTAL IS
2F10.3,7H INCH   F10.3,7H CUSECS10H AVERAGE=   F10.3,7H INCH
2F10.3,7HCUSECS )
      IF(.NOT.STMFLW)GOTO 813
      IF(.NOT.STRNCK)GOTO813
      X=SUMS(9)/QFIN
      Y=SUMS(9)/YY*TIMA/24.0
      Z=Y/QFIN
      WRITE(6,811)X,SUMS(9),Z,Y
811  FORMAT(40H ACTUAL STREAMFLOW TOTAL IS
2F10.3,7H INCH   F10.3,7H CUSECS10H AVERAGE=   F10.3,7H INCH
2F10.3,7HCUSECS )
      SUMS(15)=SUMS(15)+SUMS(10)
      YYSS=SUMS(10)/YY
      WRITE(6,700)SUMS(10),YYSS,SUMS(15)
700  FORMAT(20H SUMS OF SQUARES=   F10.3,10H AVERAGE=   F10.3,
210H TOTAL =   F10.3)
      WRITE(6,1)
      WRITE(6,1)
813  CONTINUE
      DO 809 I=1,10

```



```

809 SUMS(I)=0.0
    NPT=NPT+1
    RETURN
900 CONTINUE
    WRITE(6,812)NOPTS(NPT)
812  FORMAT(20H ERROR IN NOPTS           I4,20H SKIPPED TO NX DAY )
    NOPTS(NPT)=IDY
    IF(NPT.NE.1)NOPTS(NPT)=NOPTS(NPT-1)
    NPT=NPT+1
    GOTO 200
1   FORMAT(2H0 )
    END

```

SUBROUTINE STRMRD

```

C   *****
C   READS OFF STREAMFLOW DATA FROM TAPE 40 =ISTAPE
C   STREAMFLOW TAPE ,TAPE40) IS A BINARY TAPE WRITTEN BY ANOTHER
C   PROGRAM CALLED GURLEY.
C   *****

```

```

COMMON/TAPES/NDISK,ITMPA,ITMPB,ISTAPE,ITAPC
COMMON/REELQ/QREEL(12),STRNCK,STMFLW,IDYSS,IDYNDS,IDYS
COMMON/RDSEG/IDAY,IDYND,IDY
LOGICAL STRNCK,STMFLW
DATA IDYTST/0 /
IF(IDYS+1.GE.IDYNDS)GOTO 200
IF(IDYS+1.EQ.IDY) GOTO 100
DO 506 I=1,12
506  QREEL(I)=0.0
    RETURN
    IF(IDYTST.EQ.0) IDYTST=IDAY
2466 FORMAT(25H STRMRD ERROR IN DAYS           2I10)
100  READ(ISTAPE)IDYS,QREEL
    IF(EOF(ISTAPE)) 300,101
101  CONTINUE
    IF(IDYTST.NE.IDYS) WRITE(6,2466) IDYS, IDYTST
    IDYTST=IDYS+1
    STRNCK=.T.
    RETURN
300  IDYNDS=IDYS-1
200  CONTINUE
    WRITE(6,400)IDY,IDYS
400  FORMAT(20H END STRMRD           2I10)
    DO 201 I=1,12
201  QREEL(I)=0.0
    STRNCK=.F.
    RETURN
    END

```

SUBROUTINE READD(NSEG,IGSTA,NSDK)

```

C      *****
C      READS THE SEGMENTAL DATA OFF DATA CARDS.. ALSO WRITE OUT DATA.
C      *****

COMMON NOS( 20 ), SA( 20 ), SHX( 20 ), SHM( 20 ), SIA( 20 ), IGST(20)
COMMON SAWT( 20 ), SOF( 20 ), SSP( 20 ), GWEA(20 ), PEK( 20 ), LZEI(20)
COMMON GWOUT(20 ), ASM( 20 ), ART( 20 ), GWRR(20 ), SMN( 20 ), UZSX(20)
COMMON LZSX( 20 ), GWSX(20 ), ASTX(20), LZSNX(20), UZSNX(20)
COMMON TIMET(20,20), IELEE(20), IADD(20,20), IBDD(20,20)
COMMON SPAR(20,20)
COMMON/RDSEG/IDAY, IDYND, IDY
COMMON/TIMAA/TIMA
COMMON/DATMS/IDTAMS
COMMON/INITLL/UZSINT,LZSINT,GWSINT,ASTINT
COMMON/REELQ/OREEL(12),STRNCK,STMFLW,IDYSS,IDYNDS, IDYS
COMMON /NPTSS/NOPT,NOPTS(15),NPT
COMMON/SNOWIN/GMD(20),SNOWA(20),SNOWB(20),SNOWC(20),SNOWD(20)
COMMON/SNOW/T,GM,WE,SNWA,SNWB,SNWC,SNWD
LOGICAL STRNCK,STMFLW
COMMON/RDLOS/TITLE(8),SEGNM (2),NOSS(19),DATECD(4)
COMMON/LGPRNT/LPLOT,LPRNT,LTEST
LOGICAL LPLOT,LPRNT,LTEST
COMMON/PRNTT/IPRNT(20),PRNT(20),IPRNTA(20,20)
COMMON/PRNTA/PRNTR(13,20)
LOGICAL PRNT
REAL LZSX,LZSNX,LZSINT,LZEI
READ(5,100)TITLE
WRITE(6,103)TITLE
WRITE(6,1)
READ(5,101)ISTDY,NDAY,NOPT,STMFLW,LPLOT,LPRNT,LTEST,TIMA
WRITE(6,110)ISTDY,NDAY,TIMA
WRITE(6,637)STMFLW,LPLOT,LPRNT,LTEST
IF(NOPT.EQ.0)GOTO 201
IF(NOPT.GE.16)NOPT=15
READ(5,170)(NOPTS(I),I=1,NOPT)
WRITE(6,171)NOPT,(NOPTS(I),I=1,NOPT)
170  FORMAT(20I4)
      GOTO202
201  CONTINUE
      WRITE(6,175)
202  CONTINUE
      WRITE(6,1)
      IF(TIMA.GT.24.001.OR.TIMA.LT.0.24)STOP 1112
      READ(5,102)NSEG
      WRITE (6,111)NSEG
      WRITE(6,1)
      IF(NSEG.GT.20)STOP1111
      DO 120 II=1,NSEG
      WRITE(6,1)
      READ(5,150)NOS(II),SEGNM,IGST(II),IELEE(II),(IPRNTA(I,II),I=1,20)

```

```
WRITE(6,151)NOS(II),SEGNM,IGST(II),IELEE(II),(IPRNTA(I,II),I=1,20)
```

```
READ(5,132)SA(II),SHX(II),SHM(II),SIA(II),SAWT(II)
```

```
IF(SHX(II).GT.2.0)SHX(II)=1.0
```

```
WRITE(6,161)
```

```
WRITE(6,13)SA(II),SHX(II),SHM(II),SIA(II),SAWT(II)
```

```
READ(5,132)ASM(II),LZSNX(II),UZSNX(II),ASTX(II),UZSX(II),LZSX(II),
2GWSX(II)
```

```
WRITE(6,160)
```

```
WRITE(6,13)ASM(II),LZSNX(II),UZSNX(II),ASTX(II),UZSX(II),LZSX(II),
2GWSX(II)
```

```
READ(5,132)SOF(II),SSP(II),SMN(II),ART(II),PEK(II)
```

```
WRITE(6,162)
```

```
WRITE(6,13)SOF(II),SSP(II),SMN(II),ART(II),PEK(II)
```

```
READ(5,132)GWOUT(II),GWRR(II),GWEA(II),LZEI(II)
```

```
WRITE(6,163)
```

```
WRITE(6,13)GWOUT(II),GWRR(II),GWEA(II),LZEI(II)
```

```
IELE=IELEE(II)
```

```
READ(5,180)(TIMET(IE,II),IE=1,IELE)
```

```
WRITE(6,181)(TIMET(IE,II),IE=1,IELE)
```

```
READ(5,183)(IADD(IE,II),IE=1,IELE)
```

```
READ(5,183)(IBDD(IE,II),IE=1,IELE)
```

```
WRITE(6,14)(IBDD(IE,II),IE=1,IELE)
```

```
WRITE(6,14)(IADD(IE,II),IE=1,IELE)
```

C SNOW

```
READ( 5,132)GMD(II),SNOWA(II),SNOWB(II),SNOWC(II),SNOWD(II)
```

```
WRITE(6,422)
```

```
WRITE(6,13 )GMD(II),SNOWA(II),SNOWB(II),SNOWC(II),SNOWD(II)
```

C SPARE READS

```
READ( 5,132)(SPAR(I,II),I=1,7)
```

```
READ( 5,132)(SPAR(I,II),I=8,14)
```

```
READ( 5,132)(SPAR(I,II),I=15,20)
```

```
WRITE(6,635)(SPAR(I,II),I=1,20)
```

```
WRITE(6,1)
```

120 CONTINUE

```
READ(NDSK)TITLE
```

```
WRITE(6,114)TITLE
```

```
WRITE(6,1)
```

```
READ(NDSK)TITLE
```

```
WRITE(6,115)TITLE
```

```
WRITE(6,1)
```

```
READ(NDSK)DATECD,DATTT,DATET
```

```
WRITE(6,133)DATECD,DATTT,DATET
```

```
WRITE(6,1)
```

```

READ(NDSK) IDAY, IDYND
WRITE(6,542) IDAY, IDYND
IF(ISTDY.GT.IDAY.AND.ISTDY.LT.IDYND)GOTO 210
IDTAMS=0
GOTO 211
210 IDTAMS=ISTDY-IDAY-1
IDAY=ISTDY
211 CONTINUE
IF(NDAY.LE.0)GOTO 212
IF(NDAY.LE.IDYND-IDAY)IDYND=IDAY+NDAY-1
212 CONTINUE
WRITE(6,118) IDAY, IDYND
WRITE(6,1)
READ(NDSK) IGSTA
WRITE(6,116) IGSTA
DO117 IG=1, IGSTA
WRITE(6,1)
READ(NDSK) NSEGST, (NOSS(I), I=1, 19)
WRITE(6,140) IG, NSEGST, (NOSS(I), I=1, NSEGST)
117 CONTINUE
WRITE(6,1)
X=IDYND-IDAY+1
NAL=X*24.0/TIMA
WRITE(6,119) NAL
WRITE(6,1)
RETURN

1 FORMAT(1H0)
13 FORMAT(1H+,50X,7F10.5)
100 FORMAT(8A10)
101 FORMAT(3I4,4L1,F10.3)
102 FORMAT(20I4)
103 FORMAT(40H TITLE FOR SIMULATION RUN = 8A10)
110 FORMAT(40H START DAY LGNTH ANALYSIS TIME 2I6,F10.5)
111 FORMAT(40H NUMBER OF SEGMENTS IS I4)
112 FORMAT(1X,I3,2A8,F7.3,2F5.0,F7.3,I3,F7.3,F5.0,F5.5)
114 FORMAT(40H TITLE ON THE ORIGINAL DATA 8A10)
115 FORMAT(40H TITLE ON THE CONVERTED DATA 8A10)
116 FORMAT(40H THE NUMBER OF GAGE GROUPS SETS I4)
118 FORMAT(40H DAY ANALYSIS STARTS AND ENDS= 2I8)
119 FORMAT(40H NUMBER OF ANALYSIS POINTS IS I8)
133 FORMAT(10H INITAL 4A10,A10,10H CONVTD A10)
175 FORMAT(30H NO SUMMARY )
171 FORMAT(40H PRINT SUMMARY AT DAYS 15I5)
140 FORMAT(10H GAGE GP. I4,40H STATION NUMBERS AND TOTAL NO.=
2 I6,19I4)
132 FORMAT(10X,7F10.5)
161 FORMAT(50H PHYSICAL, SA, EVAP CORR, SHM, STA, SAWT )
160 FORMAT(50H NOMIN ASM LZSN UZSN ,INIT, AST UZS LZS GWS )
162 FORMAT(50H SURFACE ETC. SOF SSP SMN ART BZK )
163 FORMAT(50H GROUND WATER, GWOUT GWRR GWEA LZEI )
150 FORMAT(I4,2A10,I6,I2,8X,20I1)

```

```

422 FORMAT(50H SNOW - GM,WEINT,TCOF,SNWC,SNWD
151 FORMAT(30H NO NAME IGST IEL PRINT= I4,2A10,I6,I2,8X,20I1)
180 FORMAT(10X,10F5.0)
181 FORMAT(30H TIME DELAY HISTOGRAM 10F8.4)
14 FORMAT(30H ADD FLOWS FROM SEGS 20I4)
183 FORMAT(10X,20I2)
635 FORMAT(10H SPARE 7G10.3)
637 FORMAT(40H STREAMFLOW,(LPLOT), PLOTTING,(LTEST) 4(L1,2X))
542 FORMAT(40H DAY CLIMATIC DATA AVAILABLE = 2I8)
END

```

SUBROUTINE RDLOSE(NDSK)

```

C *****
C TO READ AND REJECT TITLES OFF TAPE NDSK =TAPE25.
C TAPE25 CONTAINS THE CLIMATIC DATA.
C TAPE25 IS WRITTEN BY ANOTHER PROGRAM CALLED PRECON, AND BY REEDAT
C *****

```

```

COMMON/RDLOS/TITLE(8),SEGM (2),NOSS(19),DATECD(4)
DIMENSION X(3,10)
COMMON/DATMS/IDTAMS
READ(NDSK)TITLE
READ(NDSK)TITLE
READ(NDSK)DATECD,R,R
READ(NDSK)K,K
READ(NDSK)K
DO 1 J=1,K
1 READ(NDSK)NSEGST,(NOSS(I),I=1,19)
IF(IDTAMS.LE.0)GOTO 3
DO 2 J=1,IDTAMS
READ(NDSK) M, ((X(I,IJ),I=1,3),IJ=1,K)
2 CONTINUE
3 CONTINUE
RETURN
END

```

SUBROUTINE MAIN(NS)

```

C      *****
C      THE MAIN CALLING SUBROUTINE. CALLS ALL THE HYDROLOGICAL SUBROUTINE
C      CALLED FROM SEG.
C      ALSO RETURNS VALUES TO PRNTSB WHERE ASKED FOR.
C      *****

C      CALLED EACH TIME INTERVAL AND CALLED FOR EACH SEGMENT
COMMON/TAPES/NDISK,ITMPA,ITMPB,ISTAPE,ITAPC
COMMON /NPTSS/NOPT,NOPTS(15),NPT
COMMON/VARIA/OVF,GWF,PP,PERC,QCHAN,RRS,GWOUTT,SPR,QOUT
COMMON/PRNTT/IPRNT(20),PRNT(20),IPRNTA(20,20)
COMMON/PRNTA/PRNTSR(13,20)
LOGICAL PRNT
COMMON/WRTOT/NA,QQMAX,QQMIN
COMMON/STORA/UZS,LZS,GWS,AST
COMMON/EVPA/EGS,EET
COMMON/QRRL/OREAL
COMMON/NSEGG/NSEG
COMMON/SNOW/ T,GM,WE,SNWA,SNWB,SNWC,SNWD
DIMENSION QSTR(20)
REAL LZS
COMMON/CLN /PR(24,10),CLIN(10,10),CLIM(7)
LOGICAL PRNTAL
PRNTAL=.F.

C      IF(PRNT(13))CALL PRNTSB(13,EGS ,4HEGSA)

CALL SNOW(SPR,SPRI)
IF(PRNT(16)) CALL PRNTSB(16,SPRI,4HSPRI).
C      INPUT ART,AST,ASM,SPR,      EGS EET
CALL INTERC(SPRI,RRS)
C      OUTPUT AST, RRS,      EGS EET

IF(PRNT(15))CALL PRNTSB(15,RRS,4HRRS )
C      INPUT PEK,LZEI,RRS,SIA,      LZS LZSN UZS UZSN EGS EET
CALL INFLTR(RRS,OVF,PERC,PP)
C      OUTPUT OVF, PERC, PP      UZS EGS EET

IF(PRNT(17))CALL PRNTSB(17,LZS ,4HLZSA)
IF(PRNT(18))CALL PRNTSB(18,UZS, 4HUZSB)
C      INPUT PERC PP GWOUT GWK      LZS LZSN GWS
CALL GRNDW(PERC,PP,GWF,GWOUTT)
C      OUTPUT GWF      GWS

CALL OVERFL(OVF,GWF,QCHAN)

CALL EVAPW

VAR=SPR*10.+1.0

```

```

IF (NS.EQ.1) GOTO 300
NSA=NS-1
READ(ITMPA)(QSTR(I),I=1,NSA)
OSTR(NS)=QCHAN
IF(NS.EQ.NSEG)GOTO 400
WRITE(ITMPB)(QSTR(I),I=1,NS)
GOTO 401
400 CONTINUE
WRITE(ITMPB)(QSTR(I),I=1,NS),VAR
401 CONTINUE
GOTO 301
300 CONTINUE
IF(NSEG.EQ.1) GOTO 420
WRITE(ITMPB) QCHAN
GOTO 421
420 CONTINUE
WRITE(ITMPB) QCHAN ,VAR
421 CONTINUE
301 CONTINUE
  QOUT=QCHAN
  IF(PRNT(01))CALL PRNTSB(01,SPR,3HSPR)
  IF(PRNT(02))CALL PRNTSB(02,EGS,3HEGS)
  IF(PRNT(03))CALL PRNTSB(03,EET,3HEET)
  IF(PRNT(04))CALL PRNTSB(04,OVF,3HOVF)
  IF(PRNT(05))CALL PRNTSB(05,GWF,3HGWF)
  IF(PRNT(06))CALL PRNTSB(06,QOUT,4HQOUT)
  IF(PRNT(07))CALL PRNTSB(07,PP ,3HPP )
  IF(PRNT(08))CALL PRNTSB(08,PERC,4HPERC)
  IF(PRNT(09))CALL PRNTSB(09,UZS,3HUZS)
  IF(PRNT(10))CALL PRNTSB(10,LZS,3HLZS)
  IF(PRNT(11))CALL PRNTSB(11,GWS,3HGWS)
  IF(PRNT(12))CALL PRNTSB(12,AST,3HAST)
  IF(PRNT(19)) CALL PRNTSB(19,WE,4H WE )
  IF(PRNT(14)) CALL PRNTSB(14 ,EGS,4HEGS )
  IF(PRNT(20))CALL PRNTSB(20,T,4HTEMP)
  IF(PRNTAL)WRITE(6,8424)SPR,UZS,LZS,GWS,AST,
  2OVF,PERC,PP,EGS,EET,GWF,QOUT
  IF(NOPT.GE.1)CALL PRTSUM
8424 FORMAT(1X,12E10.3)
  IF(GWF.GT.100000.0)GWF=100000.0
  RETURN
END

```

SUBROUTINE CHANEL

```

C      *****
C      CHANNEL ROUTING. DONE BY TIME-AREA TECH.
C      READS SEGMENTAL STREAMFLOWS ADDS THEM UP AND ROUTES THEM ONTO
C      OUTPUT TAPE ,ITMPB
C      *****

C INPUTS NSEG,ITMPA,ITPMB,NAL,IELEE(,),TIMET(,),IADD(,),IBDD(,)
COMMON/TIMAA/TIMA
COMMON/RDSEG/IDAY,IDYND,IDY
COMMON/TAPES/NDSK,ITMPA,ITMPB,ISTAPE,ITAPC
COMMON/WRTOT/NA,QQMAX,QQMIN
COMMON/REELQ/OREEL(12),STRNCK,STMFLW,IDYSS,IDYNDS,IDYS
COMMON/VARIA/OVF,GWF,PP,PERC,QCHAN,RRS,GWOUTT,SPR,QOUT
COMMON/NSEGG/NSEG
COMMON/NPTSS/ NOPT,NOPTS(15),NPT
COMMON NOS( 20 ), SA( 20 ),SHX( 20 ),SHM( 20 ),SIA( 20 ),IGST(20)
COMMON SAWT( 20 ),SOF( 20 ),SSP( 20 ),GWEA(20 ),PEK( 20 ),LZEI(20)
COMMON GWOUT(20 ),ASM( 20 ),ART( 20 ),GWRR(20 ),SMN( 20 ),UZSX(20)
COMMON LZSX( 20 ),GWSX(20 ),ASTX(20),LZSNX(20),UZSNX(20)
COMMON TIMET(20,20),IELEE(20),IADD(20,20),IBDD(20,20)
COMMON SPAR(20,20)
DIMENSION QSEG(1000,4)
LOGICAL STRNCK,STMFLW

ITIM=24.0/TIMA+0.0001
NAL=(IDYND-IDAY)*ITIM
REWIND ITMPA
REWIND ITPMB
I=ITMPA
ITMPA=ITMPB
ITMPB=I
QQMAX=0.0
DO 101 NA=1,NAL
READ(ITMPA)(QSEG(NA,I),I=1,NSEG),VAR
DO 200 NS=1,NSEG
NLAG=IELEE(NS)
QOUT=0.0
IF(NA.LT.NSEG) GOTO 210
IF(NA.LT.NLAG)GOTO 210
DO 220 ILAG=1,NLAG
NN=NA-ILAG+1
QOUT=QOUT+QSEG(NN,NS)*TIMET(ILAG,NS)
QSEG(NA,NS)=QOUT
220 CONTINUE
210 CONTINUE
200 CONTINUE
NS=NSEG
QOUT=QSEG(NA,NS)
IF(NA.LT.NSEG)GOTO 225
IF(NA.LT.ILAG)GOTO 225

```



```

DO 227 ILAG=1,NLAG
NN=NA-ILAG+1
IF(IADD(ILAG,NS).EQ.0) GOTO 222
J=IADD(ILAG,NS)
IF(J.GT.NSEG)GOTO 222
QOUT=QOUT+QSEG(NN,J)
222 IF(IBDD(ILAG,NS).EQ.0)GOTO 224
J=IBDD(ILAG,NS)
IF(J.GT.NSEG)GOTO 224
QOUT=QOUT+QSEG(NN,J)
224 CONTINUE
227 CONTINUE
225 CONTINUE
C WILL NOT HANDLE UPSTREAM ADDITIONS TO SEGMENTS ..
IF(STMFLW)GOTO 410
OREAL=0.0
GOTO 411
410 CONTINUE
IDY=IDAY+NA/ITIM -1
IDYY=NA/ITIM
IF(NA.EQ.IDYY*ITIM) CALL STRMRD
IF(ITIM.EQ.1) GOTO 501
ITMM=NA-IDYY*ITIM
II=ITMM*TIMA*0.5
IF(II.GT.12)II=12
IF(II.LT.1)II=1
OREAL=OREEL(II)
GOTO 502
501 CONTINUE
OREAL=0.0
DO 510 IQRL=1,12
OREAL=OREAL+OREEL(IQRL)
510 CONTINUE
OREAL=OREAL/12.0
502 CONTINUE
411 CONTINUE
IF(QOMAX.LT.QOUT)QOMAX=QOUT
IF(QOMAX.LT.OREAL)QOMAX=OREAL
IF(NOPT.GE.1) CALL OBJFUN(OREAL,QOUT)
WRITE(ITMP8)QOUT,OREAL,VAR
101 CONTINUE
WRITE(6,5465)((QSEG(I,J),I=1,20),J=1,4)
5465 FORMAT(1X,10F8.2)
RETURN
END

```

SUBROUTINE OBJFUN(QREAL,QOUT)

```

C      *****
C      PRINTS OUT THE FOUR OBJECTIVE FUNCTIONS.
C      *****

COMMON/ODAYY/ODAY
COMMON /NPTSS/NOPT,NOPTS(15),NPT
COMMON/RDSEG/IDAY, IDYND, IDY
COMMON/OVFCC/OVFKA,OVFKA,OVFKA,OFIN
COMMON/LASTT/LAST
COMMON/OPSS/OPS(10),LOPS
LOGICAL LAST
200  CONTINUE
    ODAY=ODAY+1
    IF(NPT.GT.NOPT)LAST=.T.
    IF(LAST)RETURN
    IF(NOPTS(NPT).LT.ODAY.OR.NOPTS(NPT).GT.IDYND) GOTO 900
    IF(IDAY.EQ.ODAY)QREAB=QREAL
    IF(IDAY.EQ.ODAY) QOUTB=QOUT
    IF(QREAL.LT.0.101.OR.QOUT.LT.0.101) GOTO 400
    IF(QREAB.LT.0.102)QREAB=QREAL
    IF(QOUTB.LT.0.102)QOUTB=QOUT
    ALQMQ=ALOG(QREAL)-ALOG(QOUT)
    OPS(1)=OPS(1)+ABS(ALQMQ)
    OPS(2)=OPS(2)+QOUT
    OPS(3)=OPS(3)+QREAL
    ALQLA=ALOG(QREAL)-ALOG(QOUTB)
    ALQLB=ALOG(QREAB)-ALOG(QOUT)
    QREAB=QREAL
    QOUTB=QOUT
    OPS(4)=OPS(4)+ABS(ALQLA)
    OPS(5)=OPS(5)+ABS(ALQLB)
    GOTO 410
400  CONTINUE
    LOPS=LOPS+1
410  CONTINUE
    IF(NOPTS(NPT).EQ.ODAY) GOTO 600
    RETURN
600  CONTINUE
C THIS IS PRINTING SECTION
    IF(OPS(2).LT.0.001.OR.OPS(3).LT.0.001) GOTO 430
    GOTO 441
430  CONTINUE
    WRITE(6,440)NOPTS(NPT)
440  FORMAT(30H NO OBJECTIVE FUNCTIONS UP TO           15,5H DAYS )
    LOPS=0
    GOTO 442
441  CONTINUE
    I=IDAY
    IF(NPT.NE.1)I=NOPTS(NPT-1)
    WRITE(6,1)

```

```

WRITE(6,243)I,NOPTS(NPT)
243  FORMAT(50H OBJECTIVE FUNCTIONS FOR PERIOD
2I10,10H TO ,I10)
I=IDAY
IF(NPT.NE.1)I=NOPTS(NPT-1)
YY=NOPTS(NPT)-I
YY=YY-LOPS
IF(LOPS.GE.1)WRITE(6,420) LOPS
420  FORMAT(30HONO STREAMFLOW COMPARISON FOR 15,10H DAYS /)
LOPS=0
IF(YY.LT.0.99)YY=1.0
ZA=OPS(1)
ZB=(OPS(2)-OPS(3))/OPS(3)
ZC=OPS(4)-OPS(5)
ZA=ZA*100./YY
ZB=ZB*100.
ZC=ZC*100./YY
ZD=ZA+ABS(ZB)+ABS(ZC)
OPS(6)=OPS(6)+ZA
OPS(7)=OPS(7)+ZB
OPS(8)=OPS(8)+OPS(4)
OPS(9)=OPS(9)+OPS(5)
OPSG=OPS(8)-OPS(9)
OPSG=OPSG*100./YY
OPS(10)=OPS(6)+ABS(OPS(7))+ABS(OPSG)
WRITE(6,802)
802  FORMAT(50H (PERCENT) PEAK MEAN TEMPORAL TOTAL )
WRITE(6,830)ZA,ZB,ZC,ZD
830  FORMAT(10H PARTIAL 4G10.4)
WRITE(6,820)OPS(6),OPS(7),OPSG,OPS(10)
820  FORMAT(10H TOTAL 4G10.4)
XR=OPS(2)/OFIN
YR=OPS(2)/YY
ZZR=YR/OFIN
WRITE(6,810) XR,OPS(2),ZZR,YR
810  FORMAT(40H SIMULATED STREAMFLOW TOTAL IS
2F10.3,7H INCH F10.3,7H CUSECS10H AVERAGE= F10.3,7H INCH
2F10.3,7HCUSECS )
XP=OPS(3)/OFIN
YP=OPS(3)/YY
ZZP=YP/OFIN
WRITE(6,811) XP,OPS(3),ZZP,YP
811  FORMAT(40H ACTUAL STREAMFLOW TOTAL IS
2F10.3,7H INCH F10.3,7H CUSECS10H AVERAGE= F10.3,7H INCH
2F10.3,7HCUSECS )
WRITE(60,510)I,NOPTS(NPT),ZA,ZB,ZC,ZD,ZZR,ZZP
510  FORMAT(1X,2I4,1X,7G10.3)
442  CONTINUE
WRITE(6,1)
DO 300 I=1,5
300  OPS(I)=0.0
CALL TIMER

```

```

NPT=NPT+1
RETURN
900 CONTINUE
WRITE(6,812)NOPTS(NPT)
812 FORMAT(20H ERROR IN NOPTS          14,20H SKIPPED TO NX DAY )
NOPTS(NPT)=ODAY
IF(NPT.NE.1)NOPTS(NPT)=NOPTS(NPT-1)
NPT=NPT+1
GOTO 200
1 FORMAT(2H0 )
END

```

SUBROUTINE OBJINT

```

C *****
C INITILISES THE OBJECTIVE FUNCTION ROUTINE.
C *****

```

```

COMMON/LASTT/LAST
COMMON/RDSEG/IDAY, IDYND, IDY
COMMON/ODAYY/ODAY
COMMON/NPTSS/ NOPT,NOPTS(15),NPT
COMMON/OPSS/ OPS(10),LOPS
LOGICAL LAST
DO 254 I=1,10
.254 OPS(I)=0.0
NPT=1
LAST=.F.
LOPS=0
ODAY=IDAY-1
RETURN
END

```

SUBROUTINE SEG(NS,NA,IGSTA)

```

C      *****
C      CALLED FROM KARST FOR EACH SEGMENT.
C      READS CLIMATIC DATA THEN CALLS MAIN FOR EACH ANALYSIS TIME PERIOD.
C      GENERATES SEGMENTAL STREAMFLOWS IN ITMPB.
C      *****

COMMON NDS( 20 ), SA( 20 ), SHX( 20 ), SHM( 20 ), SIA( 20 ), IGST(20)
COMMON SAWT( 20 ), SOF( 20 ), SSP( 20 ), GWEA(20 ), PEK( 20 ), LZEI(20)
COMMON GWOUT(20 ), ASM( 20 ), ART( 20 ), GWRR(20 ), SMN( 20 ), UZSX(20)
COMMON LZSX( 20 ), GWSX(20 ), ASTX(20), LZSNX(20), UZSNX(20)
COMMON TIMET(20,20), IELEE(20), IADD(20,20), IBDD(20,20)
COMMON SPAR(20,20)
COMMON/REELQ/QREEL(12), STRNCK, STMFLW, IDYSS, IDYNDS, IDYS
LOGICAL STRNCK, STMFLW
COMMON/RDSEG/IDAY, IDYND, IDY
COMMON/EVPA/EGS, EET
COMMON/CLN /PR(24,10), CLIN(10,10), CLIM(7)
COMMON/TIMAA/TIMA
COMMON/TAPES/NDSK, ITMPA, ITMPB, ISTAPE, ITAPC
REAL LZSX, LZSNX, LZEI
COMMON/PRNTT/IPRNT(20), PRNT(20), IPRNTA(20,20)
COMMON/PRNTA/PRNTR(13,20)
LOGICAL PRNT
C      CLIMATIC DATA.
C      CLIN(I,IG) ALSO CLIM(I)
C WHERE I=
C      1 DAILY PRECIPITATION
C      2 EVAPORATION
C      3 MAXIMUM TEMPERATURE
C      4 MINIMUM TEMPERATURE
C      5 WIND
C      6 SNOWFALL
C      7 SNOW ON GROUND
C      NA ANALYSIS TIME NO.
      NA=0
      DO 901 IDY=IDAY, IDYND
      IDEY=IDY
      DO 401 I=1,20
      PRNT(I)=.F.
      IF(IPRNT(I).EQ.1.AND.IDEY/10*10.EQ.IDEY)PRNT(I)=.T.
      IF(IPRNT(I).EQ.2)PRNT(I)=.T.
401 CONTINUE
403 CONTINUE
      READ(NDSK) IDEY, ((CLIN(I,IG), I=1,3), IG=1, IGSTA)
      IF(IDEY.NE.IDY)WRITE(6,520)IDY, IDEY
520 FORMAT(20H ERROR IN SEG DAYS
      IF(IDEY.LT.IDY) GOTO 403
      IF(IDEY.GT.IDY) GOTO 204
      DO203 J=1,48
      RJ=J

```

```

ITIMA=TIMA*RJ+0.99
IF(ITIMA.GT.24)GOTO 204
DO 402 I=1,20
IF(IPRNT(I).EQ.3)PRNT(I)=.T.
402 CONTINUE
NA=NA+1
CALL INTMN(J,NS)
CALL MAIN(NS)

```

```

C
203 CONTINUE
204 CONTINUE
901 CONTINUE
ENDFILE ITMPB
RETURN
END
SUBROUTINE INITAL(NS,IGSTA)

```

```

C *****
C INITIALIZES ALL DATA FOR EACH SEGMENT.
C *****

```

```

COMMON NOS( 20 ), SA( 20 ),SHX( 20 ),SHM( 20 ),SIA( 20 ),IGST(20)
COMMON SAWT( 20 ),SOF( 20 ),SSP( 20 ),GWEA(20 ),PEK( 20 ),LZEI(20)
COMMON GWOUT(20 ),ASM( 20 ),ART( 20 ),GWRR(20 ),SMN( 20 ),UZSX(20)
COMMON LZSX( 20 ),GWSX(20 ),ASTX(20),LZSNX(20),UZSNX(20)
COMMON TIMET(20,20),IELEE(20),IADD(20,20),IBDD(20,20)
COMMON SPAR(20,20)

```

```

COMMON/TIMAA/TIMA
COMMON/STORA/UZS,LZS,GWS,AST
COMMON/CINTC/ARTX,ASM
COMMON/CINFL/XIA,LZEIX,PEKX
COMMON/CCCGW/GWK,GWRRX,GWOUTX
COMMON/CEVAP/WAREA,GWEAX
COMMON /NOMIN/LZSN,UZSN
COMMON/OVFCC/OVFKA,OVFKB,QFIN
COMMON/EVPA/EGS,EET
COMMON/LGPRNT/LPLOT,LPRNT,LTEST
LOGICAL LPLOT,LPRNT,LTEST
COMMON/DATMS/IDTAMS
COMMON/VARIA/OVF,GWF,PP,PERC,QCHAN,RRS,GWOUTT,SPR,QOUT

```

```

COMMON/CLN /PR(24,10),CLIN(10,10),CLIM(7)
COMMON/ROLOS/TITLE(8),SEGNM (2),NOSS(19),DATECD(4)
COMMON/LASTT/LAST
LOGICAL LAST
COMMON/RDSEG/IDAY,IDYND,IDY
COMMON/TAPES/NOSK,ITMPA,ITMPB,ISTAPE,ITAPC
COMMON/INITLL/UZSINT,LZSINT,GWSINT,ASTINT
COMMON/REELQ/OREEL(12),STRNCK,STMFLW,IDYSS,IDYNDS,IDYS
COMMON/QRRL/OREAL

```

```

COMMON/NSEGG/NSEG
COMMON/SUMSS/SUMS(15),ASTR(5)
COMMON /NPTSS/NOPT,NOPTS(15),NPT
COMMON/OPSS/ OPS(10),LOPS
COMMON/ODAYY/ODAY
LOGICAL LOPS
COMMON/SNOWIN/GMD(20),SNOWA(20),SNOWB(20),SNOWC(20),SNOWD(20)
COMMON/SNOW/T,GM,WE,SNWA,SNWB,SNWC,SNWD
LOGICAL STRNCK,STMFLW
COMMON/WRTOT/NA,QQMAX,QQMIN
COMMON/SPARR/SPARE(20)
COMMON/SNOWAB/SHMS
COMMON/PRNTT/IPRNT(20),PRNT(20),IPRNTA(20,20)
COMMON/PRNTA/PRNTRS(13,20)
LOGICAL PRNT
REAL LZSX,LZSNX,LZEI
DIMENSION XYY(30)
REAL LZEIX,LZSN,LZS,LZSINT

```

```

TIMRAT=TIMA/24.0
GWOUTX=GWOUT(NS)
UZS=UZSX(NS)
LZS=LZSX(NS)
GWS=GWSX(NS)
AST=ASTX(NS)
LAST=.F.
NPT=1
QQMAX=0.0
QQMIN=100000000.0
DO 232 J=1,20
PRNTRS(13,J)=1.5
DO 231 I=1,12
PRNTRS(I,J)=0.0
231 CONTINUE
232 CONTINUE
DO 100 I=1,20
PRNT(I)=.F.
100 IPRNT(I)=IPRNTA(I,NS)
GWOUTX=GWOUT(NS)
XIA=SIA(NS)
PEKX=PEK(NS)*TIMRAT
LZEIX=LZEI(NS)*TIMRAT
WAREA=SAWT(NS)
GWEAX=GWEA(NS)
LZSN=LZSNX(NS)
UZSN=UZSNX(NS)
ARTX=ART(NS)
ASMX=ASM(NS)
SHMS=SHM(NS)
GM=GMD(NS)*TIMRAT
WE=SNOWA(NS)
SNWB=SNOWB(NS)

```

```
SNWC=SNWC(NS)
SNWD=SNWD(NS)
DO 118 I=1,15
118 SUMS(I)=0.0
   ASTR(1)=AST
   ASTR(2)=UZS
   ASTR(3)=LZS
   ASTR(4)=GWS
   ASTR(5)=WE
   QREAL=0.0
DO 119 I=1,12
119 QREEL(I)=0.0
   GWRRX=1.0/GWRR(NS)
   GWK=GWRRX** (TIMA/24.0)
C   CONVERSION BETWEEN INCHES AND QUSECS.
   QFIN=SA(NS)*528.0*528.0/(TIMA**432.0)
   OVFKA=0.000818* ((SMN(NS)**0.6)* (SOF(NS)**0.6)/ ((SSP(NS)**0.3)
   OVFKB=1.486* (SQRT(SSP(NS)))/ (SMN(NS)* (SOF(NS)**1.6))
   IF (IDTAMS.LE.0) GOTO 300
   IGSTA3=IGSTA*3
301 CONTINUE
   READ(NDSK) IDEY, (XYY(IYY), IYY=1, IGSTA3)
   IF (IDEY.LT.IDAY-1) GOTO 301
300 CONTINUE
   WRITE(6, 8424) QFIN, OVFKA, OVFKB, GWK
8424 FORMAT(1X, 12E10.3)
DO 400 I=1,20
400 SPARE(I)=SPAR(I, NS)
   SPARE(4)=SPARE(4)*TIMRAT
   SPARE(5)=SPARE(5)*TIMRAT
   SPARE(8)=SPARE(8)*TIMRAT
RETURN
END
```


SUBROUTINE INTMN(J,NS)

C
C
C

INITIALIZES DATA BEFORE EACH ANALYSIS PERIOD.

```

COMMON NOS( 20 ), SA( 20 ), SHX( 20 ), SHM( 20 ), SIA( 20 ), IGST(20)
COMMON SAWT( 20 ), SOF( 20 ), SSP( 20 ), GWEA(20 ), PEK( 20 ), LZEI(20)
COMMON GWOUT(20 ), ASM( 20 ), ART( 20 ), GWRR(20 ), SMN( 20 ), UZSX(20)
COMMON LZSX( 20 ), GWSX(20 ), ASTX(20), LZSNX(20), UZSNX(20)
COMMON TIMET(20,20), IELEE(20), IADD(20,20), IBDD(20,20)
COMMON SPAR(20,20)
COMMON/VARIA/OVF,GWF,PP,PERC,QCHAN,RRS,GWOUTT,SPR,QOUT
REAL LZSX,LZSNX,LZEI
COMMON/EVPA /EGS,EET
COMMON/SPARR/SPARE(20)
COMMON/QRRRL/QREAL
COMMON/REELQ/QREEL(12),STRNCK,STMFLW,IDYSS,IDYNDS,IDYS
LOGICAL STRNCK,STMFLW
COMMON/TIMAA/TIMA
COMMON/CLN /PR(24,10),CLIN(10,10),CLIM(7)
COMMON/SNOWAB/SHMS
COMMON/SNOWIN/GMD(20),SNOWA(20),SNOWB(20),SNOWC(20),SNOWD(20)
COMMON/SNOW/T,GM,WE,SNWA,SNWB,SNWC,SNWD
DIMENSION TEMP(24)
DATA TEMP/0.3,2*0.2,2*0.1,0.0,0.1,0.3,0.5,0.6,0.7,0.8,0.9,1.0,
21.0,2*0.9,0.8,0.7,0.6,0.5,0.4,0.4,0.3/
QCHAN=0.0
EET=0.0
OVF=0.0
GWF=0.0
PP=0.0
PERC=0.0
RJ=J
ITIMB=TIMA*(RJ-1.0)+1.99
ITIMA=TIMA*RJ+0.99
I=IGST(NS)
SPR=0.0
SPR=CLIN(1,I)*TIMA/24.
EGS=CLIN(2,I)*TIMA/24.0
EGS=EGS*SHX(NS)
CLIM(1)=SPR
CLIM(2)=EGS
TT=CLIN(3,I)
CLIM(3)=TT
ELDIF=SPARE(1)-SPARE(2)
T=ELDIF*0.001*SPARE(3)+TT
DO 101 K=3,7
101 CLIM(K)=0.0
RETURN
END

```

SUBROUTINE EVAPW

```

C      *****
C      EVAPORATES WATER OFF VARIOUS STORAGE LOCATION.
C      *****

C      INPUT WAREA GWEA          EGS EET
C      OUTPUT          EGS EET
COMMON/CEVAP/WAREA,GWEA
COMMON/EVPA/EGS,EET
COMMON/VARIA/OVF,GWF,PP,PERC,QCHAN,RRS,GWOUTT,SPR,QOUT
COMMON/STORA/UZS,LZS,GWS,AST
COMMON/OVFCC/OVFKA,QVFKA,QFIN
COMMON/SPARR/SPARE(20)
COMMON/NOMIN/LZSN,UZSN
REAL LZS
C      EVAPORATION FROM WATER SURFACES AND GROUND WATER
      IF(EGS.LT.0.0)EGS=0.0
      ESW=EGS*WAREA
      EGW=EGS*GWEA
      IF(GWS.GT.EGW)GOTO 100
      EGW=GWS
100    CONTINUE
      IF(EGS.GT.ESW)GOTO 101
      ESW=EGS
101    CONTINUE
      QCHAN=QCHAN-ESW*QFIN
      IF(QCHAN.GT.0.0)GOTO 104
      QCHAN=QCHAN+ESW*QFIN
      ESW=QCHAN/QFIN
      QCHAN=0.0
104    EGS=EGS-ESW
      EET=EET+ESW
      IF(EGS.GT.EGW)GOTO 102
      EGW=EGS
102    EGS=EGS-EGW
      EET=EET+EGW
      GWS=GWS-EGW
C      SPARE(8) IS THE FACTOR RELATING EVAP-T TO SOIL WATER ABOUT (0.01)
      EGSBF=EGS
      EETBF=EET
      UZS=PLUS(UZS)
      PUZEV=SPARE(8)*UZS/UZSN
      PUZEV=PLUS(PUZEV)
      EGS=PLUS(EGS)+1.0E-11
      IF(EGS.GT.PUZEV)GOTO 400
      AUZEV=EGS-(EGS*EGS)/(2.0*PUZEV)
      EGS=(EGS*EGS)/(2.0*PUZEV)
      GOTO 401
400    CONTINUE
      AUZEV=PUZEV/2.0
      EGS=EGS-AUZEV

```

```

401 CONTINUE
    EET=EET+AUZEV
    UZS=UZS-AUZEV
    RETURN
    END

```

SUBROUTINE GRNDW(PERC,PP,GWF,GWOUTT)

```

C      *****
C      CALCULATES GROUNDWAETR FLOW
C      *****
C
C      INPUT PERC PP GWOUT GWK      LZS LZSN GWS
C      OUTPUT  GWF          GWS
COMMON/CCCGW/GWK,GWRR,GWOUT
COMMON /NOMIN/LZSN,UZSN
COMMON/STORA/UZS,LZS,GWS,AST
REAL LZT,LZS,LZSN,LZX
GWF=PERC+PP
RETURN
END

```

SUBROUTINE OVERFL(OVF,GWF,QCHAN)

```

C      *****
C      FOR OVERLAND FLOW (NOT USED HERE)
C      *****
COMMON/OVFCC/OVFKA,OVFKB,QFIN
COMMON/STORA/UZS,LZS,GWS,AST
REAL LZS
GWQ=QFIN*GWF
OVFO=OVF*QFIN
QCHAN=OVFO+GWQ
RETURN
END

```

SUBROUTINE INTERC (SPR,RRS)

```

C      *****
C      INTERCEPTS WATER ON TREES ETC.
C      *****

C      INPUT ART,AST,ASM,SPR,      EGS EET
C      OUTPUT AST, RRS,          EGS EET
C      ASM MAX INTERCEPTION STORAGE
C      AST TOTAL INTERCEPTION STORAGE
C      ASD INCREMENTAL STORAGE
C      RRA RAIN IN INTERCEPTION INPUT
C      EGS EVAPORATION FROM GROUND
C      EET TOTAL EVAPORATION SO FAR.  SUMMED ALONG THE WAY
C      RRS RAIN REACHING SURFACE
C      COMMON/EVPA/EGS,EET
C      COMMON/STORA/UZS,LZS,GWS,AST
C      REAL LZS
C      COMMON/CINTC/ART,ASM
C      RRA=SPR*(1.0-ART)
C      RRS=SPR*ART
C      ASD=ASM-AST
C      IF(ASD.LT.0.0)ASD=0.0
C      IF(RRA.GT.ASD)GOTO100
C      AST=AST+RRA
C      GOTO 101
100  RRS=RRA-ASD+RRS
C      AST=ASM
C  EVAPORATION
101  CONTINUE
      IF(AST.LT.EGS)GOTO200
      AST=AST-EGS
      EET=EET+EGS
      EGS=0.0
      RETURN
,200 EGS=EGS-AST
      EET=AST+EET
      AST=0.0
      RETURN
      END

```

SUBROUTINE INFLTR(RRS,OVF,PERC,PP)

```

C      -*****
C      CALCULATES INFILTRATION.
C      *****

C      INPUT PEK,LZEI,RRS,SIA,          LZS LZSN UZS UZSN EGS EET
C      OUTPUT OVF, PERC, PP           UZS EGS EET
C      GWT IS IN FACT THE LOEER ZONE RATIO
COMMON/CINFL/SIA,LZEI,PEK
REAL LZSN,LZS,LZEI,LZEX
COMMON /NOMIN/LZSN,UZSN
COMMON/EVPA/EGS,EET
COMMON/STORA/UZS,LZS,GWS,AST
COMMON/CCCGW/GWK,GWRR,GWOUT
COMMON/SPARR/SPARE(20)

C      BZK=PEK IS THE BORTOM ZONE RECESSION CCNSTANT
      BZK=PEK
      OVF=OVF+RRS*SIA
      RSS=RRS*(1.-SIA)
      CINT=SPARE(6)
      UZS=PLUS(UZS)
      SUCO=EXP(-CINT*UZS/UZSN)
      PINFLT=SPARE(4)*SUCO+SPARE(5)
C      PINFLT IS THE POTENTIAL INFILTRATION.
C      SPARE(5) IS THE LOWEST INFILTRATION RATE (WHEN SOIL IS WET)
C      SPARE(4)+SPARE(5) IS THE HIGHEST INFILTRATION RATE RATE
C      (WHEN THE SOIL IS DRY)
C      SPARE(6) IS COEFF RELATING INFILTRATION TO SOIL MOISTURE
C      SPARE(6) IS ABOUT 1 OR 2
      IF(RSS.GT.PINFLT) GOTO 400
      AINFLT=RSS-(RSS*RSS)/(2.0*PINFLT)
      OVF=OVF+ (RSS*RSS)/(2.0*PINFLT)
      UZS=UZS+AINFLT
      GOTO 401
400  CONTINUE
      AINFLT=PINFLT*0.5
      UZS=UZS+AINFLT
      OVF=OVF+RSS-PINFLT*0.5
401  CONTINUE
C      UBCO IS THE UPPER TO BOTTOM ZONE(OFF SOIL) COELF.
      UBCO=SPARE(9)*UZS/UZSN
      UBF=UBCO*UZS
      IF(UBF.GT.UZS)GOTO, 201
      UZS=UZS-UBF
      LZS=LZS+UBF
      GOTO 202
201  CONTINUE
      UZS=0.0
      LZS=LZS+UZS
202  CONTINUE

```

C BGC0 IS BOTTOM TO GROUND WATER COEFF.

BGC0=SPARE(10)*LZS/LZSN

BGF=BGC0*LZS

IF(BGF.GT.LZS)GOTO 301

GWS=GWS+BGF

LZS=LZS-BGF

GOTO 302

301 CONTINUE

LZS=0.0

GWS=GWS+LZS

302 CONTINUE

C BZK IS THE BOTTOM ZONE CONSTANT IN RECIPROCAL DAYS

BZF=BZK*LZS

LZS=LZS-BZF

C GWK IS THE GROUND WATER CONSTANT IN RECIPROCAL DAYS.

GWK=GWK*GWS

GWS=GWS-GWK

PERC=BZF

PP=GWK

GOTO 999

999 CONTINUE

RETURN

END

SUBROUTINE SNOW(P,WATER)

```

C *****
C CALCULATES THE WATER HELD UP BY SNOWPACK.
C USES TEMPRATURE INDEX METHOD FOR MELT
C *****

C VERSION OF MARCH 26 1973
C WE IS WATER EQUIVLENT (=DEPTH) OF SNOWPACK
COMMON/SNOW/ T,GM,WE,SNWA,SNWB,SNWC,SNWD
C TCOF IS THE TEMPERATURE INDEX
TCOF=SNWB
TMELT=TCOF*(T-32.)
IF(TMELT.LT.0.0)TMELT=0.0

IF(P.LT.1.0E-6)GOTO 700
C SOME PRECIPITATION.
CALL PRECIP(T,P,CNHS,SFALL,RAINM,RAIN)
WE=WE+SFALL
IF(WE.LT.1.0E-6)GOTO 900

C SNOWPACK
AMELT=RAINM+GM+TMELT
IF(WE.LT.AMELT) GOTO 600
WE=WE-AMELT
WATER=RAIN+AMELT
C STILL SOME SNOWPACK LEFT
RETURN

700 CONTINUE
C NO RAIN OR SNOW
IF(WE.LT.1.E-6) GOTO 500
IF((TMELT+GM).GT.WE) GOTO 800
WE=WE-TMELT-GM
WATER=TMELT+GM
RETURN

500 CONTINUE
C NO RAIN OR SNOW AND NO SNOWPACK
WATER=0.0
WE=0.0
RETURN

800 CONTINUE
C NO RAIN AND SNOWPACK DISSAPEARS
WATER=WE
WE=0.0
RETURN

900 CONTINUE

```

```
C      NO SNOWPACK BUT RAIN
      WATER =RAIN
      WE=0.0
      RETURN
```

```
600  CONTINUE
C     SNOWPACK DISSIPERS
      WATER=WE+RAIN
      WE=0.0
      RETURN
```

```
END
```

```
SUBROUTINE PRECIP(T,P,CNHS,SFALL,RAINM,RAIN)
```

```
C      *****
C     CALCULATES IF PRECIPITATION IS RAIN OR SNOE.
C      *****
```

```
IF(T.GT.33.0)GOTO 100
```

```
C:   SNOWFALL
      CNHS=0.0035*P*(32-T)
      SFALL=P
      RAIN=0.0
      RAINM=0.0
      RETURN
```

```
100 CONTINUE
C     RAINFALL
```

```
      SFALL=0.0
      RAIN=P
      RAINM=0.007*P*(T-32.)
      CNHS=0.0
      RETURN
      END
```


SUBROUTINE WRTOUT

```

C      *****
C      PRINTER PLOTS THE SIMULATED AND REAL STREAMFLOWS.
C      *****

COMMON/TAPES/NDISK,ITMPA,ITMPB,ISTAPE,ITAPC
COMMON/RDSEG/IDAY,IDYND,IDY
DIMENSION QX(130),QM(130)
COMMON/TIMAA/TIMA
DIMENSION IA(4),QA(4)
DIMENSION FMT(2)
DIMENSION XAX(10)
COMMON/WRTOT/NA,QQMAX,QQMIN
AL=ALOG(10.)
QQMX=ALOG10(QQMAX)
DO 200 I=1,10
RI=I
QTST=(QQMX/10)*RI
200  XAX(I)=(10.0**QTST)
WRITE(6,243)
243  FORMAT(1H0)
WRITE(6,103)XAX
103  FORMAT(32HIDAY SIM(+) PREC(*) REAL(O) 1.0      10F10.1/
230X,1H.,10(10H*****+),1H.)
FMT(1)=10H(1H+.30X,
QMX=0.0
IND=0
IMAX=24.0/(TIMA-0.001)
DO 110 IDY=IDAY,IDYND
QMAX=0.0 $ QMIN=1000000.0
QRMX=0.0
QRMN=100000000.0
IF(IDY.EQ.(IDY/75)*75)WRITE(6,103)XAX
DO 100 I=1,IMAX
READ(ITMPB)Q,QRLEL,VAR
IF(QMIN.GT.0)QMIN=Q
IF(QMAX.LT.0)QMAX=Q
QMAX=VAR
IF(QMAX.GT.QQMAX)QMAX=QQMAX
IF(QRMN.GT.QRLEL)QRMN=QRLEL
IF(QRMX.LT.QRLEL)QRMX=QRLEL
100  CONTINUE
DO 300 I=1,4
300  QA(I)=0.0
IF(QMIN.GT.1.0)QA(1)=ALOG10(QMIN)
IF(QMAX.GT.1.0)QA(2)=ALOG10(QMAX)
IF(QRMN.GT.1.0)QA(3)=ALOG10(QRMN)
IF(QRMX.GT.1.0)QA(4)=ALOG10(QRMX)
DO 231 I=1,4
IA(I)=(QA(I)/QQMX)*100.
231  CONTINUE

```

```

QMAX=(QMAX-1.0)*0.1
WRITE(6,250)IDY,QMIN,QMAX,QRMN
250  FORMAT(1X,I4,F6.1,3X,F6.3,3X,F6.1,2H ..,100X,1H.)
DO251 I=1,4
IF(IA(I).EQ.0)GOTO 251
IF(IMAX.EQ.1.AND.I.EQ.4)GOTO 251
IF(IA(I).GT.99)IA(I)=99
ENCODE(10,501,FMT(2))IA(I)
501  FORMAT(12,5HX,A1))
AA=1H+
IF(I.GE.3)AA=1H0
IF(I.EQ.2)AA=1H*
WRITE(6,FMT)AA
251  CONTINUE
110  CONTINUE
RETURN
END

```

SUBROUTINE PRNTSB(IPT,X,ALPH)

```

C      *****
C      PRINTS OUT VARIOUS MODEL VARIABLES. CALLED FROM MAIN.
C      PRINTS OUT EACH ANALYSIS PERIOD, DAYLY, OR 10 DAYLY.
C      *****
COMMON/RDSEG/IDAY, IDYND, IDY
COMMON/PRNTT/IPRNT(20), PRNT(20), IPRNTA(20,20)
COMMON/PRNTA/PRNTRSR(13,20)
LOGICAL PRNT
C      PRNTRSR (I,J) I=STORE NO. AND J=TYPE
IF(IPT.GT.90)GOTO 400
PRNT(IPT)=.F.
IP=PRNTRSR(13,IPT)
PRNTRSR(IP,IPT)=X
PRNTRSR(13,IPT)=PRNTRSR(13,IPT)+1.0
IF(IP.EQ.12)GOTO 1101
RETURN
1101 WRITE(6,1201)ALPH,(PRNTRSR(IP,IPT),IP=1,12),IDY
1201  FORMAT(1X,A4,12G10.4,17)
PRNTRSR(13,IPT)=1.5
DO 100 I=1,12
100  PRNTRSR(I,IPT)=0.0
RETURN
400  CONTINUE
DO 401 I=1,20
401  WRITE(6,402)I,(PRNTRSR(IP,I),IP=1,12),IDYND
402  FORMAT(4H END,12,12E10.3,16)
RETURN
END

```

PROGRAM PRECON(INPUT,OUTPUT,TAPE5=INPUT,TAPE6=OUTPUT,TAPE25,TAPE21
2)

C
111 FORMAT(1H 20I5)
301 FORMAT(10H SEG NO. 13.10X,4A10)
104 FORMAT(I4,6X,4A10)
105 FORMAT(10H GAGE NO 14.6X,4A10)
100 FORMAT(20I4)
115 FORMAT(I4,6X,7(I4,F6.6))
401 FORMAT(1X,8A10)
402 FORMAT(8A10)
403 FORMAT(5H 8I10)
16 FORMAT(10X,2I4,5X,2A10,5X,3(2X,I2),2X,3(2X,I2),5X,I3,5X,A10,F5.0)
51 FORMAT(10H STATION 12.5H NO 14.7H NAME 2A10,6H DATE 3(1X,I2)
2,10H MTH LTH 12, 10H DATA ON 10(L1,1X),15H OBS HR. P
2T E 3I3)

C
COMMON TATLE(8)
COMMON NOS(50),IGAGE(10),GAGENM(4)
COMMON NSEGST(10),NOSS(20,10),NOG(10,10),IGNO(7,10,10)
COMMON GGRT(7,10,10),TITLE(8),DATECD(4)
COMMON NGAG(10),SNAM(10,2),SEGNM(4),SNAMA(2),NMOTH(10)
COMMON ELEVA(10),ITIMP(10),ITIMT(10),ITEMF(10)
COMMON CLIM(10,10),PRH(10,24),PR(24,10),CLIN(10,10)
INTEGER SDATE(10,3),FDATE(10,3),SDATEA(3)
LOGICAL LTYP(10,10),LTYPTT(10)
DIMENSION PRSUM(10)
DIMENSION THRN(7,12)

C
NDSK =25
NDISK=21
REWIND NDSK
REWIND NDISK

C
C READ THORNTHAIT DATA
DO 500 I=1,7
 READ(5,501)SNAMA,(THRN(I,J),J=1,12)
 WRITE(6,15)SNAMA,(THRN(I,J),J=1,12)
15 FORMAT(20H THORNTHAITE APPROX - 2A10,12F6.2)
500 CONTINUE
501 FORMAT(2A10,12F5.1)
 DO 577 I=1,12
 THRN(1,I)=THRN(1,I)/720.0
 THRN(2,I)=THRN(2,I)/30.0
577 THRN(6,I)=THRN(6,I)/30.0

C
 READ(5,402)TATLE
 PRINT401,TATLE
 READ(5,100)NSEG
C NSEG NO OF SEGMENTS TO BE CONSIDERED
 DO 201 II=1,NSEG
 READ(5,104)NOS(II),SEGNM

```

PRINT 301,NOS(II),SEGNM
201 CONTINUE

READ(5,100)NOGAG
C NOGAG NO OF GAGES TOTAL
DO 302 II=1,NOGAG
READ(5,104)IGAGE(II),GAGENM
PRINT 105,IGAGE(II), GAGENM
302 CONTINUE
READ(5,100)IGST
C IGST NO OF GAGE GROUP SETS
C
READ(NDISK)TITLE
PRINT 401, TITLE
READ(NDISK)DATECD,DATTT
PRINT 401 , DATECD,DATTT
READ(NDISK)NOST,MTH,IDAY,IDYND
PRINT 403 ,NOST,MTH,IDAY,IDYND
DO 408 I=1,NOST
READ(NDISK)I,NGAG(I),SNAM(I,1),SNAM(I,2),(SDATE(I,J),J=1,3),
2(FDATE(I,J),J=1,3),NMOTH(I),LOG,ELEVA(I)
WRITE(6,16)I,NGAG(I),SNAM(I,1),SNAM(I,2),(SDATE(I,J),J=1,3),
2(FDATE(I,J),J=1,3),NMOTH(I),LOG ,ELEVA(I)
408 CONTINUE
C
WRITE(NDISK)TITLE
WRITE(NDISK)TATLE
CALL DATE(DATET)
WRITE(NDISK)DATECD,DATTT,DATET
WRITE(NDISK)IDAY,IDYND
WRITE(NDISK)IGST
C
DO 310 IG=1,IGST
READ(5,100) NSEGST(IG),(NOSS(I,IG),I=1,19)
WRITE(NDISK) NSEGST(IG),(NOSS(I,IG),I=1,19)
PRINT 111, NSEGST(IG),(NOSS(I,IG),I=1,19)
C NSEGST NO OF SEMENTS IN THIS SET
C NOSS NAMES OF THE SEGMENTS BEING CONSIDERED
NSIG=NSEGST(IG)
DO 220 I=1,NSIG
DO 221 J=1,NSEG
221 IF(NOSS(I,IG).EQ.NOS(J)) GOTO 220
STOP 33003
220 CONTINUE
DO 320 J=1,10
READ 115,NOG(J,IG),((IGNO(I,J,IG),GGRT(I,J,IG)),I=1,7)
C NOG(I) NO OF GAGES BEING CONSIDERED FOR THE I TH CLIMATIC DATA
NSIG=NOG(J,IG)
IF(NSIG.EQ.0)GOTO 320
DO 230 I=1,NSIG
DO 231 II=1,NOGAG
231 IF(IGNO(I,J,IG).EQ.IGAGE(II))GOTO 230

```

```

STOP 30004
230 CONTINUE
320 CONTINUE
310 CONTINUE
C
DO 322 IMTH=1,MTH
DO 502 I=1,10
502 LTYPTT(I)=.F.
READ(NDISK)IMTH, IDYMO
DO 409 IST=1,NOST
READ(NDISK)ITT,NOGAA,SNAMA,SDATEA,LTH,(LTYP(IST,I),I=1,10)
2,ITIMP(IST),ITIMT(IST),ITEME(IST)
WRITE(6,51) IST,NOGAA,SNAMA,SDATEA,LTH,(LTYP(IST,I),I=1,10)
2,ITIMP(IST),ITIMT(IST),ITEME(IST)
DO 503 II=1,10
LTYPTT(II)=LTYP(IST,II).OR.LTYPTT(II)
503 CONTINUE
409 CONTINUE
KMT=SDATEA(2)
C
DO 321 IDAYA=1, IDYMO
READ(NDISK)IDAY
DO 332 IST=1,NOST
READ(NDISK)(CLIM(IST,I),I=2,8)
332 CONTINUE
DO 323 IST=1,NOST
DO 665 I=1,24
READ(NDISK)PRH(IST,I)
665 CONTINUE
323 CONTINUE
C
DO 350 IG=1,IGST
C
DO 460 I=1,24
460 PR(I,IG)=0.0
IF(.NOT.LTYPTT(I))GOTO 510
NOGA=NOG(I,IG)
IF(NOGA.EQ.0)GOTO 510
DO 450 K=1,NOGA
DO 451 J=1,NOST
JP=J
451 IF(IGNO(K,1,IG).EQ.NGAG(J))GOTO 453
STOP 30001
453 CONTINUE
DO 461 I=1,24
IF(.NOT.LTYP(JP,1))GOTO 520
PR(I,IG) =PRH(JP,I)*GGRT(K,1,IG)+PR(I,IG)
GOTO 461
520 CONTINUE
PR(I,IG)=THRN(1,KMT)*GGRT(K,1,IG)+PR(I,IG)
461 CONTINUE
450 CONTINUE

```

```

GOTO 519
510 CONTINUE
DO 511 I=1,24
PR(I,IG)=THRN(1,KMT)
511 CONTINUE
519 CONTINUE

```

```

DO 490 KK=2,8
IF(.NOT.LTYP(TT(KK)))GOTO 530
NOGA=NOG(KK,IG)
IF(NOGA.EQ.0)GOTO530
KJ=KK-1
CLIN(KJ,IG)=0.0
DO 480 K=1,NOGA
DO 479 J=1,NOST
JP=J
IF(IGNO(K,KK,IG).EQ.NGAG(J)) GOTO 470
479 CONTINUE
STOP 30002
470 CONTINUE
IF(.NOT.LTYP(JP,KK))GOTO 540
CLIN(KJ,IG)=CLIN(JP,KK)*GGRT(K,KK,IG)+CLIN(KJ,IG)
GOTO480
540 CONTINUE
CLIN(KJ,IG)=THRN(KJ,KMT)*GGRT(K,KK,IG)+CLIN(KJ,IG)
480 CONTINUE
GOTO490
530 CONTINUE
KJ=KK-1
CLIN(KJ,IG)=THRN(KJ,KMT)
490 CONTINUE
350 CONTINUE
WRITE(NDSK)IDAY
DO 362 IG=1,IGST
WRITE(NDSK)(PR(I,IG),I=1,24)
WRITE(NDSK)(CLIN(I,IG),I=1,7)
PRSUM(IG)=0.0
DO 635 I=1,24
635 PRSUM(IG)=PRSUM(IG)+PR(I,IG)
WRITE(6,8632)IDAY,IG,PRSUM(IG),(CLIN(I,IG),I=1,7)
8632 FORMAT(1X,2I5,8E14.2)
362 CONTINUE
321 CONTINUE
322 CONTINUE
C
ENDFILE NDSK
STOP 77777
END

```

```

PROGRAM REEDAT(INPUT,OUTPUT,TAPE5=INPUT,TAPE6=OUTPUT,TAPE21,
COMMON/DAYDA/IMONTH(I2),IYEAR(30),IMONTHC(I2)
COMMON PRH(4,744)
DIMENSION ELEVA(10)
DIMENSION ITIMP(10)
DIMENSION ITIMT(10)
DIMENSION ITEME(10)
DIMENSION TITLE(8)
DIMENSION DATECD(4)
DIMENSION NGAG(10),SNAM(10,2),SNAMA(10,2),NMOTH(10)
DIMENSION PRDIST(24)
DIMENSION PRODD(10)
DIMENSION PRD(5,31)
DIMENSION EVAP(5,31)
DIMENSION TMAX(5,31)
DIMENSION TMIN(5,31)
DIMENSION WIND(5,31)
DIMENSION SNFA(5,31)
DIMENSION SNOG(5,31)
DIMENSION PRDC(5,24)
INTEGER SDATEA(5,3),SDATE(3),SDATE(10,3),FDATE(10,3)
INTEGER CDNOB,CDNOC,CDNOD,CDNB,CDNC,CDND
LOGICAL LTY(10,10)
DIMENSION NOGAA(10),LTT(10)
DATA PRD /155*0.0/
DATA EVAP /155*0.0/
DATA TMAX /155*0.0/
DATA TMIN /155*0.0/
DATA WIND /155*0.0/
DATA SNFA /155*0.0/
DATA SNOG /155*0.0/
DATA PRDC /120*0.0/
DATA PRDIST /0.02,0.02,5*0.01,0.03,0.07,0.09,0.1
2,0.09,0.06,0.03,0.02,0.01,0.02,0.03,0.05,0.07,0.08,0.08,0.06,0.04/
DATA DATECD /10HDATA COMPI,10HLED ON THE,10H COMPUTER ,4H ON /
DO 5556 I=1,4
DO 5556 J=1,744
PRH(I,J)=0.0
5556 CONTINUE
NDISK=21
IDISK=11
REWIND IDISK
REWIND NDISK
READ(5,9) TITLE
9 FORMAT(8A10)
READ(5,10)NOST,MTH,STDATE
10 FORMAT(I2,I3,3(1X,I2))
CALL DAYM(IDAY,STDATE(1),STDATE(2),STDATE(3))
WRITE(NDISK)TITLE
CALL DATE(DATTT)
WRITE(NDISK)DATECD,DATTT
INTOT=MTH+STDATE(2)-1

```

```

ITOT=IMTOT/12 +STDATE(3)
ITOTA=STDATE(3)
ITET=IMTOT-(IMTOT/12)*12+1
CALLDAYM(IDYND,STDATE(1),ITET,ITOT)
IDYND=IDYND-1
WRITE(NDISK)NOST,MTH,IDAY ,IDYND
WRITE(6,8)TITLE
WRITE(6,7)DATECD,DATTT
7  FORMAT(5H0      5A10)
8  FORMAT(15H TITLE IS      8A10)
WRITE(6,15)NOST,MTH,STDATE,IDAY
15  FORMAT(20HNO. OF STATIONS=      12,20H NO OF MONTHS=      15,
220H STARTING DATE=      313,20H STARTING DAY=      15)
WRITE(6,62)
DO 12 I=1,NOST
READ(IDISK,20)NGAG(I),SNAM(I,1),SNAM(I,2),(SDATE(I,J),J=1,3),
2(FDATE(I,J),J=1,3),NMOTH(I),LOG,ELEVA(I)
WRITE(NDISK)I,NGAG(I),SNAM(I,1),SNAM(I,2),(SDATE(I,J),J=1,3),
2(FDATE(I,J),J=1,3),NMOTH(I),LOG,ELEVA(I)
20  FORMAT((I4,2A10,3(1X,I2),2X,3(1X,I2),I3,A10,F5.0)
WRITE(6,16)I,NGAG(I),SNAM(I,1),SNAM(I,2),(SDATE(I,J),J=1,3),
2(FDATE(I,J),J=1,3),NMOTH(I),LOG ,ELEVA(I)
16  FORMAT( 4X,2I6,5X,2A10,5X,3(2X,I2),2X,3(2X,I2),5X,I3,5X,A10,F5.0)
12  CONTINUE

```

C
C
C
C

```

ITOT IS FINISH YEAR ITOTA IS START YEAR. IXY IS YEAR.
DONE TO EFFECTIVE END OF PROGRAM
DO 30 IXY=ITOTA,ITOT
ITET=12
ISTT=1
IF(IXY.EQ.ITOTA)ISTT=STDATE(2)
IF(IXY.EQ.ITOT)ITET=IMTOT-(IMTOT/12)*12+1
DO 30 IXX=ISTT,ITET

```

C UXX IS MONTH ISTT IS START MONTH AND ITET IS FINISH MONTH
C DONE TO EFFECTIVE PROGRAM END

```

IMTH=((IXY-STDATE(3))*12+IXX-STDATE(2)+1.
IDYMO=IMONTH(IXX)
IF((IXY/4)*4.EQ.0.AND.IMO.EQ.2)IDYMO= 29
WRITE(6,62)
WRITE(6,62)
DO 40 IST=1,NOST

```

C DONE TO END OF READS. DOESNT INCLUDE WRITES

```

WRITE(6,62)
READ(IDISK,50)NOGAA(IST),SNAMA(IST,1),SNAMA(IST,2),(SDATEA(IST,I),
2I=1,3),LTT(IST),(LTYP(IST,I),I=1,10),ITIMP(IST),ITIMT(IST),ITEME(I
2ST)
50  FORMAT(I4,2A10,3(1X,I2),11X,I2,1X,10L1,6X,3(1X,I2))

```



```
WRITE(6,51)IST,NOGAA(IST),SNAMA(IST,1),SNAMA(IST,2),(SDATEA(IST,I)
2,I=1,3),LTT(IST),(LTP(IST,I),I=1,10),ITIMP(IST),ITIMT(IST),ITEME(
3IST)
```

```
51 FORMAT( 5H          12,5H  NOI4,7H NAME 2A10,6H DATE 3(1X,I2)
2,10H MTH LTH      13, 10H DATA ON      10(L1,1X),15H  OBS HR. P
2T E 3I3)
```

```
IF(NOGAA(IST).NE.NGAG(IST))STOP22210
IF(SDATEA(IST,3).NE.IXY)STOP20011
IF(SDATEA(IST,2).NE.IXX)STOP 20012
IF(LTT(IST).NE.IDYMO)STCP20014
```

C
C

```
101 IF(LTYP(IST,1))200,102
102 IF(LTYP(IST,2))250,103
103 IF(LTYP(IST,3))400,106
106 IF(LTYP(IST,4))450,107
217 CONTINUE
108 IF(LTYP(IST,6))550,109
109 IF(LTYP(IST,7))600,110
110 IF(LTYP(IST,8))650,111
111 IF(LTYP(IST,1))700,1033
1033 IF(LTYP(IST,1).AND.LTYP(IST,2))300,104
104 IF(LTYP(IST,1).AND..NOT.LTYP(IST,2))350,105
105 IF(LTYP(IST,2).AND..NOT.LTYP(IST,1))750,1066
1066 CONTINUE
GOTO 800
```

C
C

```
200 CONTINUE
DAILY PRECIPITATION
READ(IDISK,260)NOGAGB,IYRB,IMOB,LTH,PREC,CDNOB,(PRD(IST,I),I=1,12)
WRITE(6,263)NOGAA(IST),(SDATEA(IST,I),I=1,3)
263 FORMAT(12H STATION NO I4,6H DATE 3(1X,I2),18H DAILY PRECIP. )
IF(NOGAGB.NE.NGAG(IST))STOP20020
IF(IYRB.NE.IXY)STOP20021
IF(IMOB.NE.IXX)STOP20023
IF(LTH.NE.IDYMO)STOP20024
IF(PREC.NE.2HPD)STOP20025
READ(IDISK,204)CDNOC,(PRD(IST,I),I=13,24)
READ(IDISK,204)CDNOD,(PRD(IST,I),I=25,LTH)
IF(CDNOB.NE.1.OR.CDNOC.NE.2.OR.CDNOD.NE.3)STOP20001
GOTO 102
```

C
C

```
250 CONTINUE
HOURLY PRECIPITATION
WRITE(6,273)NOGAA(IST),(SDATEA(IST,I),I=1,3)
273 FORMAT(12H STATION NO I4,6H DATE 3(1X,I2),18H HOURLY PREC.. )
I=1
TOTLLA=0.0
280 CONTINUE
IIN=I*24-24+1 $ IOUT=I*24-12
```

```

READ(IDISK,281)NOGAGB,IYRB,IMOB,IDY,INX,PREC,CDNOB,
2(PRH(IST,I),I=IIN,IOUT),TOTL
IF(I.EQ.1)TOTLL=TOTL
281  FORMAT(I4,4(1X,I2),1X,A2,I1,12F4.2,8X,F4.2)
      IF(NOGAGB.NE.NGAG(IST))STOP20030
      IF(IYRB.NE.IXY)STOP20031
      IF(IMOB.NE.IXX)STOP20033
      IF(IDY.NE.I)STOP 20034
      IF(PREC.NE.2HPP)STOP20035
      IIN=I*24-12+1  $  IOUT=I*24
      READ(IDISK,281)NOGAGB,IYRB,IMOB,IDY,INX,PREC,CDNOB,
      2(PRH(IST,I),I=IIN,IOUT),TOTLA
      IF(NOGAGB.NE.NGAG(IST))STOP20030
      IF(IYRB.NE.IXY)STOP20031
      IF(IMOB.NE.IXX)STOP20033
      IF(IDY.NE.I)STOP 20034
      IF(PREC.NE.2HPP)STOP20035
      TOTLB=0.0
      INN=IOUT-23
      DO290 IJK=INN,IOUT
290  TOTLB=TOTLB+PRH(IST,IJK)
      IF(ABS(TOTLA-TOTLB).GT.0.00001)WRITE(6,291) TOTLA,TOTLB
291  FORMAT(40H TOTALS DONT AGREE                2F10.3)
      I=I+1
      IF(INX.EQ.1)      GOTO 293
      IF(INX.LE.IDY)INX=0
      IF(I.GT.IDYMO)GOTO 252
      IF(I.EQ.INX.OR.INX.EQ.0)GOTO 280
      IIN=I*24-24+1
      IOUT=INX*24
      DO 283 J=IIN,IOUT
283  PRH(IST,J)=0.0
      I=INX
      IF(I.GT.IDYMO)GOTO 252
      TOTLLA=TOTLA+TOTLLA
      GOTO 280
293  CONTINUE
      IIN=I*24-23
      IOUT=744
      DO 294 J=IIN,IOUT
294  PRH(IST,J)=0.0
252  CONTINUE
      IF(ABS(TOTLLA-TOTLL).GT.0.00001)WRITE(6,291)TOTLLA,TOTLL
      GOTO 103

C
C
C
C
400  CONTINUE
      READ(IDISK,203)NOGAGR,IYRB,IMOB,LTH,PREC,CONB,(EVAP(IST,I),I=1,12)
      IF(NOGAGR.NE.NGAG(IST))STOP20101
      WRITE(6,333)NOGAA(IST),(SDATEA(IST,I),I=1,3)

```

```

333  FORMAT(12H STATION NO  I4,6H DATE 3(1X,I2),18HEVAPORATION      )
      IF(IYRB.NE.IXY)STOP20102
      IF(IMOB.NE.IXX)STOP20104
      IF(LTH.NE.IDYMO)STOP20105
      IF(PREC.NE.2HEV)STOP20107
      READ(IDISK,204)CDNC,(EVAP(IST,I),I=13,24)
      READ(IDISK,204)CDND,(EVAP(IST,I),I=25,LTH)
      IF(CDNB.NE.1.OR.CDNC.NE.2.OR.CDND.NE.3)STOP20150
      GOTO 106

```

```

C
C
450  CONTINUE
      WRITE(6,463)NOGAA(IST),(SDATEA(IST,I),I=1,3)
463  FORMAT(12H STATION NO  I4,6H DATE 3(1X,I2),18HMAX. TEMP      )
      READ(IDISK,205)NOGAGB,IYRB,IMOB,LTH,PREC,CDNB,(TMAX(IST,I),I=1,12)
      IF(PREC.NE.2HTL)STOP20107
      IF(NOGAGB.NE.NGAG(IST))STOP20101
      IF(IYRB.NE.IXY)STOP20102
      IF(IMOB.NE.IXX)STOP20104
      IF(LTH.NE.IDYMO)STOP20105
      READ(IDISK,206)CDNC,(TMAX(IST,I),I=13,24)
      READ(IDISK,206)CDND,(TMAX(IST,I),I=24,36)
      IF(CDNB.NE.1.OR.CDNC.NE.2.OR.CDND.NE.3)STOP20150
      TOTT=0.0
      DO 464 J=1,LTH
464  TOTT=TOTT+TMAX(IST,J)
      RLTH=LTH
      IF(ABS(TOTT*RLTH-TMAX(IST,36)*10.0).GT.0.1)WRITE(6,465)TOTT
465  FORMAT(30H TEMPERATURE MEANS DONT AGREE      F10
      GOTO 107

```

```

C
C
500  CONTINUE
      WRITE(6,503)NOGAA(IST),(SDATEA(IST,I),I=1,3)
503  FORMAT(12H STATION NO  I4,6H DATE 3(1X,I2),18H MINIMUM TEMP.  )
      READ(IDISK,205)NOGAGR,IYRB,IMOB,LTH,PREC,CDNB,(TMIN(IST,I),I=1,12)
      IF(NOGAGR.NE.NGAG(IST))STOP20101
      IF(IYRB.NE.IXY)STOP20102
      IF(IMOB.NE.IXX)STOP20104
      IF(LTH.NE.IDYMO)STOP20105
      IF(PREC.NE.2HTS)STOP20107
      READ(IDISK,206)CDNC,(TMIN(IST,I),I=13,24)
      READ(IDISK,206)CDND,(TMIN(IST,I),I=24,36)
      IF(CDNB.NE.1.OR.CDNC.NE.2.OR.CDND.NE.3)STOP20150
      TOTT=0.0
      DO 510 J=1,LTH
510  TOTT=TOTT+TMIN(IST,J)
      RLTH=LTH
      IF(ABS(TOTT*RLTH-TMIN(IST,36)*10.).GT.0.1)WRITE(6,465)TOTT
      GOTO 108

```

```

550 CONTINUE
WRITE(6,553)NOGAA(IST),(SDATEA(IST,I),I=1,3)
553 FORMAT(12H STATION NO I4,6H DATE 3(1X,I2),18H WIND FLOW )
READ(IDISK,203)NOGAGB,IYRB,IMOB,LTH,PREC,CDNB,(WIND(IST,I),I=1,12)
IF(NOGAGB.NE.NGAG(IST))STOP20101
IF(IYRB.NE.IXY)STOP20102
IF(IMOB.NE.IXX)STOP20104
IF(LTH.NE.IDYMO)STOP20105
IF(PREC.NE.2HWD)STOP20107
READ(IDISK,204)CDNC,(WIND(IST,I),I=13,24)
READ(IDISK,204)CDND,(WIND(IST,I),I=25,LTH)
IF(CDNB.NE.1.OR.CDNC.NE.2.OR.CDND.NE.3)STOP20150
GOTO109

```

C

C

```

600 CONTINUE
WRITE(6,603)NOGAA(IST),(SDATEA(IST,I),I=1,3)
603 FORMAT(12H STATION NO I4,6H DATE 3(1X,I2),18H SNOWFALL )
READ(IDISK,203)NOGAGB,IYRB,IMOB,LTH,PREC,CDNB,(SNFA(IST,I),I=1,12)
IF(NOGAGB.NE.NGAG(IST))STOP20101
IF(IYRB.NE.IXY)STOP20102
IF(IMOB.NE.IXX)STOP20104
IF(LTH.NE.IDYMO)STOP20105
IF(PREC.NE.2HSF)STOP20107
READ(IDISK,204)CDNC,(SNFA(IST,I),I=13,24)
READ(IDISK,204)CDND,(SNFA(IST,I),I=25,LTH)
IF(CDNB.NE.1.OR.CDNC.NE.2.OR.CDND.NE.3)STOP20150
GOTO 110

```

C

C

```

650 CONTINUE
WRITE(6,653)NOGAA(IST),(SDATEA(IST,I),I=1,3)
653 FORMAT(12H STATION NO I4,6H DATE 3(1X,I2),18H SNOW ON GRND. )
READ(IDISK,203)NOGAGB,IYRB,IMOB,LTH,PREC,CDNB,(SNOG(IST,I),I=1,12)
IF(NOGAGB.NE.NGAG(IST))STOP20101
IF(IYRB.NE.IXY)STOP20102
IF(IMOB.NE.IXX)STOP20104
IF(LTH.NE.IDYMQ)STOP20105
IF(PREC.NE.2HSG)STOP20107
READ(IDISK,204)CDNC,(SNOG(IST,I),I=13,24)
READ(IDISK,204)CDND,(SNOG(IST,I),I=25,LTH)
IF(CDNB.NE.1.OR.CDNC.NE.2.OR.CDND.NE.3)STOP20150
GOTO 111

```

C

C

```

700 CONTINUE
C TO READ THE FIRST DAY OF THE NEXT MOUNTHS PRECIPITATION FIGURES.
IF(IMTH.EQ.MTH)GOTO1033
READ(IDISK,701)PRDDD(IST)
701 FORMAT(/,20X,F5.2) -
BACKSPACE IDISK
BACKSPACE IDISK

```

GOTO 1033

C

C

300 CONTINUE

C

ASSUME THE DILY PRECIPITATION IS MORE ACCURATE CORREST THE HOURLY

DO 302 J=1,LTH

SUM=0.0

IF(J.EQ.1)GOTO313

DO 303 I=1,24

IN=J*24-24+I-24+ITIMP(IST)

303 SUM=PRH(IST,IN)+SUM

GOTO 316

313 CONTINUE

IF(IMTH.EQ.1)GOTO317

IIN=ITIMP(IST)+1

DO314 I=IIN,24

314 SUM=SUM+PRDC(IST,I)

317 CONTINUE

IIN=ITIMP(IST)

DO 315 I=1,IIN

315 SUM=SUM+PRH(IST,I)

IF(IMTH.EQ.1)SUM=SUM*24/IIN

316 CONTINUE

IF(J.EQ.1)GOTO320

DO 304 I=1,24

IN=J*24-24+I-24+ITIMP(IST)

304 PRH(IST,IN)=PRH(IST,IN)*PRD(IST,J)/SUM

GOTO 330

320 CONTINUE

IIN=ITIMP(IST)

DO 321 I=1,IIN

321 PRH(IST,I)=PRH(IST,I)*PRD(IST,I)/SUM

IF(IMTH.EQ.1)GOTO330

IIN=ITIMP(IST)+1

DO 323 I=IIN,24

323 PRDC(IST,I)=PRDC(IST,I)*PRD(IST,I)/SUM

330 CONTINUE

302 CONTINUE

GOTO 103

C

C

350 CONTINUE

C

ASUMES NO HOURLY PRECIPITATION. USES DISTRUBUTION TO GRT HOURLY

IF(IMTH.EQ.1)GOTO361

IIN=ITIMP(IST)+1

DO 360 I=IIN,24

PRDC(IST,I)=PRD(IST,I)*PRDIST(I)

360 CONTINUE

361 CONTINUE

DO 353 J=2,LTH

DO 354 I=1,24

IN=J*24-24+I-24+ITIMP(IST)

```

IX=I+ITIMP(IST)
IF(IX.GE.25)IX=IX-24
354 PRH(IST,IN)=PRD(IST,J)*PRDIST(IX)
353 CONTINUE
IF(IMTH.NE.MTH) GOTO 370
IIN=ITIMP(IST)+1
DO 362 I=IIN,24
IX=LTH*24-24+I
362 PRH(IST,IX)=PRDD(IST)*PRDIST(I)
WRITE(6,3856)IMTH
3856 FORMAT(I10)
IF(IMTH.NE.1)GOTO 370
IIN=ITIMP(IST)+1
DO 371 I=1,IIN
PRH(IST,I)=PRH(IST,IIN)
371 CONTINUE
370 CONTINUE
GOTO105

```

C
C

```

750 CONTINUE
C ASSUMES NO DAYLY PRECIPITATION ADD UP HOURLY TO GET DAILY
IF(ITIMP(IST).EQ.0)ITIMP(IST)=7
IF(ITIMP(IST).EQ.0.AND.ITIMT(IST).NE.0)ITIMP(IST)=ITIMT(IST)
IF(ITIMP(IST).EQ.0.AND.ITEME(IST).NE.0)ITIMP(IST)=ITEME(IST)
PRD(IST,1)=0.0
IIN =ITIMP(IST)
IF(IMTH.NE.1)GOTO 760
DO 751 I=1,IIN
PRD(IST,1)=PRD(IST,1)+PRH(IST,I)
751 CONTINUE
PRD(IST,1)=PRD(IST,1)*(24/ITIMP(IST))
GOTO 770
760 CONTINUE
DO 761 I=1,IIN
761 PRD(IST,1)=PRD(IST,1)+PRH(IST,I)
IIN=IIN+1
DO 762 I=IIN,24
762 PRD(IST,1)=PRD(IST,1)+PRDC(IST,I)
770 CONTINUE
DO 753 J=2,LTH
PRD(IST,J)=0.0
DO 754 I=1,24
II=J*24-24+I-24+ITIMP(IST)
PRD(IST,J)=PRH(IST,II)+PRD(IST,J)
754 CONTINUE
753 CONTINUE
GOTO 1066

```

C
C

```

800 CONTINUE
40 CONTINUE

```

C
C

```

IF (INTH.EQ.1) GOTO 962
DO 961 IST=1, NOST
DO 961 IIN=1, 24
WRITE (NDISK) PRDC (IST, IIN)
961 CONTINUE
962 CONTINUE
WRITE (NDISK) INTH, IDYMO
DO 963 IST=1, NOST
WRITE (NDISK) IST, NOGAA (IST), SNAMA (IST, 1), SNAMA (IST, 2), (SDATEA (IST, I
2), I=1, 3), LTT (IST), (LTP (IST, I), I=1, 10), ITIMP (IST), ITIMT (IST), ITEME
3 (IST)
963 CONTINUE
LTH=IDYMO
DO 821 IST=1, NOST
DO 821 I=1, 24
IIN=I+LTH*24-24
821 PRDC (IST, I)=PRH (IST, IIN)
CALL DAYM (IDEY, I, IXX, IXY)
IIN=LTH-1
DO 950 J=1, IIN
IDAY=IDEY+J-1
WRITE (NDISK) IDAY
DO 953 IST=1, NOST
WRITE (NDISK) PRD (IST, J), EVAP (IST, J), TMAX (IST, J), TMIN (IST, J)
2, WIND (IST, J), SNFA (IST, J), SNOG (IST, J)
953 CONTINUE
DO 954 IST=1, NOST
DO 951 I=1, 24
IN=J*24-24+I
951 WRITE (NDISK) PRH (IST, IN)
954 CONTINUE
950 CONTINUE
IDAY=IDEY+LTH-1
WRITE (NDISK) IDAY
J=LTH
DO 955 IST=1, NOST
WRITE (NDISK) PRD (IST, J), EVAP (IST, J), TMAX (IST, J), TMIN (IST, J)
2, WIND (IST, J), SNFA (IST, J), SNOG (IST, J)
955 CONTINUE
30 CONTINUE

C
C
DO 981 IST=1, NOST
DO 981 IIN=1, 24
WRITE (NDISK) PRDC (IST, IIN)
981 CONTINUE

C
C
ENDFILE NDISK
WRITE (6, 9999)

```

9999 FORMAT(20H * END OF EXECUTION)
STOP77777

C

260 FORMAT(14,3(1X,12),4X,A2,11,12F5.2)
204 FORMAT(19X,11,12F5.2)
203 -FORMAT(14,3(1X,12),4X,A2,11,12F5.2)
205 -FORMAT(14,3(1X,12),4X,A2,11,12F5.0)
206 FORMAT(19X,11,12F5.0)
62 FORMAT(1H)

END

SUBROUTINE DAYM (IDAY, IDY, IMO, IYR)

C

CALCULATES THE DAY FROM 1940

COMMON/DAYDA/ IMONTH(12), IYEAR(30), IMONTHC(12)

DATA IMONTH/31,28,31,30,31,30,31,31,30,31,30,31/

DATA IMONTHC/0,31,59,90,120,151,181,212,243,273,304,334/

DATA IYEAR/0,365,730,1096,1461,1826,2191,2557,2922,3287,3652,
24018,4383,4748,5113,5479,5844,6209,6574,6940,7305,7670,8035,8401,
38766,9131,9496,9862,10227,10592/

IF(IDY.LT.1.OR.IDY.GT.31)GOTO 800

IF(IMO.LT.1.OR.IMO.GT.12)GOTO 800

IF(IYR.LT.50.OR.IYR.GT.79)GOTO 800

IYR=IYR-49

IDAY=IYEAR(IYR)+IMONTHC(IMO)+IDY

IF(((IYR/4)*4-IYR).EQ.0.AND.IMO.GE.3)IDAY=IDAY+1

RETURN

800 WRITE(6,801)IDY,IMO,IYR

801 FORMAT(50H *****ERROR IN DATE =

3110)

STOP 10007

ENTRY DATM

IF(IDAY.GT.10957.OR.IDAY.LE.0)GOTO 400

DO 200 I=1,30

II=I

200 IF(IYEAR(I).GE.IDAY)GOTO 210

IYR=30

GOTO 220

210 IYR=II-1

220 ITEM=IDAY-IYEAR(IYR)

IYR=IYR+49

DO 300 I=1,12

II=I

300 IF(IMONTHC(I).GE.ITEM)GOTO 310

IMO=12

GOTO 320

310 IMO=II-1

320 IDY=ITEM-IMONTHC(IMO)

RETURN

400 WRITE(6,401)IDAY

401 FORMAT(50H *****ERROR IN IDAY=

110)

STOP 10001

END


```

PROGRAM RATNGC(INPUT,OUTPUT,TAPE5=INPUT,TAPE6=OUTPUT
2,TAPE10
2,MYPC,TAPE8=MYPC,
2OUTA,OUTB,OUTC,
2TAPE3=OUTA,TAPE4=OUTB,TAPE9=OUTC,
2MYPNCH,TAPE7=MYPNCH)
DIMENSION STR(372),STRX(372)
DIMENSION RLOG(100)
DIMENSION QHUND(12)
DIMENSION STG(100)
DIMENSIONRATNG(100),TITLE(8),SWAG(12),Q(12),QM(130),OX(130)
IDAYLS=0
READ(5,1)TITLE
WRITE(6,50)
WRITE(7)TITLE
WRITE(6,3)TITLE
C NUMBER OF POINTS ON THE RATING CURVE AND DIVISIONS BETWEEN
C READ(5,4)NUM, DIV, START
DISCHARGES AT THESE POINTS
DO 435 I=1, NUM
435 STG(I)=START+FLOAT(I)*DIV
READ(5,2)(RATNG(I), I=1, NUM)
DO 440 I=1, NUM
RATN=RATNG(I)
RLOG(I)=ALOG10(RATN)
WRITE(6,441) STG(I),RATNG(I),RLOG(I)
441 FORMAT(1X, F8.2,1H=F8.2,10X,F8.4)
440 CONTINUE
READ(5,1)TITLE
WRITE(6,51)
WRITE(7)TITLE
WRITE(6,3)TITLE
READ(5,600)IDAYA, IDAYB, IPLT, IPPLT
WRITE(7)IDAYA, IDAYB
600 FORMAT(4I4)
WRITE(6,801)IDAYA, IDAYB
801 FORMAT(20H DAYS START END 218)
INU=0
98 INO=0
99 READ(5,103)NIN, IYR, IMH, IDY, TOTLL, SWAG
IF(NIN.EQ.8888)GOTO 888
IF(NIN.EQ.9999)GOTO 999
CALL DAYN(IDAY, IDY, IMH, IYR)
IF(IDAYLS.NE.IDAY)WRITE(6,568)IDAY, IDY, IMH, IYR
568 FORMAT(20H MISSING DAY 515)
IDAYLS=IDAY+1
OMAX=0.0 SQMIN=1000000000.0
TOTLL=0.0
ODAY=0.0
DO 110 I=1,12
ILES=I-1
IF(ILES.EQ.0)ILES=1

```

```

IF(SWAG(I).LT.0.000001)SWAG(I)=SWAG(I*LES)
TOTLLL=TOTLLL+SWAG(I)
STAGE=SWAG(I)
RNUM=NUM
IF(STAGE.GT.RNUM/DIV)GOTO 200
CALL RATING(STAGE,QQ,RATNG,NUM,DIV,START)
GOTO 201
200 QQ=RATNG(NUM)
201 CONTINUE
QDAY=QDAY+QQ
Q(I)=QQ
IF(QMIN.GT.Q(I))QMIN=Q(I)
IF(QMAX.LT.Q(I))QMAX=Q(I)
110 CONTINUE
DO 530 I=1,12
INX=INU+I
STRX(INX)=INX
STR(INX)=Q(I)
530 CONTINUE
INU=INU+12
DO 827 I=1,12
827 OHUND(I)=Q(I)*100.
WRITE(8,400)IN, IDY, IMH, IYR, OHUND
400 FORMAT(11,1HD,3I2,12F6.0)
WRITE(7)IDAY,0
QDAY=QDAY/12
CALL BARSTR(QDAY,TITLE, IDY, IMH, IYR)
IF(IPLT.LT.1)GOTO 845
845 CONTINUE
WRITE(9,624)IDY, IMH, IYR, QDAY, IDAY, QMIN, QMAX
624 FORMAT(1X,2(12,1H/),12,9H FLOW= F10.3,10H IDAY= 14
2,20H MAX MIN FLOW 2F10.2)
WRITE(4,546)IDAY, SWAG
546 FORMAT(1X,14,12F10.2)
WRITE(3,547)Q
547 FORMAT(1H04X,12F10.3)
IF(TOTLL.LT.0.1)GOTO 540
IF(ABS(TOTLLL-TOTLL).GT.0.000001)WRITE(6,253)TOTLLL,TOTLL , IDY, IMH
253 FORMAT(20H TOTALS DONT AGREE 2F7.2,2I5)
540 CONTINUE
DO 425 I=1,6
J=I+INO
JJ=I*2
JI=JJ-1
OM(J)=Q(JJ)
OX(J)=Q(JI)
425 CONTINUE
INO=INO+6
IF(INO.GT.124)GOTO 97
GOTO 99
97 IF(IPLT.LT.1)GOTO 842
CALL PLOT2(QM,OX,RATNG(NUM),0.0,126.0,0.0,50,INO,12)

```

```

842 CONTINUE
   GOTO 98
888 CONTINUE
   READ(5,858)
858 FORMAT(//)
859 CONTINUE
   INU=0
   GOTO 99
999 IF(IPLT.LT.1)GOTO 843
   CALL PLOT2(QM,QX,RATNG(NUM),0.0,126.0,0.0,50,INO,12)
843 CONTINUE
   IF(IPLT.LT.1)GOTO 847
847 CONTINUE
   STOP

1   FORMAT(8A10)
2   FORMAT(8F10.0)
3   FORMAT(1H+,50X,8A10)
4   FORMAT(14,2F6.0)
50  FORMAT(40H TITLE FOR RATING NUMBERS
51  FORMAT(40H TITLE FOR THE STAGE RECORDS
103 FORMAT(14,3I3,F5.2,2X,12F5.2)
121 FORMAT(1H 15,12(F5.2,F5.0)
   END

SUBROUTINE RATING(S,O,RATNG,NUM,DIV,START)
DIMENSION RATNG(NUM)
I=(S-START)/DIV
IF(I.LE.0)GOTO 100
IP=I+1
IF(IP.GT.NUM)GOTO 200
S=S-START
YX=S/(DIV*DIV)-FLOAT(I)/DIV
O=RATNG(I)*(1./DIV-YX )*DIV+RATNG(IP)*DIV*YX
RETURN
100 O=RATNG(1)
    RETURN
200 CONTINUE
    O=RATNG(NUM)+1.0
    RETURN
END

```

```
SUBROUTINE BARSTR(X,TITLE,IDY,IMH,IYR)
DIMENSION STR(40),TITLE(8),TATLE(3)
DATA LTH/0/
DATA AVE,IAVE/0.0,0/
DATA STR/40*0.0/
AVE=AVE+X
IAVE=IAVE+1
IF (IDY.EQ.1.AND.LTH.NE.0)GOTO 200
STR(IDY)=0.0
IF(X.GT.1.0)STR(IDY)=ALOG10(X)
MTH=IMH
LTH=IDY
JYR=IYR
RETURN
200 CONTINUE
TATLE(1)=TITLE(1)
TATLE(2)=TITLE(2)
TATLE(3)=10H LOG STRMF
WDT=LTH*0.3
HGT=3.0
RMAX=4.0
RIAVE=IAVE
AVER=AVE/RIAVE
WRITE(8,563)AVER
WRITE(3,563)AVER
WRITE(4,563)AVER
WRITE(9,563)AVER
563 FORMAT(1H1,20H AVERAGE FLOE IS
IAVE=0
AVE=0.0
STR(IDY)=0.0
IF(X.GT.1.)STR(IDY)=ALOG10(X)
RETURN
END
```

F10.4)

SUBROUTINE DAYM (IDAY, IDY, IMO, IYR)

DECK RESEQUENCED AND DUPLICATED ON 02/16/70 BY COMPUTER
DAY TO DATE CONVERSION

C
C
C
C

CALCULATES THE DAY FROM 1940
COMMON/DAYDA/ IMONTH(12), IYEAR(30), IMONTHC(12)
DATA IMONTH/31,28,31,30,31,30,31,31,30,31,30,31/
DATA IMONTHC/0,31,59,90,120,151,181,212,243,273,304,334/
DATA IYEAR/0,365,730,1096,1461,1826,2191,2557,2922,3287,3652,
24018,4383,4748,5113,5479,5844,6209,6574,6940,7305,7670,8035,8401,
38766,9131,9496,9862,10227,10592/
IF (IDY.LT.1.OR.IDY.GT.31)GOTO 800
IF (IMO.LT.1.OR.IMO.GT.12)GOTO 800
IF (IYR.LT.50.OR.IYR.GT.79)GOTO 800
IYR=IYR-49
IDAY=IYEAR(IYR)+IMONTHC(IMO)+IDY
IF (((IYR/4)*4-IYR).EQ.0.AND.IMO.GE.3)IDAY=IDAY+1
RETURN
800 WRITE(6,801)IDY,IMO,IYR
801 FORMAT(50H *****ERROR IN DATE = 3110)
RETURN
ENTRY DATM
IF (IDAY.GT.10957.OR.IDAY.LE.0)GOTO 400
DO 200 I=1,30
II=I
IF (IYEAR(I).GE.IDAY)GOTO 210
200 CONTINUE
IYR=30
GOTO 220
210 IYR=II-1
220 ITEM=IDAY-IYEAR(IYR)
IYR=IYR+49
DO 300 I=1,12
II=I
IF (IMONTHC(I).GE.ITEM)GOTO 310
300 CONTINUE
IMO=12
GOTO 320
310 IMO=II-1
320 IDY=ITEM-IMONTHC(IMO)
RETURN
400 WRITE(6,401)IDAY
401 FORMAT(50H *****ERROR IN IDAY= 110)
STOP 10001
END

APPENDIX II

PROGRAM OUTPUT AND FULL SIMULATION RESULTS FOR THE FOUR BASINS

On the graphs of the simulated and recorded streamflow, the precipitation figures are plotted for comparison. In order to achieve a reasonable precipitation plot the figures were transformed as:

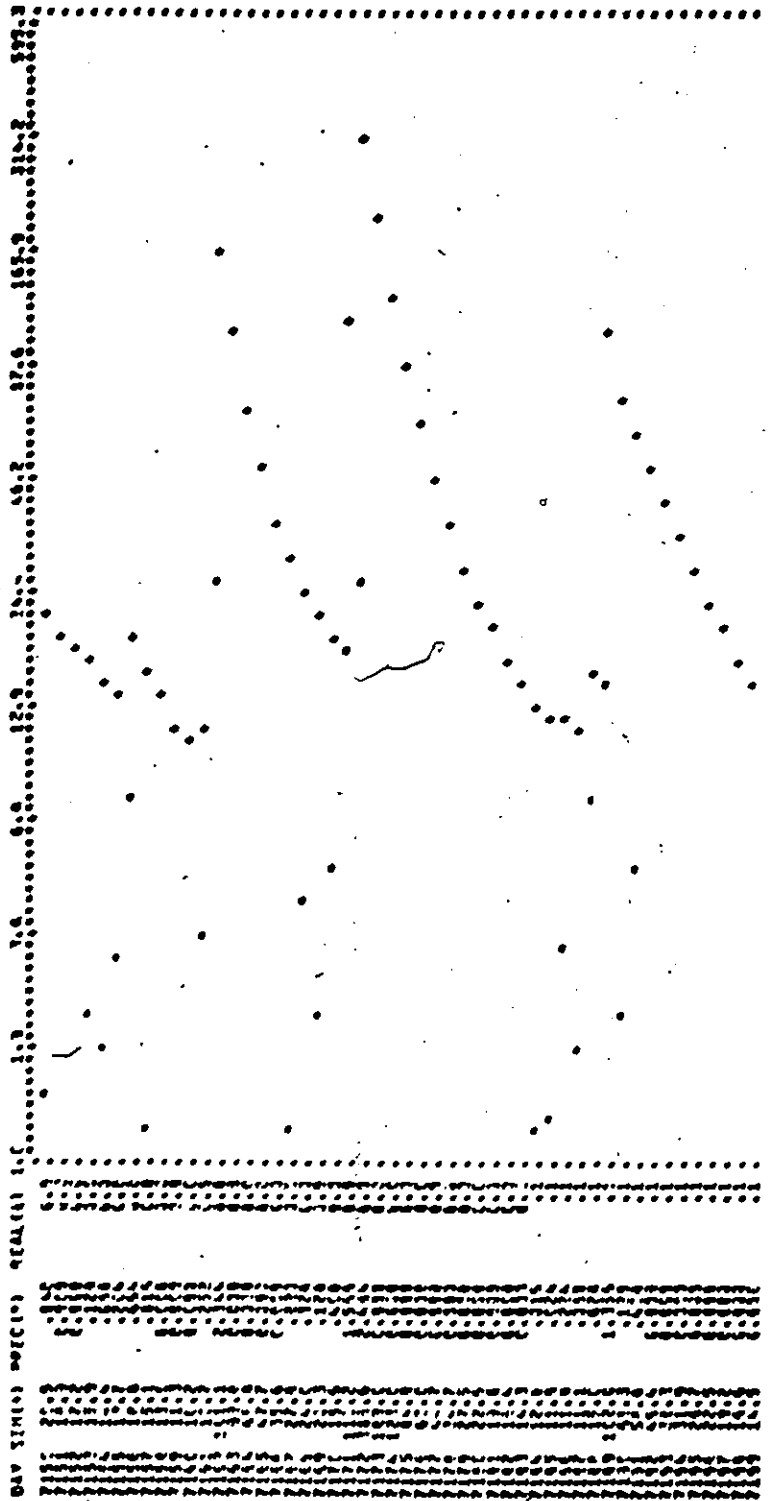
$$\text{PLOT} = 10. * (\text{P} + 1.)$$

where PLOT is the plotted figure, and

P is the precipitation figure,

before plotting.

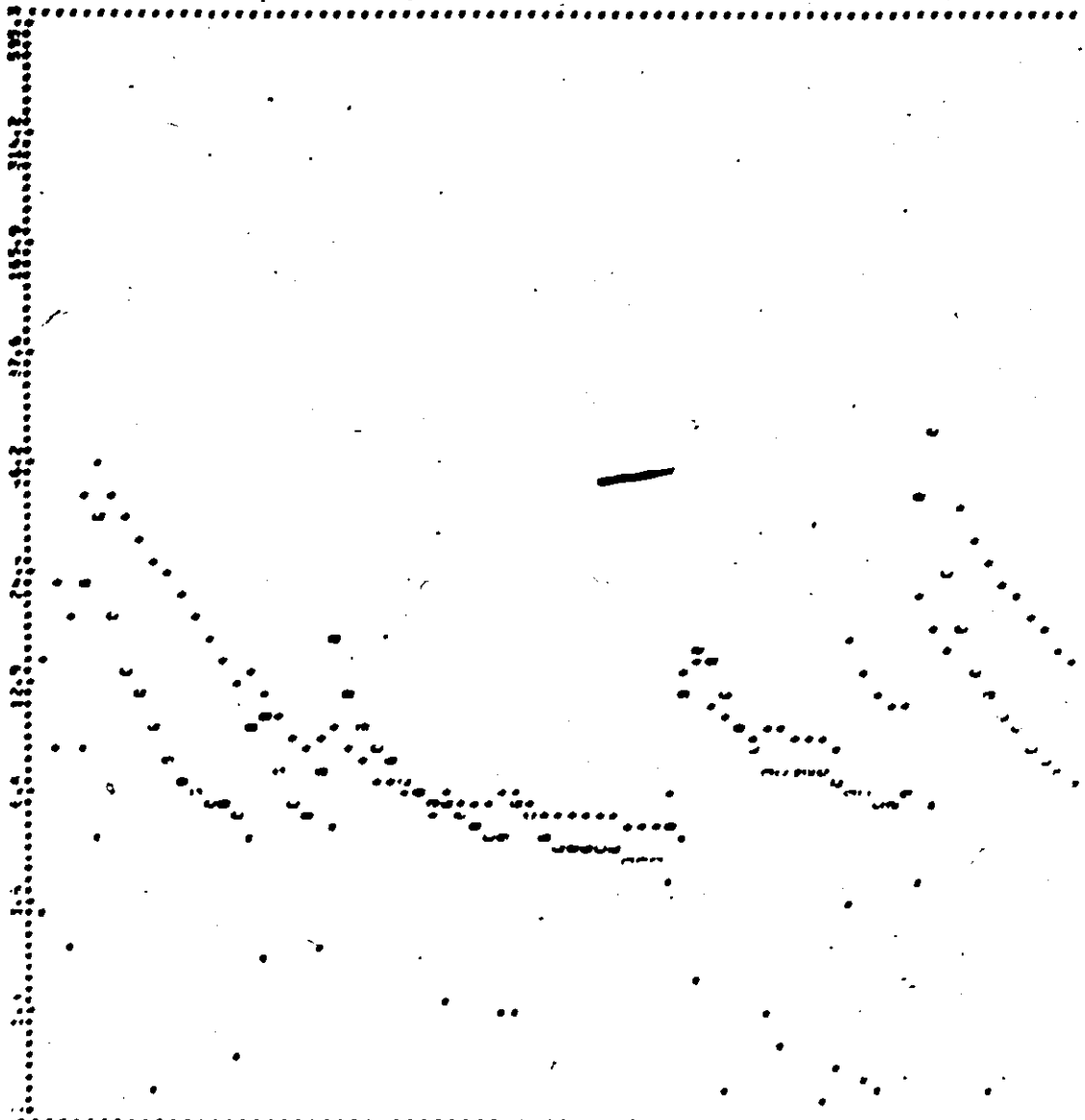
1969
 2002
 2001
 2000
 1999
 1998
 1997
 1996
 1995
 1994
 1993
 1992
 1991
 1990
 1989
 1988
 1987
 1986
 1985
 1984
 1983
 1982
 1981
 1980
 1979
 1978
 1977
 1976
 1975
 1974
 1973
 1972
 1971
 1970
 1969



August 1969

September 1969

Simulation at Swago Creek

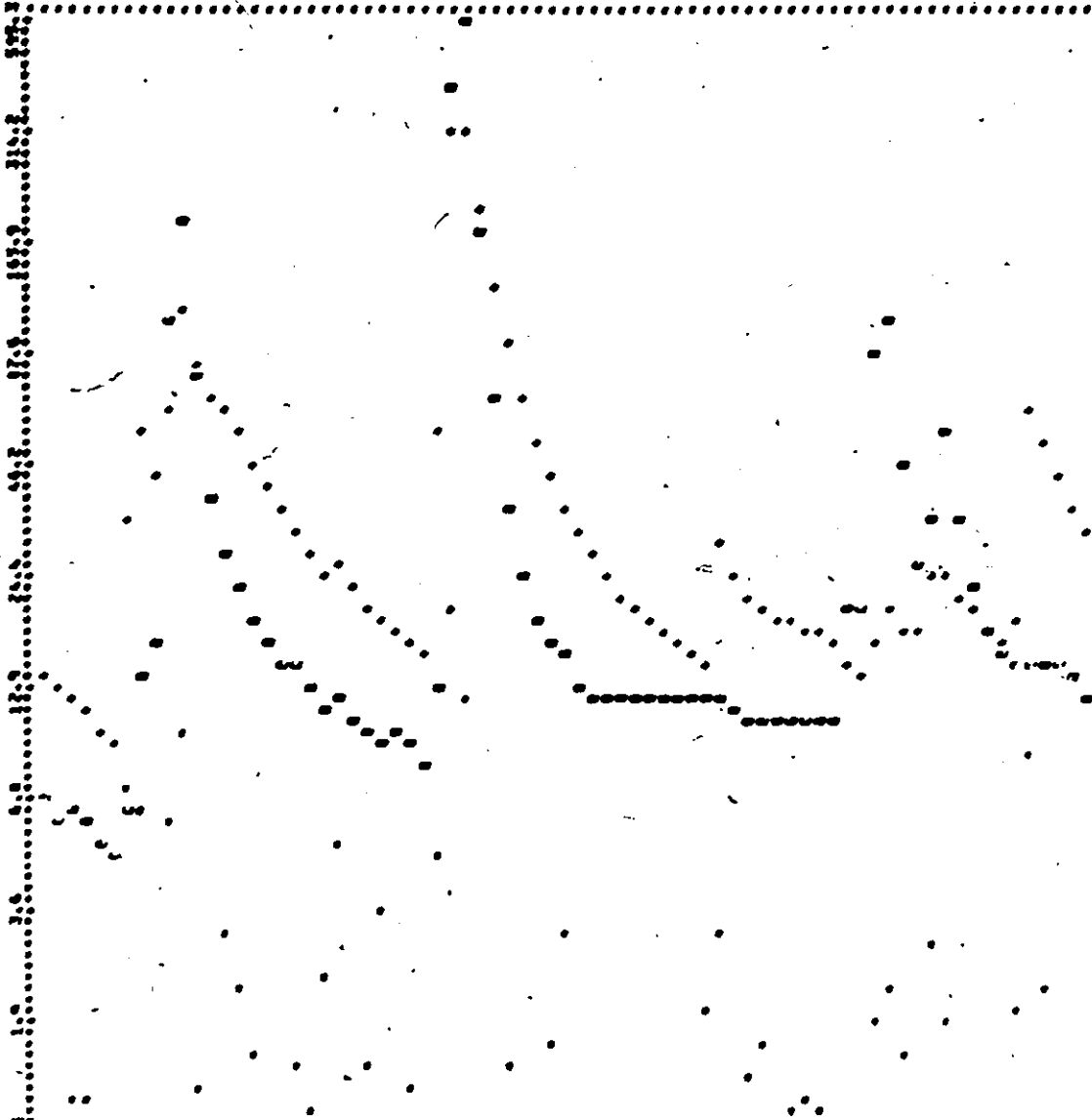


The following information is provided for your information and is not intended to be used as a basis for any action. It is the policy of the Department of Health, Education and Welfare to disseminate information on the progress of research and development in the field of health, education and welfare. This information is being provided to you for your information and is not intended to be used as a basis for any action.

The following information is provided for your information and is not intended to be used as a basis for any action. It is the policy of the Department of Health, Education and Welfare to disseminate information on the progress of research and development in the field of health, education and welfare. This information is being provided to you for your information and is not intended to be used as a basis for any action.

The following information is provided for your information and is not intended to be used as a basis for any action. It is the policy of the Department of Health, Education and Welfare to disseminate information on the progress of research and development in the field of health, education and welfare. This information is being provided to you for your information and is not intended to be used as a basis for any action.

Sept. 1969	October 1969	November 1969
------------	--------------	---------------

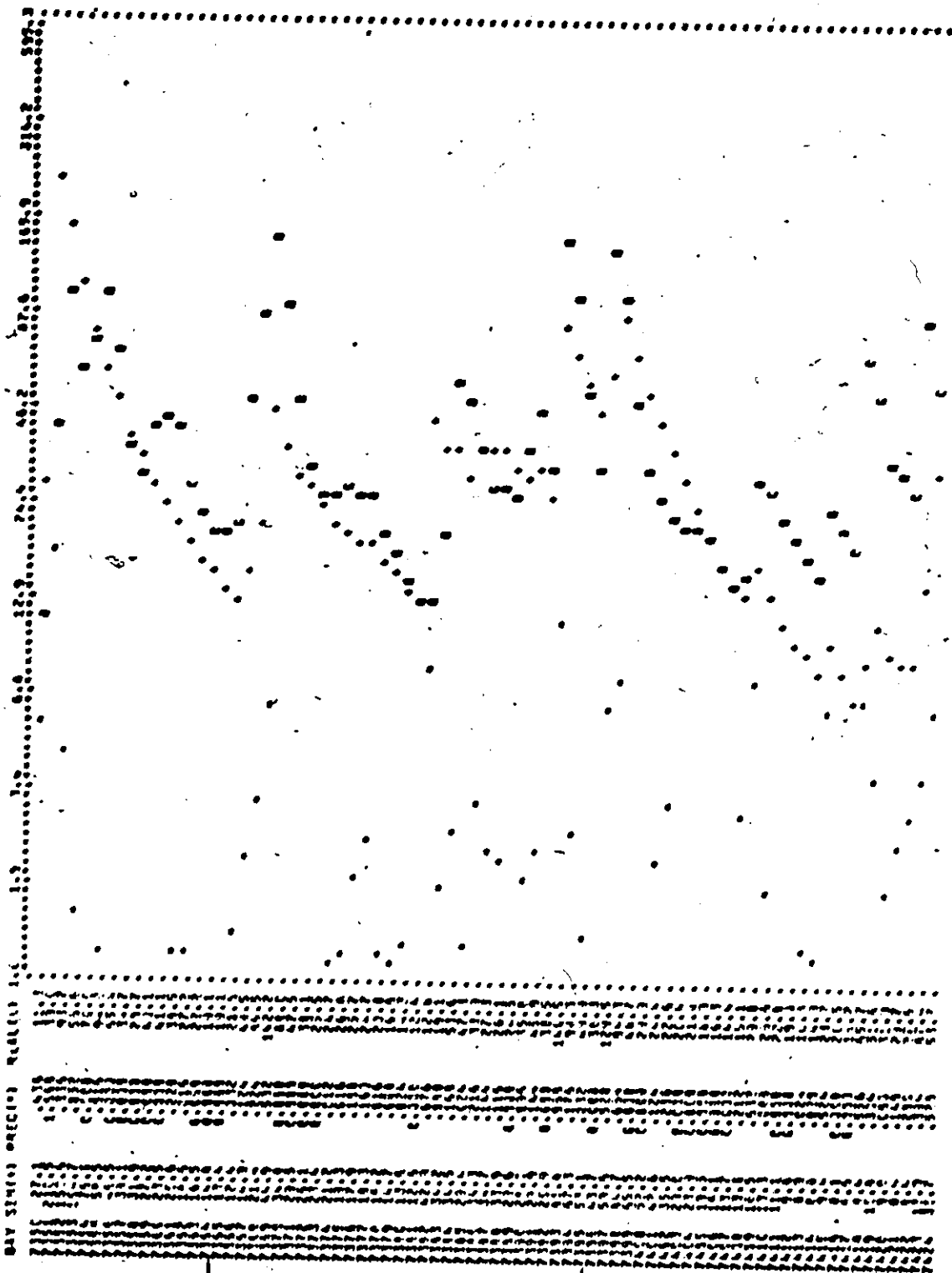


RAY SINCE PRECISE

REAR 1 2 3 4 5 6 7 8 9 10 11 12 13 14 15 16 17 18 19 20 21 22 23 24 25 26 27 28 29 30 31 32 33 34 35 36 37 38 39 40 41 42 43 44 45 46 47 48 49 50 51 52 53 54 55 56 57 58 59 60 61 62 63 64 65 66 67 68 69 70 71 72 73 74 75 76 77 78 79 80 81 82 83 84 85 86 87 88 89 90 91 92 93 94 95 96 97 98 99 100

December 1969 January 1970 Feb. 1970



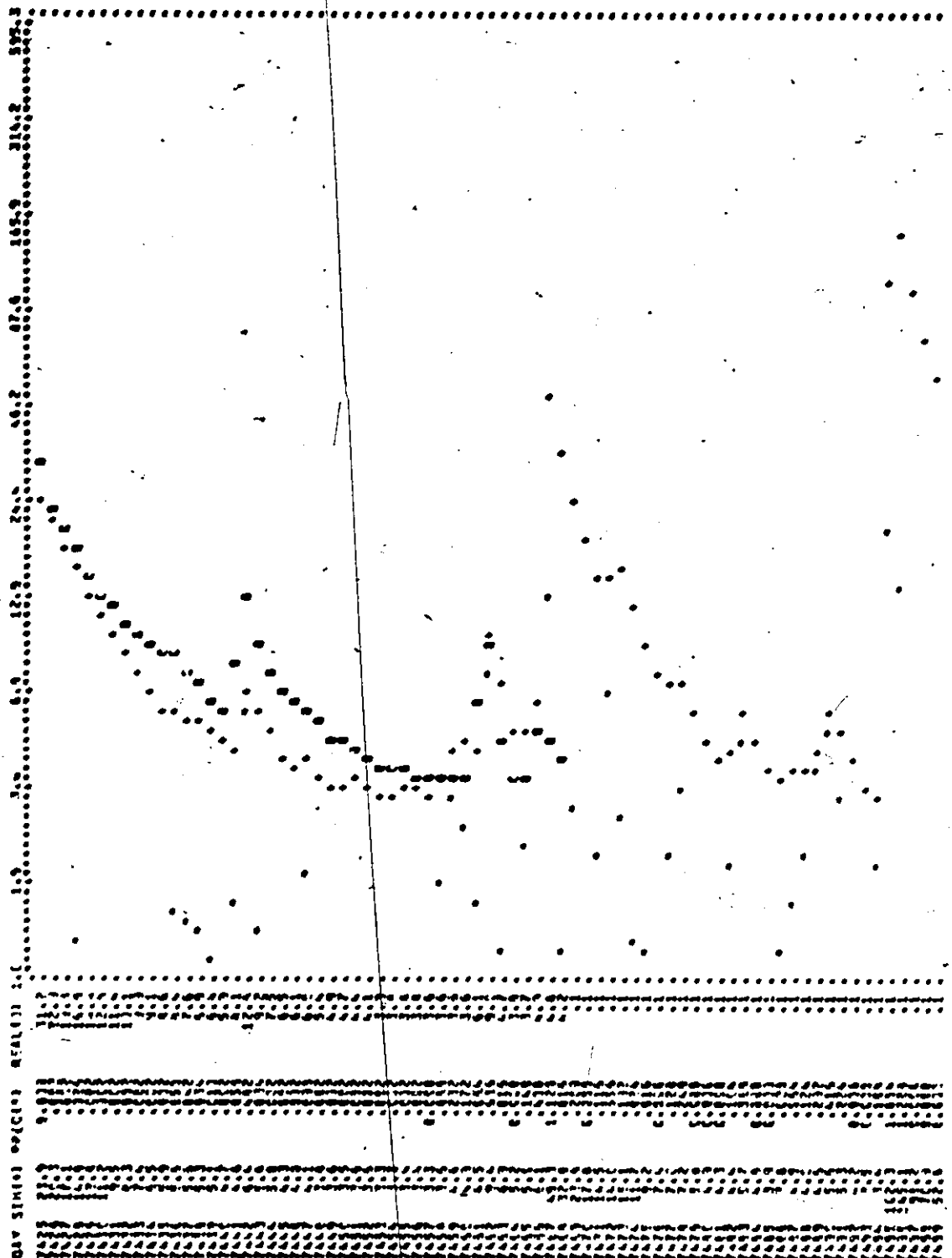


Feb. 1970

March 1970

April 1970



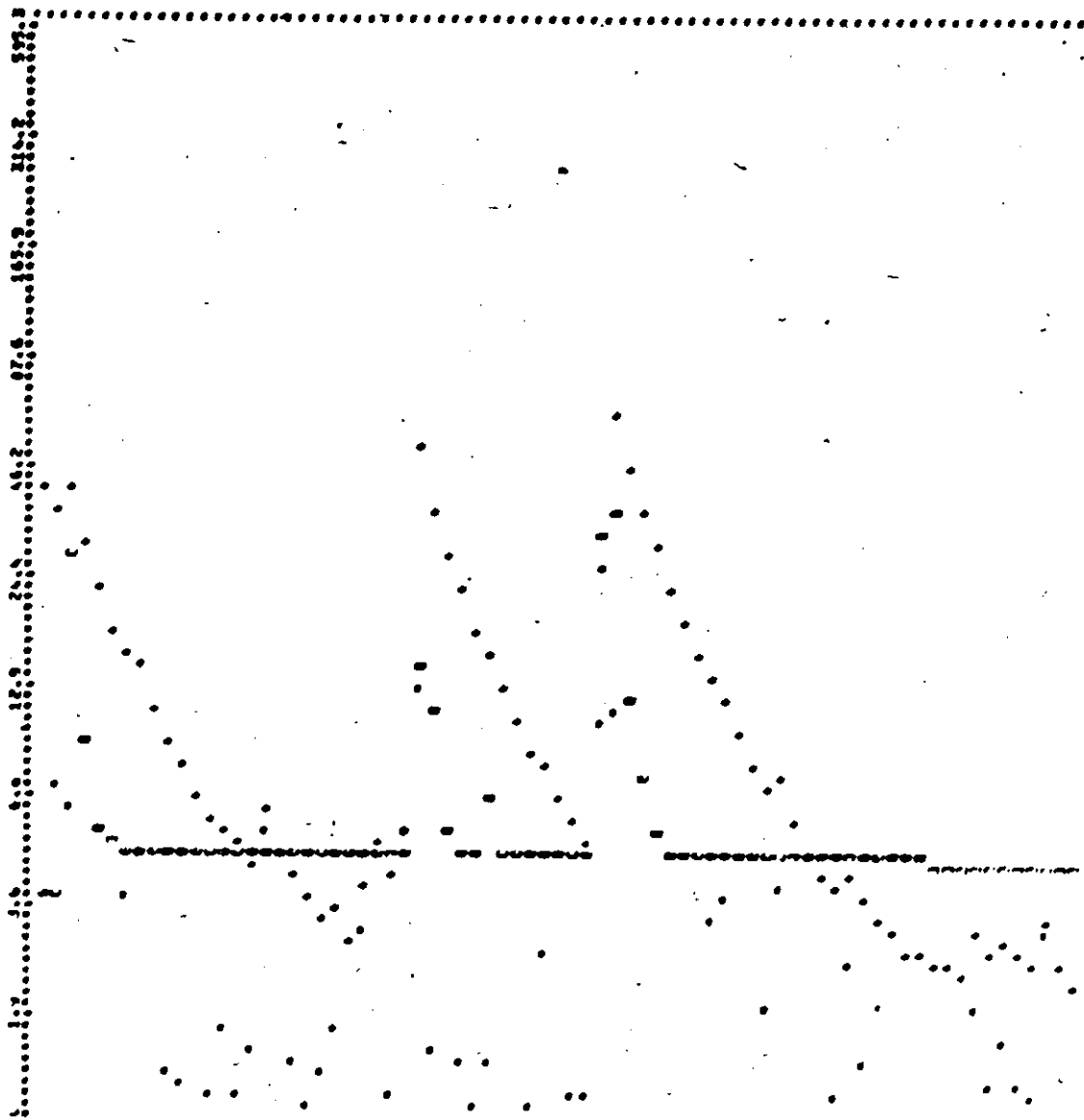


May 1970

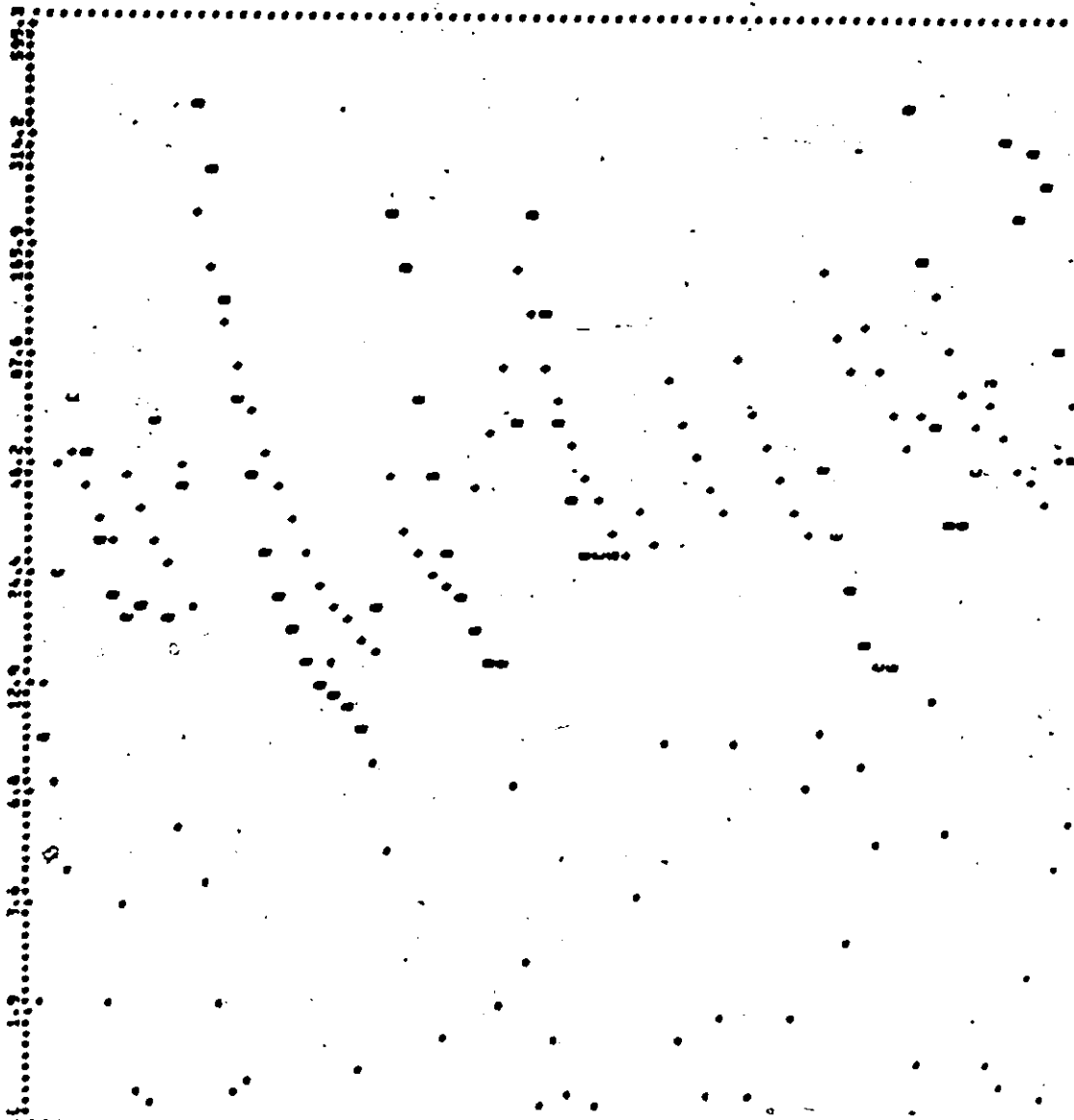
June 1970

July 1970





JULY 1970
 AUGUST 1970
 SEPTEMBER 1970



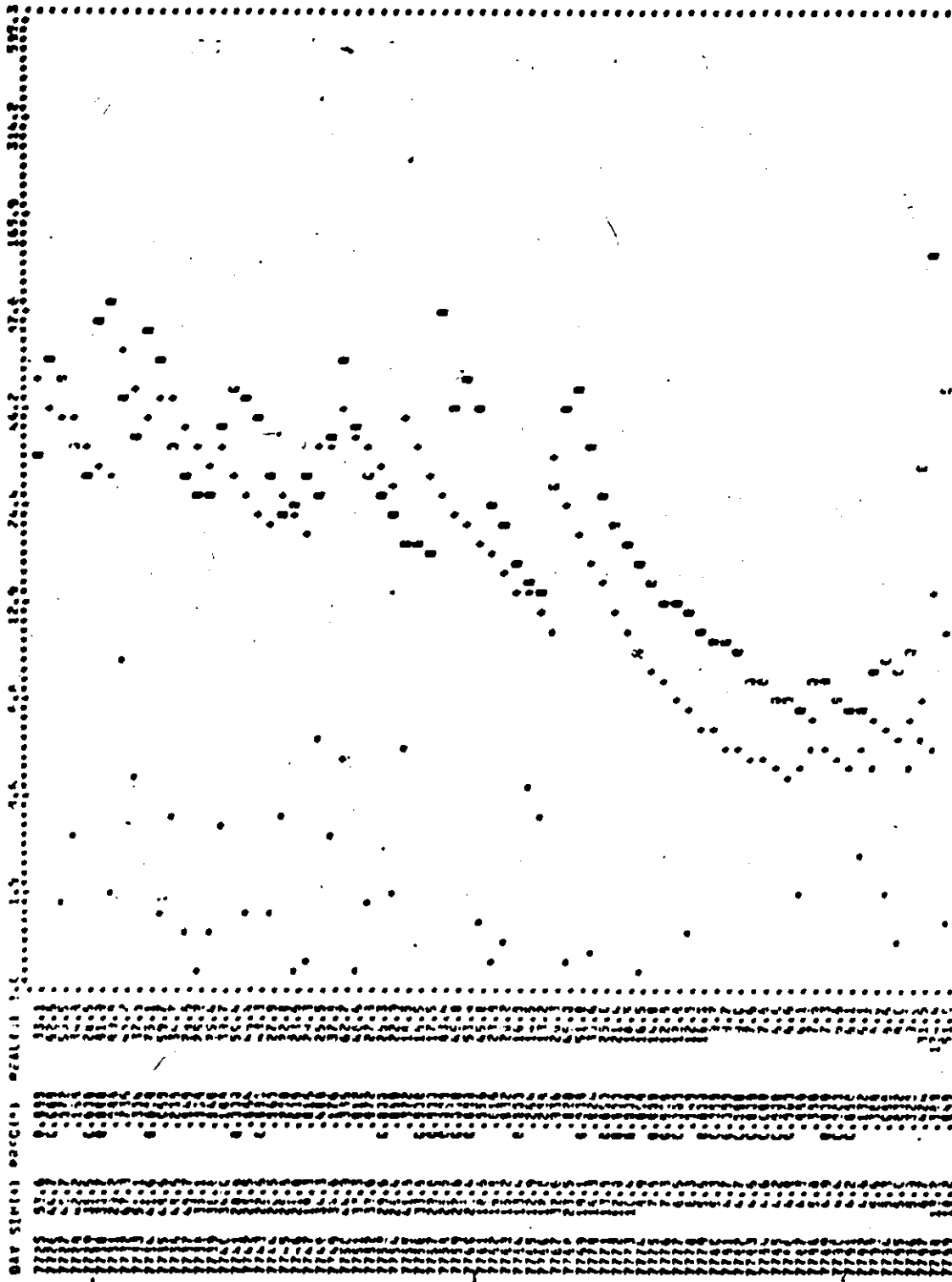
The following information is provided for the purpose of identifying the data points in the scatter plot. The data points are arranged in a grid pattern, with the horizontal axis representing the month and the vertical axis representing the year. The data points are arranged in a grid pattern, with the horizontal axis representing the month and the vertical axis representing the year.

The following information is provided for the purpose of identifying the data points in the scatter plot. The data points are arranged in a grid pattern, with the horizontal axis representing the month and the vertical axis representing the year. The data points are arranged in a grid pattern, with the horizontal axis representing the month and the vertical axis representing the year.

The following information is provided for the purpose of identifying the data points in the scatter plot. The data points are arranged in a grid pattern, with the horizontal axis representing the month and the vertical axis representing the year. The data points are arranged in a grid pattern, with the horizontal axis representing the month and the vertical axis representing the year.

December 1970 | January 1971 | February 1971.

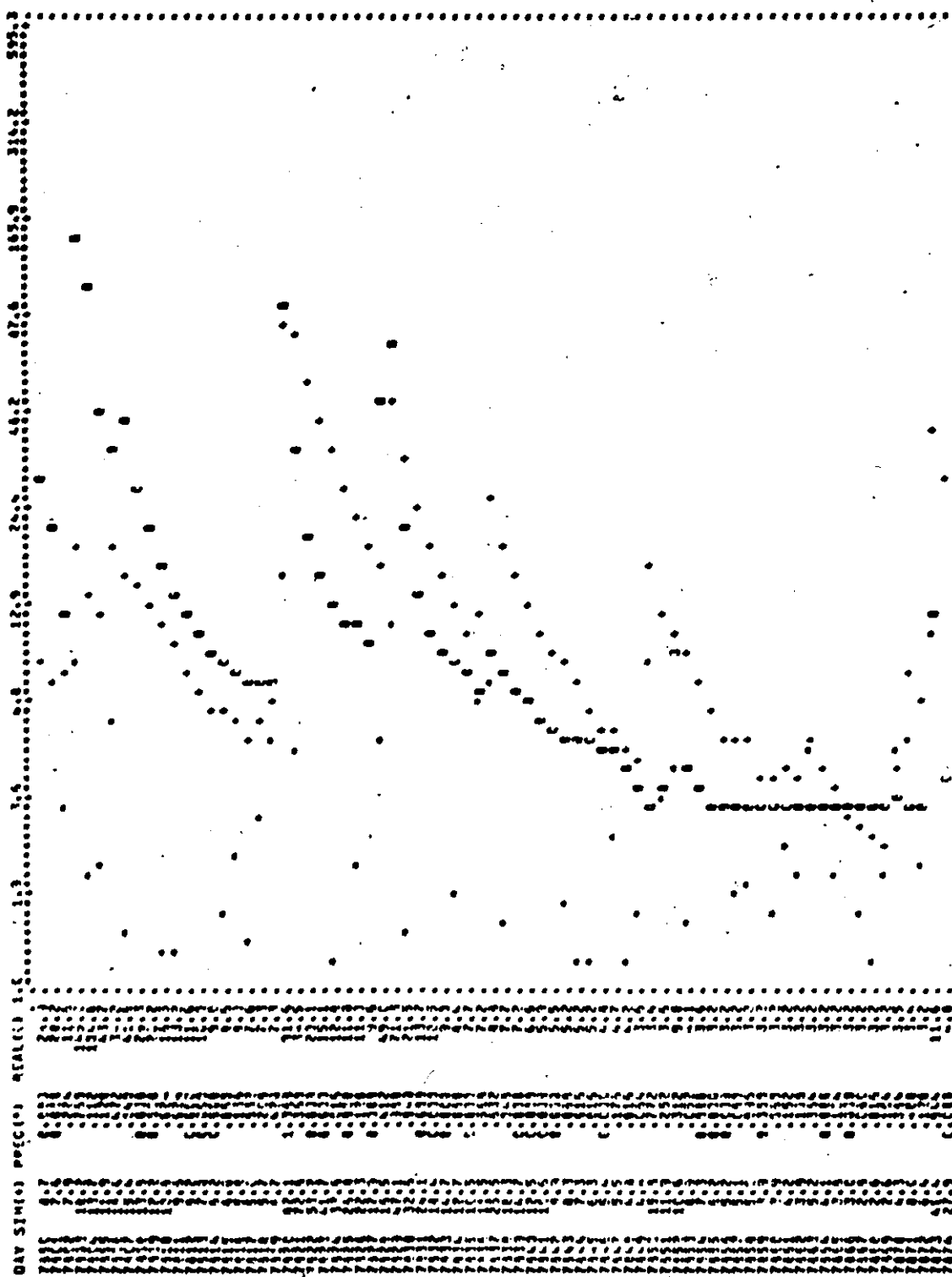




March 1971

April 1971

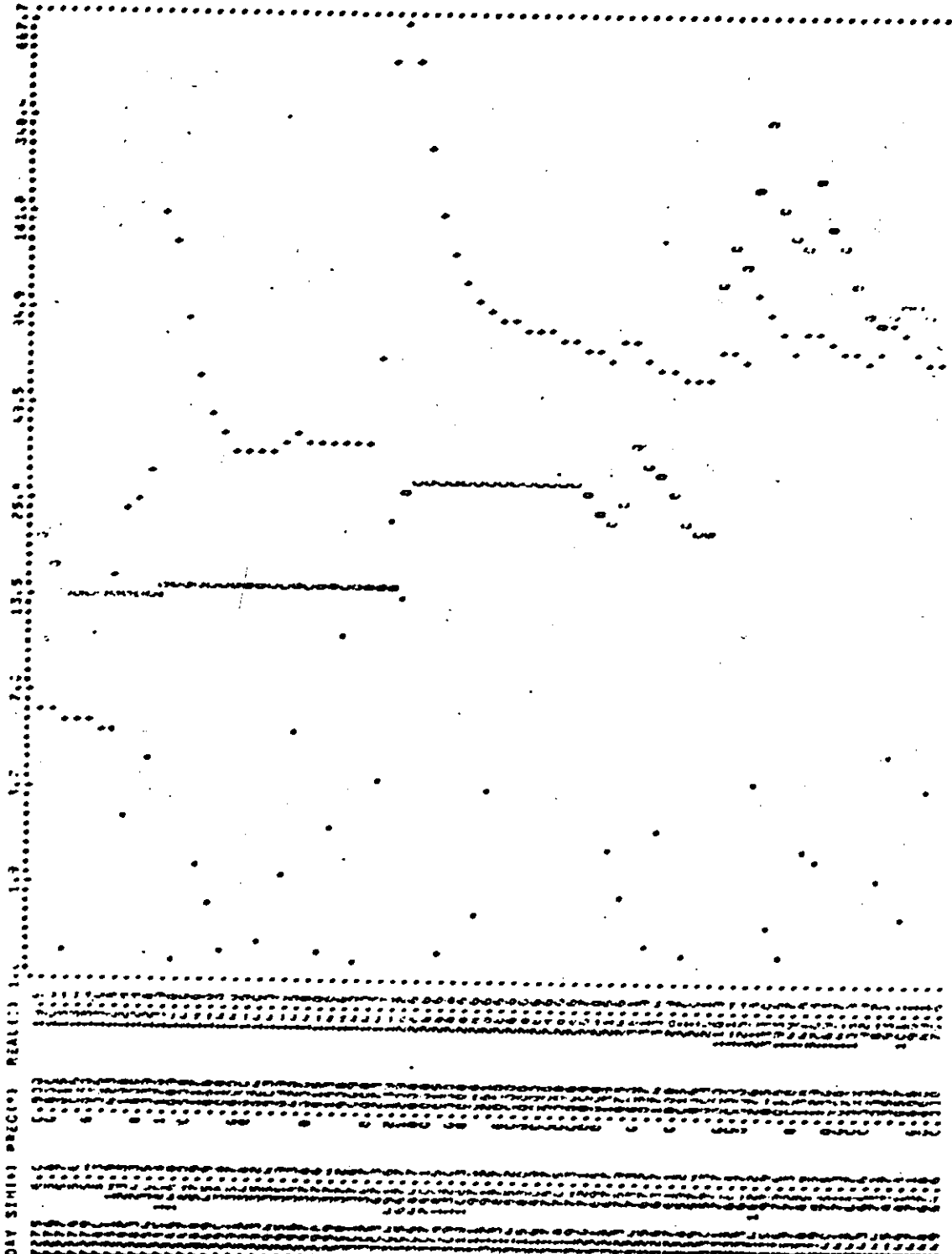
May 1971



May 1971..

June 1971

July 1971



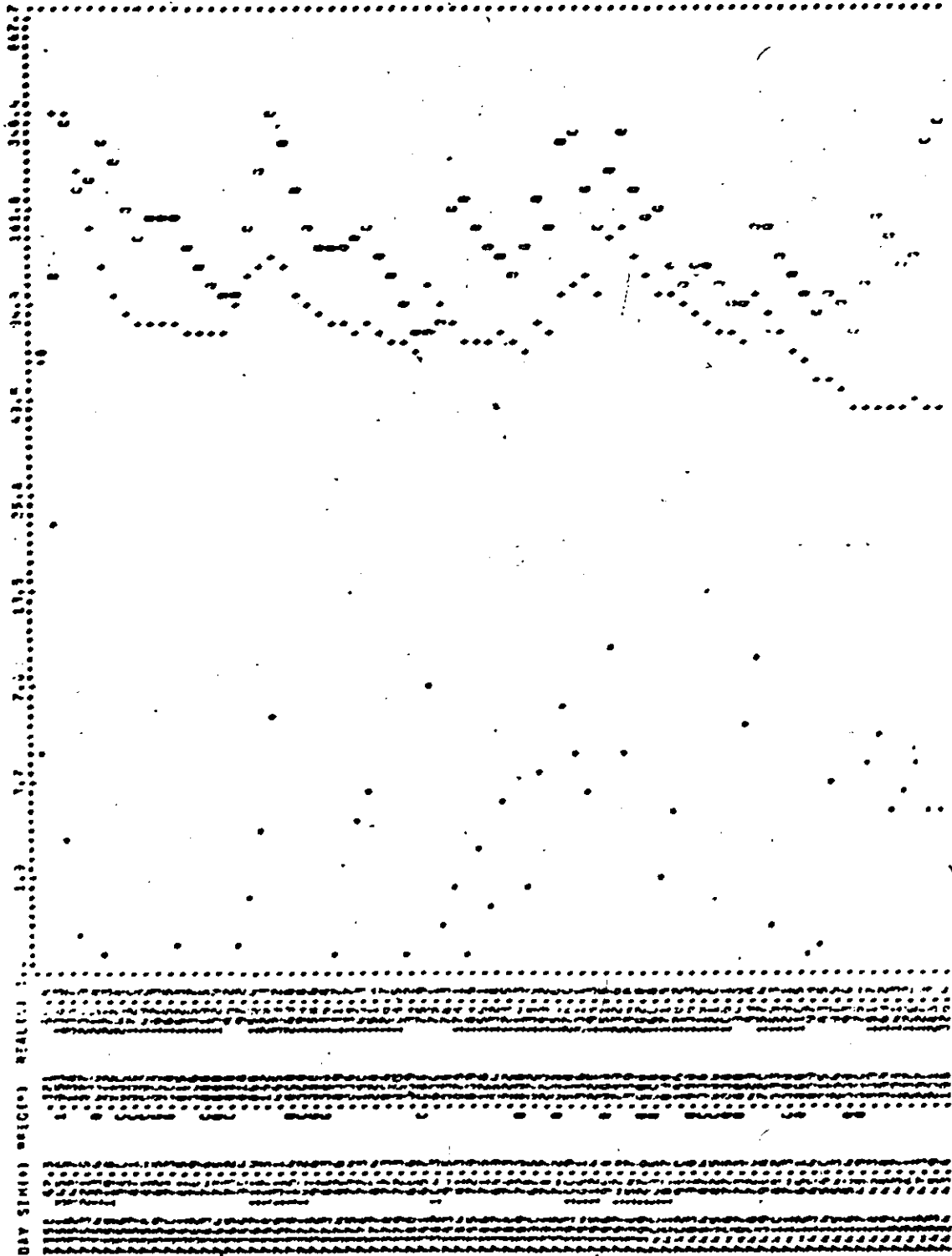
December 1969

January 1970

Feb. 1970

Simulation at Locust Creek

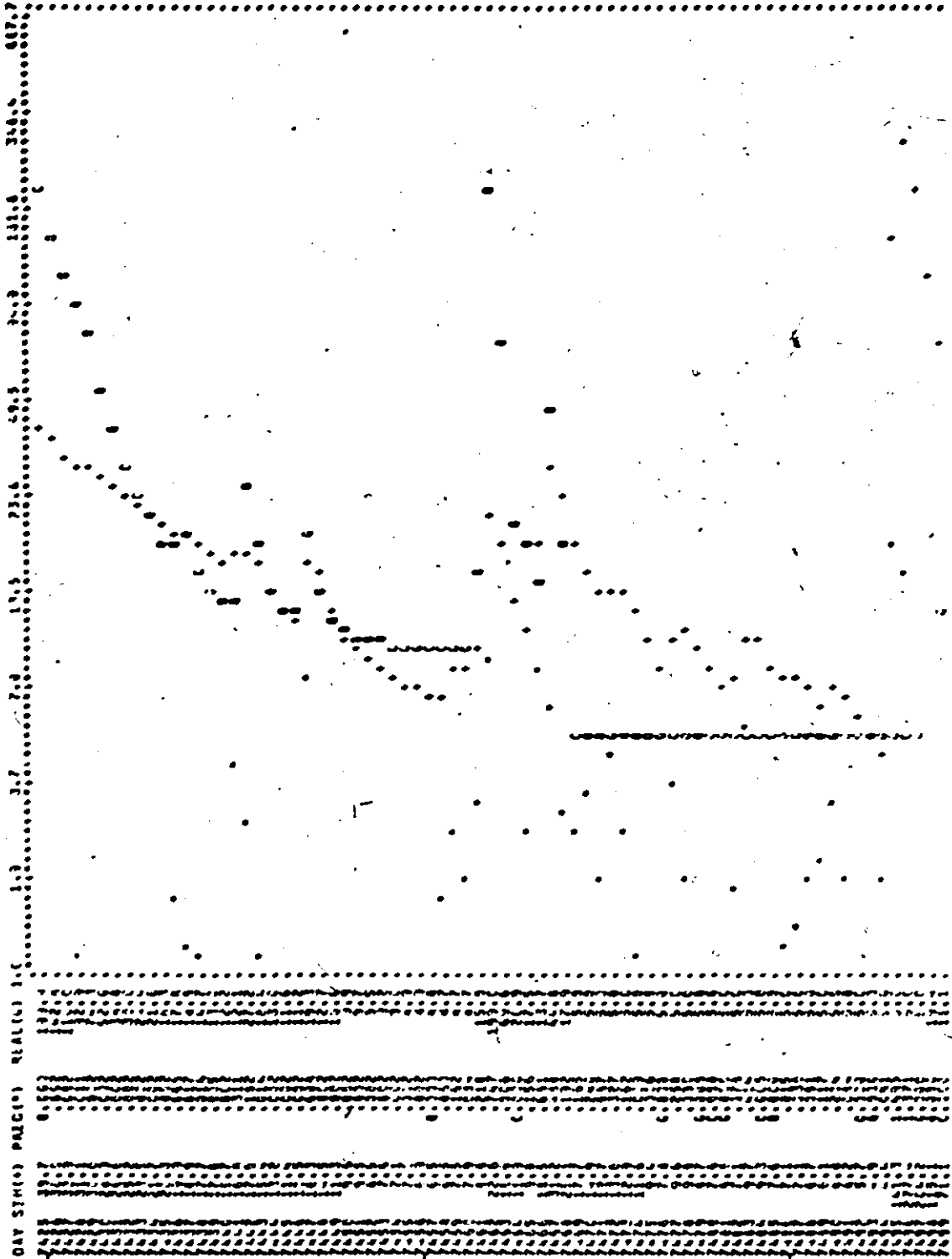




Feb. 1970

March 1970

April 1970

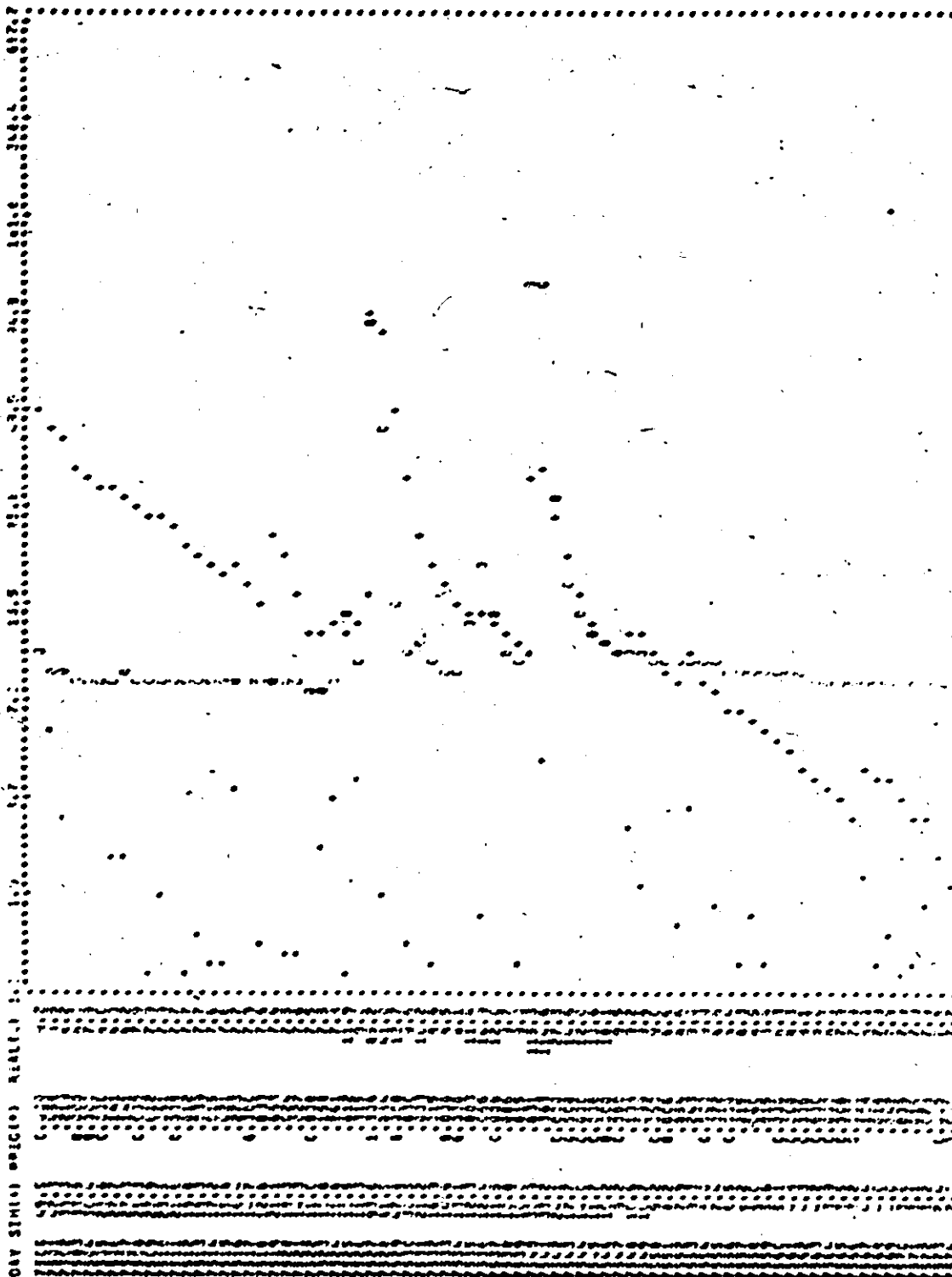


May 1970

June 1970

July 1970



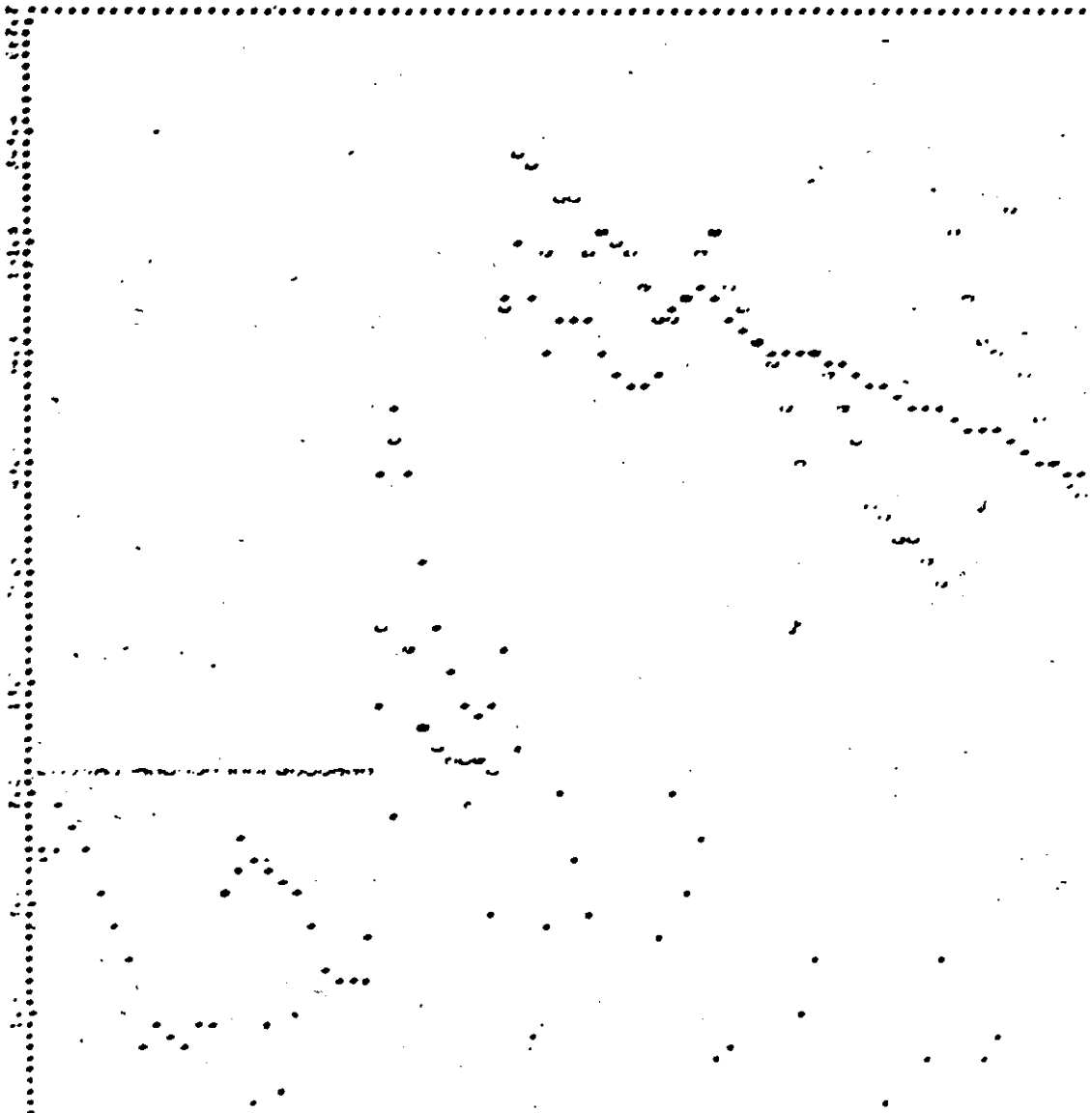


July 1970

August 1970

September 1970





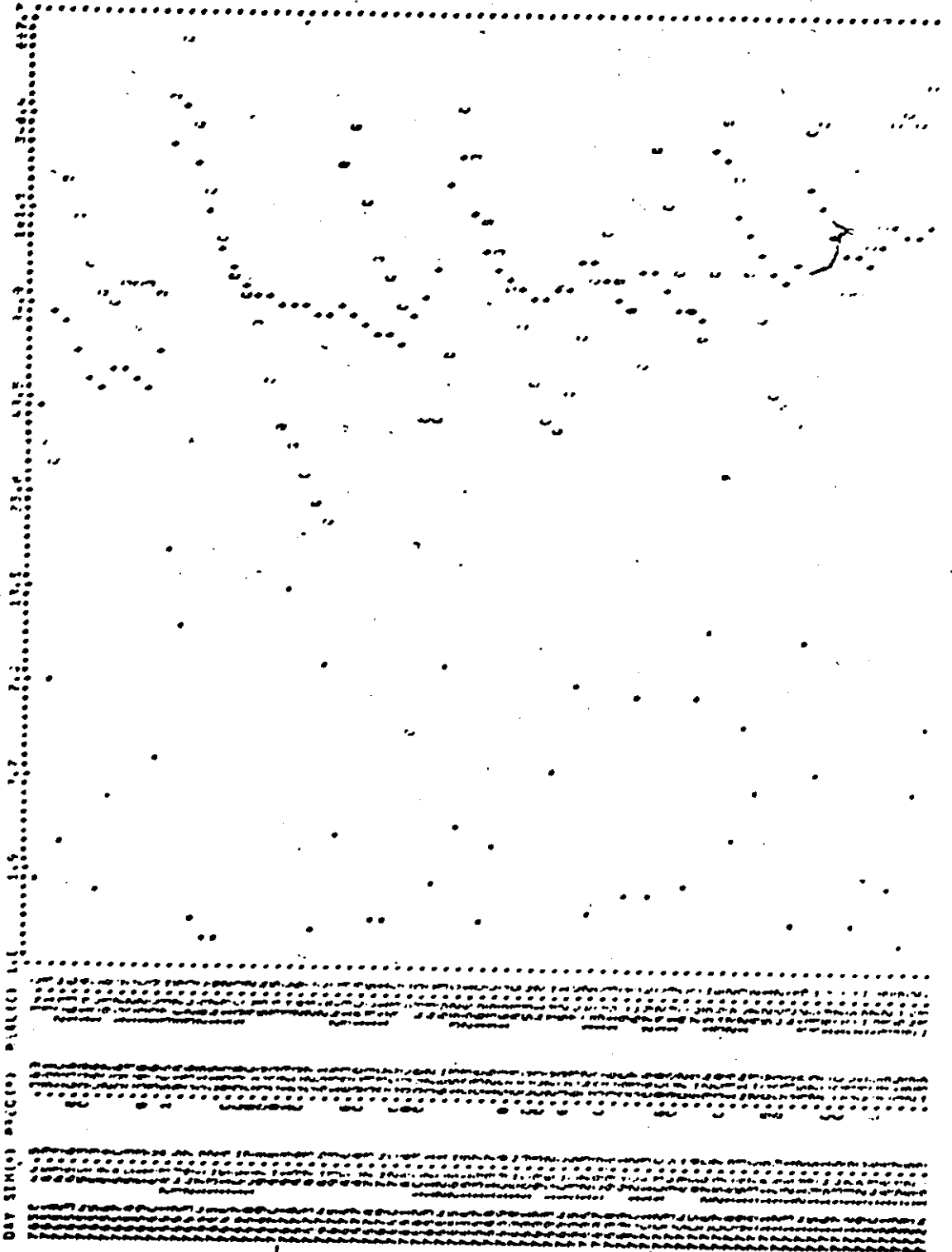
The following table shows the results of the analysis of the data for the period October 1970 to December 1970. The data shows a clear downward trend in the number of cases over the period, with a slight increase in November 1970. The overall trend is consistent with the scatter plot shown above.

October 1970

November 1970

Dec. 1970



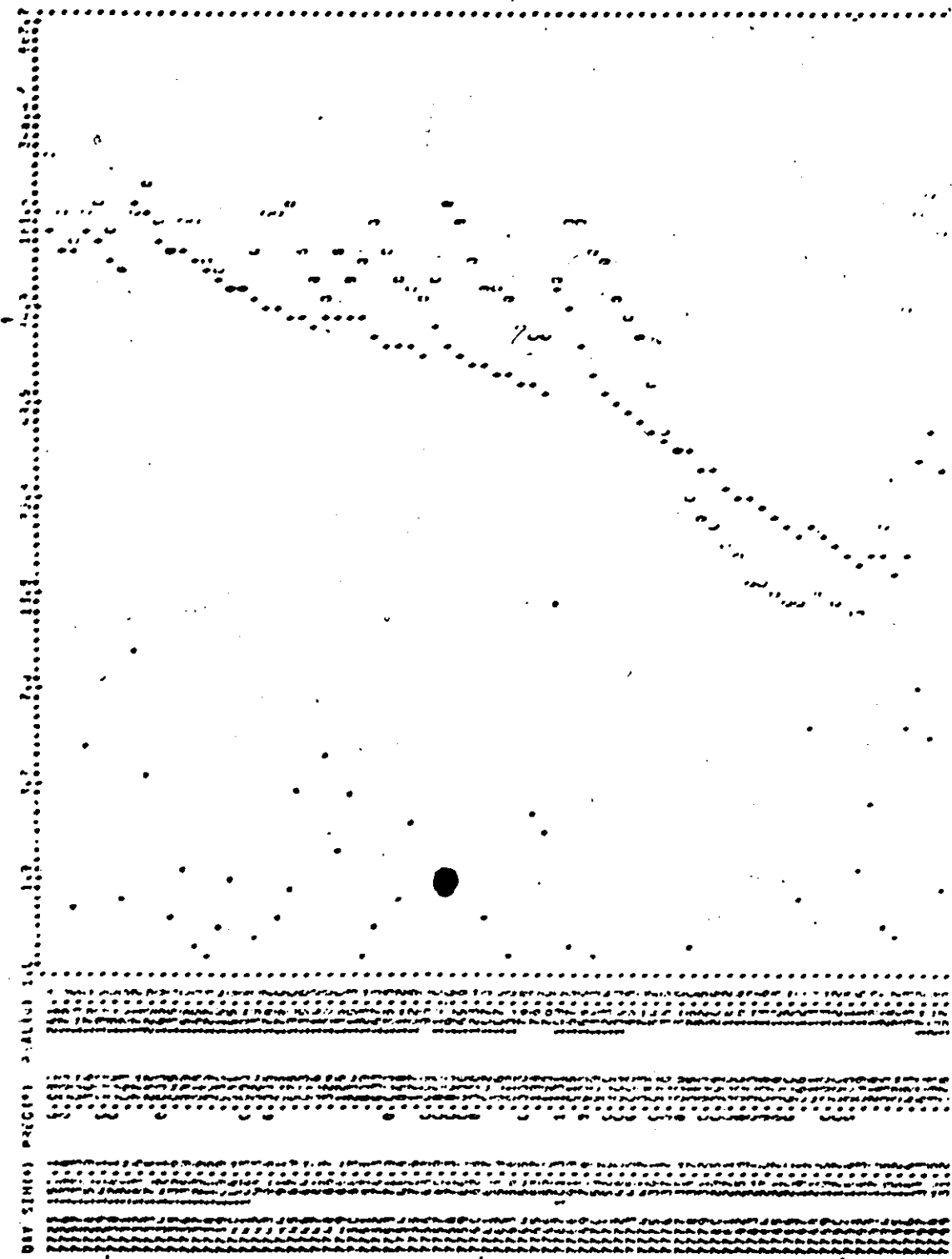


December 1970

January 1971

February 1971



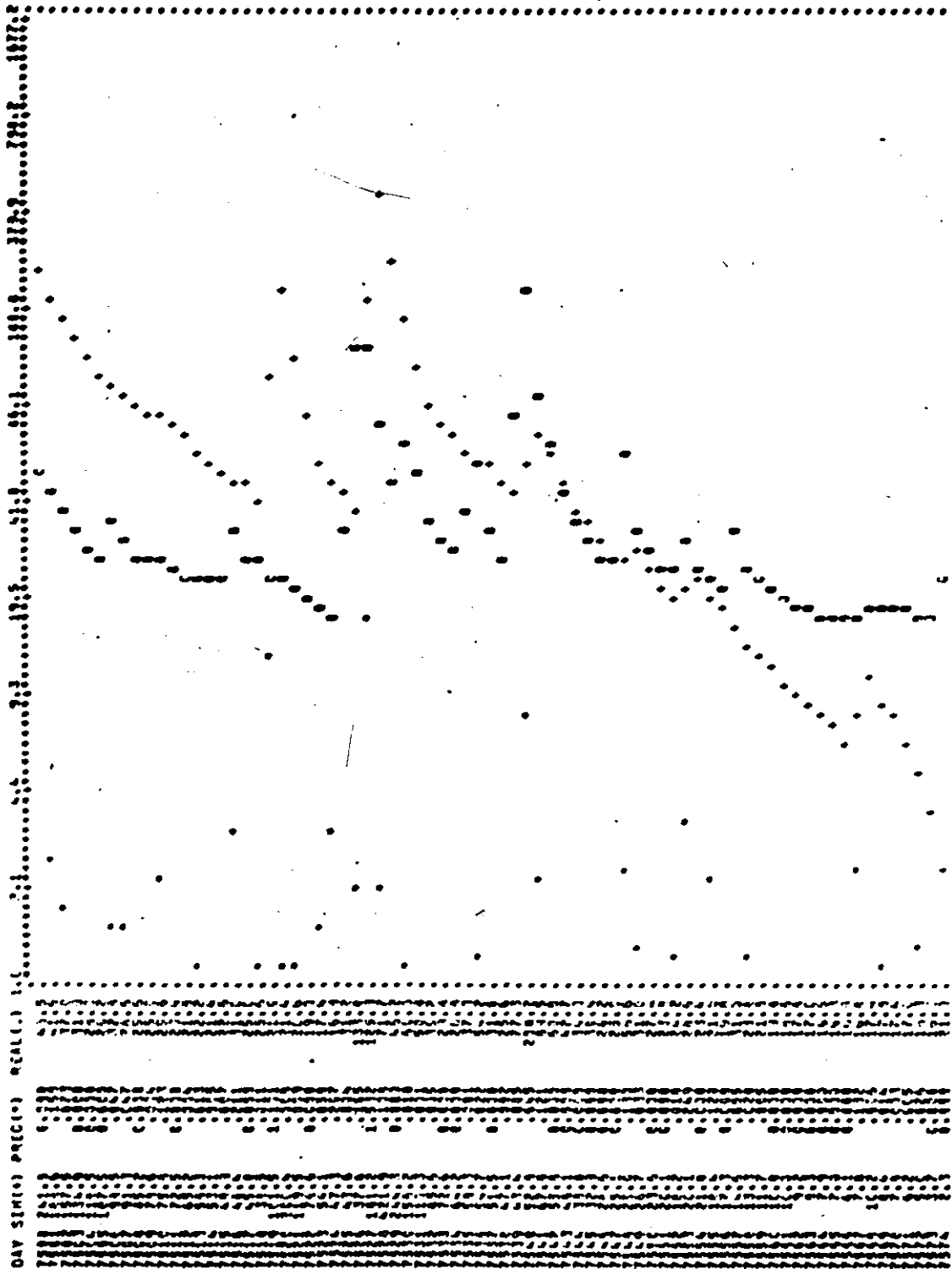


March 1971

April 1971

May 1971



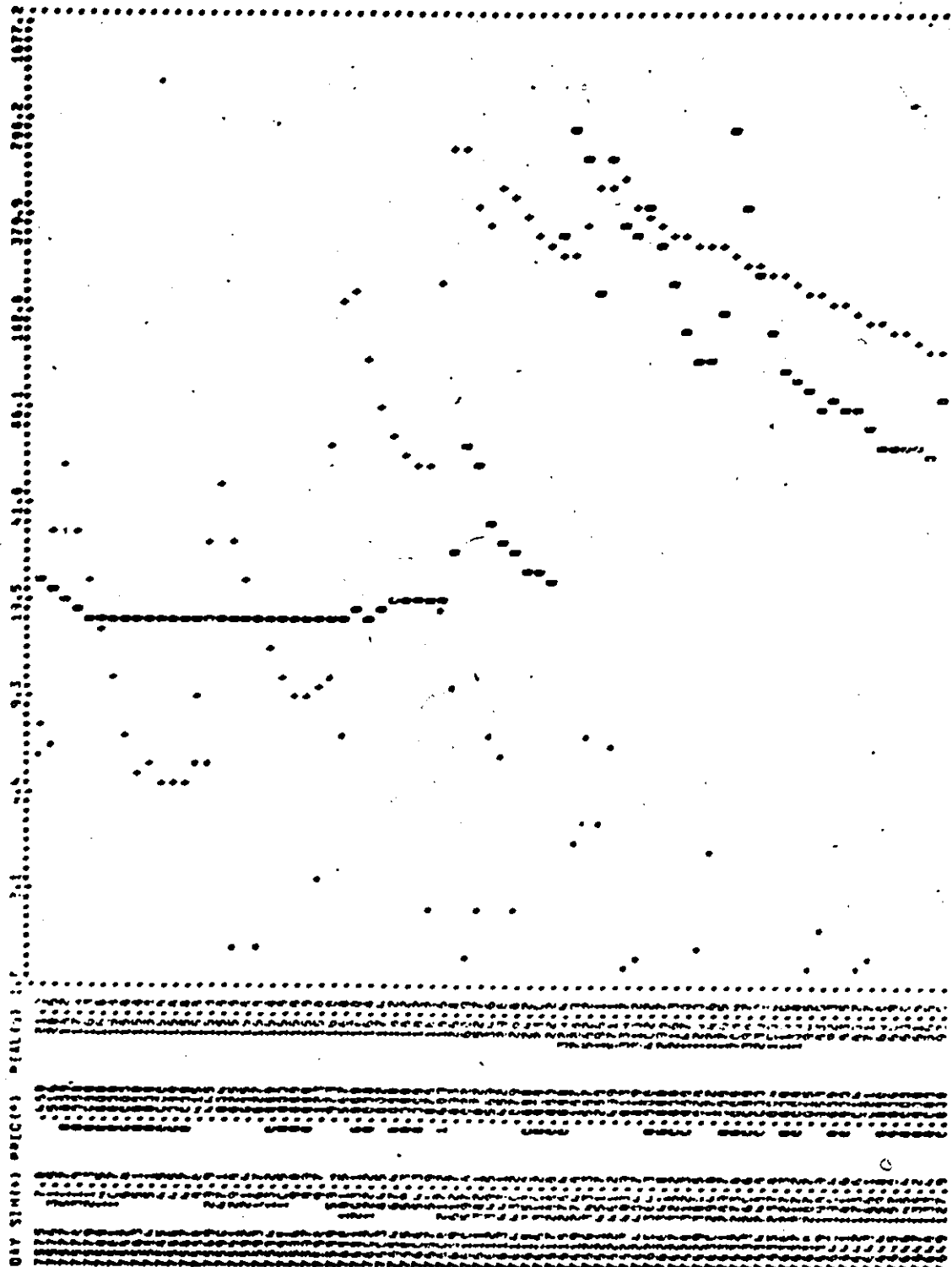


July 1970

August 1970

September 1970

Simulation at Spring Creek



DAY SINCE RECORDED

.....

.....

.....

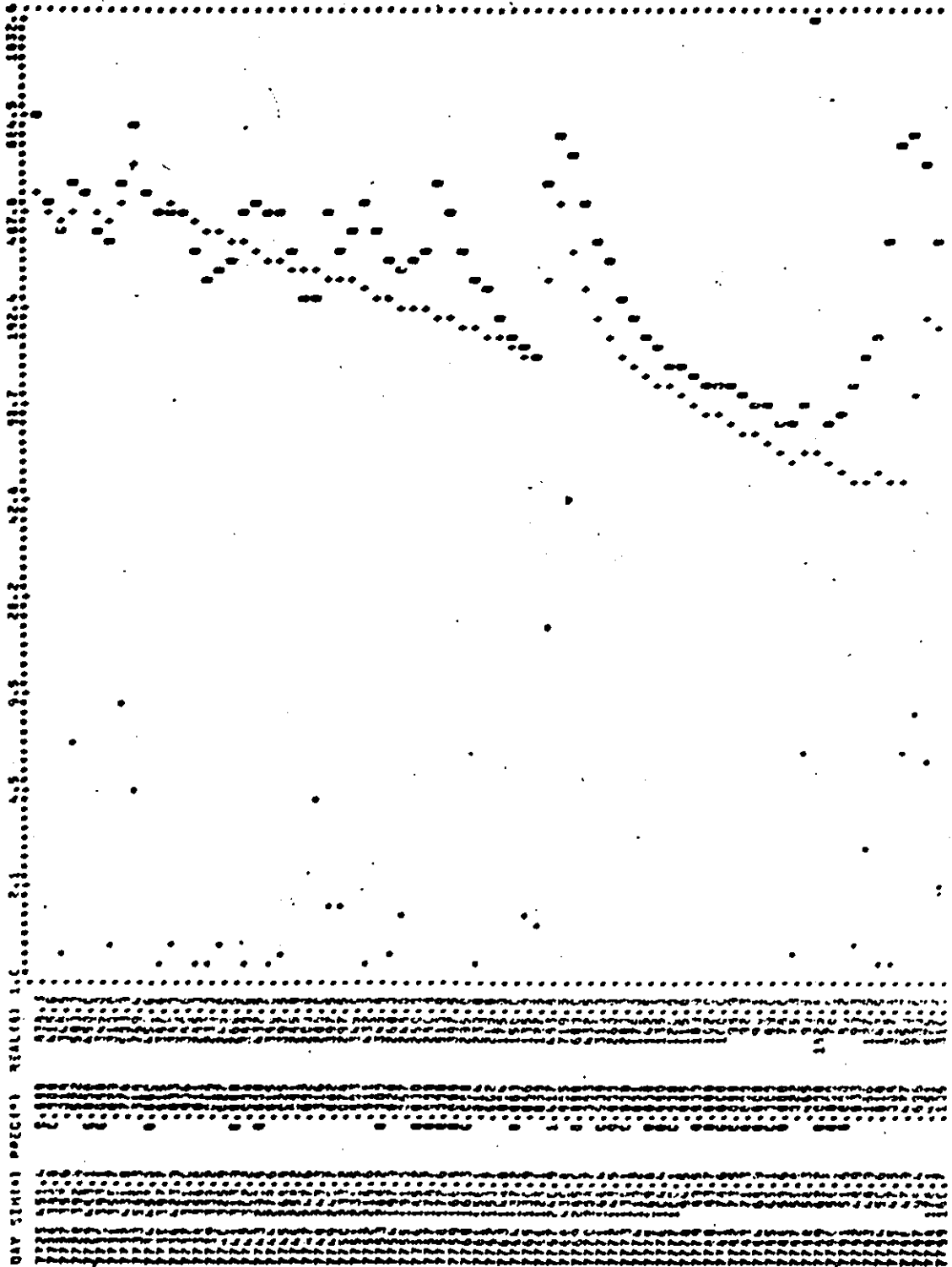
.....

October 1970

November 1970

Dec. 1970



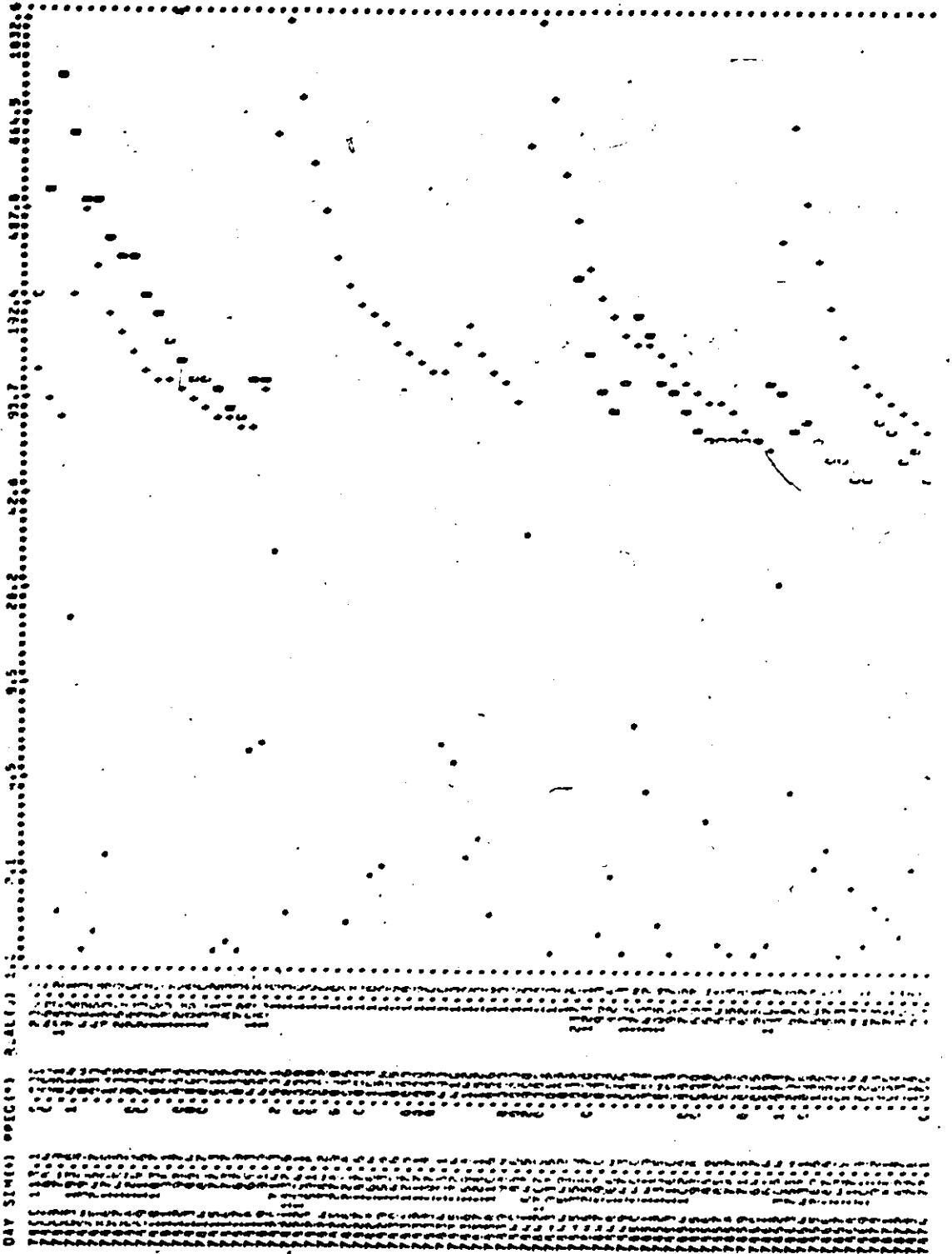


March 1971

April 1971

May 1971

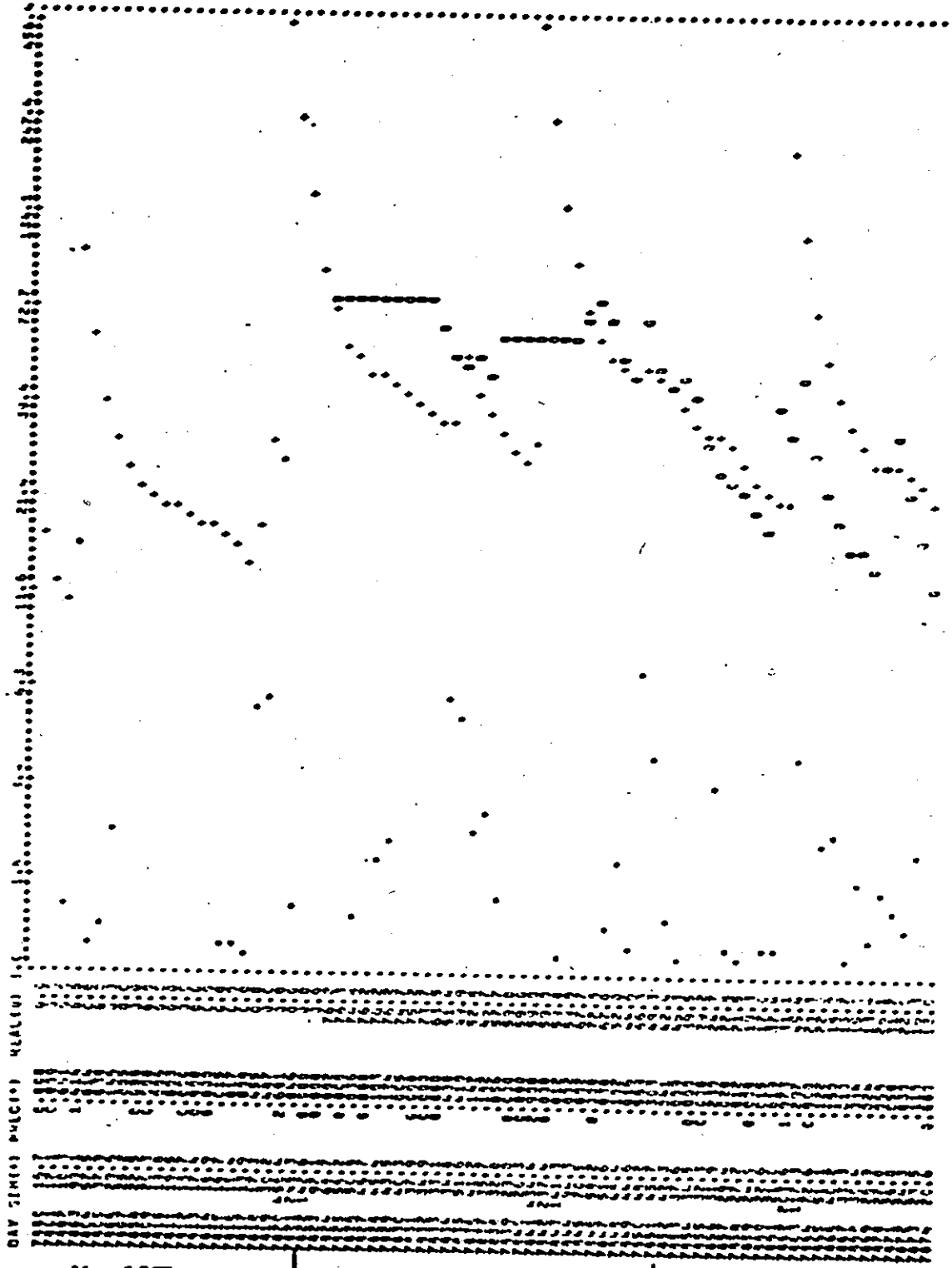




May 1971

June 1971

July 1971



May 1971

June 1971

July 1971

Simulation at Wildcat Basin

APPENDIX III

DATA CARD INPUT FOR KARST

<u>Card No.</u>	<u>Columns</u>	<u>Format</u>	<u>Program Variable</u>	<u>Comments</u>
1	1-80	10A8	TITLE(8)	Title for the simulation run.
2	1-4	I4	ISTDY	First Day Number for the simulation.
	5-8	I4	NDAY	Number of days for simulation.
	9-12	I4	NOPT	Number of water balance periods.
	13	I1	STMFLW	"T" if streamflow records are available.
	14			Not used.
	15	I1	LPRNT	"T" if a printer plot is required.
	16	I1	LPUNCH	"T" if a card deck of simulated and real streamflow is required.
	17-26	F10.0	TIMA	Analysis time in hours.
3	1-4	20I4	NOPTS(20)	Day Numbers when water balance and objective function calculations are to be made.
	5-8			
	etc.			
4	1-4	I4	NSEG	Number of segments in this simulation.
5	1-4	I4	NOS	Segment number.
	5-24	2A10	SEGNM	Segment name.
	25-30	I6	IGST	Gauge group from PRECON that this segment receives its input data from.
	31-32	I2	IELEE	Number of time delays for the histogram.
	33-40			Not used.
	41-60	20I1		Used for printing control of intermediate variables. 'Blank' or '0' means 'no printing'. '1' Printing ever 10 days. '2' Printing every day. '3' Printing every analysis point.
	41	I1	(SPR)	Precipitation.
	42	I1	(EGS)	Potential evaporation (after analysis).
	43	I1	(EET)	Actual evapotranspiration.
	44	I1	(OVF)	Overland flow.
	45	I1	(GWF)	Ground water flow.
	46	I1	(QOUT)	Segment runoff.
	47	I1	(PP)	Percolation.
	48	I1	(PERC)	Interflow.

<u>Card No.</u>	<u>Columns</u>	<u>Format</u>	<u>Program Variable</u>	<u>Comments</u>
5 (cont'd)	49	Π	(UZS)	Upper zone storage.
	50	Π	(LZS)	Lower zone storage.
	51	Π	(GWS)	Ground water storage.
	52	Π	(AST)	Interception storage.
	53	Π	(EGSA)	Potential evaporation.
	54	Π	(EGSB)	Evaporation after call from EVAPC.
	55	Π	(HRS)	Rain reaching surface.
	56	Π	(UZSA)	Upper zone storage before infiltration.
	57	Π	(LZSA)	Lower zone storage before ground water flow.
	58	Π	(UZSB)	Upper zone storage before ground water flow.
59	Π	(EET)	Initial evaporation.	
60	Π	(EETA)	Evaporation from interception.	
6	1-10			Not used.
	11-20	F10.5	SA	Segment area (square miles).
	21-30	F10.5	SHX	Evaporation correction (ratio).
	31-40			Not used.
	41-50	F10.5	SIA	Impervious area (ratio).
	51-60	F10.5	SAWT	Area of water (ratio).
7	1-10			Not used.
	11-20	F10.5	ASM	Interception storage, maximum (inches).
	21-30	F10.5	LZSNX	Nominal lower zone storage (inches).
	31-40	F10.5	UZSNX	Nominal upper zone storage (inches).
	41-50	F10.5	ASTX	Initial interception storage (inches).
	51-60	F10.5	UZSX	Initial upper zone storage (inches).
	61-70	F10.5	LZSX	Initial lower zone storage (inches).
	71-80	F10.5	GWSX	Initial ground water storage (inches).
8	1-40			Not used.
	41-50	F10.5	ART	Proportion of area not intercepted (ratio).
	51-60	F10.5	BZK	Interflow recession constant (1/days).
9	1-20			Not used.
	21-30	F10.5	GWRR	Ground water recession rate (days).
	31-40	F10.5	GWEA	Ground water evaporation coefficient.
	41-50	F10.5	LZEI	Lower zone evaporation coefficient.
10	1-10			Not used.
	11-15	10F5.0	TMET(20)	Time delay histogram (ratio).
	16-20			
	etc.			
11	1-10			Not used.
	11-12	20I2	IADD	Addition of flows from upstream segment numbers.
	13-14			
	etc.			

<u>Card No.</u>	<u>Columns</u>	<u>Format</u>	<u>Program Variable</u>	<u>Comments</u>
12	1-10 11-12 13-14 etc.	2012	IBDD	Not used. Addition of flows from upstream segment numbers.
13	1-10 11-20 21-30 31-40	F10.5	GMD SNOWA SNOWB	Not used. Ground melt (inches/day). Initial snow pack depth (inches). Temperature melt factor (inches/day/ F).
14	1-10 11-20 21-30 31-40 41-50 51-60 61-70	F10.5	SPARE(1) SPARE(2) SPARE(3) SPARE(4) SPARE(5) SPARE(6)	Not used. Mean climatic station elevation (feet). Mean segment elevation (feet). Lapse rate (F/1000 feet). Maximum infiltration rate (inches/day). Minimum infiltration rate (inches/day). Infiltration coefficient.
15	1-10 11-20 21-30 31-40	F10.5	SPARE(8) SPARE(9) SPARE(10)	Not used. Soil evaporation coefficient. Upper to lower zone coefficient. Lower to ground water coefficient.
16	1-80			Not used.

Cards 5 to 16 are repeated for each segment in the model.

Example of Data Input Cards

In this example the control cards are included for running the job. For this job it is assumed that the programs REEDAT and PRECON have been run to generate the climatic data tape which is stored as the first record on the tape (VSN = 1106). The program RATNG has also been run to generate the streamflow data which is stored as the second record on the tape, and the program KARST has been compiled and is stored as the final record on the tape. The data for this example is the Swago Creek data described in Chapter V.

123456789012345678901234567890123456789012345678901234567890123456789012

HFFC, CM70000, T40, MT1. (JOB CARD)

: COWA

LABEL (JCA, R, VSN=1106) READ/1106 (JC05)

REWIND (JCA, TAPE40, TAPE25, KARST)

COPYBR (JCA, TAPE25)

COPYBR (JCA, TAPE40)

COPYBF (JCA, KARST)

REWIND (KARST)

KARST.

7 END OF RECORD.

SWAGO RUN

697309390010TTTTF24.

70007100720073007400750076007700780079007912

1	1	2	111	3	1	1	1	11	1
12.	1.	0.	0.01		0.01				
0.5	2.0	1.1	0.02		0.1		0.2		5.
1.3	0.001	0.2	0.1		0.15				
0.	200.	0.05	0.2						
0.5	0.5								
SNOW	0.02	0.	0.08						
	2150.	3500.	-5.	2.	0.3		0.1		
	0.8	0.5	0.2						

6 END OF FILE